Hetu Sheth

A Photographic Atlas of Flood Basalt Volcanism

Springer

A Photographic Atlas of Flood Basalt Volcanism

Hetu Sheth

A Photographic Atlas of Flood Basalt Volcanism

Springer

Hetu Sheth
Department of Earth Sciences
Indian Institute of Technology Bombay
Mumbai, Maharashtra, India

ISBN 978-3-319-67704-0 ISBN 978-3-319-67705-7 (eBook)
https://doi.org/10.1007/978-3-319-67705-7

Library of Congress Control Number: 2017958544

Cover illustration: Gently-dipping, >1000 m thick Neogene flood basalts, Reyðarfjörður, Eastern Iceland. Photo © *Hervé Bertrand*

Printed on acid-free paper

This Springer imprint is published by Springer Nature
The registered company is Springer International Publishing AG
The registered company address is: Gewerbestrasse 11, 6330 Cham, Switzerland

Foreword

Flood basalt volcanism is an important form of large igneous provinces (LIPs), the term introduced in the early 1990s for unusually large, short-lived, mafic volcanic episodes that do not fit typical plate tectonic models. Flood basalts can be found in every continent and ocean basin, and throughout Earth's history. The origin of these LIPs has been controversial, though most geologists have favoured a mantle plume origin. The literature on that topic is abundant, but one important item lacking so far is a comprehensive catalogue of the physical volcanology of the huge lava flows and intrusions that make up these provinces. There is nothing like an actual field visit to a particular flood basalt province to understand its physical and volcanological features, ideally in the company of a specialist researcher familiar with that province. However, time and funding constraints mean that no single geologist will have the opportunity to see most flood basalt provinces of the world. Besides, not all flood basalts are easily accessible, and even the more accessible ones are often so large as to require decades, or even the entire span of a geologist's career, to see properly and adequately.

The flood basalt literature is full of written descriptions, which sometimes contain an "overview" photograph or two. These photographs however cannot do justice to the physical characteristics typical of each flood basalt. Besides, the flood basalt literature itself is scattered over many different journals and books, not always easily accessible. Thus, trying to get a good feel for the physical volcanological features of a specific flood basalt (not to speak of several flood basalts of the world), from the existing literature, is a frustrating task.

As an old saying goes, however, "One good picture is worth a thousand words", so how about a single volume that shows geologists of the world *five hundred* good flood basalt pictures? This is the idea that occurred to Hetu Sheth, an experienced flood basalt researcher enthusiastic about field geology and the author of this volume. He collected field photographs of typical volcanological features from researchers studying flood basalt provinces of the world. After careful selection, he has compiled hundreds of great photographs, showing the best volcanological features of global flood basalts, in one place, the present volume. Geologists reading this volume can now easily get a broad understanding of the physical volcanological features shared by flood basalt provinces as well as those distinct to specific provinces. The photographs in this book cover every conceivable topic one might want to see from a flood basalt province. Chapters range from landscapes and geomorphology, lava

flow structures related to emplacement and solidification, intrusive rocks, and even alteration and weathering.

The whole task at hand, being substantial and challenging, required high enthusiasm and motivation and efficient execution, and Hetu Sheth and Springer deserve our congratulations and appreciation for having produced this beautiful, scientifically valuable and long-needed volume. This photographic atlas should become a major reference and field guide for researchers studying flood basalts around the world and for students of volcanology and petrology.

Washington State University Tri-Cities Stephen P. Reidel
Richland, WA, USA

Acknowledgements

This work would not have been possible without the support of a large number of people, and here I place on record my indebtedness to them.

Sherestha Saini (Sher), Senior Editor, Environmental Sciences (Springer), invited me in late 2016 to do a book project, and had my book proposal reviewed quickly by early 2017. Sher and her editorial assistant Aaron Schiller always responded promptly to my queries and concerns. Sher gave me great freedom to produce the book the way I wanted, and to even cross 300 pages for the sake of completeness of the scientific material and to show the world what I wanted to show.

Karoly Németh, one of the top volcanologists we have today, reviewed and supported the initial book proposal for Springer and encouraged me with his comments, while also contributing significantly to the book.

The book, though it contains a large number of photographs by myself, would never have been completed without the enthusiastic support and contributions of 89 other people around the world, who gave many more photographs together (from one to as many as 49 each). It is one of the beautiful photos by Hervé Bertrand which is on the book's cover. Many of these contributors also helped me to write accurate captions for my photos taken in flood basalt provinces of their expertise.

Several contributors asked that they should retain copyright to their photographs in this book for future use, and that this should be indicated explicitly in their figure captions. I thank Springer (via Sher) for agreeing to this request and also for making a handsome offer of a free print copy of the book to the top 30 contributors (those with the maximum accepted photographs). That certainly did the trick for me, in part.

Once the component parts of the book were in place, and before the book went into production, the materials were kindly reviewed by such experts as Edgardo Cañón-Tapia (Mexico), Agust Gudmundsson (UK), J. Gregory McHone (Canada), Cliff D. Ollier (Australia), and Thorvaldur Thordarson (Iceland). Their constructively critical reviews helped me to present the material in a better way and to remove some errors. Stephen P. Reidel (USA), one of the best flood basalt experts in the world, and a contributor himself, kindly wrote a Foreword for the book at my request.

After I had revised all material following peer review, Murugesan Tamilselvan of SPi Global, Project Coordinator (Books) for Springer Nature, and his staff, particularly S. Rajesh (Project Manager, SPi Global), worked on the book's production, and performed the hard task of arranging the 582 photos and their captions in the final book as per my instructions. Murugesan and Rajesh always provided prompt responses and support to me.

On the domestic and family front, my wife Chaitali has provided great support over many years while I have been busy with flood basalts. Having interests in life rather distant from geology (whether continental, oceanic, or planetary, and Archaean through Recent), she wisely kept her distance whenever I worked on this book from home. It was very different with my seven-year-old, dinosaur-enthusiast son Shikhar ("summit", "peak"). Shikhar even knows that the dinosaurs did not die alone, but that all other wild animals, domestic animals, and pet animals also died with them. Shikhar would frequently thrust his head between me and my laptop, and commented, on seeing the opening photograph of Chap. 8, that he would like to "take that puzzle apart and put it back". May you, little Shikhar, in time solve every flood basalt puzzle and climb every summit that I could not.

Finally, there is no place like the field, and no feeling like being on the rocks without people within miles around. I dedicate this book to all lovers of field geology and to the numerous people who, over the years, have shown and taught me something about flood basalts and other igneous phenomena in the field.

IIT Bombay Hetu Sheth

About the Author

Hetu Sheth (1972–) is a Professor of Igneous Petrology and Volcanology in the Department of Earth Sciences, Indian Institute of Technology Bombay (IIT Bombay, Mumbai). He earned his B.Sc. (Geology) from Mumbai University in 1992, and his M.Sc. (Applied Geology) in 1994 and Ph.D. in 1998 from IIT Bombay. He then did post-doctoral work at the Physical Research Laboratory (PRL, Ahmedabad, India), the National Autonomous University of Mexico (UNAM), the University of Hawaii (USA), and the Homi Bhabha Centre for Science Education (TIFR, Mumbai). He was Deputy Website Manager of www.mantleplumes.org (2003–05), Associate, Indian Academy of Sciences (2003-07), and Associate Editor of the *Journal of Earth System Science* (2004–07). He has published and reviewed dozens of papers, co-edited two research volumes, and won several awards including the Indian National Science Academy (INSA) Young Scientist Medal (2003), the IIT Bombay Young Investigator Award (2007), the Indian Geophysical Union (IGU) Krishnan Medal (2010), the National Geoscience Award of the Ministry of Mines, Govt. of India (2010), and the M. R. Srinivasa Rao Award in Petrology of the Geological Society of India (2017). His major research interests are flood basalt volcanism and volcanic rifted margins, and he has additional broader interests in intraplate and arc volcanism, anorthosites, granites and rhyolites, and crustal evolution.

Contents

List of Contributors

Giulia Airoldi Torino, Italy
e-mail: g.airoldi.a@gmail.com

Sultan Ali Oil and Natural Gas Corporation (ONGC), Sundargarh, Odisha, India
e-mail: ali_md2@ongc.co.in

Carla Joana Santos Barreto Department of Geology, Center of Technology and Geosciences, Federal University of Pernambuco (UFPE), Arquitectura Avenue, Cidade Universitária, Recife, Pernambuco, Brazil
e-mail: carlabarreto.geo@hotmail.com

Jean Bédard Geological Survey of Canada, Québec, QC, Canada
e-mail: jeanh.bedard@canada.ca

Brian R. Bell University of Glasgow, Glasgow, UK
e-mail: Brian.Bell@glasgow.ac.uk

Hervé Bertrand Laboratoire de Géologie de Lyon, Ecole Normale Supérieure de Lyon et Université Lyon 1, Lyon, France
e-mail: herve.bertrand@ens-lyon.fr

Benjamin Black Department of Earth and Atmospheric Sciences, City University of New York, New York, NY, USA
e-mail: ben.black@gmail.com

Ninad R. Bondre Elevate Scientific, Hägersten, Sweden
e-mail: nrbondre@gmail.com

C. Kent Brooks Natural History Museum of Denmark, Copenhagen, Denmark
e-mail: kent2039@live.com

Adam Bumby Department of Geology, University of Pretoria, Pretoria, South Africa
e-mail: adam.bumby@up.ac.za

Victor Camp Department of Geological Sciences, San Diego State University, San Diego, CA, USA
e-mail: vcamp@mail.sdsu.edu

Kenneth Chakma Department of Earth Sciences, Indian Institute of Technology Bombay, Mumbai, India
e-mail: kennethchakma2008@gmail.com

El Hassane Chellai Faculty of Sciences-Semlalia, Geology Department, Cadi Ayyad University, Marrakech, Morocco
e-mail: chell@uca.ma

Raymond A. Duraiswami Department of Geology, Savitribai Phule University of Pune, Pune, India
e-mail: raymond.duraiswami@gmail.com

Linda Elkins-Tanton School of Earth and Space Exploration, Arizona State University, Tempe, AZ, USA
e-mail: ltelkins@asu.edu

David H. Elliot School of Earth Sciences and Byrd Polar Research Center, Ohio State University, Columbus, OH, USA
e-mail: elliot.1@osu.edu

Richard E. Ernst Department of Earth Sciences, Carleton University, Ottawa, ON, Canada
Faculty of Geology and Geography, Tomsk State University, Tomsk, Russia
e-mail: Richard.Ernst@ErnstGeosciences.com

Trevor J. Falloon School of Physical Sciences, Discipline of Earth Sciences, University of Tasmania, Hobart, Tasmania, Australia
e-mail: trevor.falloon@utas.edu.au

J. Godfrey Fitton School of GeoSciences, University of Edinburgh, Grant Institute, Edinburgh, UK
e-mail: godfrey.fitton@ed.ac.uk

Thomas H. Fleming Department of Earth Sciences, Southern Connecticut State University, New Haven, CT, USA
e-mail: flemingt1@southernct.edu

Gillian R. Foulger Science Laboratories, Department of Earth Sciences, Durham University, Durham, UK
e-mail: g.r.foulger@durham.ac.uk

Purva Gadpallu Department of Geology, Savitribai Phule University of Pune, Pune, India
e-mail: purva.gauri28@gmail.com

Hripsime Gevorgyan Institute of Geological Sciences, Armenian National Academy of Sciences, Yerevan, Republic of Armenia
e-mail: rippa@geology.am

Naresh C. Ghose (Formerly) University of Patna, Bangalore, India
e-mail: ghosenc2008@gmail.com

Vivek Ghule District Mining Office, Palghar (West), Maharashtra, India
e-mail: vivekforgeology@gmail.com

Chandrahas Halai Mumbai, India
e-mail: chandrahas.halai@gmail.com

William K. Hart Department of Geology and Environmental Earth Science, Miami University, Oxford, OH, USA
e-mail: hartwk@miamioh.edu

Arsen Israyelyan Institute of Geological Sciences, Armenian National Academy of Sciences, Yerevan, Republic of Armenia
e-mail: arsen.israelyan@gmail.com

Alexei V. Ivanov Center for Geodynamics and Geochronology, Institute of the Earth's Crust, Siberian Branch of the Russian Academy of Sciences, Irkutsk, Russia
e-mail: aivanov@crust.irk.ru

G.N. Jadhav Department of Earth Sciences, Indian Institute of Technology Bombay, Mumbai, India
e-mail: jadhav@iitb.ac.in

Vishwas S. Kale Department of Geography, Savitribai Phule University of Pune, Pune, India
e-mail: vskale.unipune@gmail.com

Andranik Keshishyan Ashtarak, Armenia
e-mail: gallery-ak@yandex.ru

Laszlo Kestay (Keszthelyi) U. S. Geological Survey, Astrogeology Science Center, Flagstaff, AZ, USA
e-mail: laz@usgs.gov

Martin B. Klausen Department of Earth Sciences, Stellenbosch University, Matieland, South Africa
e-mail: klausen@sun.ac.za

Lotte Melchior Larsen Geological Survey of Denmark and Greenland (GEUS), Copenhagen, Denmark
e-mail: lml@geus.dk

Rais Latypov School of Geosciences, University of the Witwatersrand, Johannesburg, South Africa
e-mail: Rais.Latypov@wits.ac.za

Vladimir A. Lebedev Institute of Geology of Ore Deposits, Petrography, Mineralogy and Geochemistry, Russian Academy of Sciences, Moscow, Russia
e-mail: vlad18011971@mail.ru

Nils Lenhardt Department of Geology, University of Pretoria, Pretoria, South Africa
e-mail: nils.lenhardt@up.ac.za

Jean-Paul Liégeois Geodynamics and Mineral Resources, Royal Museum for Central Africa, Tervuren, Belgium
e-mail: jean-paul.ligeois@africamuseum.be

José Madeira Faculdade de Ciências, Instituto Dom Luiz and Departamento de Geologia, Universidade de Lisboa, Lisbon, Portugal
e-mail: jmadeira@fc.ul.pt

Andrea Marzoli Dipartimento di Geoscienze, Università Degli Studi di Padova, Padova, Italy
e-mail: andrea.marzoli@unipd.it

Samson Masango Department of Physics and Geology, University of Limpopo, Sovenga, South Africa

Department of Geology, University of Pretoria, Pretoria, South Africa
e-mail: u04220773@tuks.co.za

George Mathew Department of Earth Sciences, Indian Institute of Technology Bombay, Mumbai, India
e-mail: gmathew@iitb.ac.in

Khachatur Meliksetian Institute of Geological Sciences, Armenian National Academy of Sciences, Yerevan, Republic of Armenia
e-mail: km@geology.am

Kiran S. Misra Earth Science Research Center, University of Petroleum & Energy Studies, Dehradun, India
e-mail: drksmisra@gmail.com

Saumitra Misra Department of Geology, School of Agricultural, Earth and Environmental Sciences, University of Kwazulu-Natal, Durban, South Africa
e-mail: misrasaumitra@gmail.com

Dhananjay Mohabey Department of Geology, RTM Nagpur University, Nagpur, India
e-mail: dinomohabey@yahoo.com

Lucia Castanheira de Moraes CEFET-MG—Centro Federal de Educação Tecnológica de Minas Gerais, Araxá, Minas Gerais, Brazil
e-mail: 2013luciam@gmail.com

Danielle K. Moyer Department of Biodiversity, Earth and Environmental Science, Drexel University, Philadelphia, PA, USA
e-mail: dkm64@drexel.edu

James D. Muirhead Syracuse University, Syracuse, NY, USA
e-mail: james.muirhead@fulbrightmail.org

Ria Mukherjee School of Geosciences, University of the Witwatersrand, Johannesburg, South Africa
e-mail: ria.mkrj@gmail.com

Karoly Németh Institute of Agriculture and Environment, Massey University, Palmerston North, New Zealand
e-mail: k.nemeth@massey.ac.nz

Ralph Neuwerth Section des Sciences de la Terre, Université de Genève, Geneva, Switzerland
e-mail: ralph.neuwerth@gmail.com

Troels F.D. Nielsen Geological Survey of Denmark and Greenland (GEUS), Copenhagen, Denmark
e-mail: tfn@geus.dk

Berthold Ottens Walsdorf, Germany
e-mail: ottens-mineralien@t-online.de

Ishita Pal Institute of Geophysics and Planetary Physics, Scripps Institution of Oceanography, University of California San Diego, La Jolla, CA, USA
e-mail: palishita13@gmail.com

Kreesan Palan Department of Geology, School of Agricultural, Earth and Environmental Sciences, University of Kwazulu-Natal, Durban, South Africa
e-mail: kreesanpalan@gmail.com

Asger Ken Pedersen Natural History Museum of Denmark, Copenhagen, Denmark
Geological Survey of Denmark and Greenland (GEUS), Copenhagen, Denmark
e-mail: akp@snm.ku.dk

Peng Peng Institute of Geology and Geophysics, Chinese Academy of Sciences, Beijing, China
e-mail: pengpengwj@mail.iggcas.ac.cn

Anthony R. Philpotts Department of Geology and Geophysics, University of Connecticut, Storrs, CT, USA
e-mail: philpotts@charter.net

Erika Rader NASA Ames Research Center, Moffett Field, CA, USA
e-mail: erika.rader@nasa.gov

Stephen P. Reidel School of the Environment, Washington State University, Pullman, WA, USA
e-mail: sreidel@wsu.edu

Julie Rowland School of Environment, University of Auckland, Auckland, New Zealand
e-mail: j.rowland@auckland.ac.nz

Arnav H. Samant Department of Geology, St. Xavier's College, Mumbai, India
e-mail: arnav.samant@gmail.com

Hrishikesh P. Samant Department of Geology, St. Xavier's College, Mumbai, India
e-mail: hrishikesh.samant@xaviers.edu

Satish J. Sangode Department of Geology, Savitribai Phule University of Pune, Pune, India
e-mail: sangode63@gmail.com

Eraiyoli Sankaran Thane (West), Maharashtra, India
e-mail: eraiyoli@yahoo.com

Hildor José Seer CEFET-MG—Centro Federal de Educação Tecnológica de Minas Gerais, Araxá, Minas Gerais, Brazil
e-mail: hildorster@gmail.com

Stephen Self Department of Earth and Planetary Science, University of California Berkeley, Berkeley, CA, USA
e-mail: steve.self1815@gmail.com

Bibhas Sen Geological Survey of India, North Eastern Region, Shillong, Meghalaya, India
e-mail: bibhas.sen@gmail.com

P. Senthil Kumar Planetary Geosciences, CSIR-National Geophysical Research Institute (NGRI), Hyderabad, India
e-mail: senthilngri@yahoo.com

Priyanka Shandilya Department of Earth Sciences, Indian Institute of Technology Bombay, Mumbai, India
e-mail: priyankashandilay@gmail.com

Kamal Kant Sharma Government Postgraduate College, Sirohi, Rajasthan, India
e-mail: sharmasirohi@yahoo.com

J. Gregory Shellnutt Department of Earth Sciences, National Taiwan Normal University, Taipei, Taiwan
e-mail: jgshelln@ntnu.edu.tw

Hetu Sheth Department of Earth Sciences, Indian Institute of Technology Bombay, Mumbai, India
e-mail: hcsheth@iitb.ac.in

Leonid Shumlyanskyy M.P. Semenenko Institute of Geochemistry, Mineralogy and Ore Formation, National Academy of Sciences of Ukraine, Kiev, Ukraine
e-mail: lshumlyanskyy@yahoo.com

Alan Smith Department of Geology, School of Agricultural, Earth and Environmental Sciences, University of Kwazulu-Natal, Durban, South Africa
e-mail: asconsulting@telkomsa.net

Erik Vest Sørensen Geological Survey of Denmark and Greenland (GEUS), Copenhagen, Denmark
e-mail: evs@geus.dk

Chantal Souche The Rectorate of the Academy of Montpellier, Montpellier, France
e-mail: chantal.souche@hotmail.fr

Bjørn Thomassen Geological Survey of Denmark and Greenland (GEUS), Copenhagen, Denmark
e-mail: bjorn.thomass@gmail.com

Thorvaldur Thordarson Faculty of Earth Sciences, University of Iceland, Reykjavík, Iceland
e-mail: torvth@hi.is

Loÿc Vanderkluysen Department of Biodiversity, Earth & Environmental Science, Drexel University, Philadelphia, PA, USA
e-mail: loyc@drexel.edu

Dhananjai Verma Geological Survey of India, Gandhinagar, Gujarat, India
e-mail: geodhananjai@gmail.com

Margrethe Watt Søborg, Denmark
e-mail: margrethewatt@mail.dk

W. Stuart Watt Geological Survey of Denmark and Greenland (GEUS), Copenhagen, Denmark
e-mail: wsw@geus.dk

Dominique Weis Department of Earth, Ocean and Atmospheric Sciences, The University of British Columbia, Vancouver, BC, Canada
e-mail: dweis@eos.ubc.ca

James D.L. White Department of Geology, University of Otago, Dunedin, New Zealand
e-mail: james.white@otago.ac.nz

Yigang Xu Guangzhou Institute of Geochemistry, Chinese Academy of Sciences, Guangzhou, China
e-mail: yigangxu@gig.ac.cn

Mahua Yadav Department of Earth Sciences, Indian Institute of Technology Bombay, Mumbai, India
e-mail: mahuay27@gmail.com

Nasrrddine Youbi Faculty of Sciences-Semlalia, Geology Department, Cadi Ayyad University, Marrakech, Morocco

Faculdade de Ciências and Instituto Dom Luís, Departamento de Geologia, Universidade de Lisboa, Lisbon, Portugal
e-mail: youbi@uca.ac.ma; nayoubi@fc.ul.pt

Introduction

1

Flood basalts represent the largest magmatic events on Earth and the terrestrial planets (e.g., Head and Coffin 1997; Bryan et al. 2010; Ernst 2014). *Continental flood basalt* (CFB) provinces are volcanic constructs that are laterally extensive (many hundreds to thousands of kilometers) and thick (up to several kilometers). The Late Cretaceous to Palaeocene (~65 Ma) Deccan Traps cover 0.5 million km^2 of western and central India today (with small outcrops in Pakistan) and have an estimated original extent of 1.5 million km^2. The 250 Ma Siberian Traps of Russia are an order of magnitude larger, whereas even comparatively small CFB provinces such as the Columbia River province in the USA are well over 200,000 km^2. Oceanic flood basalt provinces, forming the so-called *oceanic plateaus* such as the Ontong Java in the western Pacific, may also be millions of square kilometers in areal extent, and are vastly thicker (tens of kilometers) than CFB provinces.

The importance of flood basalt volcanism in the geological evolution of the Earth is manifold, making them a very interesting topic of study for volcanologists, igneous petrologists, geochemists, geochronologists, palaeomagnetists, geodynamicists, palaeontologists, and climate and atmospheric scientists. Flood basalts represent events of major crustal growth, in the form of eruption and intrusion of very large volumes (millions of cubic kilometers) of mantle-derived magma on the Earth's surface and into the crust, in relatively short time periods of one to a few million years (e.g., Mahoney and Coffin 1997 and references therein). Whereas oceanic plateaus are relatively inaccessible, CFB provinces are observed to be products of fissure eruptions on a grand scale, represented in mafic dyke swarms which are valuable in understanding mantle-crust evolution, lithospheric stress regimes and geodynamics, and palaeocontinental reconstructions (e.g., Ernst et al. 2001). The larger intrusions found in CFB provinces, such as the famous Skaergaard Intrusion of East Greenland, are where many current standard ideas in igneous petrology saw significant development (e.g., Wager and Deer 1939; Wager et al. 1960; see Young 2003). CFB provinces are dominated by subalkalic basalts and basaltic andesites, but also typically contain non-basaltic rocks, including ultrabasic-ultramafic, alkaline and silicic rocks. The petrogenetic evolution and mineral resources of all these rocks are of much interest to academia and industry (e.g., Garland et al. 1995; Lightfoot and Hawkesworth 1997; Melluso et al. 2008, 2009). Many CFB provinces of the world formed during the rifting and breakup of continents, and both phenomena have been ascribed variously to deep mantle plumes, normal plate tectonic processes, and asteroid impacts (e.g., Foulger et al. 2005 and Foulger and Jurdy 2007, and references therein; Ernst 2014). Because many prehistoric flood basalt events correlate with biological mass extinctions (e.g., Rampino and Stothers 1988; Wignall 2001, 2005; Ernst and Youbi 2017), topics such as the physical emplacement of flood basalt lava flows, their emplacement duration, and volatile release are of major past and current interest (e.g., Thordarson and Self 1996; Self et al. 2014).

It is therefore not surprising that the current flood basalt research community consists of many hundreds of researchers worldwide, specializing in various disciplines. Thousands of research papers on flood basalts exist. Many research volumes and books on the broad theme of flood basalt volcanism exist, including *Continental Flood Basalts* (ed. Macdougall, Kluwer Acad. Publ., 1988), *Large*

H. Sheth, *A Photographic Atlas of Flood Basalt Volcanism*, https://doi.org/10.1007/978-3-319-67705-7_1

Igneous Provinces: Continental, Oceanic, and Planetary Flood Volcanism (eds. Mahoney and Coffin, Am. Geophys. Union Geophysical Monograph 100, 1997), and *Large Igneous Provinces* (Ernst, Cambridge Univ. Press, 2014). Many more volumes exist on specific flood basalts of the world. Among these are volumes on the Deccan Traps (e.g., *Deccan Volcanism*, eds. Subbarao and Sukheswala, Geol. Soc. Ind. Mem. 3, 1981; *Deccan Flood Basalts*, ed. Subbarao, Geol. Soc. Ind. Mem. 10, 1988; *Deccan Basalts*, eds. Deshmukh and Nair, Gondwana Geol. Soc., 1996; *Deccan Volcanic Province*, ed. Subbarao, Geol. Soc. Ind. Mem. 43, 1999). There are volumes on the Central Atlantic Magmatic Province (e.g., *Eastern North American Mesozoic Magmatism*, eds. Puffer and Ragland, Geol. Soc. Am. Spec. Pap. 268, 1992; *The Central Atlantic Magmatic Province: Insights from Fragments of Pangaea*, eds. Hames et al., Am. Geophys. Union Geophysical Monograph 136, 2003). There are also volumes on the Columbia River province (e.g., *Volcanism and Tectonism in the Columbia River Flood-Basalt Province*, eds. Reidel and Hooper, Geol. Soc. Am. Spec. Pap. 239, 1989; *The Columbia River Flood Basalt Province*, eds. Reidel et al., Geol. Soc. Am. Spec. Pap. 497, 2013a). In addition, many special issues of the standard research journals have been devoted to individual CFB provinces, or groups of CFB provinces associated in space or time. Examples are *Mesozoic Magmatism of the Eastern Margin of India* (guest-editors Ghose et al., J. Asian Earth Sci., 1996), *Flood Basalts of Asia* (guest-editors Sheth and Vanderkluysen, J. Asian Earth Sci., 2014), and *Permian Large Igneous Provinces: Characteristics, Mineralization and Palaeo-Environmental Effects* (guest-editors Xu et al., Lithos, 2014a). Speaking of oceanic flood basalt provinces, available research volumes include *Origin and Evolution of the Ontong Java Plateau* (eds. Fitton et al., Geol. Soc. Lond. Spec. Publ. 229, 2004) and *The Origin, Evolution, and Environmental Impact of Oceanic Large Igneous Provinces* (eds. Neal et al., Geol. Soc. Am. Spec. Pap. 511, 2015). This is by no means an exhaustive list but is large enough to indicate the great past and current interest and activity in this field, which will undoubtedly continue in the decades to come. Indeed, there are few subjects as "hot" and interdisciplinary as flood basalt volcanism.

Despite the wealth of geological, geochemical and geophysical information available on flood basalt volcanism, few volumes exhibit the *field geology* of flood basalts in any detail. One such volume, packed with geological information and beautiful maps and field photographs, is *The Palaeogene Volcanic Districts of Scotland* (4th ed., Emeleus and Bell, British Geol. Surv., 2005). However, over the past few years I have increasingly felt a need for a photographic field atlas covering the flood basalt provinces of the world. No such work exists, but I thought that such an atlas, containing great field photographs of large-, medium-and small-scale geological features of global flood basalts, would be a valuable addition to flood basalt literature specifically, and volcanological and geological literature in general. Such an atlas would be a valuable field guide to flood basalts for a large audience including, say, specialists focussing on geochemistry or palaeomagnetism, nonspecialists who want to know more about flood basalts, field geologists (such as those working in geological surveys), aspiring students beginning a research career, or even people in the industry. It is worth pointing out that field features of flood basalts, such as vesicles and jointing patterns, are not features of academic interest alone, useful only in understanding flood basalt emplacement. They are also of high potential economic, engineering, and industrial importance: consider hydrocarbon maturation by magma intrusions (e.g., Muirhead et al. 2017), flood basalt-hosted petroleum reservoirs (e.g., Farooqui et al. 2009), carbon dioxide sequestration and nuclear waste storage in flood basalts (e.g., U.S. Department of Energy 1988; Reidel et al. 2002), groundwater resources (e.g., Pawar et al. 2012; Lite 2013), economic mineralization (e.g., Lightfoot and Hawkesworth 1997; Ernst and Jowitt 2013), and geothermal energy and hydropower (e.g., Kristjánsdóttir 2015).

It is with these thoughts that I have produced the present book, **A Photographic Atlas of Flood Basalt Volcanism**. Because no single person has seen all the flood basalts of the world, or all their features, I asked researchers around the world, studying various flood basalt provinces, to contribute good field photographs with short captions (without limits on how many), complementing my own and covering various topics for this volume. I realized that people who are nonspecialists (or even

nongeologists) may also possess great flood basalt photos. It is worth noting that the 90 contributors spread over 23 countries, who have contributed the 582 photos appearing in this book (selected from nearly 1150 received), include not only many flood basalt specialists and other geologists-volcanologists, but also my former students (Ali, Chakma, Ghule, Pal, Yadav), a Moroccan sedimentologist (Chellai), a French mathematics professor (Souche), an Armenian professional photographer (Keshishyan), and two college friends of mine who are avid trekkers and gifted nature photographers (Halai, Sankaran). And why not? Their photographs speak for themselves. I could convince these 89 contributors (other than myself) that this book could be a great place for the many valuable field photos they must have and which could never go into the standard research papers and books, that this book was an opportunity to showcase their favourite flood basalt and their own photographic talent, and, for the active researchers, that a short break from "that perpetual pending research paper" would be to everyone's benefit.

The reader should be clear about what this volume offers and what it does not. The volume is the first of its kind in offering hundreds of photographs illustrating the field geological features of flood basalt volcanism, classified by theme into landscapes (Chap. 2), lava flow morphology and stacking patterns (Chap. 3), lava flow structures (Chaps. 4 and 5), subaqueous volcanism, volcanosedimentary sequences and lava-sediment interaction (Chap. 6), explosive volcanism and pyroclastic rocks (Chap. 7), the intrusive component of flood basalt volcanism (dykes, sills and plutons, Chap. 8), compositional diversity and magmatic processes (Chap. 9), tectonic deformation (Chap. 10), secondary mineralization (Chap. 11), and alteration and weathering (Chap. 12). The last three chapters are shorter than the rest, as these deal with topics not directly related to flood basalt volcanism itself, though still very much contributing to flood basalt geology as we observe it today.

The geographic coverage of flood basalts in this book is global (Fig. 1.1). All major CFB provinces (the British Palaeogene, Central Atlantic Magmatic Province, Columbia River, Deccan, East Greenland, Emeishan, Ethiopian, Ferrar, Iceland, Karoo, Paraná, Siberian, and West Greenland) are well covered, and many others (such as the Rajmahal-Kerguelen and the Indo-Madagascar) are also included. Intermediate-sized to small-sized flood basalts of the world (Hoggar, Libya, Patagonia, Saudi Arabia, South Caucasus) are also included in the book, the last two being particularly well-covered. To me, these examples, as well as others like the Miocene Altos de Jalisco basalt plateau in central Mexico (Ferrari et al. 2000; Mori et al. 2009) or the numerous Cenozoic basalt plateaus in Vietnam and Laos (Hoang and Flower 1998), indicate that boundaries between "small", "intermediate" and "large" flood basalt provinces are artificial, and flood basalt size a continuum. This has significance for our conceptual understanding of flood basalt volcanism and associated mantle-crust geodynamics (see Cañón-Tapia 2010, and a brief discussion in Sheth et al. 2015), and is worthy of an entire future research paper.

Also included in the book are Precambrian CFB provinces (and some greenstone belts which may be CFBs) such as the Volyn, Natkusiak, and others. Precambrian giant dyke swarms that may represent the feeders of now-eroded flood basalts (such as across Greenland) are also covered. Planetary flood basalts are *not* included; giving them the attention and coverage they deserve would have meant a book of impossible size in the present circumstances. Places like Hawaii were excluded from consideration for several and evident reasons. The emphasis has been on exhibiting the widest range of geological *features* possible, and it is significant that all or nearly all major field geological features of flood basalts are covered in this book. They cover a range of sizes, from lava toes and dykelets centimeters in thickness to sheet flows and giant dykes many tens of meters to >100 m thick. Some of the intriguing features are not well understood, such as the "war bonnet" structures of the Columbia River flood basalt province (Chap. 5). Other, similarly intriguing and puzzling features are located at places not well known (e.g., see Titan's Piazza in Chap. 5). It would be nice to see research studies of these being initiated by the capable readers of this book.

A *Glossary* of technical terms is provided, more for the benefit of flood basalt nonspecialists, with ample references. Otherwise this atlas, being a collection of field geological photographs and their explanatory captions, purposely contains no

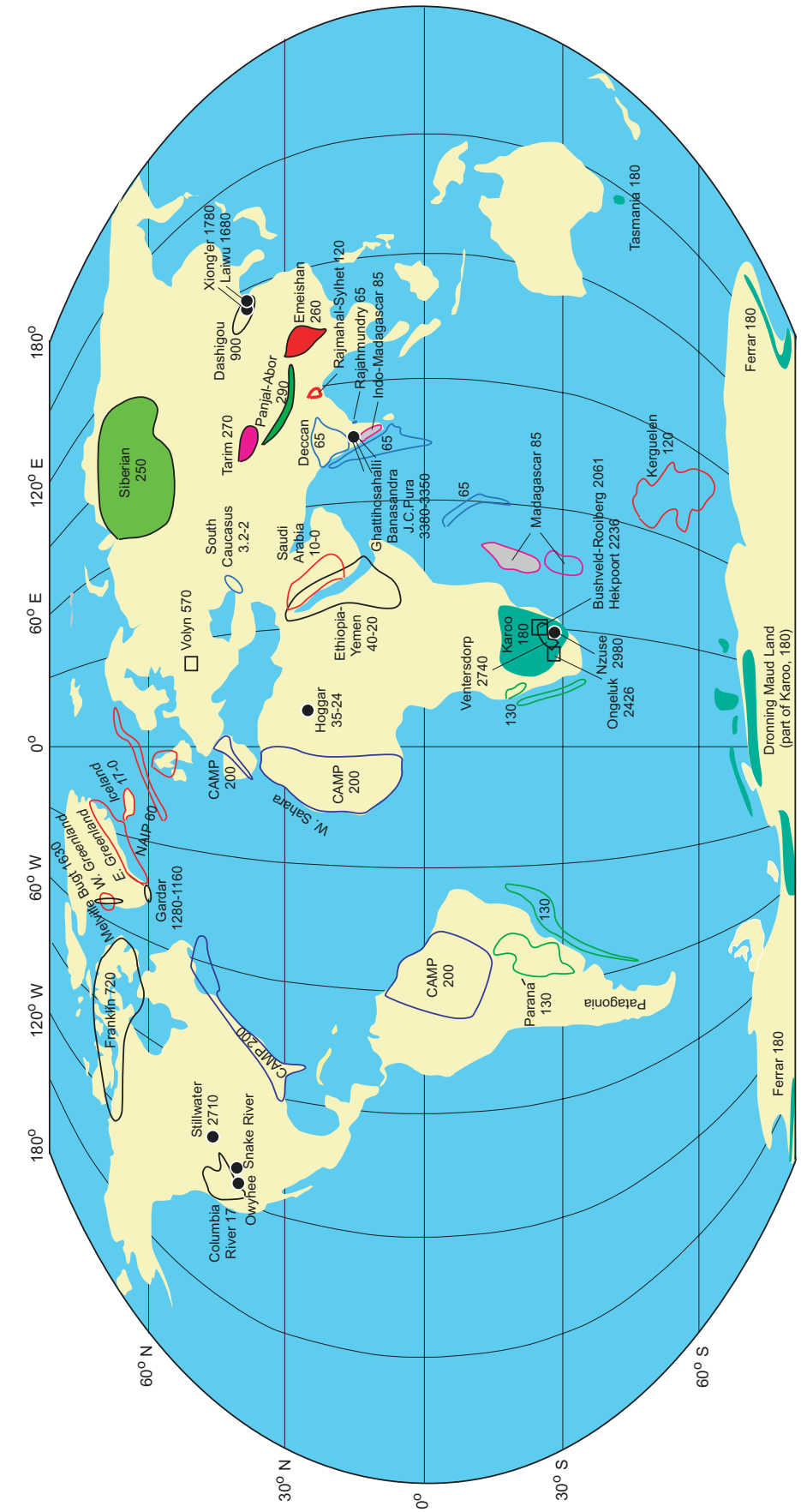

Fig. 1.1 Map of the world showing the flood basalt examples covered in this atlas (see the *Flood Basalt Index* at the end of the book for a list). Parts of the same flood basalt event are indicated by outlines or fills of the same colour, and average ages of the flood basalt events (in million years) are also given. Robinson projection; modified from Ernst (2014)

maps (location or geological), sketches of the features illustrated, lithologs, geochemical data, etc., all of which can be found in the many publications listed in the *References* and *Suggested Reading* sections of the book. An index of technical terms is not included, as it would be superfluous in a volume in which the photographs are classified by broad topics into chapters, and by narrower topics within each chapter. An *Author Index* (with the specific photograph numbers shown against contributor name) and a *Flood basalt Index* (with specific photograph numbers for particular flood basalt examples) are provided, as is a *List of Contributors* with their affiliations and contact information. Following modern usage, and as explained in Harris et al. (2017), the standard and frequently appearing lava-type terms pāhoehoe and ʻa'ā, ascribed to Dutton (1883), are spelt everywhere with the Hawaiian-language diacritical marks. Following the recommendation of Thorvaldur Thordarson, one of the reviewers of this volume, Icelandic place names are given with Icelandic spelling, for which it is only necessary to know, for present purposes, that the letter Þ nearly corresponds to the English "Th" (pronounced as in "thin") and the letter ð to the English "d". Note that the captions to the photographs supplied by the contributors, after editing by me to various extents (and the contributors' approval of my edits), retain the writing style of the contributors themselves.

The 582 photographs appearing in this book were selected based on their scientific and aesthetic value, and show the great similarities *and* differences between flood basalts of the world. The book takes the reader on a virtual field geological tour, and could be classified as a contribution not only in technical volcanology but also in volcanic geotourism and geoheritage, studies of which are of increasing interest (e.g., Moufti and Németh 2016). This book project (involving obtaining, selecting, arranging hundreds of photos, editing and re-editing their captions, compiling and checking the references and so on, and above all working with the contributors) was both challenging and stimulating for me. The finished outcome of everyone's combined effort and contribution is now in the reader's hands. If the book gives the reader the "Wow, I want to go there" feeling, my intensive work of more than a year will not have been wasted.

It is my hope that this photographic atlas on flood basalts will motivate readers (and contributors of this atlas) to bring out more such atlases in the future, such as on arc volcanism, ocean island volcanism, monogenetic volcanism, individual flood basalt provinces of the world, planetary flood volcanism, and more. The themes and possibilities seem limitless.

Flood Basalt Landscapes

2

Fig. 2.1 Waterfalls plunging ~200 m over a large amphitheatrical cliff, carved through several flows of Deccan basalt. Rajmachi area near Khandala, Western Ghats, India. Such amphitheatrical valleys abound in this region, which is very dry and hot in summer but very wet, lush green and cool in the monsoon. There is an additional 100 m or so of height traversed by smaller cascades above the cliff Photo © *Chandrahas Halai*

H. Sheth, *A Photographic Atlas of Flood Basalt Volcanism*, https://doi.org/10.1007/978-3-319-67705-7_2

Chapter Overview

Flood basalts create beautiful and impressive landscapes, whether these landscapes be humid tropical and thickly forested, frozen and snow-covered, hot and arid, or any other. The larger-scale elements of flood basalt landscapes are plateaus and escarpments, canyons and gorges, mesas and buttes, formed on the typically horizontal lava stacks. Sigurdsson (1999, p. 113) ascribes the term "Trap" (referring to their step-like topography, and derived from an Old Norse word *trappa*, a step in a stair), to the Swedish scientist and philosopher Emanuel Swedenborg (1688–1772). Flood basalt landscapes covered in this chapter are necessarily all continental, with the sole exception of Iceland. An emergent oceanic plateau, Iceland is well known for its striking scenery: vast empty plains, broken by high, dark mountains capped by glaciers, whose meltwaters produce thunderous rivers and magnificent waterfalls during summertime. Indeed, flood basalts of the world are home to waterfalls ranging in size from small cascades to those bigger than the Niagara.

Despite their common features, flood basalts of the world show a considerable diversity in landscapes owing to climate conditions. Compare the modern landscapes of the Paraná and the West Greenland flood basalts and the Saudi Arabian *harrats* (volcanic fields). Or compare the modern landscapes on large dolerite sills of the Karoo, Ferrar and Tasmania, formed together in a single Jurassic magmatic burst on Gondwanaland (Ivanov et al. 2017) and now separated by many thousands of kilometers due to continental drift. Even individual flood basalt provinces such as the Deccan show much regional and seasonal variation in climate, rainfall and vegetation cover, and the resultant landscape. The Western Ghats of India receive large amounts of rainfall from the Arabian Sea, are densely vegetated, and are in fact one of the major biodiversity hotspots of the world. In contrast, a large region of the Deccan plateau to the east of the Ghats escarpment, due to the rain shadow effect, is semi-arid to arid. (It is for the same rainshadow effect that a large part of the Columbia River flood basalt province in the Pacific Northwest USA, east of the Cascades Range, is a desert.) There are interesting geomorphological puzzles which remain not only unsolved but also untouched, such as the magnificent Ajanta gorge in the central Deccan Traps, illustrated in this chapter. In an arid region where modern summer temperatures typically reach 47 °C, when were the large incised meanders of the gorge carved, and under what favourable interplay of climate and tectonics?

When you are a geologist and love your work, even a family holiday is a geological field trip and an opportunity for education, just as a geological field trip is equally a pleasure trip. Take the world tour with this book, and return impressed and enriched.

Fig. 2.2 Typical landscape in the high areas in central-western Disko, West Greenland. A thick, monotonous-looking succession of basalt lava flows of the Maligât Formation, dipping very gently to the west (to the right) is seen. The snow accumulates preferentially on the ledges formed by the easier-eroded top rubble of the flows. The mountain wall in the foreground is situated at 1000–1470 m a.s.l.
Photo: *Asger Ken Pedersen, Geological Survey of Denmark and Greenland (GEUS)*

Fig. 2.3 Flood basalt lava flows of the Geikie Plateau Formation of the Blosseville Group. Eastern Gåseland close to the Inland Ice, inner Scoresby Sund region, central East Greenland (Larsen et al. 1989). Footprints in the snow provide a nice human touch and a feel for the experience of field work in this beautiful but harsh terrain
Photo: *W. Stuart Watt, Geological Survey of Denmark and Greenland (GEUS)*

Fig. 2.4 Panorama of basaltic plateaus of the Paraná CFB province, Brazil. The road and the houses in the valley below provide an approximate scale
Photo © *Carla Barreto*

Fig. 2.5 View of the upper part of the 1400 m thick Karoo flood basalt sequence of the Drakensberg Group in the Sani Pass, Lesotho (S29°35′, E29°17′). The winding road provides an approximate scale
Photo © *Adam Bumby*

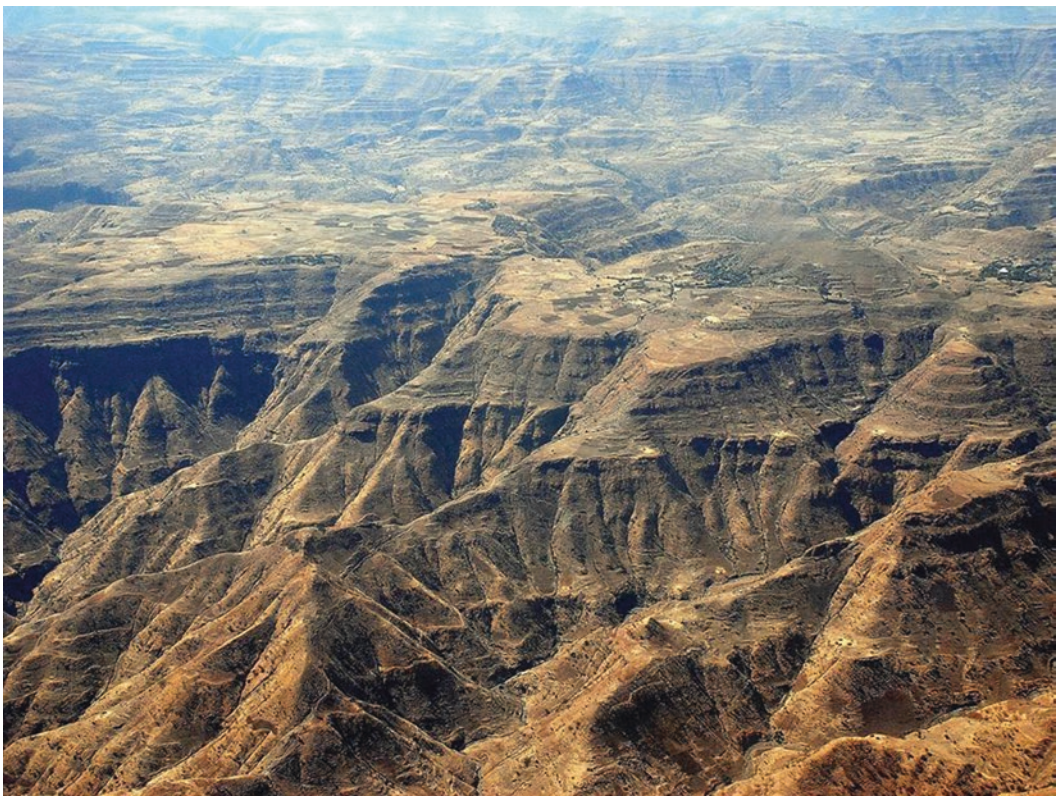

Fig. 2.6 Aerial view of the Ethiopian Traps (30 Ma) between Addis Ababa and Lalibela, Ethiopia. The Traps are 1500 m thick
Photo © *Hervé Bertrand*

Fig. 2.7 The 1500 km long Western Ghats escarpment in India is cut through the Deccan flood basalts in its northern half. The road from Poladpur town on the Konkan Plain, nearly at sea level, winds through the many spurs that this escarpment sends down to the plain, and through ~1350 m of flood basalts capped by extensive ferricrete (laterite), to reach the hill town of Mahabaleshwar (1436 m) on the top. More information: Ollier and Powar (1985), Gunnell and Radhakrishna (2001), Kale (2010)
Photo © *Hetu Sheth*

Fig. 2.8 The Mesa Range in north Victoria Land, Antarctica, has the greatest thickness (ca. 700 m) of Kirkpatrick Basalt flows. The capping, cliff-forming, black flow is up to about 80 m thick and is tachylitic. More information: Elliot and Fleming (2008)
Photo © *David H. Elliot*

Fig. 2.9 The highly eroded Drakensberg mountain range about 115 km west of Durban, South Africa. The mountains reach 2800 m above sea level, and rise 1500 m above the foreground
Photo © *Saumitra Misra & Kreesan Palan*

Fig. 2.10 Flood basalts in northern Iceland, forming sequences 500–600 m thick. The lake in the foreground is Vatnshlíðarvatn, next to the circum-Iceland ring road, Route 1, about 10 km from the town of Varmahlíð
Photo © *Dominique Weis*

Fig. 2.11 View from Portree harbour, Isle of Skye, of Ben Tianavaig (413 m), dominated by the Palaeogene Beinn Edra Formation, unconformably overlying Middle Jurassic strata. The Formation comprises basal hyaloclastites (not obvious in photograph), overlain by compound pāhoehoe and simple sheet lavas. More information: Emeleus and Bell (2005)
Photo © *Hetu Sheth*

Fig. 2.12 Scenic view of the Columbia River Gorge, cutting through the Columbia River Basalts, near Portland, Oregon, USA
Photo © *Loÿc Vanderkluysen*

Fig. 2.13 The Snake River canyon (USA) exposes several volcanoes (tuff cones and tuff rings) that formed due to magma-water explosive interaction. However, the presence of lava deltas also indicates that a large portion of the lava flows entered a lacustrine basin. The walls of the canyon to the left expose multiple lava flows, while the walls to the right, capped by the buttes, expose hydromagmatic volcanoes
Photo © *Karoly Németh*

Fig. 2.14 The southwestern tip of the Reykjanes Peninsula (Smokey Point), Iceland, with Holocene lava flows (dark, foreground). Also seen are the Reykjanes lighthouse (Reykjanesviti) and the Reykjanes geothermal field and power plant (Reykjanesvirkjun)
Photo © *Dominique Weis*

Fig. 2.15 One of the youngest lava flows in the Harrat Khaybar in western Saudi Arabia emitted from the Jebel Qidr volcano (the distant, dark, symmetrical volcano in the lava field). The lava field spreads across older silicic (rhyolitic, trachytic) lava domes, tuff rings and mafic scoria cones. The lava flow shows exquisite pāhoehoe lava surface textures in its proximal areas, but where ground slope angle suddenly increases, or behind breakouts of ponded zones, the lava flow texture becomes more like rubbly pāhoehoe. More information: Camp et al. (1991), Moufti and Németh (2016)
Photo © *Karoly Németh*

Fig. 2.16 Tholeiitic-transition flood basalts (vertical development 600 m, altitude above sea level ~1000 m) in the Baie Larose (Larose Bay), south of Mount Ross stratovolcano (1850 m), Kerguelen Islands, southern Indian Ocean
Photo © *Dominique Weis*

Fig. 2.17 Quiraing on the Trotternish peninsula, northern Skye, Scotland, with rounded topography on flood basalt. Since the Pleistocene glaciations, large basalt masses overlying Jurassic sedimentary rocks have detached from the scarp and slided towards the sea. Some movements continue today. More information: Emeleus and Bell (2005)
Photo © *Hetu Sheth*

Fig. 2.18 Reyðarfjörður in eastern Iceland, fjord carved by Ice Age glaciers into Neogene flood basalts. The gently-dipping basalts are ~1000 m thick. More information: Walker (1959)
Photo © *Dominique Weis*

Fig. 2.19 Extensive flood basalt flows, mainly of the Geikie Plateau Formation. In the background is the Watkins Bjerge escarpment crowned by the Gunnbjørn Fjeld massif, including Greenland's highest mountain at 3707 m altitude. The basalts were uplifted by the Kangerlussuaq dome (Brooks 2011). Southern Blosseville Kyst, East Greenland
Photo: *Margrethe Watt, Geological Survey of Denmark and Greenland (GEUS)*

Fig. 2.20 Splendid isolation, especially for someone from a city of 20 million and 25,000 people per square kilometer. Grassy and water-logged summer landscape of the Isle of Skye between Preshal More (dark hill in the background), and Preshal Beg, from where the photograph was taken. Distance between the two is 2 km. A late-arriving member of the field party provides a scale
Photo © *Hetu Sheth*

Fig. 2.21 Pāhoehoe lava flow terminus at the foot of Jebel Bayda silicic tuff ring in Harrat Khaybar. Note the uplifted pāhoehoe slabs in the terminus and their slightly rotated nature; flow behaviour was controlled by local topography rather than the location of the main lava flow axis. The silicic tuff ring rises about 100 m above the surroundings
Photo © *Karoly Németh*

Fig. 2.22 Road through the Columbia River flood basalts in the vicinity of Portland, Oregon, with the majestic pyramid of Mount Hood in the background. Mount Hood (3429 m above sea level), a stratovolcano of the Cascade arc, is about 500,000 years old, and thus much younger than the Miocene Columbia River flood basalts. However, the Cascade arc has existed since ~40 Ma, and several of the huge Columbia River flood basalt flows travelled hundreds of kilometers from their sources located inland to the Pacific Ocean, through a "trans-arc lowland" (e.g., Reidel 2006; Reidel and Hooper 1989; Reidel et al. 2013a)
Photo © *Hetu Sheth*

Fig. 2.23 Akhurian (Arpaçay) River gorge carved in the Pliocene basaltic sequence of the Kars plateau (eastern Turkey), near the ruins of the ancient Armenian city of Ani. The gorge here is ~80 m deep
Photo © *Vladimir A. Lebedev*

Fig. 2.24 Upalluk/Giesecke Monument, south coast of Nuussuaq, West Greenland. This 1580 m high landmark peak consists of subaerial basalt flows of the Maligât Formation. The height of the exposed part shown here is 500 m (photogrammetric interpretation in Pedersen et al. 1993) Photo: *Erik Vest Sørensen, Geological Survey of Denmark and Greenland (GEUS)*

Fig. 2.25 Spectacular lava butte with a cleft summit, near Bhamer, 10 km NNE of Sakri, in the arid central Deccan Traps. The butte, which rises 100 m from the foreground, is made up of small-scale compound pāhoehoe. Low ridge in the foreground is a 3.5–5 m wide and 5.2 km long dyke trending N85°. The dyke continues to the back of the butte. More information: Ray et al. (2007) Photo © *Hetu Sheth*

Fig. 2.26 Monsoon scenery of the Deccan flood basalts in the Western Ghats escarpment, a paradise for trekkers (Kapadia 2003). Here, in the Malshej Ghat area, a remarkable waterfall "goes up" rather than down, bathing the surrounding countryside in a fine spray, because of shearing by forceful winds as this is the very edge of the escarpment here, ~700 m above the Konkan Plain. Mountains in the background rise to >1500 m. Person photographing the scenery is Chandrahas Halai
Photo © *Hetu Sheth*

Fig. 2.27 Monsoon at its peak in the Western Ghats, India, with innumerable streams and cascades everywhere, as here on the road to Matheran tableland. The cliff in Deccan basalt is ~100 m high
Photo © *Eraiyoli Sankaran*

Fig. 2.28 The beautiful Ófærufoss in the Eldgjá chasm (A.D. 934–940), southern Iceland. The lower four-fifths of the cliffs are made up of hyaloclastites formed in subglacial eruptions during the last glacial period. The top one-fifth is fountain-fed lavas of the Eldgjá 934–940 eruption
Photo © *Gillian R. Foulger*

Fig. 2.29 Pleistocene basaltic lava pile cut by the mighty and thunderous Gullfoss waterfall, southern Iceland. The spray of fine water droplets present in the air produces rainbows on sunny days. Tourists on the trail on the left and at the edge of the waterfall provide a scale
Photo © *Hervé Bertrand*

Fig. 2.30 The Iguazu Falls on the border of Brazil and Argentina drop an impressive 82 m over the Paraná Traps basalts; the Niagara Falls on the USA-Canada border are a third shorter
Photo © *Hervé Bertrand*

Fig. 2.31 When the taps run dry: the spectacular Ajanta gorge in the central Deccan Traps, on the walls of which the famous Ajanta Caves are situated. These 26 Buddhist caves, carved in basalt between the second century B.C. and the seventh century A.D., are an Archaeological Survey of India monument and a UNESCO World Heritage Site. A spectacular development of compound flows can be seen here as remarked by Walker (1971); see several photos in this volume. An interesting unanswered question is when and how this horseshoe-shaped gorge of the Waghora River, a huge incised meander, was carved, because the present-day climate of the region is arid, with summer temperatures typically reaching 47 °C. Note already dry riverbed at the beginning of summer in March 2016. Straight-line distance from the bottom left to the bottom right corners of the photo is 500 m; bridge across the river provides a sense of scale
Photo © *Hetu Sheth*

Fig. 2.32 Golden summit of Emeishan, 3099 m above sea level, from where the Emeishan flood basalt of Late Permian age (259 Ma) is named
Photo © *Yigang Xu*

Fig. 2.33 A typical entry point of a large lava tube system in the Harrat Khaybar. Note the whaleback-style, gently sloping surface of the lava field and the few decimeter-thick flow units in the wall of the tube itself. The extreme arid climate and the high altitude (>1500 m above sea level) together strongly affect the lava surface textures, and finer features quickly vanish making the lava field surface fairly smooth in a short time
Photo © *Karoly Németh*

Fig. 2.34 The north-trending Kiger Gorge is a glaciated U-shaped valley near the summit of Steens Mountain, SE Oregon. The eastern wall (left) is juxtaposed against the headwall of the Steens escarpment, thus forming a knife-edge arête from glacial plucking to the east and west. About 500 m of Steens pāhoehoe flow lobes can be observed on both sides of the gorge
Photo © *Victor Camp*

Fig. 2.35 Aerial photo of the flat-topped plateaus formed by the Late Pliocene-Early Pleistocene South Caucasus flood basalts (Sheth et al. 2015), here 300 m thick and dissected by the canyon of the Debed River in the Lori province, northern Armenia. The village of Dsekh is situated on the top of the plateau. The ridge in the background is formed of folded Jurassic to Lower Cretaceous volcanic and volcanosedimentary units of the Lesser Caucasus island arc
Photo © *Andranik Keshishyan*, description: *Khachatur Meliksetian*

Fig. 2.36 The Great Face, SW Staffa, NW Scotland, west of Fingal's Cave, viewed looking towards the NW. The main crag comprises the classic colonnade–entablature doublet of the Palaeogene Fingal's Cave Lava, overlying bedded pyroclastic–volcaniclastic deposits. The lava is approximately 50 m thick (although only ca. 30 m is preserved on The Great Face). The base of the lava is sharp and planar, and dips at a shallow angle towards the east. The cliff is ca. 42 m high. People on cliff top for scale
Photo © *Brian R. Bell*

Fig. 2.37 Palaeogene lavas forming the summit of Ben Meabost (345 m) on the Strathaird Peninsula, Isle of Skye, NW Scotland. The underlying strata are part of the Middle Jurassic Great Estuarine Group. Note houses on the left for scale. In the left background is the gabbro-dominated summit of Bla Bheinn (Blaven, 926 m), the easternmost part of the Cuillin Intrusive Complex, whereas in the right background are the rounded granite summits of the Eastern Red Hills Intrusive Complex: Beinn Dearg Mhor (709 m), Beinn Dearg Bheag (582 m), and Beinn na Caillich (732 m)
Photo © *Brian R. Bell*

Fig. 2.38 An inclined Ferrar Dolerite sheet cross-cutting a concordant 200 m thick dolerite sill intruding Devonian sandstones (light-coloured rocks) at Finger Mountain, south Victoria Land, Antarctica. The concordant sill terminates on the left in a dyke-like body. More information: Elliot and Fleming (2004)
Photo © *David H. Elliot*

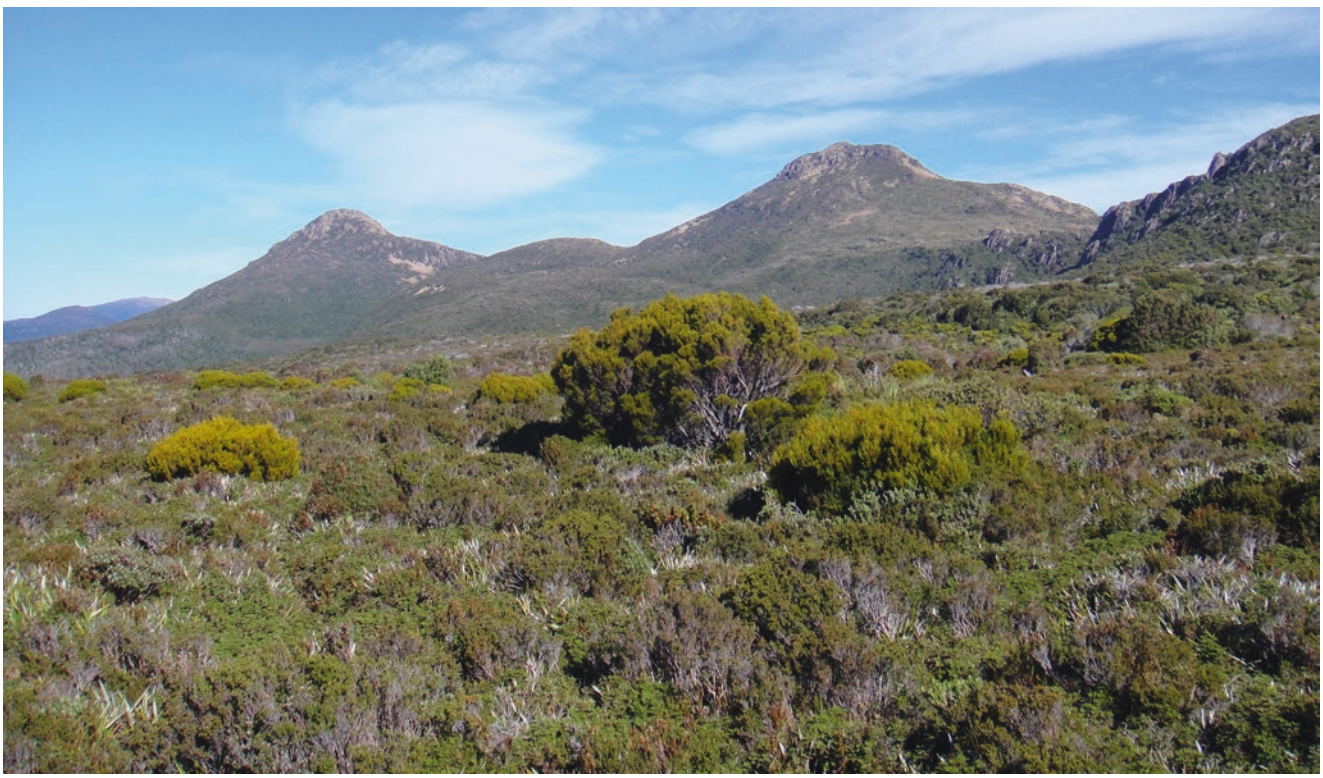

Fig. 2.39 Tasmanian Jurassic dolerite forming peaks in the Hartz Mountains National Park, Tasmanian Wilderness World Heritage Area. Mount Hartz (peak right of centre) is 1254 m high. View is towards the southwest
Photo © *Trevor J. Falloon*

Fig. 2.40 Karoo doleritic sills intruding various levels of Permian-Triassic sedimentary rocks northwest of Maclear, South Africa. The sequence exposed in the foreground is 450 m thick
Photo © *Hervé Bertrand*

Fig. 2.41 Photo to the south from Friis Hills in the McMurdo Dry Valleys, Antarctica. The Basement Sill of the Ferrar large igneous province (LIP) is observed below the Peneplain Sill (each ~250 m thick). Prominent peaks in the background include Beacon Heights and Knobhead Mountain. Geologist is Giulia Airoldi
Photo © *James Muirhead*

Fig. 2.42 Bouldery outcrop of the York Haven diabase sheet (part of the ~200 Ma Central Atlantic Magmatic Province, CAMP), at Little Round Top, Gettysburg National Military Park, Pennsylvania, USA. The sheet is 330–675 m thick (Mangan et al. 1993). Note irregular polygonal jointing in the rock. Geologist is Hetu Sheth
Photo © *Loÿc Vanderkluysen*

Fig. 2.43 Bouldery outcrop of a sill of the Draa Valley/Zemoul sill complexes intruding the Devonian sedimentary cover of the Anti-Atlas (Morocco), Central Atlantic Magmatic Province (CAMP). Photo was taken from the road between the towns of Foum Zguid and Tissinnt near Mrimnna at Oued Zguid. Geologists are Sofie Lindström and Gunver K. Pedersen
Photo © *Nasrrddine Youbi*

Fig. 2.44 Prominent olivine dolerite dyke ridge near Babra in central Saurashtra. Such long, linear ridges with the erosion-resistant dykes along their central axes are the typical expression of dykes here and elsewhere in the Deccan Traps. Outcrops next to person are of weathered compound pāhoehoe host. More information: Ray et al. (2007), Cucciniello et al. (2015)
Photo © *Hetu Sheth*

Fig. 2.45 Landscape near Foum Zguid town, Morocco, with the famous Great Foum Zguid gabbro dyke forming a ridge 40 m high. The dyke is 201 Ma in age, >200 km long and 100–150 m wide, and belongs to the Central Atlantic Magmatic Province (CAMP) (e.g., Youbi et al. 2003)
Photo © *Andrea Marzoli*

Fig. 2.46 The Guli massif in the Maymecha-Kotui alkaline ultramafic province, at the northeastern margin of the Siberian Traps. The Maymecha River cuts through the massif
Photo © *Benjamin Black*

Fig. 2.47 Landscape of the Sodium Group of the Ventersdorp Supergroup between Prieska and Britstown, Northern Cape Province, South Africa. The Sodium Group is ~2739 ± 39 Ma (Altermann and Lenhardt 2012). The Ventersdorp Supergroup is a volcanosedimentary sequence, ca. 4 km thick on average but up to 8 km thick, predominantly composed of subaerial lavas and pyroclastics and sedimentary rocks (mainly lacustrine siliciclastic, but also carbonate). It covers an area of ca. 300,000 km^2 between Johannesburg and Marydale in South Africa and is best exposed in the southern and western Transvaal basin, in the Northern Cape Province and southeastern Botswana. With this extent and thickness, the Ventersdorp Supergroup represents the biggest large igneous province (LIP) on the Kaapvaal craton, with the volcanic rocks ranging from komatiites and basalts to andesites, trachytes and dacites (Altermann and Lenhardt 2012)
Photo © *Nils Lenhardt*

Morphology and Architecture of Flood Basalt Lava Flows and Sequences

3

Fig. 3.1 Pāhoehoe sheet lobes tens of meters thick, Arthur's Seat (1347 m) near Mahabaleshwar, Western Ghats escarpment, Deccan Traps. Vertical cliff exposes four such lobes, crudely columnar-jointed. Groups of tourists at the scenic viewpoints along the top of the cliff provide a scale. Photo was taken in evening light, when the setting sun imparts the west-facing cliffs a golden glow
Photo © *Hetu Sheth*

H. Sheth, *A Photographic Atlas of Flood Basalt Volcanism*, https://doi.org/10.1007/978-3-319-67705-7_3

Chapter Overview

The morphological types of flood basalt lava flows (pāhoehoe, ‘a’ā, etc.) are guides to their emplacement dynamics, with the relationships between flow conditions and lava flow morphology being established through observations of modern basaltic eruptions at places like Hawaii or Réunion Island. This is an excellent example of the application of the fundamental geological axiom, “The present is the key to the past”. Of course, the volumes of even single prehistoric flood basalt eruptions (commonly reaching 500–1000 km^3, e.g., Self et al. 1997) are hundreds or thousands of times larger than any modern basaltic eruptions (~1 km^3), though historical eruptions such as the 1783–1784 Laki eruption in Iceland (15 km^3, Guilbaud et al. 2005) provide an intermediate step through the size spectrum. The older flood basalts that formed vast lava plateaus are now mainly exposed in vertical section. The flow morphology and stacking geometry of their eruptive units, as observed in vertical section, reveal the gradual build-up of the stratigraphy by lava flows sourced from different eruptive vents, and how eruption rates and flow dynamics varied through time.

Flood basalts have been divided into *compound* and *simple* flows (Walker 1971): compound flows are made up of hundreds or thousands of small (meter-size) individual flow-units which erupted one after the other, and simple flows are much larger, single eruptive units, typically columnar-jointed and much wider than the outcrop. Whereas compound and simple are convenient field terms, what appears to be a simple flow at a given outcrop may simply be a large flow-unit, ending against other such units when followed laterally, in what is a compound flow on a larger size scale (Self et al. 1997). Sometimes, pāhoehoe flows have been equated to compound and ‘a’ā flows to simple flows, though these terms are not equivalent: ‘a’ā flows are usually compound, though less commonly so than pāhoehoe (Walker 1971). Flood basalts are dominantly pāhoehoe and rubbly pāhoehoe, and contain few true ‘a’ā flows, partly due to the very low ground slopes ($\ll 1°$) on which these fluid lava flows advance.

There are some other intersting observations to note. Many individual Deccan lava flows, though vastly larger than Hawaiian flows, are compound on the same size scale as Hawaiian flows, and this must indicate a similarly low eruption rate, albeit sustained over greatly longer time periods than for Hawaiian lavas (Sheth et al. 2017a). Several provinces also show systematic transitions from, say, dominantly compound flows in the lower part of the stratigraphy to dominantly simple flows in the upper part; examples are the Deccan and the Central Atlantic Magmatic Province (CAMP) in Morocco (Bondre et al. 2004a, b; El Hachimi et al. 2011). As Bondre et al. (2004a, b) have cautioned, any generalization about lava flow morphologies and emplacement mechanisms across flood basalt provinces, or even for a flood basalt province, should be avoided.

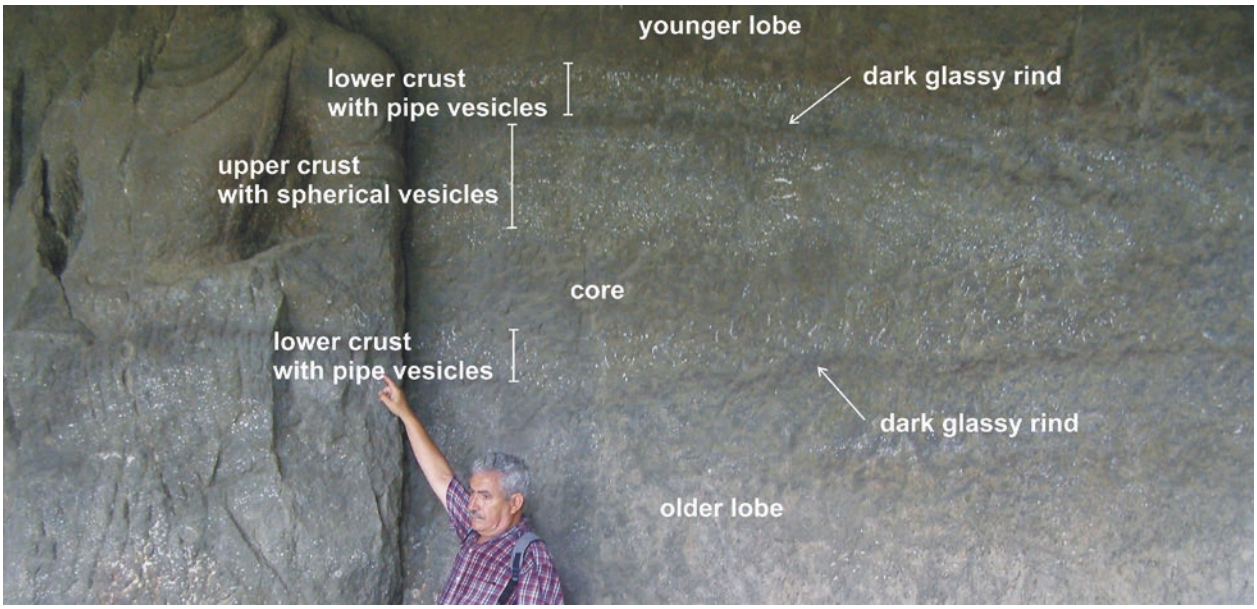

Fig. 3.2 A well-formed pāhoehoe lava lobe, underlain and overlain by other lobes. The lobe shows a thin lower crust with pipe vesicles, a thicker (40 cm) upper crust with spherical vesicles, and a dense and largely aphyric core between these two. Interlobe contacts (dark lines), possibly glassy originally, are emphasized by weathering. The lobe was apparently emplaced in a depression between two older lobes, as indicated by its V-shaped base, and then inflated, resulting in its gently convex top. Geologist is El Hassane Chellai. Cave 3, Elephanta Caves on Elephanta Island, Mumbai harbour, western Deccan Traps. The mid-sixth century Elephanta Caves are a UNESCO World Heritage Site. More information: Sheth et al. (2017a)
Photo © *Hetu Sheth*

Fig. 3.3 Small lobes in a compound pāhoehoe lava flow from the Lower Formation basalts (Central Atlantic Magmatic Province, CAMP) in the Oued Lhar (Herrissane) section, Morocco. Note central vug in one of the lobes. Visible part of the walking stick is 1 m high. Details in El Ghilani et al. (2017)
Photo © *José Madeira*

Fig. 3.4 A small lava lobe among numerous such lobes forming a compound pāhoehoe flow, Paraná CFB province. Note cooling joints in the upper crust of the lobe. The lobe is vesicular-amygdaloidal throughout; also note large horizontally elongated cavities filled by secondary minerals
Photo © *Carla Barreto*

Fig. 3.5 A pāhoehoe toe, somewhat oxidized, in the Deccan basalts of Manmad area, Maharashtra. Both the outer chilled margin and inner vesicular (amygdular) core of this toe are visible in the broken face
Photo: *Bibhas Sen, Geological Survey of India*

Fig. 3.6 Vesicle-rich lava of the Sodium Group of the Ventersdorp Supergroup. The Sodium Group is ~2739 ± 39 Ma (Altermann and Lenhardt 2012). The perfectly spherical vesicles and their great abundance throughout this outcrop suggest a lava type similar to the modern Hawaiian S-type (spongy) pāhoehoe lobes
Photo © *Nils Lenhardt*

Fig. 3.7 Cross section through lava toes of the ~2.98 Ga Nzuse Group basalts within the lower Pongola Supergroup, South Africa (see Wilson and Grant 2006). Note concentric internal structures and brecciated material between toes. Camera lens in the left foreground provides a scale
Photo © *Martin B. Klausen*

Fig. 3.8 Stacking of small P-type and S-type flow-units in a compound pāhoehoe flow of the Paraná CFB province, Brazil. The P-type ("pipe vesicle-bearing") units have pipe vesicles at the base and vesicle-free cores, whereas the S-type (spongy) units lack pipe vesicles but contain spherical vesicles throughout their volume (Wilmoth and Walker 1993). More information: Barreto et al. (2014, 2017)
Photo © *Carla Barreto*

Fig. 3.9 Juxtaposition of P-type and S-type flow-units in a compound pāhoehoe flow of the Bhimashankar Formation, western Deccan Traps, at Shivneri Fort, ~1000 m above sea level. This is a view of a vertical rock face; pen (15 cm long) separates two adjacent P-type units (with pipe vesicles at their bases and a vesicle-free core above) from an underlying S-type unit (with spherical vesicles throughout its thickness and vesicle sizes increasing from the upper crust into the core)
Photo © *Ishita Pal*

Fig. 3.10 Roadcut exposure in compound flow, showing several small (Hawaiian-size) pāhoehoe lobes, highly weathered and amygdaloidal throughout. A set of pipe vesicles pitching to the right is seen in one of the lobes, occupying the left of the photo at middle height. Pen positioned against that lobe is 15 cm long. This exposure is now destroyed by urban development. Chandni Chowk, Pune, western Deccan Traps
Photo © *Nasrrddine Youbi*

Fig. 3.11 Detail of small lava lobes in a carved vertical rock face. Cave 1, Ajanta Caves (a UNESCO World Heritage Site), central Deccan Traps. Note lateral contacts between lobes, pipe vesicles at the base of all lobes, and spherical vesicles near their tops. The prominent elongated lobe appears to feed small breakout toes, on the right and particularly on the left just above the hand, which also provides a scale. More information: Walker (1971), Bondre et al. (2004a, b), Sheth (2006)
Photo © *Hetu Sheth*

Fig. 3.12 "Finger" of younger pāhoehoe lava filling an existing inflation cleft in an older, highly vesicular lobe. A similar cleft-fill appears to exist in the lower right of the photo, separated from the first by two small lava toes. Glassy margins of these lobes and toes are now represented by highly weathered yellowish brown material. Vertical rock face, Cave 11, Ellora Caves. Pen is 15 cm long
Photo © *Hetu Sheth*

Fig. 3.13 Vertical carved face exposing small, highly vesicular pāhoehoe toes in basalts of the Deccan Traps. Kailasa Temple (mid-eighth century), Cave 16, Ellora Caves, Maharashtra, India. Note how the lobes neatly fill pre-existing microtopography. Pebbly patches are just concrete fillings for maintenance. Geologist is Stephen Self
Photo © *Loÿc Vanderkluysen*

Fig. 3.14 Superimposed and juxtaposed compound pāhoehoe flow lobes above the entrance of Cave 16 (mid-eighth century), Ellora Caves, central Deccan Traps. Each lobe shows pipe vesicles at the base and vesicle banding in the upper crust. Tourist standing above, in top right corner of photo, provides a scale
Photo © *Erika Rader*

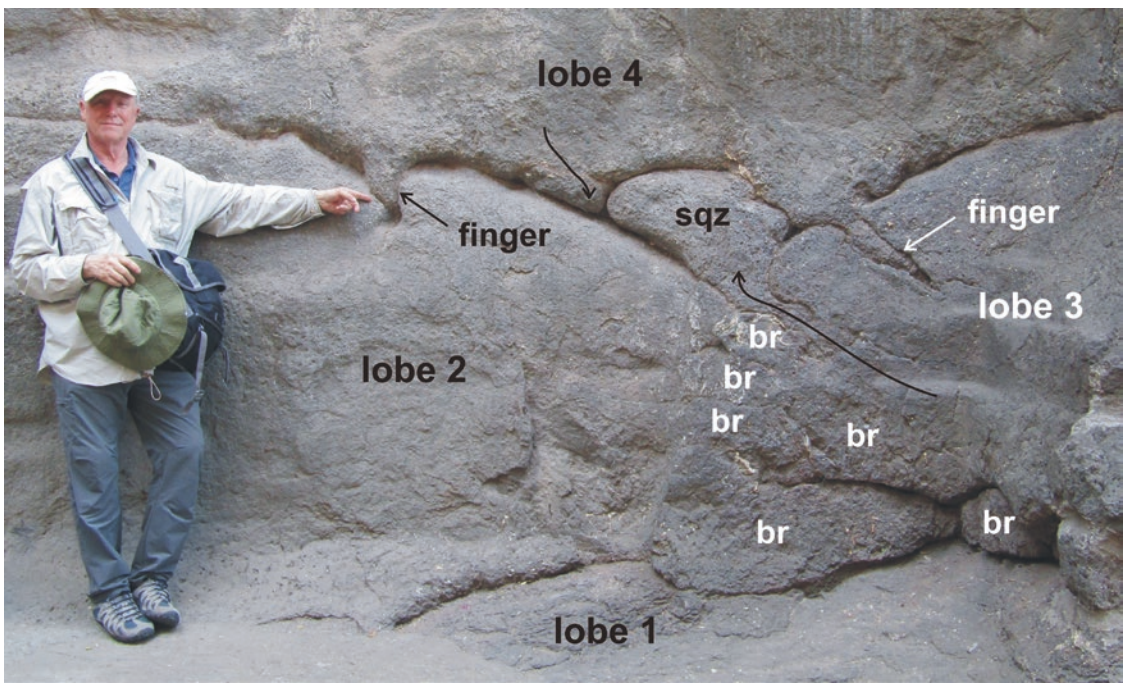

Fig. 3.15 Striking combination of lava lobes and toes, a squeeze-up, and lava "fingers" infilling existing inflation clefts. A large lobe (lobe 1) is exposed at ground level, overlain by two large, convex-upward lobes on the left and right (lobes 2 and 3). Small lobes and toes present at their junction are breakouts (br). Lobes 2 and 3 both have inflation clefts, and through one of them a lava squeeze-up (dome-top feature labelled sqz) has been extruded (long arrow). A fourth, large lobe has spread itself over lobes 2 and 3 and the squeeze-up, perfectly moulding itself to the microtopography (e.g., small arrow), and has sent two pointed fingers of lava into the lobes 2 and 3. In three dimensions, the "fingers" are likely "wedges". Kailasa Temple, Ellora Cave 16, central Deccan Traps. Geologist is Stephen Self
Photo © *Hetu Sheth*

Fig. 3.16 A stack of basaltic lava lobes in the ~9000 year B.P. Thingvallahraun lava flow field exposed at Almannagjá, Þingvellir, Iceland. The section is 20 m high
Photo © *Hervé Bertrand*

Fig. 3.17 Roadcut exposure (10 m high) in the "Barrage" (Dam) section in the Middle Atlas, Morocco, showing overlapping lobes of a compound pāhoehoe flow of the Intermediate Formation, CAMP
Photo © *Hervé Bertrand*

Fig. 3.18 Packing of compound pāhoehoe lobes of various sizes exposed in a carved wall, Ajanta Caves, central Deccan Traps. Note vesicle banding in the lowermost, thick lobe, the flat and long middle lobe, and the sharp but cuspate contacts of that lobe with the other lobes. Note also the small toe exactly at photo centre. The tourist provides a scale
Photo © *Hetu Sheth*

Fig. 3.19 A pāhoehoe flow lobe (up to 6 m thick) fills the topography formed by underlying compound pāhoehoe flow (with flow lobes <2 m thick). Paraná CFB province, Brazil. Geologist is Carla Joana Santos Barreto. More information: Barreto et al. (2014, 2017)
Photo © *Carla Barreto*

Fig. 3.20 Ropy surface of a pāhoehoe lava flow, Sprengisandur, Iceland
Photo © *Hervé Bertrand*

Fig. 3.21 Lava ropes in the proximal pāhoehoe lava flow field of the A.D. 1256 Al Madinah eruption site near Al Madinah city, Harrat Rahat, western Saudi Arabia
Photo © *Karoly Németh*

Fig. 3.22 Small pāhoehoe lava lobes, toes, and breakouts with ropy surfaces indicating local flow directions. Stream bed near Bhorande village, 200 m elevation, Malshej Ghat section, Western Ghats, Deccan Traps. The outcrops belong to the Thakurvadi Formation
Photo © *Hetu Sheth*

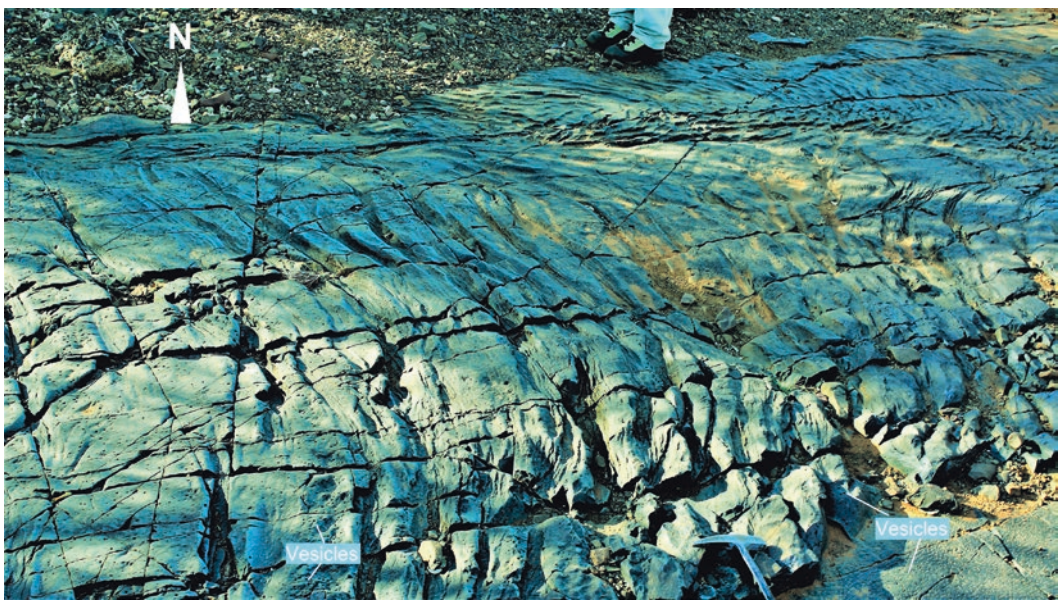

Fig. 3.23 Pāhoehoe flow lobe, showing smooth, ropy surface, from the Ongeluk LIP, formally known as the Ongeluk Formation, in the Griqualand West sub-basin (Transvaal Supergroup, South Africa). The Ongeluk LIP is Palaeoproterozoic (2426 Ma) in age (Gumsley et al. 2017). The lava flow contains well-rounded vesicles (>2% vol, ~4 mm radius) throughout, with higher concentration in the core of the flow. The outcrop (S29°17′32.94″ E022°46′33.06″) was discovered by Mr. Petrus Noeth on his farm
Photo © *Samson Masango*

Fig. 3.24 Ropy lava exposed in a small roadcut exposure, Malshej Ghat, Western Ghats escarpment, Deccan Traps. This is a vertical face
Photo © *Danielle K. Moyer*

Fig. 3.25 Lava ropes on the ceiling of Cave 4, Ajanta Caves, central Deccan Traps. Field of view is ~10 m wide. Because ropes can only form on the upper surfaces of pāhoehoe flows, this ceiling exposure implies a cast, i.e., an overlying flow of fluid pāhoehoe lava filled the surface microtopography of ropes of a lower flow; the lower flow has been removed in carving the cave
Photo © *Erika Rader*

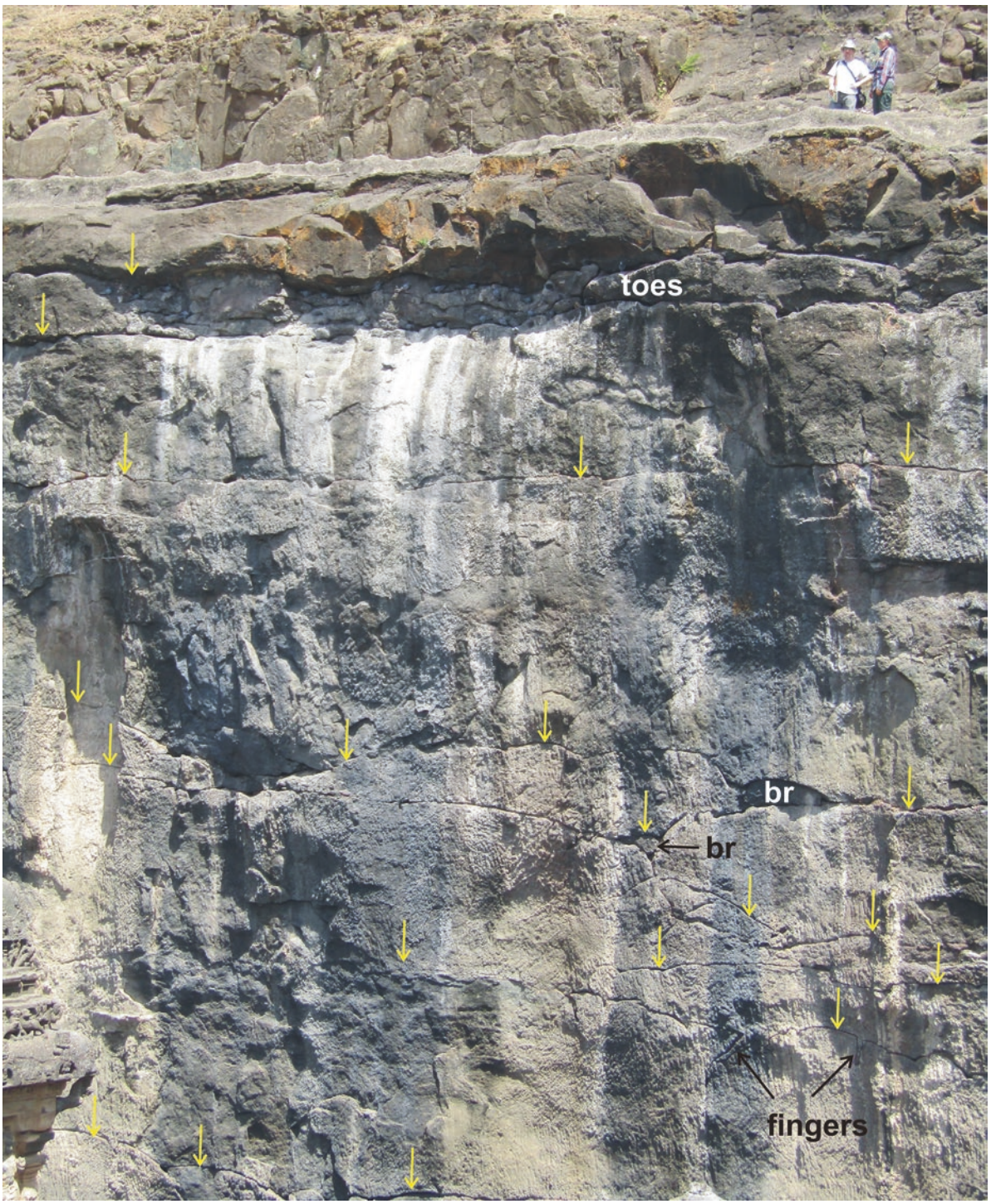

Fig. 3.26 The architecture of meter-size pāhoehoe lobes in lateral juxtaposition and stacked on top of each other, as beautifully seen in the cliff section behind the Kailasa Temple, Cave 16, Ellora Caves, central Deccan Traps. Many internal contacts in this sequence are noticeable (yellow arrows); note the lateral pinching and wedge shape of several lobes. Some of the lobes have also produced smaller breakouts (br) at their termini, and in the lower left, fingers of overlying lava occur in inflation clefts in the underlying lobe. Interestingly, just under the "ledge" at the top of this cliff (and therefore in shadow) are a number of decimeter-size, closely packed, lava toes. Geologists Loÿc Vanderkluysen and Erika Rader at the top of the cliff provide a scale. Behind and above them are additional thicker lobes. The UNESCO World Heritage Sites of the Ellora and Ajanta Caves in the central Deccan Traps, and the Elephanta Caves near Mumbai (Sheth et al. 2017a), are important not only for their tremendous historical and artistic value (1000–2000 years old religious sculptures and paintings in Deccan basalt). They are also to be viewed as great ancient engineering feats (C. Halai, pers. comm. 2013), and also provide invaluable insights into the architecture and emplacement of compound pāhoehoe lava flows with lobes meters to tens of meters in size (Walker 1971; Keszthelyi et al. 1999; Sheth 2006)
Photo © *Hetu Sheth*

Fig. 3.27 Columnar-jointed pāhoehoe sheet lobes juxtaposed against and stacked above each other, as seen in a road section near Alaverdi, northern Armenia, South Caucasus flood basalt province (Sheth et al. 2015). Cliff is ~50 m in height. Note the lenticular shape of several of the lobes, with their contacts often marked by vegetation. These flows are compound on a larger scale than typical Hawaiian-size compound flows
Photo © *Arsen Israyelyan*

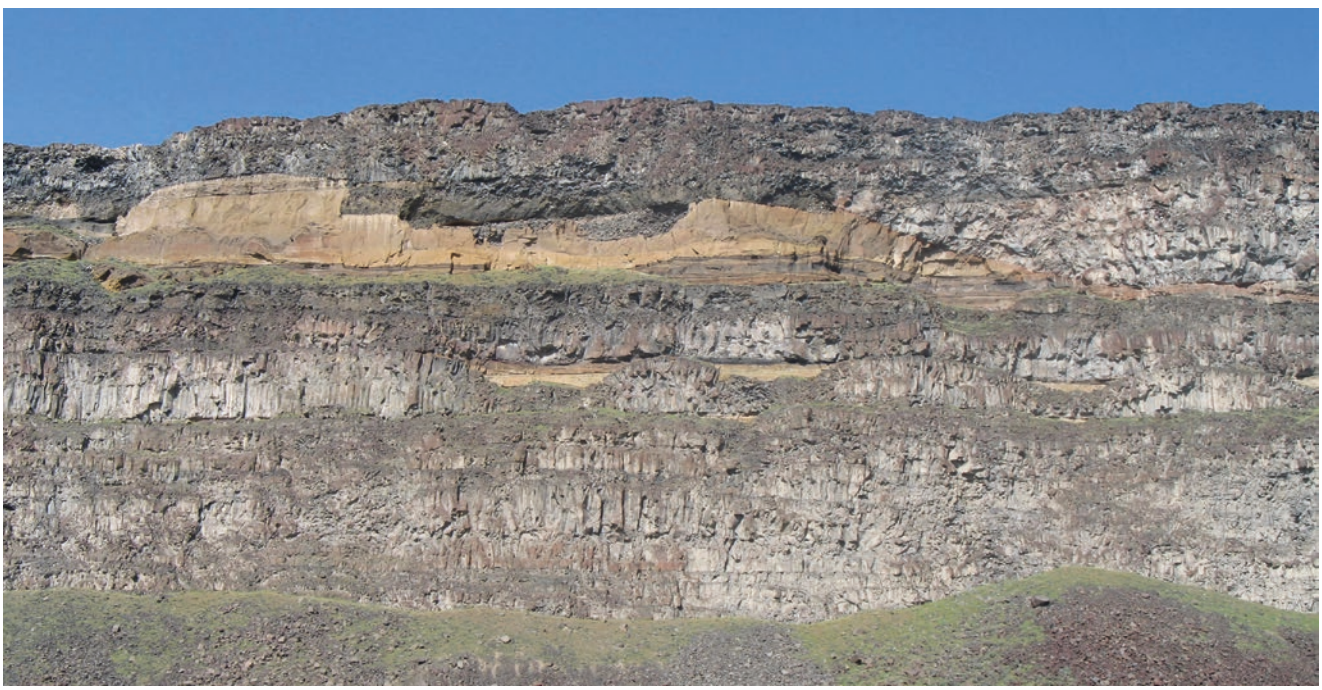

Fig. 3.28 Typical section (~40 m high) of multiple stacked pāhoehoe lava lobes (a few meters thick and columnar-jointed) in the Snake River Plain, USA. Pyroclastic deposits (brown) within the lava sequence indicate explosive eruptions in between effusive ones. Note the distinctly convex-upward tops of some of the pāhoehoe lobes which appear to be tumuli. Three of them can be perceived adjacent to each other, at middle height. Note also how the thin pyroclastic deposits, exactly at the photo's centre, occupy the low areas between the adjacent flow lobes and the tumuli
Photo © *Karoly Németh*

Fig. 3.29 Cliff section ~12 m in height, beautifully exposing 2–4 m thick, columnar-jointed pāhoehoe sheet lobes with a wedge shape that are stacked on top of one another. Grande River channel, northern part of the Paraná CFB province, Brazil. Location is near the city of Iturama, in the Minas Gerais province. More information: Pacheco et al. (2017)
Photo © *Lucia C. Moraes*

Fig. 3.30 Cliff section beautifully exposing the stacking of columnar-jointed pāhoehoe sheet lobes which are a few meters thick and with a wedge-shaped geometry. Grande River channel, northern part of the Paraná CFB province. Location is near the city of Iturama, in the Minas Gerais province, Brazil. Geologist is Lucia C. Moraes. More information: Pacheco et al. (2017)
Photo © *Hildor J. Seer*

Fig. 3.31 Section in a roadcut, showing four flows of Deccan basalt, Chandni Chowk, Pune, western India. The lower flow is a compound flow with small (Hawaiian-size) lava lobes, and the overlying three are crudely columnar-jointed pāhoehoe sheet lobes. The lower three flows belong to the Bushe Formation and the uppermost flow to the Poladpur Formation of the Western Ghats stratigraphy. Geologists provide a scale. The section has subsequently been destroyed owing to urban development
Photo © *Nasrrddine Youbi*

Fig. 3.32 Three pāhoehoe sheet lobes at the top of the Moti Gop section, Saurashtra, northwestern Deccan Traps. Each lobe is several meters thick, has a tabular shape and low aspect ratio (thickness/length), and shows crude columnar jointing. A large number of closely spaced vesicle cylinders occur in the middle lobe, directly above geologist Tarulata Das (see also Fig. 4.20)
Photo © *Vivek Ghule*

Fig. 3.33 Pāhoehoe sheet lobe with an entablature containing many randomly oriented, small-scale columnar sets (some horizontal), underlain by a tier of distinctly platy, centimeter-scale horizontal jointing, underlain by a brown bole (base of the photo, behind talus pile). The bole was not disturbed by the flow of lava above. Location 3 km southwest of Talaja on the road to Mahuva, in Saurashtra, northwestern Deccan Traps. Geologist is Tarulata Das; see also Fig. 5.45, 12.14
Photo © *Vivek Ghule*

Fig. 3.34 Thick pāhoehoe sheet flow with three tiers, near Odzun, northern Armenia. The flow has an upper colonnade (left edge of photo), a laterally discontinuous entablature with hackly jointing below it, and a well-developed lower colonnade with columns ~1 m wide below the entablature and above the geologists Hetu Sheth and Arsen Israyelyan. Above this flow is a stack of slabby pāhoehoe and rubbly pāhoehoe flows. More information: Sheth et al. (2015)
Photo © *Hripsime Gevorgyan*

Fig. 3.35 Panorama of the lava successions of the Snake River canyon, USA, situated far from hydromagmatic volcanoes, and exposing multiple thin pāhoehoe lava lobes stacked above each other. The individual lobes are typically a few meters thick and columnar-jointed. Cliff is ~200 m high
Photo © *Karoly Németh*

Fig. 3.36 230 m high cliff of Late Pliocene to Early Pleistocene plateau basalts in the canyon of the Debed river ~3 km ENE of Alaverdi (Lori province, northern Armenia). The cliff exposes a sequence of columnar-tiered pāhoehoe sheet flows with well-developed colonnade and entablature tiers, capped by a stack of slabby pāhoehoe and rubbly pāhoehoe flows. The boundaries between the flows are not quite flat; note the columnar flow exactly at the photo centre which is thick in the middle and thins towards the left and right, and fills a low area in the top of the immediately older flow. Geologists are Iain Neill and Gevorg Navasardyan. More information: Sheth et al. (2015)
Photo © *Khachatur Meliksetian*

Fig. 3.37 Large sheet lobes of the Columbia River Basalt Group at Banks Lake, Washington. Individual sheet lobes are traceable for kilometers and terminate against other sheet lobes, implying that a flow which appears "simple" in a single outcrop may also be "compound", only on a very large (kilometer) scale. The cliffs are 200 m in height. More information: Self et al. (1997). Note also the funnel-shaped structure two thirds of the way from the left. The significance of this and associated "basaltic ring structures", formed by lava flows inflating around phreatovolcanic cones, is described in Keszthelyi and Jaeger (2015)
Photo: *Laszlo Kestay (Keszthelyi), US Geological Survey*

Fig. 3.38 Columnar-jointed pāhoehoe sheet lobes of the Columbia River Basalt Group at Steamboat Rock State Park, Washington. The cliffs are 200 m high
Photo: *Laszlo Kestay (Keszthelyi), US Geological Survey*

Fig. 3.39 The flat, tabular geometry of pāhoehoe sheet lobes is beautifully seen in the two photos on this page though the top of the upper flow is an eroded surface. This exposure near Ambajogai in the southeastern Deccan Traps shows a columnar-jointed sheet lobe which is kilometers long, and is underlain by flow-top breccia of the preceding flow. Plant moulds are present in the highly weathered rock and palaeosol at the contact. Geologist is Loÿc Vanderkluysen
Photo © *Erika Rader*

Fig. 3.40 The flat, tabular geometry of pāhoehoe sheet lobes as seen near Ambajogai in the southeastern Deccan Traps. The columnar-jointed sheet lobe is kilometers long, and is underlain by flow-top breccia of the preceding flow. Plant moulds are present in the highly weathered rock and palaeosol at the contact (see Fig. 6.40). Geologist is Loÿc Vanderkluysen
Photo © *Erika Rader*

Fig. 3.41 Pāhoehoe sheet lobes tens of meters thick, Arthur's Seat (1347 m) near Mahabaleshwar, Western Ghats escarpment, Deccan Traps. The main parting in the middle of the photo is the base of a 60–70 m thick sheet lobe. The horizon with overhangs is the core-upper crust boundary of this sheet lobe; note crude columnar jointing in the core. Below and above this thick lobe, thinner (~20 m thick) sheet lobes occur, each with an upper crustal zone marked by a vegetated slope above and a cliff-forming core below
Photo © *Stephen Self*

Fig. 3.42 A view of the Western Ghats Escarpment in the Deccan basalts at Mahabaleshwar, Maharashtra, western India. The escarpment is >1.3 km high and exposes several tens of lava flows, mostly extensive and thick sheet lobes. The part in the photo is ~500 m high
Photo: *Bibhas Sen, Geological Survey of India*

Fig. 3.43 The 60 m high Palouse Falls, Washington, cuts through a number of flows of the Columbia River Basalt
Photo © *Anthony R. Philpotts*

Fig. 3.44 Columnar-jointed basaltic lavas of the Palaeogene Staffa Lava Formation, above Malcolm's Point, Ross of Mull, on the Isle of Mull, NW Scotland. Height of section is ca. 300 m
Photo © *Brian R. Bell*

Fig. 3.45 Multiple compound pāhoehoe flows unconformably overlying undulating ash-flow tuff topography, Owyhee River canyon, SE Oregon, USA. Basalt pack ~100 m thick in the centre of the photo. See Shoemaker and Hart (2002) for more information
Photo © *William K. Hart*

Fig. 3.46 Thin flow lobes of Steens Basalt form the 200 m cliff face at Abert Rim, about 55 km north of Lakeview, Oregon. The gentler slope beneath Steens Basalt contains a 300 m thick section of basaltic to basaltic trachyandesite flows of Late Oligocene age
Photo © *Victor Camp*

Fig. 3.47 Stacking of basalt lava flows along the coastal road in east Iceland. Note dykes cutting the basalt stack. The cliffs are ~100 m high Photo © *Dominique Weis*

Fig. 3.48 Landscape of The Storr, on the Trotternish peninsula of the Isle of Skye, NW Scotland, part of the British Palaeogene igneous province. The cliff exposes several columnar-jointed sheet lobes, as well as dykes (left) standing out because of greater resistance to erosion. Grazing cows (black) and sheep (white) provide a scale Photo © *Hetu Sheth*

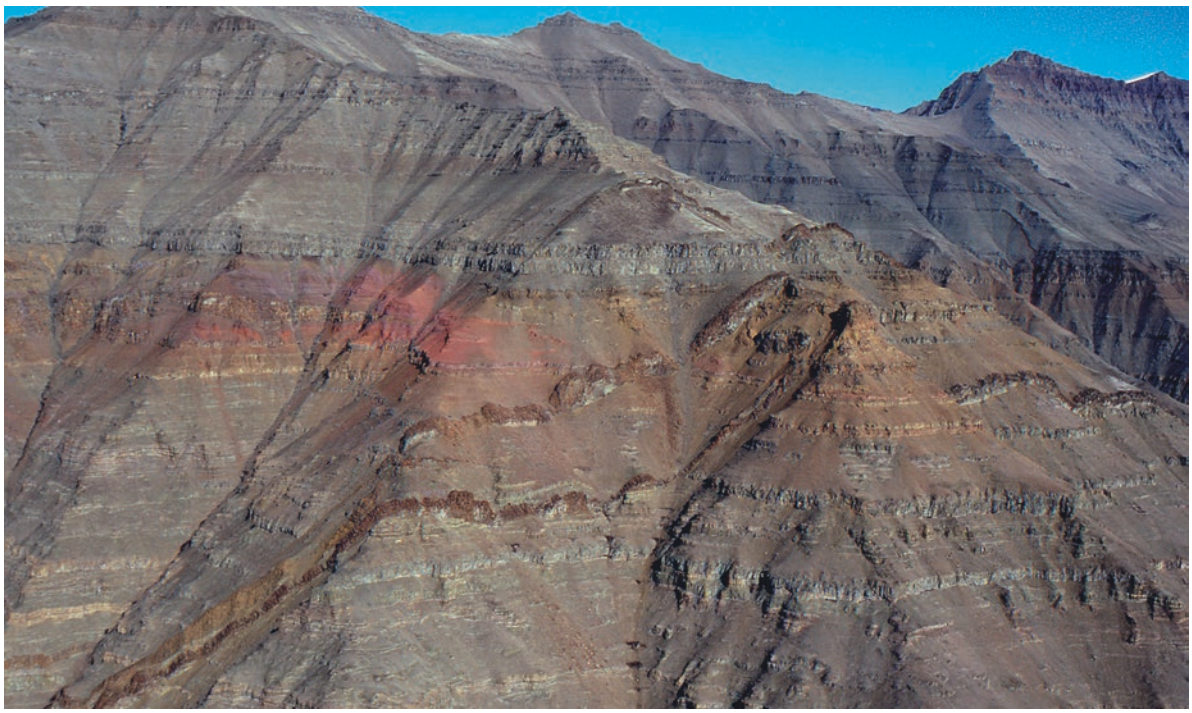

Fig. 3.49 Typical picrite landscape of grey crumbling subaerial lava flows. Most flows are only a few meters thick but others are massive and up to 10 m thick. The brown lava series in the middle of this picture comprises the crustally contaminated lava flows of the Kûgánguaq Member with a brick-red oxidised tuff crater in the centre (Pedersen 1985). The whole succession is cut by late brown basalt dykes. Vaigat Formation, northern Disko, West Greenland
Photo: *Asger Ken Pedersen, Geological Survey of Denmark and Greenland (GEUS)*

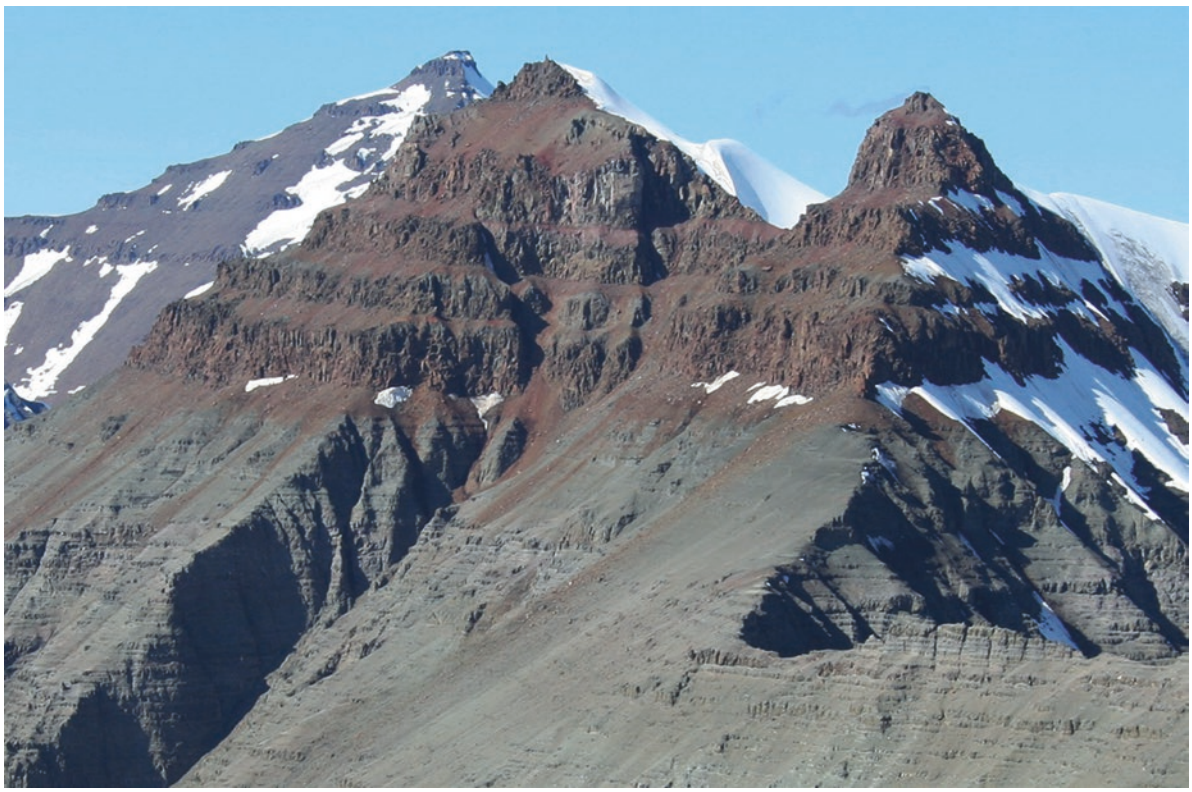

Fig. 3.50 The two major Palaeocene volcanic formations on Disko and Nuussuaq, West Greenland: Thin grey, crumbling picrite flows of the Vaigat Formation are near-conformably overlain by 15–30 m thick brown basalt flows of the Maligât Formation (Larsen and Pedersen 2009). Southern Nuussuaq
Photo: *Asger Ken Pedersen, Geological Survey of Denmark and Greenland (GEUS)*

Fig. 3.51 Late Triassic (201 Ma) basaltic volcanic pile (350 m thick) of the Central Atlantic Magmatic Province (CAMP), Tiourjdal, southern High Atlas, Morocco. About 80% of the section is composed of basalt, which is capped by 50 m of Jurassic limestones above red clays and siltstones with a thin basalt flow in between. The Tiourjdal section is one of the most complete CAMP sections of the High Atlas that comprises four lava flow fields or formations, namely the Lower, Intermediate, Upper and Recurrent Formations. More information: Bertrand et al. (1982), Bertrand (1991) and Marzoli et al. (2004)
Photo © *Hervé Bertrand*

Fig. 3.52 Lower lava flows of the CAMP volcanic pile of the Aït Ourir section, Morocco. The section, though only 170 m thick, is one of the most complete sections of the High Atlas that comprises four lava flow fields or Formations, namely the Lower, Intermediate, Upper and Recurrent Formations
Photo © *Nasrrddine Youbi*

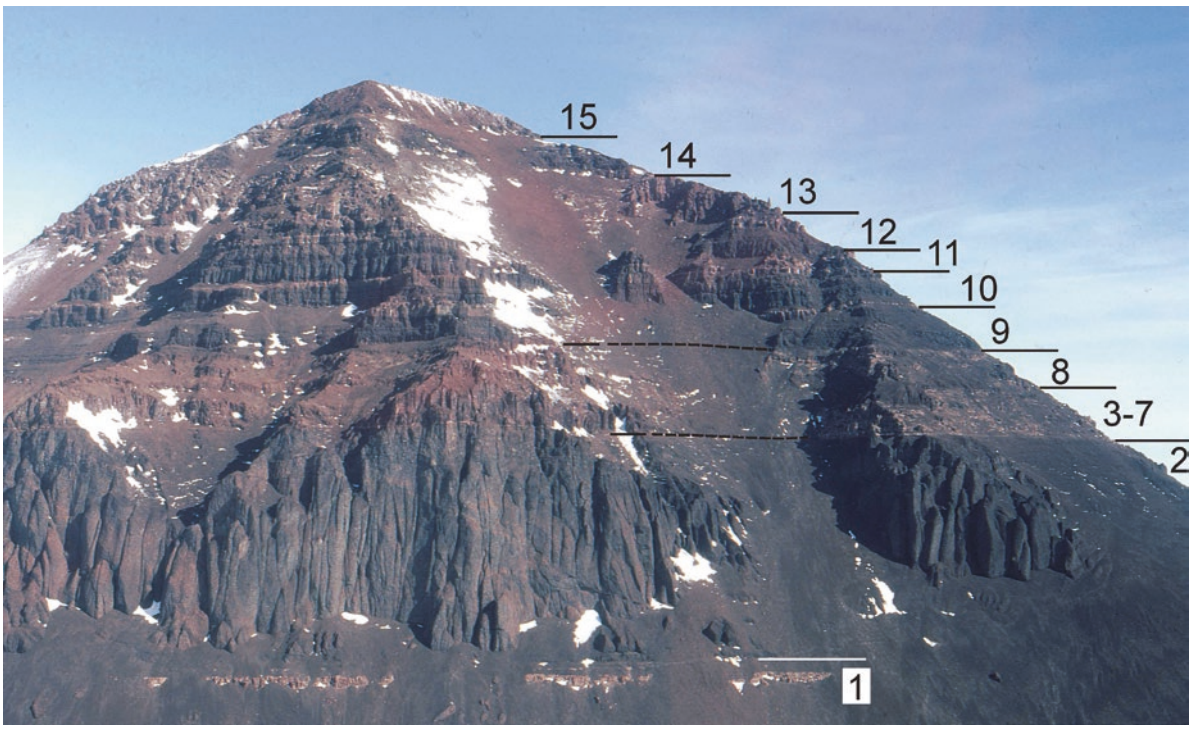

Fig. 3.53 Fifteen Kirkpatrick Basalt flows with a cumulative thickness of 480 m are exposed at Storm Peak, central Transantarctic Mountains. Note the 135 m thick flow (#2). In the centre and on the left, a single flow above flow #2 is represented on the right hand ridge by multiple flows. More information: Elliot and Fleming (2008)
Photo © *David H. Elliot*

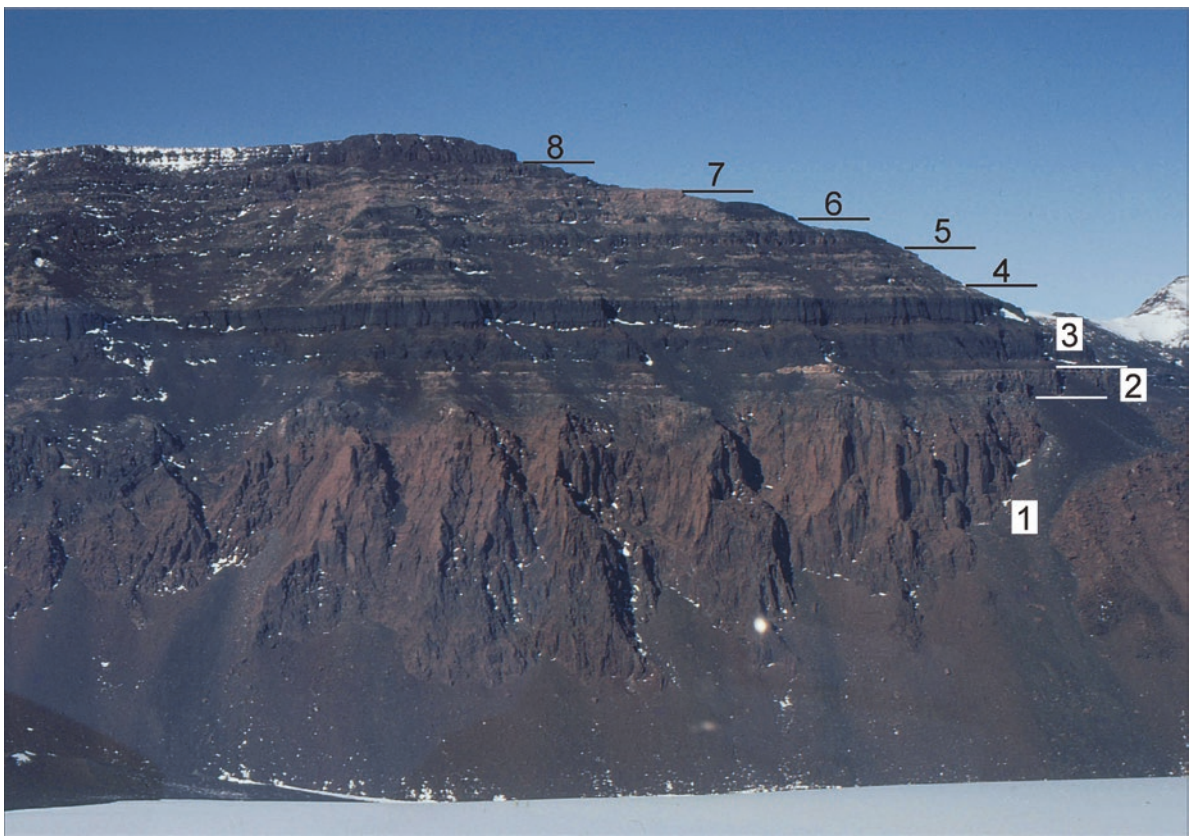

Fig. 3.54 Kirkpatrick Basalt flows with a cumulative thickness of 397 m are exposed at Mt. Bumstead, central Transantarctic Mountains. The basal flow is 175 m thick and is almost certainly ponded. The unit designated "7" consists of multiple thin flows. More information: Elliot and Fleming (2008)
Photo © *David H. Elliot*

Fig. 3.55 Basaltic lava pile in Mt. Skessa in Reyðarfjörður, eastern Iceland. The gently-dipping basalts are ~500 m thick
Photo © *Dominique Weis*

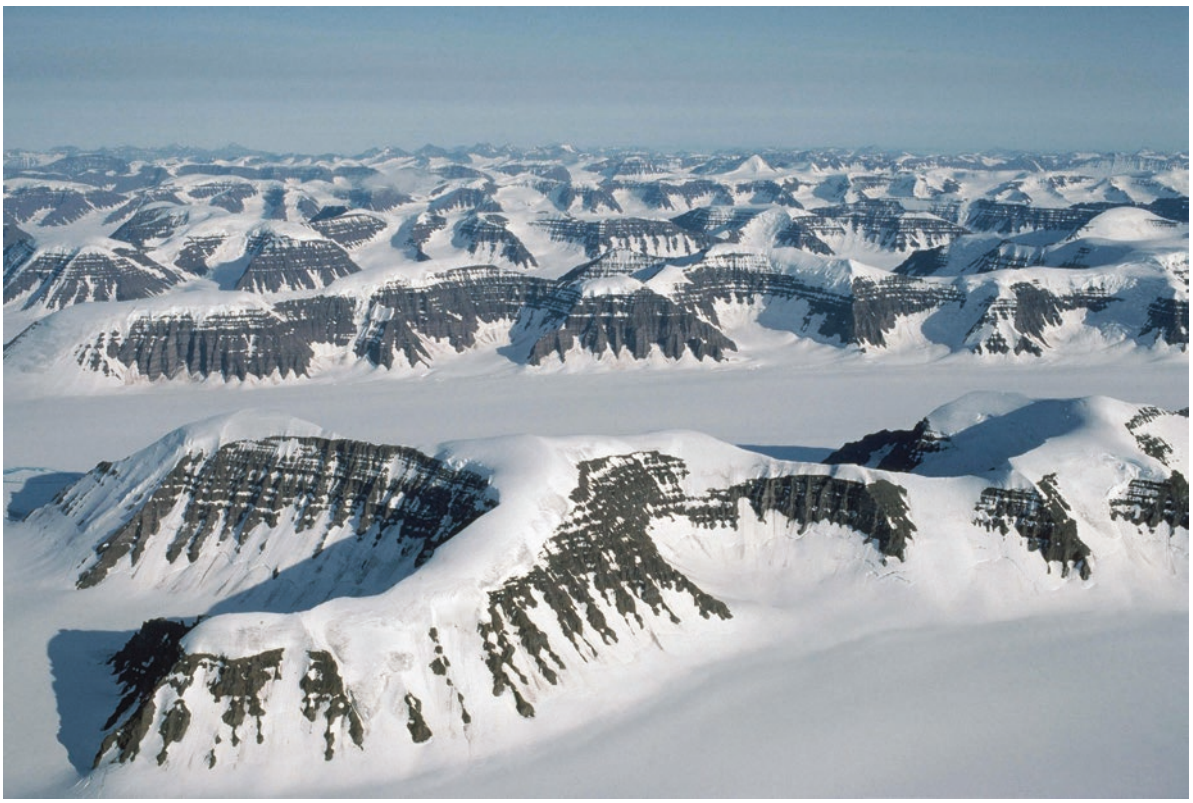

Fig. 3.56 Flat-lying basalt lava flows, mainly of the Skrænterne Formation of the Blosseville Group. Inland from the central Blosseville Kyst, East Greenland. The mountains rise several hundred meters above the valley glacier
Photo: *Asger Ken Pedersen, Geological Survey of Denmark and Greenland (GEUS)*

Fig. 3.57 A view of the Drakensberg Escarpment at Sani Pass between South Africa and Lesotho. Mountain on the left (~1450 m above sea level) is composed of the Karoo flood basalts in its upper part, which overlie Karoo sedimentary rocks. The rocks in the right foreground are Clarens Formation sandstones
Photo © *Saumitra Misra & Alan Smith*

Fig. 3.58 Photo from near the 2900 m high summit of Steens Mountain, SE Oregon, looking southwest into the Alvord Desert below. Steens Mountain is a fault-scarp mountain range with numerous, thin pāhoehoe flow lobes cut by NE-trending feeder dykes exposed in the glaciated walls of the escarpment. This is the major source of volcanism for Steens Basalt (the oldest stratigraphic unit of the Columbia River Group), and may represent an ancient shield volcano whose interior is now well exposed by Late Miocene to recent faulting. More information: Camp et al. (2013)
Photo © *Victor Camp*

Fig. 3.59 A stacked succession of Grande Ronde Basalt sheet flows of the Columbia River Basalt Group is exposed here in the incised meanders of the Grande Ronde River canyon near the small village of Troy in northeastern Oregon. The total thickness of Grande Ronde Basalt here is about 500 m but increases to about 800 m at the Grande Ronde type section located 40 km downstream, beyond the far ridge seen in the photo background. The gentle upper slopes above the canyon walls in the foreground are underlain by poorly exposed flows of Wanapum and Saddle Mountains Basalt. Geologist Simone Cogliati, and the road below beside the river, provide a sense of scale
Photo © *Victor Camp*

Fig. 3.60 Type section of the Grande Ronde Basalt, Columbia River Basalt Group. Location: Grande Ronde River, Washington. Approximately 1000 m of Grande Ronde Basalt are exposed. The Grande Ronde Basalt has four magnetic polarity reversals, and this section contains the first three
Photo © *Stephen P. Reidel*

Fig. 3.61 The Late Permian Emeishan flood basalt of southwestern China: A >1000 m thick sequence along the Jinshajiang River, a part of the Yangtze River. More information: Xu et al. (2001)
Photo © *Yigang Xu*

Fig. 3.62 Intracanyon basalt along the crest of Weissenfels Ridge, looking north down the Snake River about 7 km south of Asotin, Washington. Here, hackly jointed basalt of the Pomona Member (Saddle Mountains Basalt) is exposed as rounded topography at the top of the west (left) canyon wall where it fills an 11 million-year-old canyon of the ancestral Snake River. The western cliff face is 300 m high; road below provides a scale
Photo © *Victor Camp*

Fig. 3.63 The Hnevank monastery (seventh to twelfth centuries A.D.) near Kurtan village, Lori province, northern Armenia. An ~150 m thick stack of Late Pliocene-Early Pleistocene flood basalt lavas forms the cliff behind the monastery and the "wall" on the right. The flood basalts erupted and flowed in canyons within older basement rocks, which form the high mountain ranges (with cloud shadows) seen in the upper background. The basalt stack here is itself dissected by the modern gorge of the Dzoraget River. More information: Sheth et al. (2015)
Photo © *Andranik Keshishyan*, description: *Khachatur Meliksetian*

Fig. 3.64 An excellent example of intracanyon flood basalts is the Late Pliocene to Early Pleistocene South Caucasus flood basalt province (Sheth et al. 2015), found in parts of Armenia, Georgia and Turkey. This photo, taken near Alaverdi town in northern Armenia, beautifully shows flat-topped plateaus produced by the basalts that flowed within pre-existing canyons in basement rocks (Jurassic-Cretaceous island arc rocks) that rise to much greater heights. These intracanyon flows which erupted in quick succession formed stacks of lavas >200 m thick, without significant erosional breaks or sedimentary interbeds. This is how the famous Columbia River flood basalt province of northwestern USA would have looked at an early stage, after the intracanyon Imnaha flood basalts were erupted (S. Reidel, pers. comm., 2014; Sheth et al. 2015). The Armenian basalt stacks and plateaus are now being cut through by modern rivers such as the Debed and the Dzoraget
Photo © *Hripsime Gevorgyan*

Fig. 3.65 Pliocene basaltic sequences of Akhalkalaki plateau near Khertvisi fortress, Lesser Caucasus, Republic of Georgia (Lebedev et al. 2008)
Photo © *Vladimir A. Lebedev*

Fig. 3.66 Smaller-scale flood basalts: The Anahef-Taharaq basaltic plateau in the Hoggar, Tuareg Shield, Algeria. These fissure-fed basalts are Upper Eocene to Oligocene (35–24 Ma) in age with a current surface area of 400 km² and volume of 200 km^3, but they have a thickness of 700 m and an estimated volume before erosion of 1000 km^3. The basalts are intruded by a dozen subvolcanic ring complexes (Liégeois et al. 2005; Rougier et al. 2013, and references therein)
Photo © *Jean-Paul Liégeois*

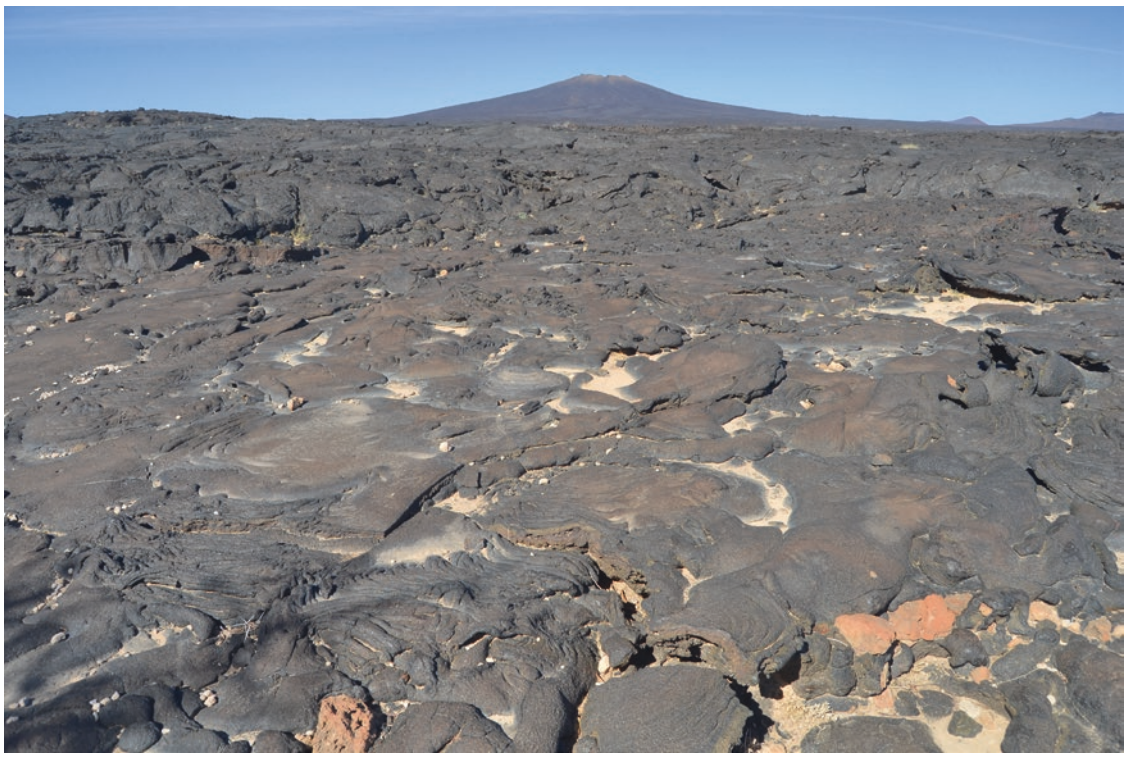

Fig. 3.67 Typical pāhoehoe surface of the lava flow suspected to be about 1000 years old and emitted from Jebel Qidr (background) in Harrat Khaybar in Saudi Arabia. The foreground is about 5 m wide. Jebel Qidr rises 322 m above a plateau 1700 m above sea level. More information: Moufti and Németh (2016)
Photo © *Karoly Németh*

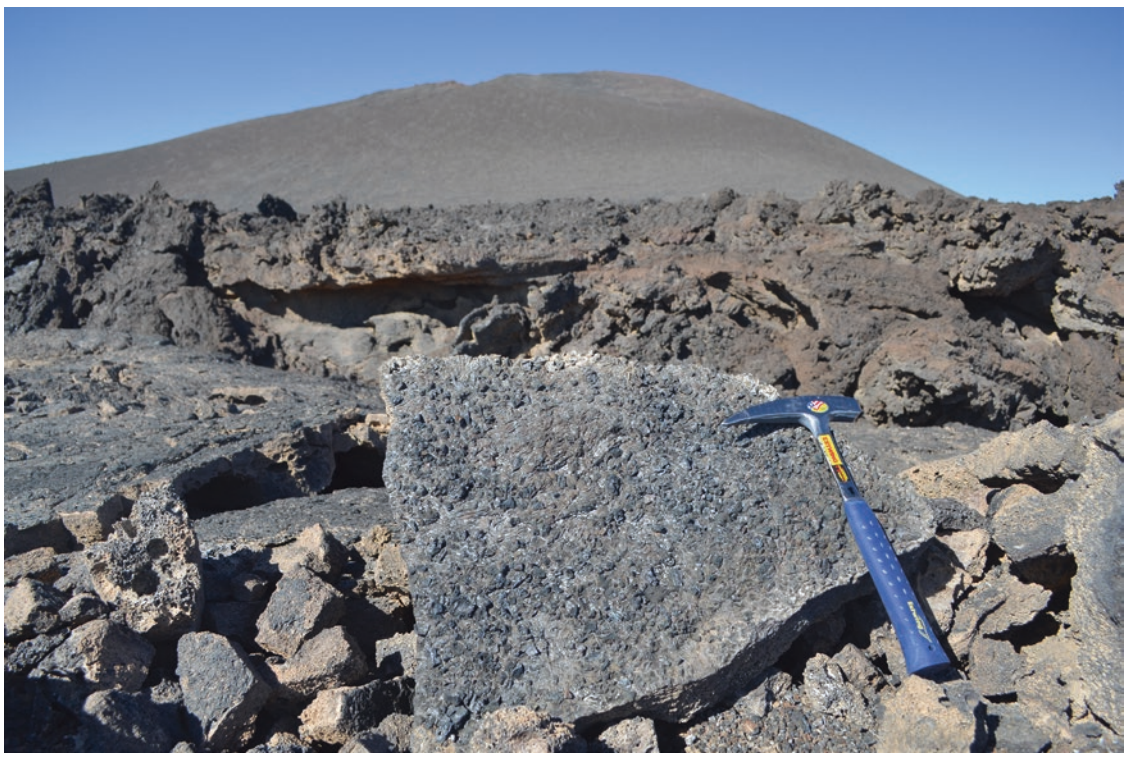

Fig. 3.68 Detail of a slabby pāhoehoe lava flow emitted from the A.D. 1256 Al Madinah historic eruption near Al Madinah city, in the Harrat Rahat, western Saudi Arabia. Note the fused scoria, lapilli and ash attached to the base of the slab that has been lifted up and incorporated into the interior of the rubbly pāhoehoe lava flow about 3 km from its source volcano, seen in the background. More information: Murcia et al. (2014), Moufti and Németh (2016)
Photo © *Karoly Németh*

Fig. 3.69 Typical slabby pāhoehoe lava in the proximal section of the A.D. 1256 Al Madinah eruption site. Large (meter-scale) and relatively thin (centimeter- to decimeter-thick) slabs of pāhoehoe are stacked against the steep slope of the main scoria cone chain of the eruption site. The individual slabs are 1–2 m across; the view in the front is about 10 m across
Photo © *Karoly Németh*

Fig. 3.70 Slabby pāhoehoe containing subangular, vesicular crustal fragments on top of the Barshiv lava flow. The Barshiv lava flow is unique in the Deccan Traps as it records transitional lava morphotypes over a short distance of ~600 m. More information: Duraiswami et al. (2003a)
Photo © *Raymond Duraiswami*

Fig. 3.71 Slabby pāhoehoe in vertical section, in road cut near Odzun, northern Armenia, showing slabs 10–30 cm thick, with gaps between some slabs and rough undersides of the slabs, containing shark's tooth-like lava stalactites, and the uppersides of other slabs showing lava stalagmites, possibly formed by similar mechanisms. More information: Sheth et al. (2015)
Photo © *Hetu Sheth*

Fig. 3.72 Stacking of several slabby pāhoehoe and rubbly pāhoehoe flows in the upper part of the Debed River basalt sequence, near Odzun, northern Armenia. Note the thick, dense cores of many of the flows and well-developed flow-top breccia above the geologist Arsen Israyelyan. More information: Sheth et al. (2015)
Photo © *Hripsime Gevorgyan*

Fig. 3.73 Road cut exposure near Odzun, northern Armenia, showing an older flow combining slabby pāhoehoe and rubbly pāhoehoe characters, overlain by the dense, massive core of a younger flow (which itself grades into slabby pāhoehoe at its top, not seen here). Note the tilted pāhoehoe slabs of the lower flow to the right, grading into flow-top breccia, and the absence of slabs and the much thicker flow-top breccia just above the centre of the photo, implying that the slabs here completely brecciated to produce flow-top breccia. The upper flow followed the topography of the upper surface of the lower flow, without eroding or incorporating the loose flow-top breccia. Geologist is Arsen Israyelyan. More information: Sheth et al. (2015)
Photo © *Hetu Sheth*

Fig. 3.74 Rubbly pāhoehoe in the 1783–1784 Laki lava flow field, south Iceland. Note a columnar-jointed interior below flow-top rubble. The surface of the flow is covered in moss. More information: Guilbaud et al. (2005)
Photo © *Hetu Sheth*

Fig. 3.75 Rubbly pāhoehoe (Keszthelyi and Thordarson 2000; Duraiswami et al. 2008; Sen 2017; Sheth et al. 2017b). Well-developed flow-top breccia in a tholeiitic lava flow, overlain by another tholeiitic flow whose columnar base is seen here. Location is between Dhandhalpur and Adala, Sayla Taluka, Surendranagar district, Saurashtra, northwestern Deccan Traps. Geologist is Tarulata Das
Photo © *Vivek Ghule*

Fig. 3.76 Flow-top breccia of a rubbly pāhoehoe flow underlying giant plagioclase basalt. Shivneri Fort near Junnar, western Deccan Traps, India. Geologist is Shubhankar Majhi
Photo © *Ishita Pal*

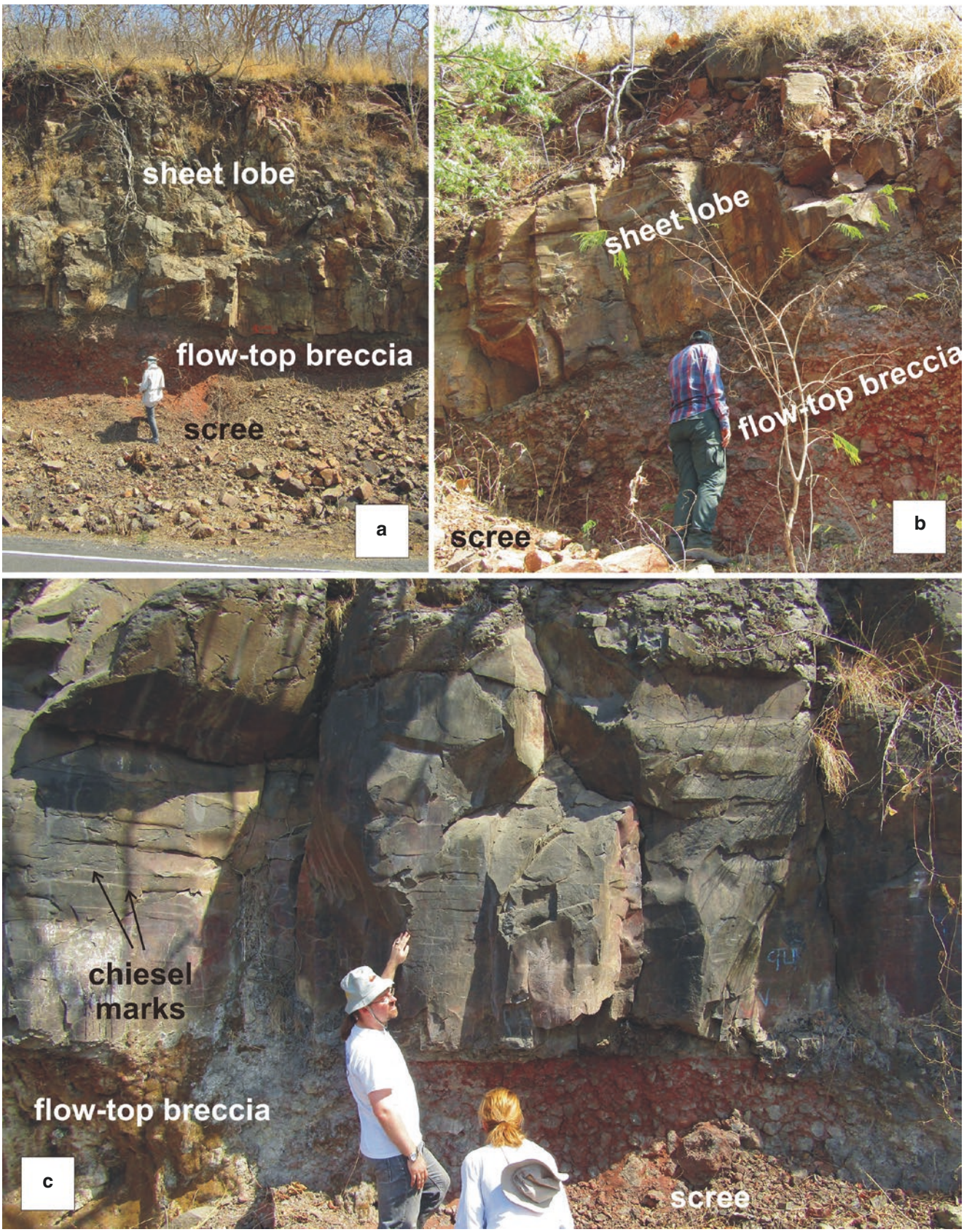

Fig. 3.77 Road cut in the Buldana section, central Deccan Traps, exposing a pāhoehoe sheet lobe with thick basal columns, resting on highly weathered and reddened flow-top breccia of the preceding flow. Note horizontal chiesel marks on the columns. Geologists are Stephen Self in (**a**), Erika Rader in (**b**), and Loÿc Vanderkluysen and Amanda Clarke in (**c**)
Photos © *Hetu Sheth*

Fig. 3.78 Contact between the two flows of the Elephant Mountain Member (Saddle Mountains Basalt, Columbia River Basalt Group) at Yakima River Canyon. The Elephant Mountain Member is one flow that traveled 200 km from its vent. As it exited its main channel and slowed as it spread in the Pasco Basin, an upstream portion of the flow broke out and overtopped the earlier portion. Here, the lower flow contains a rubbly, brecciated flow top with rafted masses of the flow. The white material is sediment. The flow burrowed into the sedimentary interbed below it (above the Pomona flow). This wet sediment mixed with the flow forming the flow-top breccia and now the sediment coats the basalt clasts. The exposure is about 5 m high. More information: Reidel et al. (2013b)
Photo © *Stephen P. Reidel*

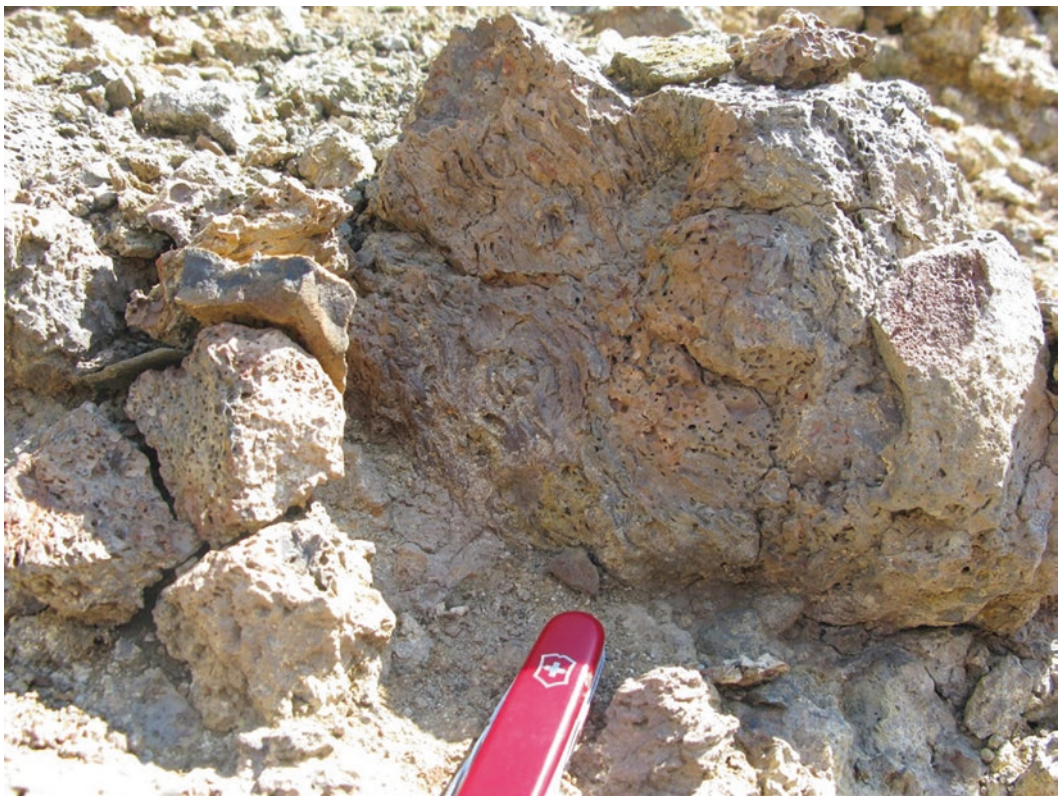

Fig. 3.79 Clasts with pāhoehoe surfaces in a rubbly pāhoehoe flow of the Columbia River Basalt Group at Armour Draw, Washington
Photo: *Laszlo Kestay (Keszthelyi), US Geological Survey*

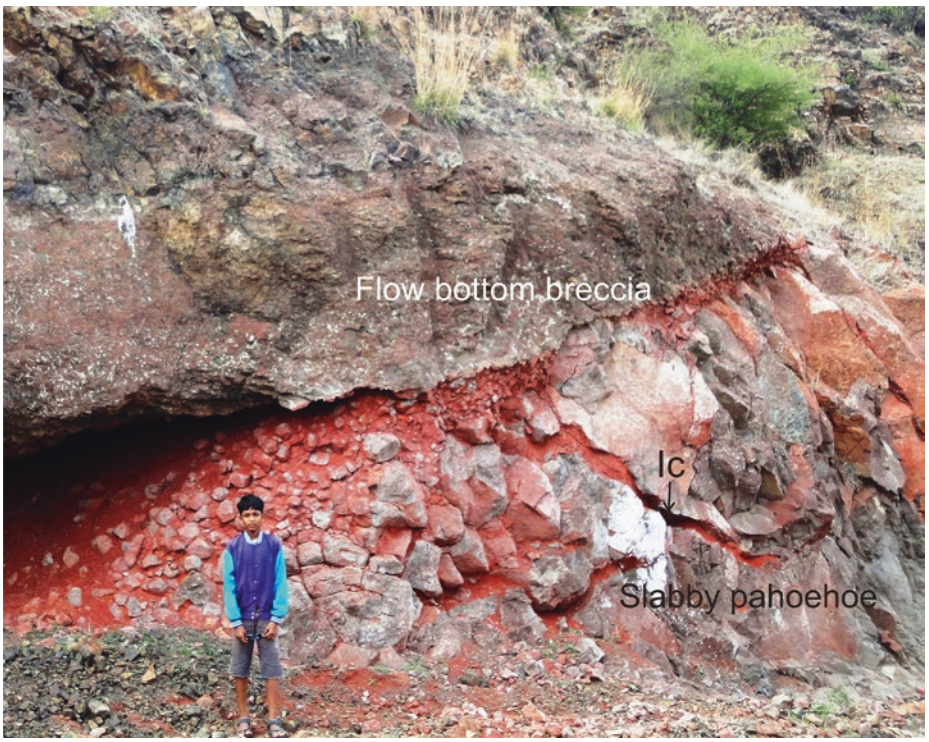

Fig. 3.80 Contact between slabby pāhoehoe flow (below) and ‘a’ā flow (above) exposed in the Bhuleshwar Ghat, Yewat, Deccan plateau. Note the large inflation cleft (Ic) and the pāhoehoe slabs in the lower lava flow behind Neil Duraiswami. The fine flow-bottom breccia of the overlying ‘a’ā lava flow is also seen. Transitions between pāhoehoe and ‘a’ā (such as slabby and rubbly pāhoehoe) are common in the compound flow fields of the western Deccan Traps. More information: Duraiswami et al. (2014)
Photo © *Raymond Duraiswami*

Fig. 3.81 Toothpaste lava in the distal flow fields of the A.D. 1256 Al Madinah historic eruption site near Al Madinah city. This texture is evidence of the viscosity increase of the lava over a distance due to heat loss and partial crystallization, and such textures are common in the distal flow lobes of many of the western Saudi Arabian lava flow fields
Photo © *Karoly Németh*

Fig. 3.82 ʻA'ā lava flow from the 1973 eruption of Eldfell scoria cone, on the island of Heimaey in the Vestmannaeyjar (Westman Islands), off the southern coast of Iceland. House destroyed by the flow provides a scale
Photo © *Gillian R. Foulger*

Fig. 3.83 Breccia zone separating ʻa'ā flows of the mid-Miocene Steens Basalt, Catlow Rim, SE Oregon, USA. Ninad Bondre is the geologist; see Bondre and Hart (2008) for more information
Photo © *William K. Hart*

Fig. 3.84 Flow-bottom breccia at the base of an 'a'ā flow, with the core of the flow exposed above. The breccia is very red because of weathering and oxidation. Pasarni Ghat section between Satara and Mahabaleshwar, Western Ghats, Deccan Traps. Geologist is Nasrrddine Youbi. 'A'ā flows are relatively uncommon in the Deccan (see Brown et al. 2011 for additional examples)
Photo © *Nasrrddine Youbi*

Fig. 3.85 Spinose surface of a clast in the upper clinker zone of a Deccan 'a'ā flow. The clast surface bears scratch marks indicating abrasion of fragments against each other. Diveghat section, Pune, Maharashtra
Photo: *Bibhas Sen, Geological Survey of India*

Fig. 3.86 Welded flow-top breccia in the crustal clinkery zone of a Deccan lava flow in the Phaltan area, Maharashtra. The deformed shapes of these vesicles are characteristic of ‘a’ā clinker. Lens cap is 6.5 cm in diameter
Photo: *Bibhas Sen, Geological Survey of India*

Fig. 3.87 The terminus of an ‘a’ā lava flow emitted from a large scoria and tuff ring complex of the Aslaj volcano, in the northern Harrat Kishb, western Saudi Arabia. The lava is alkali basalt and commonly contains decimeter-size mantle peridotite nodules. The foreground is several meters wide.
Photo © *Karoly Németh*

Fig. 3.88 Distal pāhoehoe breakout in an ‘a’ā lava flow terminus zone associated with the A.D. 1256 Al Madinah eruption, Harrat Rahat, western Saudi Arabia. More information: Moufti and Németh (2016)
Photo © *Karoly Németh*

Structures Formed during Transport, Inflation, and Degassing of Flood Basalt Lavas

4

Fig. 4.1 Spreading ridge about 50 m long, exposed in the A.D. 1256 Al Madinah lava field, Harrat Rahat, western Saudi Arabia
Photo © *Karoly Németh*

H. Sheth, *A Photographic Atlas of Flood Basalt Volcanism*, https://doi.org/10.1007/978-3-319-67705-7_4

Chapter Overview

Various structures, i.e., outcrop-scale features, are produced in flood basalt lava flows during the movement, transport, inflation, and degassing of lava. These include vesicles left by escaping gas bubbles, lava tubes under thick solidified crust transporting lava tens of kilometers or greater distances with negligible ($\ll$1 °C/km) heat loss, tumuli (domal uplifts in lava crust above overpressurized or blocked lava tubes), lava squeeze-ups ejected from the tumuli's extensional surface clefts, and open channels transporting 'a'ā flows much as they do on Kilauea, Etna, or Barren Island today. Interestingly, many large Deccan lava flows, which are small-scale compound pāhoehoe flows like Hawaiian flows, contain tumuli with sizes, aspect ratios, and calculated magmatic overpressures comparable to those of Hawaiian and Icelandic tumuli (Sheth et al. 2017a). These large Deccan flows must therefore have been emplaced in an essentially identical and gradual manner, over long time periods, and possibly from very long feeder dykes (Ray et al. 2007).

The structures illustrated in this chapter are all primary structures directly related to the processes of flood basalt emplacement. Surprisingly, though much is known, some most basic and universal structures like pipe vesicles are still poorly understood.

Pipe vesicles are the tens to hundreds of elongated, tube-like vesicles, found at the bases of pāhoehoe flows. They are much more frequently inclined than vertical, and often also bent, in vertical sections, but all associated pipe vesicles typically remain parallel. In Walker's (1987) widely cited model, an individual pipe vesicle forms when a buoyant gas bubble rises vertically from the base of the lava, and the lava solidification front moves upward fast enough to prevent the host lava (postulated as now having a yield strength) from closing the space left by the escaped bubble. However, a rising spherical bubble cannot leave behind a tube as postulated. Either there must be a *train* of rising bubbles, in which case pipe vesicles would not be fundamentally different from vesicle cylinders (Goff 1996; Costa et al. 2006). Or, there must be vertical stretching of a bubble, somehow, making a tube. A perplexing aspect of the Walker (1987) model is that pipe vesicles, which are very frequently inclined in concert, are viewed as having become tilted due to flowage of the lava, and to even indicate lava flow directions (at least local) and palaeoslopes, while their very origin and form are ascribed to the host lava having already become rigid. Philpotts and Lewis (1987) have provided a fundamentally different interpretation of pipe vesicles in which these features are not related to bubble buoyancy at all. Much interesting work remains for understanding these universal features, the rarer "half-moon" vesicles, and so on.

Fig. 4.2 Close-up of perfectly spherical vesicles (indicating the host lava to be pāhoehoe) in a 2.74 Ga Sodium Group (Ventersdorp Supergroup) lava flow, South Africa. Coin provides a scale
Photo © *Nils Lenhardt*

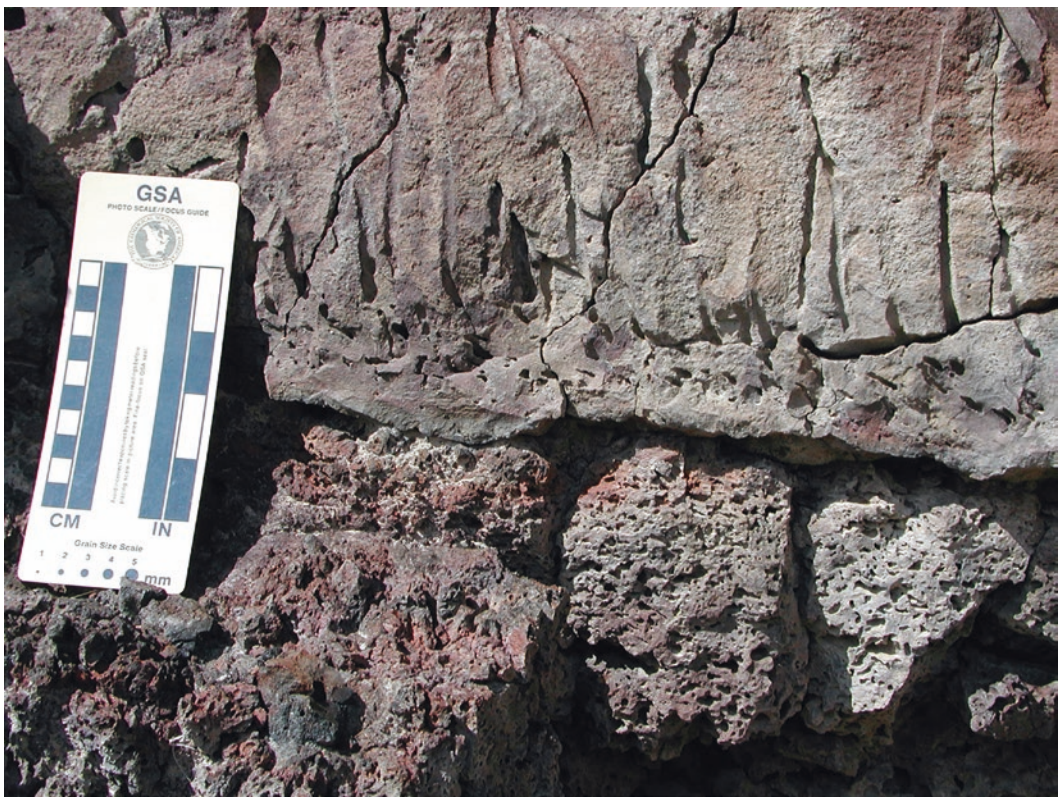

Fig. 4.3 Open pipe vesicles in the basal crust of a mid-Miocene Steens Basalt pāhoehoe flow lobe, SE Oregon, USA. See Bondre and Hart (2008) for additional information
Photo © *William K. Hart*

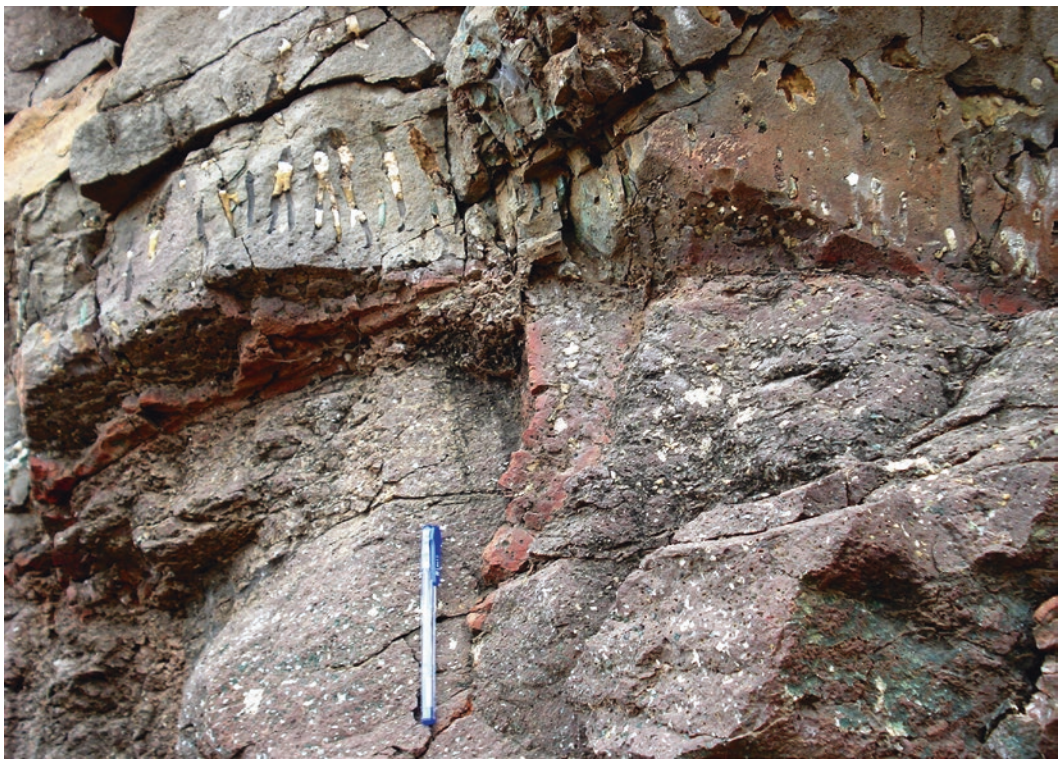

Fig. 4.4 Deccan lava belonging to a younger compound flow lobe infilling the inflation cleft in the thoroughly vesicular-amygdaloidal upper crust of a lower lobe (centre of the photograph). The upper lobe shows well-developed, inverted V-shaped and Y-shaped pipe amygdules in its lower crust. Pen is 15 cm long. Tamniwadi area, Pune district, Maharashtra
Photo: *Bibhas Sen, Geological Survey of India*

Fig. 4.5 Pipe amygdules in the lower vesicular zone of a pāhoehoe lobe, originating just above the oxidized lower chilled margin of the lobe (red). The pipes coalesce upwards to make inverted Y-shapes and are bent into the local direction of lava movement (Walker 1987; but see also Peterson and Hawkins 1971; Philpotts and Lewis 1987). The core of the lobe in the upper part is largely vesicle-free. Pen is 15 cm long. Deccan Basalts of Alandi, Maharashtra
Photo: *Bibhas Sen, Geological Survey of India*

Fig. 4.6 Three-dimensional view of pipe vesicles in high-alumina olivine tholeiite of northern Owyhee Plateau, SE Oregon, USA. The pipes are ~1 cm in diameter
Photo © *William K. Hart*

Fig. 4.7 Well-formed, unfilled pipe vesicles (both in section and top view) in a boulder of the Holyoke Basalt (CAMP) in the Tariffville gorge, Connecticut, USA. The Farmington River is in the background. Pen is 15 cm long
Photo © *Hetu Sheth*

Fig. 4.8 Pipe vesicles in CAMP basalt, Aït Ourir section, High Atlas of Morocco
Photo © *El Hassane Chellai*

Fig. 4.9 Row of stone elephants in the Kailasa Temple monument (mid-eighth century), Cave 16, Ellora Caves, central Deccan Traps. The elephants are ~2 m tall and have had their trunks broken along a flow lobe contact marked by a prominent horizon of pipe vesicles. Dipping vesicular-amygdaloidal banding in the upper crust of the same lobe, above the elephants' heads, is also seen well in this photo. Note also the wavy and cuspate base of the lobe, and vesicle banding in the upper crust of the underlying lobe
Photo © *Erika Rader*

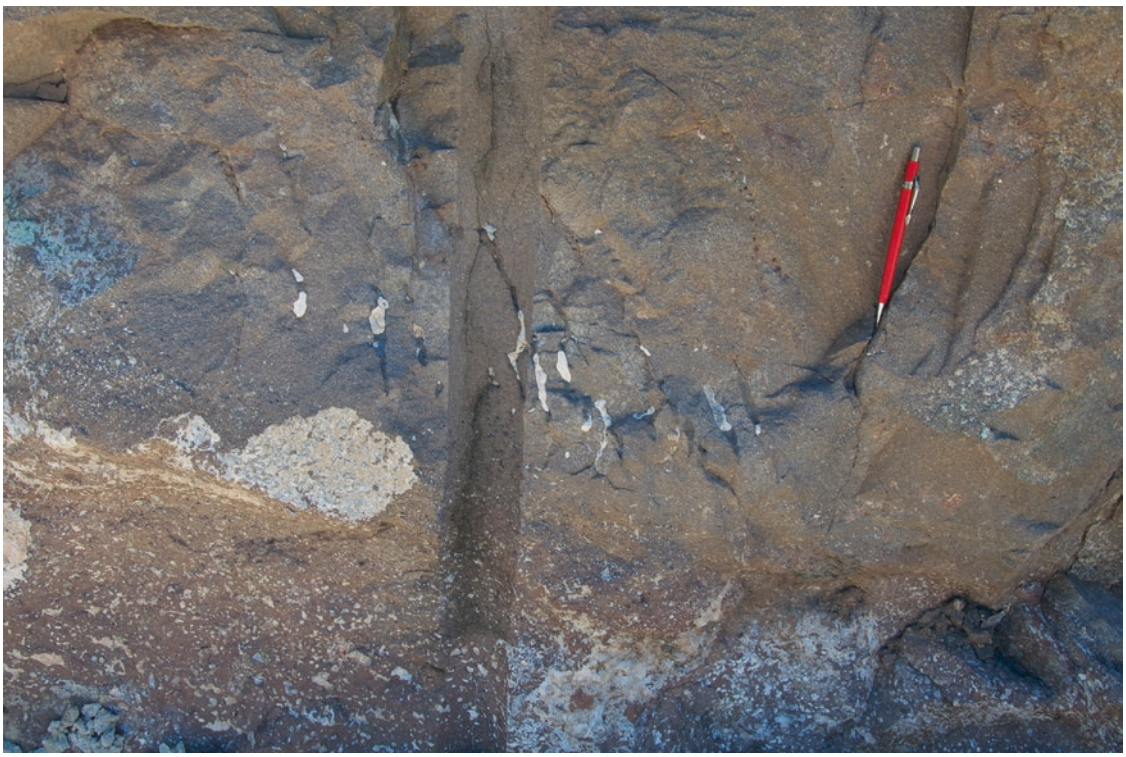

Fig. 4.10 Pipe vesicles and proto-cylinder (vertical trail of vesicles, left of the 15 cm long pen) at the base of a simple pāhoehoe lava flow in the Paraná CFB province. The lower part of the photo is the highly vesicular-amygdaloidal top of the underlying flow unit
Photo © *Carla Barreto*

Fig. 4.11 Vertical trail of vesicles (proto-cylinder) at the base of a simple pāhoehoe lava flow of the Paraná CFB province. Note the dense, non-vesicular and relatively coarse-grained lava surrounding the proto-cylinder. Paper clip for scale. More information: Barreto et al. (2014, 2017)
Photo © *Carla Barreto*

Fig. 4.12 Vesicle cylinder in the core of a simple pāhoehoe lava flow in the Paraná CFB province, Brazil
Photo © *Carla Barreto*

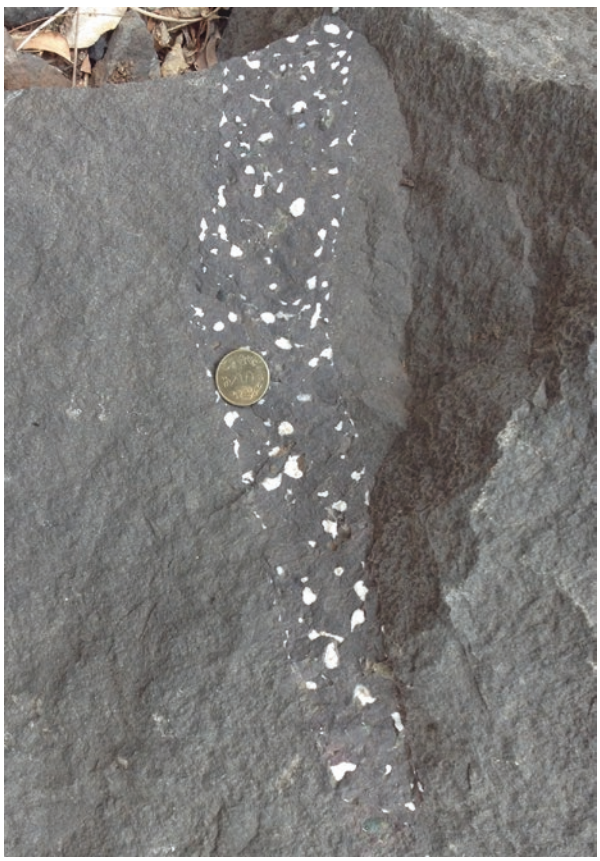

Fig. 4.13 A vesicle cylinder with vesicles later filled by secondary zeolites and calcite. Note the vesicle-free basalt surrounding it. Coin diameter is 2 cm. Parsik Hill, Belapur, New Mumbai, western Deccan Traps
Photo © *Hrishikesh P. Samant*

Fig. 4.14 Section view of vesicle cylinders developed in the massive core of a pāhoehoe flow lobe, near Alandi, Maharashtra, Deccan Traps. Besides the cylinder adjacent to the coin (diameter 2.5 cm), three other cylinders on the right are indicated with arrows. Vesicle cylinders are common in the compound pāhoehoe flows of the western Deccan (e.g., Sarkar and Mude 2010; Sarkar et al. 2015)
Photo: *Bibhas Sen, Geological Survey of India*

Fig. 4.15 Segregation structures in the core of a plagioclase-phyric, mid-Miocene Steens Basalt pāhoehoe flow lobe, Steens Mountain, SE Oregon, USA. See Bondre and Hart (2008) for additional information
Photo © *William K. Hart*

Fig. 4.16 Plan view (horizontal section) of a vesicle cylinder in a simple pāhoehoe lava flow of the Paraná CFB province. Note the dense, non-vesicular lava, with a relatively coarse grain size and diktytaxitic texture, in which the vesicle cylinder occurs. Paper clip for scale. More information: Barreto et al. (2014, 2017); see also Waichel et al. (2006)
Photo © *Carla Barreto*

Fig. 4.17 Plan view of abundant vesicle cylinders (Goff 1996; Costa et al. 2006) in small pāhoehoe lobes, significantly more vesicular than host lava. Elephanta Island, Mumbai harbour, western Deccan Traps. Fourteen cylinders are observed here. Coin diameter 2.5 cm. See also Fig. 4.21. More information: Sheth et al. (2017c)
Photo © *Hetu Sheth*

Fig. 4.18 Top view of a vesicle cylinder in a 2.22 Ga Hekpoort Formation lava. The 300–850 m thick Hekpoort Formation in the Transvaal Basin of South Africa comprises subaerial lava flows (dominantly basalts), pyroclastics, and their reworked counterparts (Lenhardt et al. 2012 and references therein). The picture shows the weathered surface on the right and a fresh rock surface on the left
Photo © *Nils Lenhardt*

Fig. 4.19 Well-preserved vesicle cylinder (left of the hammer) in the core of a pāhoehoe flow, Lower Formation (CAMP), in the Oued Lhar (Herrissane) section, Morocco
Photo © *Nasrrddine Youbi*

Fig. 4.20 Parts of two thick, crudely columnar pāhoehoe sheet lobes exposed near the top of the Moti Gop section (see Fig. 3.32) in Saurashtra, northwestern Deccan Traps. The lower lobe shows an upper crust with spherical vesicles now filled by secondary minerals. The upper lobe shows pipe vesicles at the base and a dense, aphyric core, which however shows a large number of very closely spaced vesicle cylinders, also filled by secondary minerals. There are additional cylinders towards the left. The pipe vesicles indicate that the prominent horizontal discontinuity is indeed a contact between two flows, and not just a horizontal fracture within a single flow. Geologist is Tarulata Das
Photo © *Raymond Duraiswami*

Fig. 4.21 Unusually profuse development of vesicle cylinders in small pāhoehoe lobes, Elephanta Island, Mumbai harbour, western Deccan Traps. More than 100 cylinders, a majority located on prismatic joints or their intersections, are seen here. Oblique view of horizontal surface; the compass provides a scale. See also Fig. 4.17. More information: Sheth et al. (2017c)
Photo © *Hetu Sheth*

Fig. 4.22 Vesicle cylinder showing a prominent deflection, in the aphyric, massive core of a pāhoehoe flow of the Paraná CFB province. Note the dense, non-vesicular core with a notably coarse grain size and diktytaxitic texture. In the upper left of the photo, a T-junction made up of a vertical vesicle cylinder passing into a horizontal vesicle sheet is seen. Pen is 15 cm long. More information: Barreto et al. (2014, 2017)
Photo © *Carla Barreto*

Fig. 4.23 Horizontal vesicle sheet in the core of a simple pāhoehoe lava flow from the Paraná CFB province, Brazil. View of vertical face; pen is 15 cm long. The vesicle sheet has sharp margins with the host basalt. Note the dense and non-vesicular core with a notably coarse grain size and diktytaxitic texture. More information: Barreto et al. (2014, 2017)
Photo © *Carla Barreto*

Fig. 4.24 Large "half-moon vesicle" of the type described from the CAMP basalts in the northeastern USA (Puffer and Student 1992; Puffer and Laskowich 2012), here in New Jersey. View is of vertical rock face; note the sparse and tiny vesicles in the rock. Pen is 15 cm long
Photo © *Hetu Sheth*

Fig. 4.25 Roadcut exposure in compound flow, showing several small (Hawaiian-size) pāhoehoe lobes, highly weathered, and amygdaloidal at their contacts. Two gas blisters are seen, and are lined by zeolites. Dark area on the right is covered in water. Geologist is Raymond Duraiswami. The exposure no longer exists due to urban development. Chandni Chowk, Pune, western Deccan Traps
Photo © *Nasrrddine Youbi*

Fig. 4.26 Well-preserved internal architecture (a dense lava core underlying an upper crust with vesicle banding, see Self et al. 1997) of a pāhoehoe flow of the Lower Formation, CAMP. The Jbel Imzar section, Morocco. The geologist Idris Ali Ahmadi Bensaid has his hand on the boundary between the core and the crust
Photo © *Nasrrddine Youbi*

Fig. 4.27 Horizontal vesicle banding seen on and behind stone elephant, Cave 19, Ajanta Caves, central Deccan Traps. The banding may indicate periodic injection of new volatile-bearing lava into an inflating pāhoehoe lobe, with the rising bubbles derived from each injection being trapped against a progressively downward-solidifying upper crust. Erika Rader is the geologist
Photo © *Hetu Sheth*

Fig. 4.28 Internal vesicle zone in the Cohasset flow, Grande Ronde Basalt, Columbia River Basalt Group. The Cohasset flow formed as four distinct pulses of lava inflated the flow. The internal vesicular zone pictured here formed as the last pulse which was rich in volatiles inflated the flow. Meter stick for scale. Location: Sentinel Gap, Saddle Mountains, near Vantage, Washington
Photo © *Stephen P. Reidel*

Fig. 4.29 Horizontal vesicle banding seen in a single lobe of Deccan pāhoehoe lava, the bands showing large variations in vesicle numbers and vesicle size. The bands are separated by much thinner and discontinuous patches of aphyric lava. Note that no internal contacts are present, and this banding may indicate periodic inflation of the lobe (Self et al. 1997), with repetitive injection of volatile-rich lava and the upward escape and trapping of bubbles against solidified lava. Note the spherical shapes of the vesicles, typical of pāhoehoe. Vertical face, pen 15 cm long. Cave 19, Ajanta Caves
Photo © *Hetu Sheth*

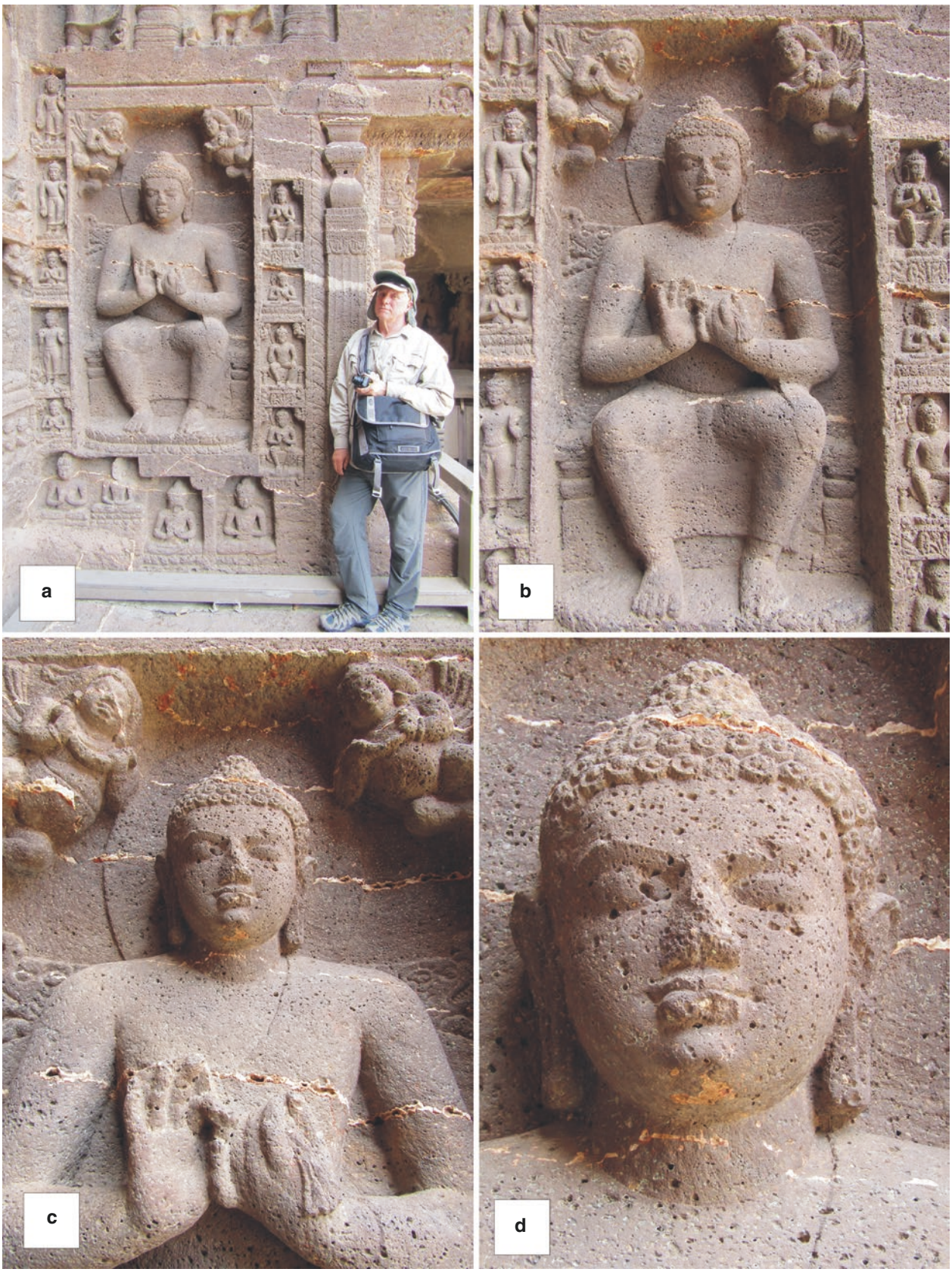

Fig. 4.30 (**a–d**) Horizontal vesicle banding seen on and around Buddha idol, Cave 19, Ajanta Caves (second century B.C. to seventh century A.D., a UNESCO World Heritage Site), central Deccan Traps. Some of the horizontal bands are filled by white secondary zeolites. Geologist in (**a**) is Stephen Self. Note the spherical, undeformed vesicles seen on the Buddha's face in (**d**), indicating that the lava is pāhoehoe (Macdonald 1953). The lava is also porphyritic, with numerous small white plagioclase laths, better seen on the panel behind the Buddha
Photos © *Hetu Sheth*

Fig. 4.31 Lava channels with levees, exposed at the village Gunjale, Ahmednagar district, western Deccan Traps. The levees are large and wide. Person in the bottom left corner provides a scale, as do the distant buffaloes (small black objects to the right of the levees at the centre of the photo). More information: Misra (2002)
Photo: *Kiran S. Misra, Geological Survey of India*

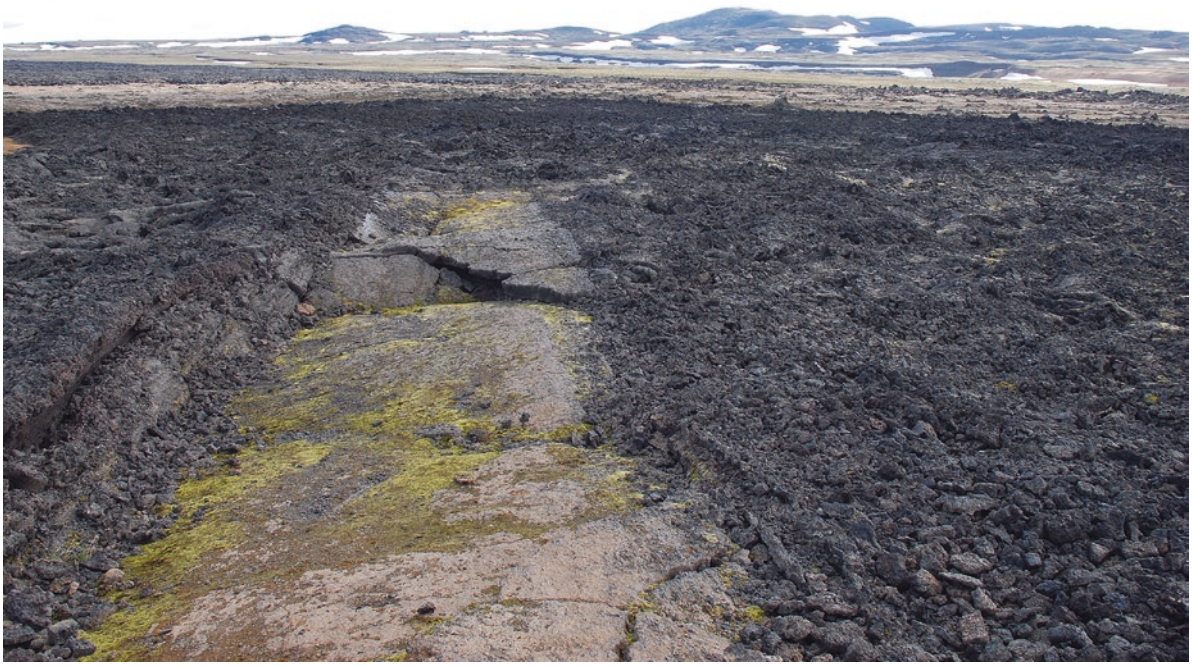

Fig. 4.32 Two-meter-wide channel of smooth-surfaced lava in a flow which is a hybrid of slabby and rubbly pāhoehoe, Ódáðahraun, Iceland
Photo © *Hervé Bertrand*

Fig. 4.33 Close-up view of one margin of a lava channel initiated from the A.D. 1256 Al Madinah eruption site. The levee of the channel is about 25 cm thick
Photo © *Karoly Németh*

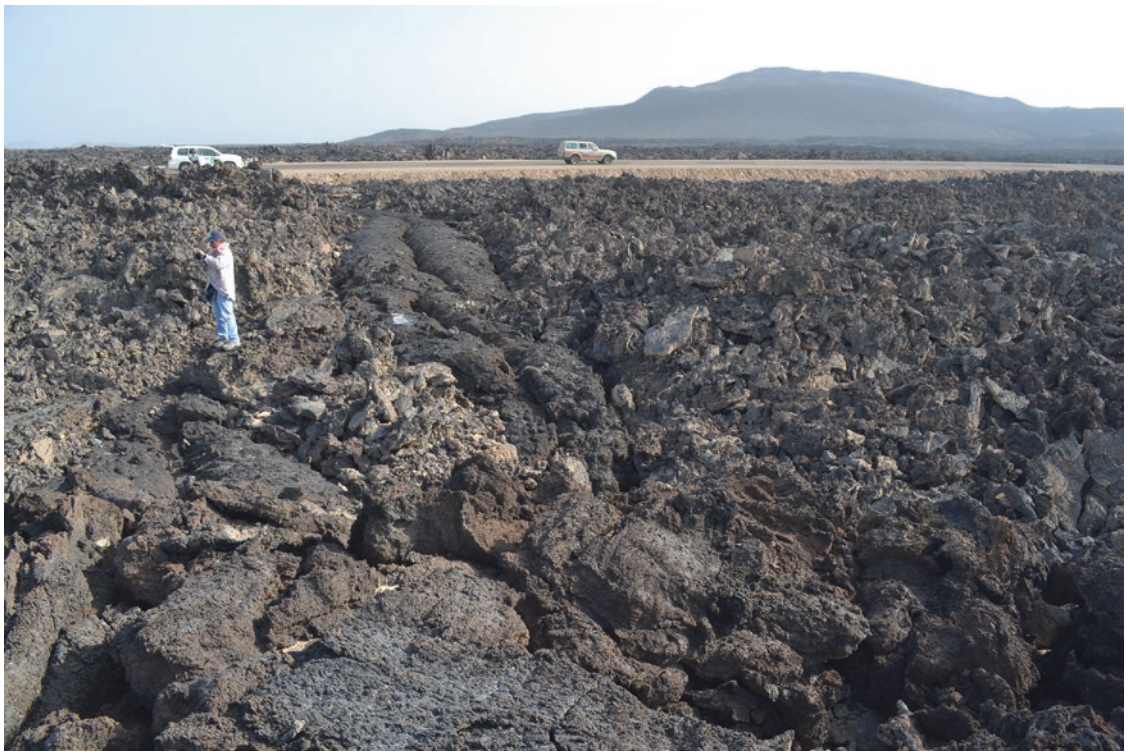

Fig. 4.34 Exposed lava spreading ridge (right of the person) in the northern side of the A.D. 1256 Al Madinah historic eruption site near Al Madinah city, Harrat Rahat, western Saudi Arabia. Such spreading ridges are overlain by lava showing textural features in between typical slabby and rubbly pāhoehoe
Photo © *Karoly Németh*

Fig. 4.35 Lava tubes are common features in the Harrat Khaybar, and rank among the largest across the western Saudi Arabian post-Miocene intracontinental volcanic provinces. The large lava caves in the Harrat Khaybar are associated mostly with the main arteries of extensive pāhoehoe lava flow fields inferred to have filled a rift where they outpoured. Lava caves on such a scale also commonly host rich Pleistocene palaeontological as well as archaeological sites. More information: Moufti and Németh (2016)
Photo © *Karoly Németh*

Fig. 4.36 Exposed lava stalactites in a small collapsed lava tube in the proximal lava field of the A.D. 1256 Al Madinah eruption site, Harrat Rahat, western Saudi Arabia. The view is about 2 m across
Photo © *Karoly Németh*

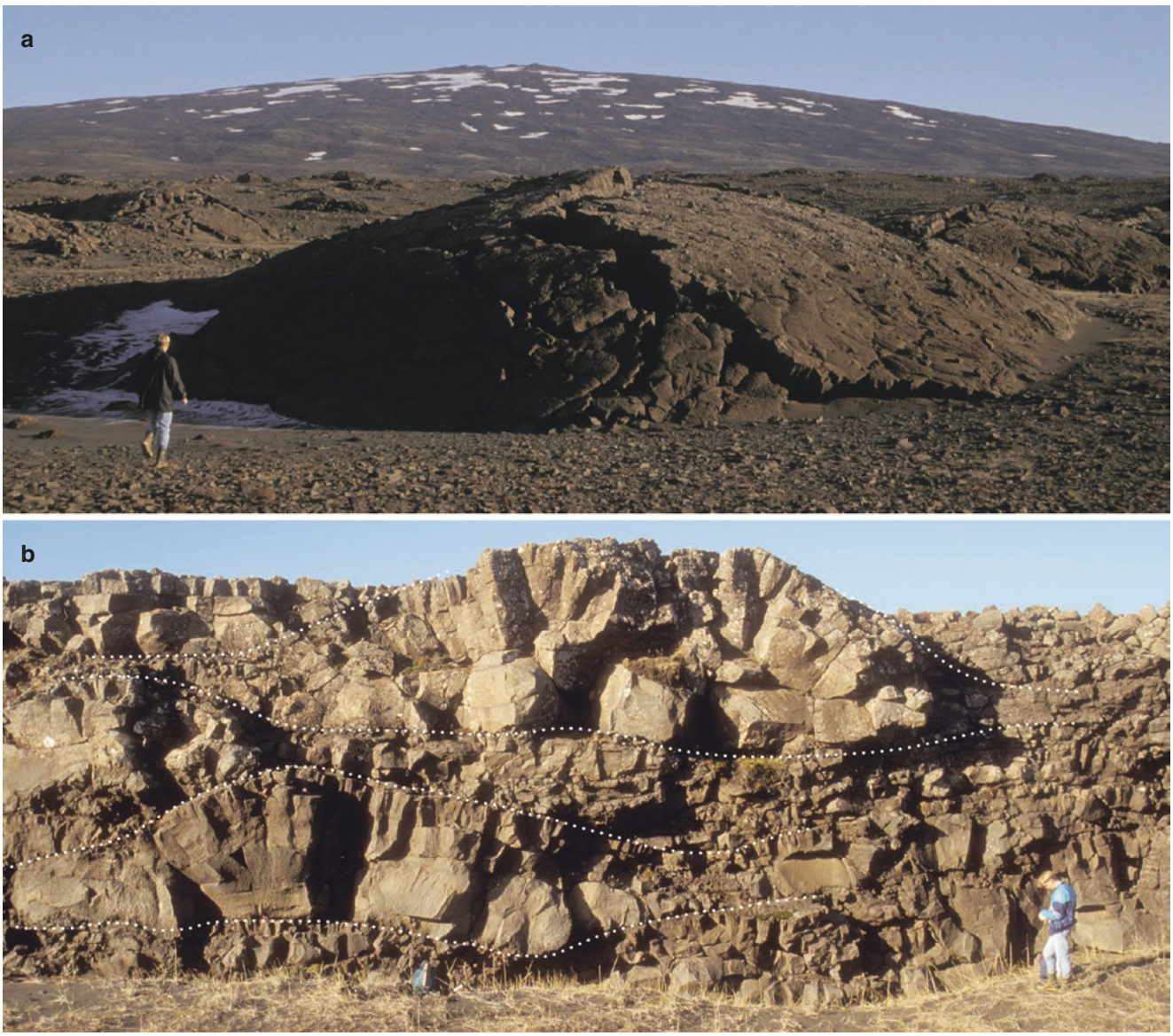

Fig. 4.37 Tumuli in Icelandic lava flow fields. (**a**) Tumulus below the western flank of the archetypal Skjaldbreiður shield volcano rising nearly 600 m above foreground. Lava flowing down the flank of the shield volcano generates interior lava overpressure where it accumulates at the foot of the slope (e.g., Walker 1991; Rossi and Gudmundsson 1996). (**b**) Southeast-facing surface of normally faulted fissure exposing a cross-section through two tumuli (outlined). Matti Rossi provides a scale in each photograph
Photos © *Martin B. Klausen*

Fig. 4.38 Large star-like tumulus in the Pleistocene-age Crater Basalt Volcanic Field (CBVF) in Chubut, northern Patagonia, Argentina. The CBVF represents one of the smallest volcanic fields with only a few preserved scoria cones; however, the field is part of a large volcanic province developed behind the Andes in the continental basement of Patagonia. Tumuli like this are common features in these Patagonian volcanic fields where the surface slope changes and lava flows can undergo ponding. To recognize them in a semi-arid and shrub-covered landscape turns out not to be an easy task and they have commonly been interpreted as eruptive point sources. Gabriella Massafero is the geologist. More information: Németh et al. (2007)
Photo © *Karoly Németh*

Fig. 4.39 Typical star-like tumulus in an eroded pāhoehoe lava flow field of the Al Haruj al Abyad in central Libya. The tumulus is about 20 m across and 5 m tall, and split in its middle with no sign of lava outflow. The tumulus is surrounded by a depression as a result of the subsequent deflation of the pāhoehoe field after reduction of the magmatic pressure (hence drop of magma flux) in the system
Photo © *Karoly Németh*

Fig. 4.40 Pāhoehoe lava flow front with tumuli, blocked by the gently sloping tephra ring of the Al Wahbah maar volcano, in the Harrat Kishb, western Saudi Arabia. Geologist is Mohammed Rashad Moufti
Photo © *Karoly Németh*

Fig. 4.41 As the gently sloping tephra ring of the Al Wahbah maar volcano in the Harrat Kishb, western Saudi Arabia, acts as a barrier to younger pāhoehoe lava flows, the lavas surround the tephra ring and gradually inflate forming relatively small (about 2–10 m across) distorted, convolute-shaped tumuli. View is about 4 m across in the foreground. Note prominent axial cleft of tumulus
Photo © *Karoly Németh*

Fig. 4.42 "Whaleback" tumulus exposed in the course of the Bhima River at Daund, western Deccan Traps. Geologist is Pulin Goswami. Several large elongated tumuli are also seen in the background. Tumuli such as these are commonly found in hummocky-surfaced pāhoehoe with meter-sized relief, and experience variable amounts of uplift due to inflation and/or variable lava supply rates due to constrictions in the lava tube systems. The Deccan hummocky pāhoehoe flows with tumuli resemble Hawaiian flows, suggesting a similarity in the nature and style of eruptions. More information: Duraiswami et al. (2001, 2004); see also Sheth et al. (2017a)
Photo © *Raymond Duraiswami*

Fig. 4.43 Bulbous flow-lobe tumulus exposed at Sonwadi near Daund, western Deccan Traps. Note the disposition of the lava inflation clefts occupied by squeeze-ups. The presence of such flow-lobe tumuli in the hummocky pāhoehoe lava flows is consistent with the tube-fed nature of these flows and suggests emplacement by mechanism of inflation. Hammer above photo centre provides a scale. More information: Duraiswami et al. (2002, 2004)
Photo © *Raymond Duraiswami*

Fig. 4.44 Large tumulus (centre of the photo) in compound pāhoehoe flows of the Deccan basalts. Note the vesicular banding in the upper crust dipping towards the left, the wedge shape of the lava lobe that overlies and abuts the tumulus, a long and thin lobe that covers both of them, and a thick lobe at the top. The other side of the tumulus, away from the viewer, is not exposed because of carving and plaster cover. Near Cave 6 and the bridge over Waghora River, Ajanta Caves, central Deccan Traps. Tourists provide a scale. The tumulus indicates a hummocky pāhoehoe flow (see e.g., Sheth et al. 2017a)
Photo © *Hetu Sheth*

Fig. 4.45 Hummocky pāhoehoe flow with several tumuli that are several meters wide, Harrat Kishb, Saudi Arabia. Many tumuli have ropy surfaces and bilateral symmetry with well-developed central clefts. Atef Qaddah stands on the uplifted flank of a large tumulus, and a lava squeeze-up about a meter wide is seen to have extruded through the axial cleft of the tumulus behind him
Photo © *Karoly Németh*

Fig. 4.46 Pervasively altered ~4.5 Ma basalt (brown) unconformably overlain by canyon-filling ~0.4 Ma basalt (grey) along the modern Snake River canyon, southcentral Idaho, USA. Note preserved inflation features in lobes of the lower basalt (brown), including a large tumulus at the centre of the photo and another on the right edge. See Godchaux and Bonnichsen (2002) for more information
Photo © *William K. Hart*

Fig. 4.47 Squeeze-ups in a CAMP pāhoehoe flow lobe in the Alemzi North section, Argana Basin, Morocco. The outcrop also contains horizontal squeeze-ups elsewhere. Geologist is Mohamed Khalil Bensalah. Details in El Hachimi et al. (2011)
Photo © *Nasrrddine Youbi*

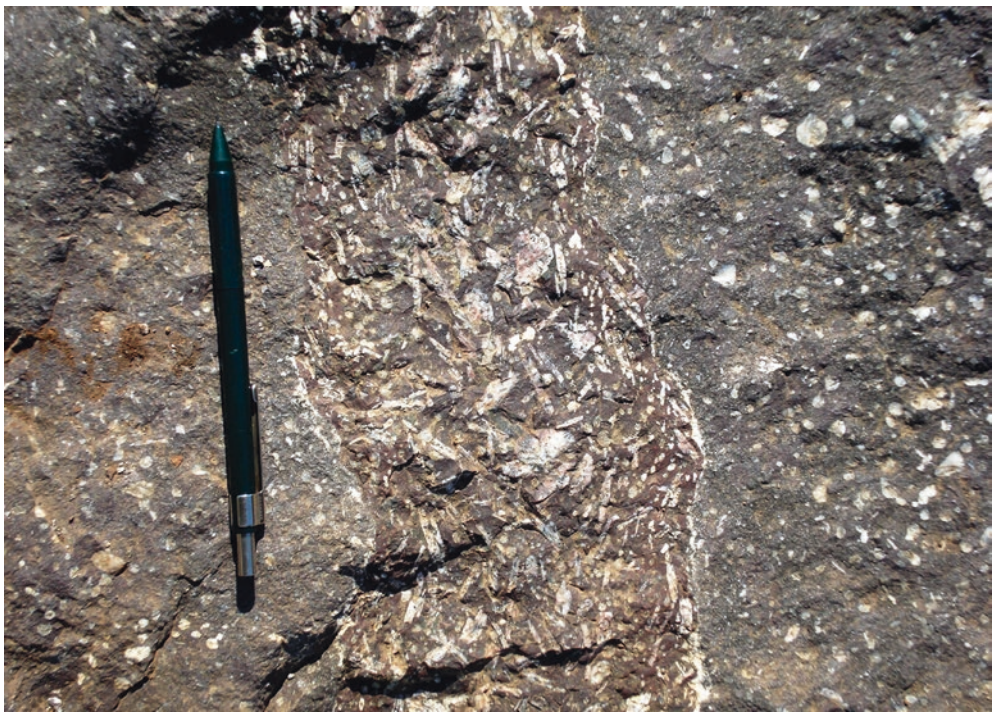

Fig. 4.48 Plan view of a squeeze-up of plagioclase phenocryst-laden basalt injected in the upper, phenocryst-poor but vesicular (now amygdaloidal) part of the same pāhoehoe flow lobe. Location near Chandwad, Maharashtra, Deccan Traps. Pen is 15 cm long
Photo: *Bibhas Sen, Geological Survey of India*

Fig. 4.49 Part of a large (~5 m high and 50 cm wide) breccia-filled lava inflation cleft in an ‘a’ā flow at Bhuleshwar Ghat near Pune. Vertical face; hammer is 36 cm long. Note the irregular, wavy contact between the breccia and a squeeze-up in the upper part of the inflation cleft. Breccia-filled inflation clefts are common in the Deccan Traps, but the occurrence of lava inflation clefts and squeeze-ups of evolved composition in ‘a’ā flows is uncommon. This photo proves that thick ‘a’ā lava flows can also inflate and produce segregations during emplacement
Photo © *Purva Gadpallu*

Fig. 4.50 Elongated tumulus on a basaltic lava flow, Þingvellir, Iceland. The axial crack is one meter wide. In the background, running across the photo, are normal faults of the Þingvellir graben, located on the Eurasian-North American plate boundary
Photo © *Hervé Bertrand*

Fig. 4.51 Elongated tumulus on basaltic lava flow, Sprengisandur, Iceland. The central cleft is 2 m wide
Photo © *Hervé Bertrand*

Structures Formed during Cooling and Solidification of Flood Basalt Lavas

5

Fig. 5.1 The Great Face, west of Fingal's Cave, on southwestern Staffa, NW Scotland. The main crag comprises the classic colonnade-entablature doublet of the Palaeogene Fingal's Cave Lava, overlying bedded pyroclastic-volcaniclastic deposits. The lava is approximately 50 m thick (although only ca. 30 m is preserved on The Great Face). The base of the lava is sharp and planar, and dips at a shallow angle towards the east. The cliff is ca. 42 m high. Person on top of cliff provides a scale
Photo © *Brian R. Bell*

H. Sheth, *A Photographic Atlas of Flood Basalt Volcanism*, https://doi.org/10.1007/978-3-319-67705-7_5

Chapter Overview

Despite their name, *joints* are not joins between blocks of rock, but fractures along which a larger rock mass has been split into blocks. In flood basalt lava flows, jointing, particularly columnar jointing, develops due to contraction of the lava on cooling and solidification, and is a primary and universal structural feature, seen everywhere in various degrees of perfection. Joint columns are typically five-, six- or seven-sided, often beautiful and exquisite enough to appear man-made, and ascribed by legends to creation by mythological giants (see Sigurdsson 1999). Chapter 9 of Sigurdsson (1999), titled "Columnar Basalt and the Neptunists", and Chapter 2 of Young (2003), titled "Basaltes Prismatiques: Lava, Columnar Basalt, and Ancient Volcanoes", describe how several medieval European philosophers and scientists interpreted the beautifully formed, symmetrical and hexagonal columns of basaltic lava flows as giant crystals of basalt precipitated from a primordial ocean. Yet other European field geologists were able to physically trace columnar basalt flows to their eruptive vents on known volcanoes, and a volcanic origin for basalt was thus postulated and ultimately accepted.

World-famous localities for columnar basalt include the Giant's Causeway in Northern Ireland, and Staffa in the Inner Hebrides of Scotland. By popular (and likely true) accounts, even the unusual and striking exterior of Reykjavik's Hallgrímskirkja church (built during 1945–1986, and the largest in Iceland at 74.5 m high) has been designed to mimic basalt columns. Interestingly, there is also the commercial side to columnar basalt: well-formed columns of the Columbia River basalt, of various colours, are prized for their use in landscaping homes and office buildings, and fetch high prices.

Joint columns in the horizontal flood basalt lava flows are typically vertical. Thick flood basalt lava flows take several years to solidify completely. Their cooling history and jointing patterns can be affected by external conditions, most importantly the ingress of meteoric water (rain and streams) into the upper parts of solidifying flows, resulting in haphazardly arranged and twisted columns which can be interpreted by the unwary as indicating tectonic deformation. (The same process can operate in shallow-level intrusions.) Tiers of regular, vertical and thicker columns in thick flood basalt lava flows, called *colonnades*, can alternate with tiers of irregular and thinner columns, called *entablatures*. Colonnades represent slow, conductive cooling but entablatures indicate rapid, convective cooling aided by meteoric water ingress, with abundant glass found in the quenched lava (e.g., Tomkeieff 1940; Long and Wood 1986; Lyle 2000). Well-developed, strikingly contrasted colonnade-entablature tiers are a universal feature of the Columbia River flood basalts, yet such colonnade-entablature tiers are rare in the Deccan lava flows, even in the Western Ghats escarpment where the sequence is at its thickest (~2 km). Again, many Deccan flows in central India do show well-developed colonnade-entablature tiers. The reasons for these interprovince and intraprovince differences in the flows' jointing characters are not yet understood, and constitute one of the interesting broader "palaeovolcanological" questions remaining to be answered.

Fig. 5.2 Columnar joints in the core of a ponded pāhoehoe lava flow of the Paraná CFB province that filled interdune regions of the Botucatu palaeoerg. Geologist is Lucas Magalhães May Rossetti. More information: Barreto et al. (2014, 2017), Rossetti et al. (2017)
Photo © *Carla Barreto*

Fig. 5.3 Joint columns in basalt flow forming the base of the Upper Formation of the Central Atlantic Magmatic Province (CAMP), in the Aït Ourir section, High Atlas of Morocco. Geologist is El Hassane Chellai
Photo © *El Hassane Chellai*

Fig. 5.4 Large plumose markings on joint faces of the Higganum dyke in Connecticut, USA. Geologist Loÿc Vanderkluysen provides a scale. This is a CAMP feeder dyke exposed in southern New England over 250 km. More information: Philpotts and Martello (1986) Photo © *Hetu Sheth*

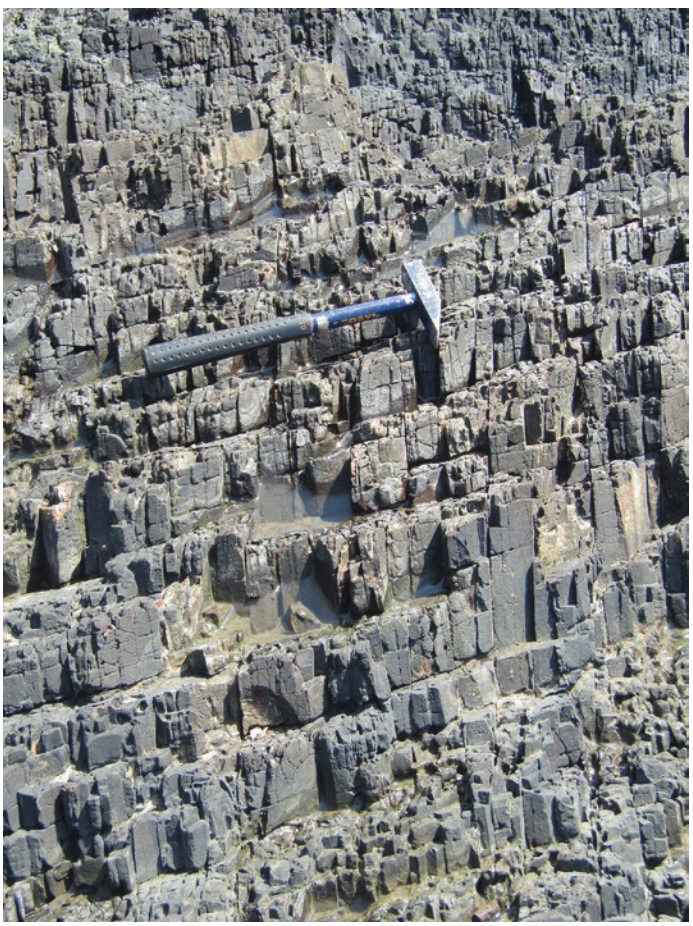

Fig. 5.5 Pervasive, closely spaced and beautifully formed prismatic joints in a basaltic sheet intrusion, on the southern wave-cut platform of Elephanta Island, Mumbai harbour, western Deccan Traps (see Fig. 8.67). View is oblique, of a face inclined towards the viewer Photo © *Hetu Sheth*

Fig. 5.6 Spectacularly curved and splintery columnar joints in the thick core of a rubbly pāhoehoe flow of the Paraná CFB province, Brazil. The flow overlies another rubbly pāhoehoe flow whose reddened, brecciated top is seen just above the road. Geologist is Fernando Varella
Photo © *Carla Barreto*

Fig. 5.7 Very large, prominently curved columns in basaltic andesite at Sanmenxia, Henan. This lava flow is part of the 1780 Ma Xiong'er volcanic province of the North China craton. More information: Peng (2010)
Photo © *Peng Peng*

Fig. 5.8 Slightly curved basalt columns, exposed in the Chhindwara-Narsinghpur section, Mandla lobe, northeastern Deccan Traps Photo © *Raymond Duraiswami*

Fig. 5.9 Two symmetrical sets of columnar jointing within a so-called brown dolerite dyke in SE Iceland (e.g., Klausen 2006), which during their formation presumably propagated inwards from both chilled contacts and connected along the last crystallized central plane of the dyke. Halfdís Eygló Jónsdóttir provides a scale Photo © *Martin B. Klausen*

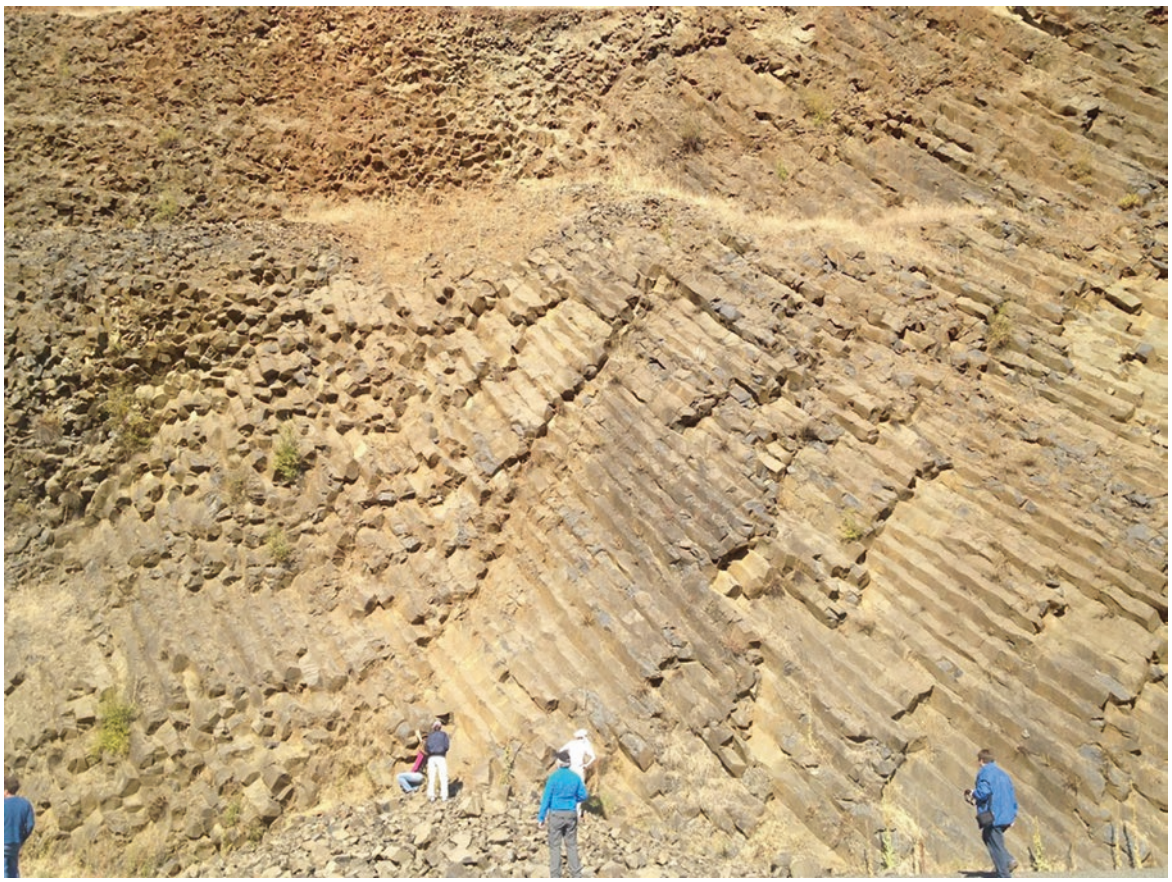

Fig. 5.10 Large, inclined basalt columns in the water-cooled entablature of a lava flow of the Columbia River Basalt Group. Locality just north of Kendrick, Idaho on Highway 3
Photo: *Laszlo Kestay (Keszthelyi), US Geological Survey*

Fig. 5.11 Large, inclined basalt columns in the water-cooled entablature of a lava flow of the Columbia River Basalt Group. Locality just north of Kendrick, Idaho on Highway 3
Photo: *Laszlo Kestay (Keszthelyi), US Geological Survey*

Fig. 5.12 The contact between colonnade and entablature (Tomkeieff 1940) in an olivine tholeiite lava flow of the Talisker Bay Group. Preshal More, Isle of Skye, Scotland. The entablature of the flow is several times as thick as the colonnade, and the whole flow 120 m thick. More information: Williamson and Bell (1994)
Photo © *Hetu Sheth*

Fig. 5.13 Colonnade-entablature boundary in a basalt flow on the east side of the Columbia River, at the Sentinel Gap, Washington. Doreen Philpotts provides a scale. Topographic bench at mid-height of photo is not a flow contact
Photo © *Anthony R. Philpotts*

Fig. 5.14 A Plio-Pleistocene basaltic lava flow (15 m thick), Aldeyjarfoss, Iceland. Note the distinct two-tier structure of the flow with a colonnade of regular joint columns below and an entablature with irregular columns above
Photo © *Hervé Bertrand*

Fig. 5.15 Close-up of a basaltic lava flow with a colonnade tier below and an entablature tier above (see Tomkeieff 1940; Saemundsson 1970; Lyle 2000). Aldeyjarfoss, Iceland. Note the fan-shaped geometry of the colonnade on the left, formed as the lava flow was confined on the left by a valley wall. The exposure is 12 m high
Photo © *Hervé Bertrand*

Fig. 5.16 Columnar jointing in 20 m thick CAMP basalt flow resting above Rhaetian-Hettangian red clays at Agouim, southern High Atlas, Morocco. This is the youngest CAMP basaltic flow ("Recurrent Formation") of the High Atlas rift, dated at c. 196 Ma (Verati et al. 2007). Note its colonnade of crudely formed, thicker columns overlain by an entablature zone of irregular, much thinner columns. Geologist is Karine Allenbach. Location southeast of Agouim, 70 km west of Ouarzazate
Photo © *Ralph Neuwerth*

Fig. 5.17 Sharp boundary between the entablature (with chevrons of columns) and the colonnade (vertical columns) in a Deccan basalt flow, exposed in a quarry 20 km west of Rajahmundry, southeastern India
Photo © *P. Senthil Kumar*

Fig. 5.18 Colonnade and entablature in Pliocene basalt of Kars plateau in the Arax (Aras) River gorge in eastern Turkey. The flow is ~50 m thick
Photo © *Vladimir A. Lebedev*

Fig. 5.19 Basaltic lava flow of the Jordan Valley Volcanic Field, a few tens of meters thick, exposed along the Owyhee River canyon in southeastern Oregon, USA. The flow, which unconformably overlies a volcanic and volcaniclastic package, shows well-developed columnar jointing with entablature between upper and lower colonnades. After emplacement via inflation, the flow cooled from the top and bottom, which led to the formation of the colonnades. The entablature probably resulted from interaction with meteoric water that found its way into the molten interior via inflation clefts, which would have led to much quicker and irregular cooling of the core of the flow. This scenario receives support from the presence of many lava dams and well-documented river-lava interaction at this location
Photo © *Ninad R. Bondre*

Fig. 5.20 Well-formed colonnade of lava flow exposed in an abandoned quarry pit, Gangakhed-Ambajogai section, southeastern Deccan Traps. Note the distinct chiesel marks (Ryan and Sammis 1978; Grossenbacher and McDuffie 1995) on many columns. Loÿc Vanderkluysen is the geologist
Photo © *Hetu Sheth*

Fig. 5.21 Well-developed colonnade in Deccan basalt with upright columns showing large-wavelength curvature. Towards the right, the columns significantly depart from the vertical. Amarkantak Group, Chhindwara-Narsinghpur road section, Karabdol, Madhya Pradesh (central India). Geologist is Bandana Samant
Photo © *Dhananjay Mohabey*

Fig. 5.22 Large basalt columns exposed both in section and plan view in the northeastern part of the Paraná CFB province. Erosion has loosened the top columns, some of which have become tilted and even toppled. Geologist is Lucia C. Moraes
Photo © *Hildor J. Seer*

Fig. 5.23 Prominent chiesel marks on joint columns in the colonnade of a Columbia River Basalt, Picture Gorge, Oregon. Note the entablature tier of the same flow immediately above. Geologist is Tony Philpotts
Photo © *Anthony R. Philpotts*

Fig. 5.24 Columnar jointing, Giant's Causeway, County Antrim, Northern Ireland. Outcrop is ~10 m high. The basalt is part of the North Atlantic Palaeogene igneous province. More information: Tomkeieff (1940), Lyle and Preston (1993), Lyle (2000)
Photo © *Chantal Souche*

Fig. 5.25 The 570 Ma Volyn continental flood basalt province in the southwestern part of the East European craton (Shumlyanskyy et al. 2016). This photo shows a quarry in Basaltove village (also known as Yanova Dolyna, at 50.92 N, 26.24 E) with well-developed columnar jointing in a high-Ti basalt flow that belongs to the uppermost Ratne Suite. Person at the centre of the photo provides a scale
Photo © *Leonid Shumlyanskyy*

Fig. 5.26 Pliocene basaltic lava flow with a perfectly formed, 25 m thick colonnade at Svartifoss, Iceland. More information: Tanner (2013)
Photo © *Hervé Bertrand*

Fig. 5.27 Detail of basaltic columns (1.5 m high), Svartifoss, Iceland. Note the well-formed horizontal striations (chiesel marks)
Photo © *Hervé Bertrand*

Fig. 5.28 "Biscuit" segmentation in columnar-jointed basalts of Giant's Causeway, County Antrim, Northern Ireland, part of the North Atlantic Tertiary igneous province
Photo © *Loÿc Vanderkluysen*

Fig. 5.29 "Pile of Dutch cheese" columns (Spry 1962) in a lava flow in a road exposure, Gangakhed-Ambajogai section, southeastern Deccan Traps. Erika Rader is the geologist
Photo © *Hetu Sheth*

Fig. 5.30 Plumose markings on the top surfaces of joint columns, Giant's Causeway, Northern Ireland. The columns are 40–45 cm in diameter
Photo © *Chantal Souche*

Fig. 5.31 Prismatic jointing in small and thin pahoehoe lava lobes, Malshej Ghat, Western Ghats, Deccan Traps. Hammer for scale. Note the dominance of curved-T junctions, with a few T- and Q (quadruple) junctions of the joints (Aydin and DeGraff 1988), and the absence of Y-junctions with angles of 120°, indicating that these surfaces represent the original crusts, or near-surface levels, of the lobes
Photo © *Hetu Sheth*

Fig. 5.32 Top of a columnar-jointed basaltic lava flow showing the well-formed polygonal sections of columns (diameter 30–40 cm) at Kirkjubæjarklaustur, Iceland. The formation is known locally as the "church floor"
Photo © *Hervé Bertrand*

Fig. 5.33 Hexagonal basalt column in cross-section. Exposure is in the Araguari river, between the cities of Sacramento and Araxá, in the northeastern part of the Paraná CFB province, Brazil
Photo © *Hildor J. Seer*

Fig. 5.34 Hourglass columnar jointing in the entablature zone of the Holyoke Basalt flow. Tariffville gorge, Hartford Basin of Connecticut, USA. The basalt is a part of the 200 Ma Central Atlantic Magmatic Province (CAMP). Geologist is Loÿc Vanderkluysen
Photo © *Hetu Sheth*

Fig. 5.35 Hourglass columnar jointing in a Deccan basalt flow in central India. Location is near Ghatia, about 23 km NNE of Ujjain, Madhya Pradesh (central India). The legs of a person standing in the top right corner provide a scale
Photo © *P. Senthil Kumar*

Fig. 5.36 Radiating sets of columnar joints in the entablature of a Columbia River Basalt flow near Austin, Oregon
Photo © *Anthony R. Philpotts*

Fig. 5.37 A "war bonnet" structure (Waters 1960) in the intracanyon Pomona Member, Saddle Mountains Basalt, Columbia River Basalt Group. At this location (Mesa, Washington), the Pomona lava is just emerging from the ancestral Salmon-Clearwater River Canyon into the Pasco Basin of central Washington State. Note well-developed spheroidal weathering in the area of convergence of the columns. Geologist is Simone Cogliati
Photo © *Stephen P. Reidel*

Fig. 5.38 War bonnet structure in the Columbia River Basalt Group. Location: Mesa, Washington. The radiating columns are of the intracanyon Pomona Member, Saddle Mountains Basalt. This feature is in the same roadcut as the preceding. Geologist is Karoly Németh
Photo © *Stephen P. Reidel*

Fig. 5.39 Another war bonnet structure in the Pomona Member, Saddle Mountains Basalt, Columbia River Basalt Group. Location: Mesa, Washington. This feature is in the roadcut facing the preceding two examples. Karoly Németh provides a scale
Photo © *Stephen P. Reidel*

Fig. 5.40 Complex radiating patterns of columnar joints in a thick Columbia River Basalt flow in Devil's Canyon, north of Walla Walla, Washington. Cliff face is approximately 25 m high
Photo © *Anthony R. Philpotts*

Fig. 5.41 Chevron columnar jointing, consisting of many small individual fans of cooling columns, chaotically arranged. This is the entablature; no colonnade is present. The flow is underlain by a thin "red bole" horizon (orange), below which is reddened and oxidized flow-top breccia of the underlying flow. In the top left corner are parts of this flow's top breccia and the colonnade of another flow. Dive Ghat section, Pune, western Deccan Traps. Raymond Duraiswami watches out for traffic before crossing the busy *ghat* road (a road winding up and down a mountain, essentially a pass)
Photo © *Nasrrddine Youbi*

Fig. 5.42 (**a–c**) Titan's Piazza, a poorly known and maintained geological site in the Mount Holyoke Range in Massachusetts, USA. This is 200 Ma CAMP basalt with a highly unusual and striking jointing pattern of the entablature, above a regular colonnade (with chiesel marks, and a 28 cm long hammer for scale). The entablature's jointing pattern resembles the "bow-tie" patterns formed by surface traces of curviplanar joints described from Jurassic dolerite in Tasmania (Hill 1965, see his Fig. 3). Geologist is Loÿc Vanderkluysen. Thanks to Tony Philpotts for directing us to this site Photos © *Hetu Sheth*

Fig. 5.43 A large fan of beautifully curved and downward-diverging joint columns in the entablature of a Deccan basalt flow of the Kalisindh Formation, Malwa Group. Vishal Verma provides a scale. Location is Singhana, Dhar district, Madhya Pradesh (central India). In the Columbia River province, this structure would be called a "war bonnet"
Photo © *Dhananjay Mohabey*

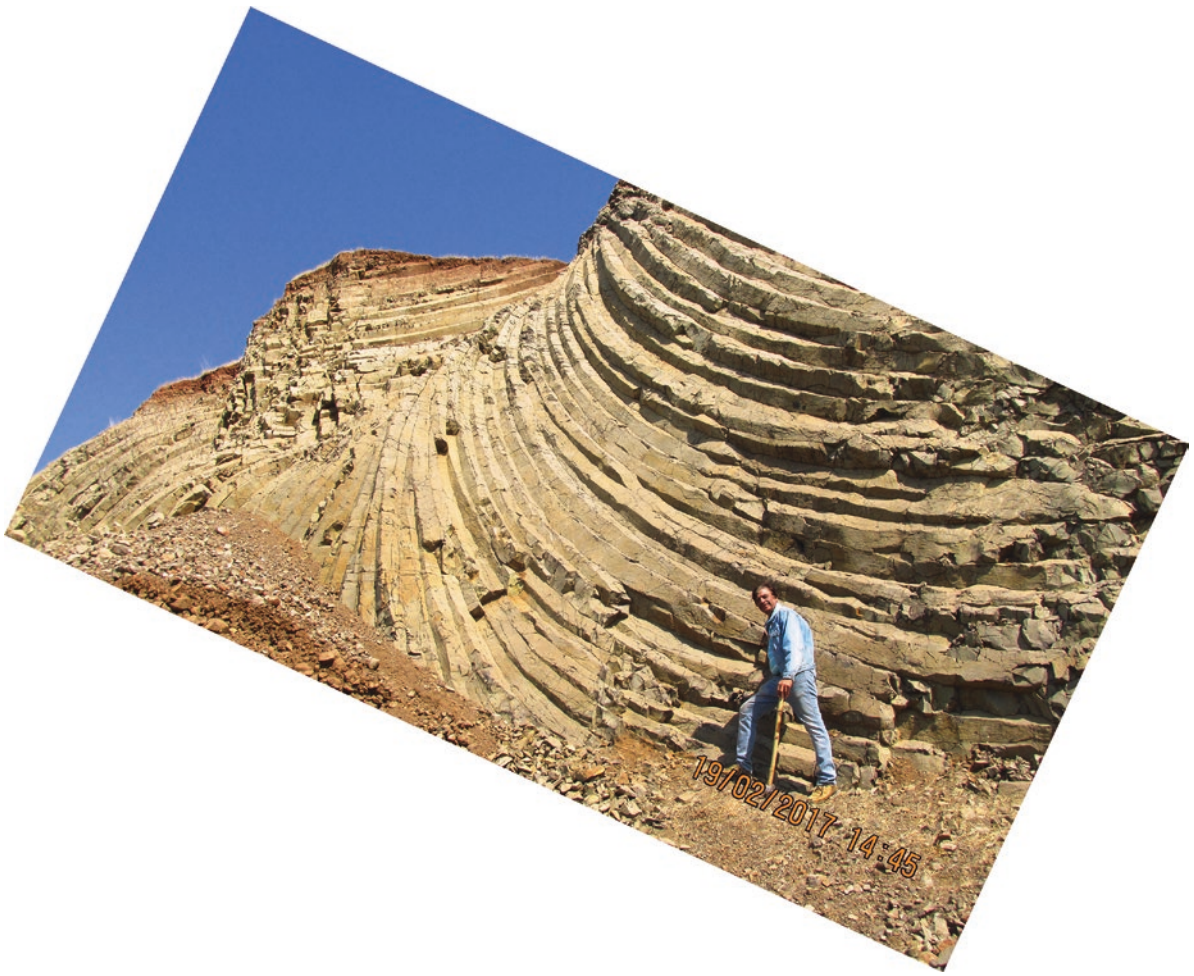

Fig. 5.44 Close-up of a striking example of a large fan of joint columns diverging downward in the entablature of a Deccan basalt flow of the Kalisindh Formation, Malwa Group. Location is Singhana, Dhar District, Madhya Pradesh (central India). Dhananjay Mohabey is the geologist
Photo © *Dhananjay Mohabey*

Fig. 5.45 Detail of a zone of distinctly platy, horizontal jointing at the base of a pāhoehoe sheet lobe and above a brown bole which was not disturbed by the flow of lava above. Above the zone of platy jointing is the entablature of this sheet lobe with many randomly oriented columnar joint sets, some of which are very small-scale and horizontal (as seen here, thus forming polygons in vertical faces). Such a geometry may indicate continued passage of meteoric water along a vertical fracture. No colonnade exists. Location 3 km southwest of Talaja on the road to Mahuva, in Saurashtra, northwestern Deccan Traps. Geologist is Tarulata Das; see also Figs. 3.33, 12.14
Photo © *Vivek Ghule*

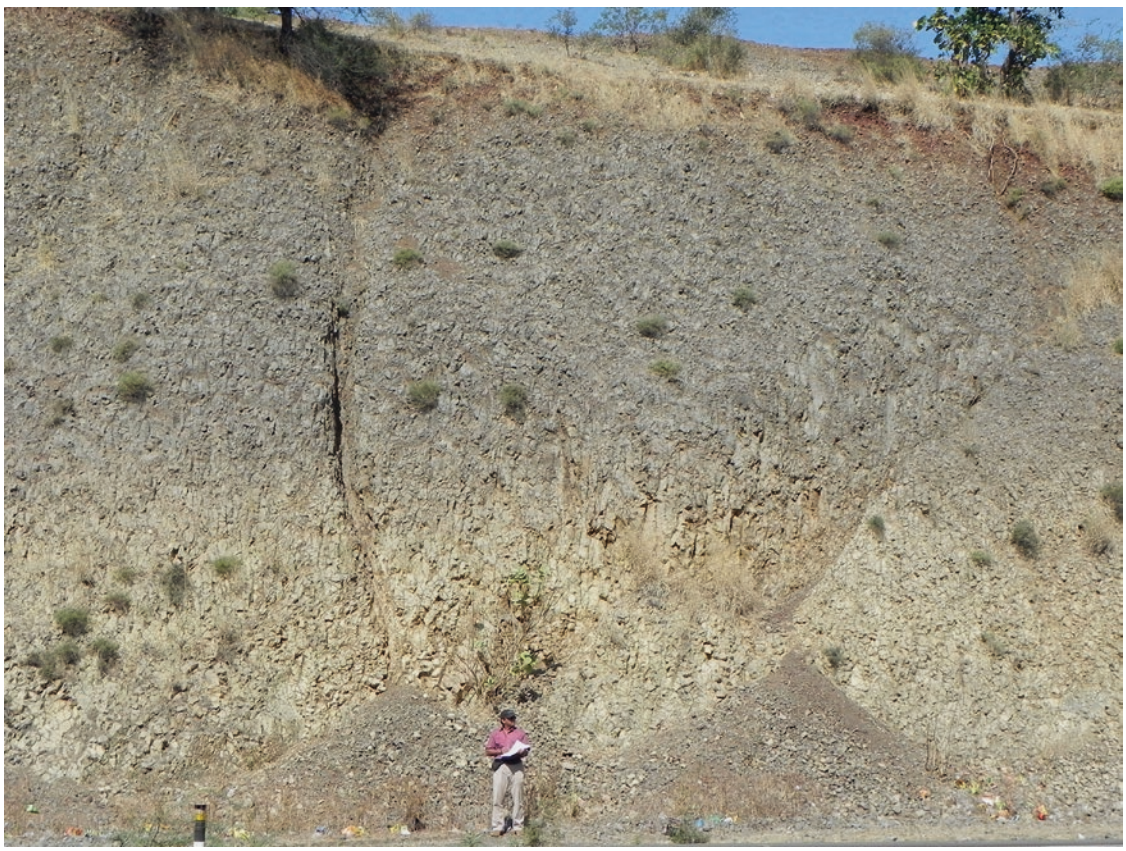

Fig. 5.46 Thick entablature zone (10 m exposed) with very small and irregular columns throughout. Location 18 km west of Chotila on the highway to Rajkot, Saurashtra, northwestern Deccan Traps. Geologist is Hetu Sheth. On his left is a master joint, and such subvertical joints are approximately regularly spaced in the flow at 7 m distance
Photo © *Vivek Ghule*

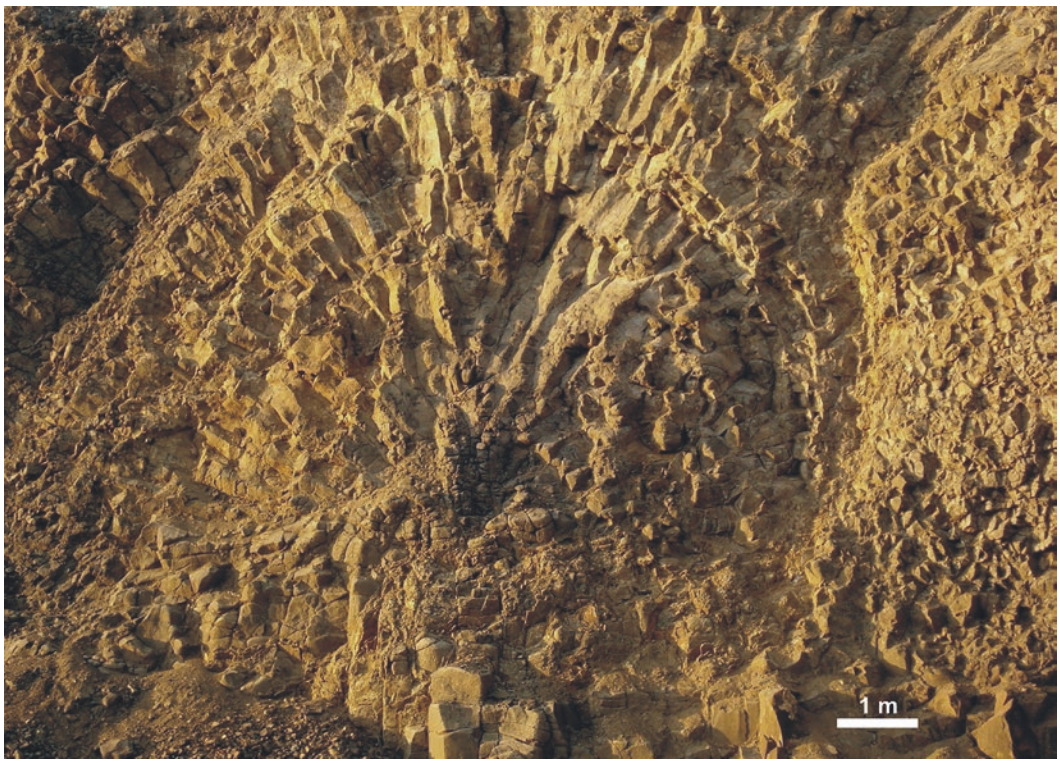

Fig. 5.47 Large, almost complete rosette of joint columns developed in the entablature zone just above the colonnade. View is of a vertical section in a quarry face. The Rajahmundry Traps, Duddukuru area, Andhra Pradesh (see Sen and Sabale 2011)
Photo: *Bibhas Sen, Geological Survey of India*

Fig. 5.48 Cliff of ~80 m height in the Snake River canyon, USA, showing numerous stacked pāhoehoe flows of tabular geometry with occasional thin interbeds of volcaniclastic material indicating that effusive and explosive eruptions alternated in this area. The large vertical face with radial jointing is the eroded entablature tier of a thicker flow. Its colonnade, with much more regular, vertical columns, is situated just below the entablature
Photo © *Karoly Németh*

Fig. 5.49 Large partial rosette of joint columns surrounding flow-top breccia in the Koya quarry, Koynanagar, southwestern Deccan Traps. Note the chilling of the lava against the breccia core (indicated by finer-scale jointing), gradual widening of the columns away from the breccia core, and their eventual mergence with the massive flow core. More information: Sheth et al. (2011a, 2017b)
Photo © *P. Senthil Kumar*

Fig. 5.50 Core of a pāhoehoe sheet lobe with narrow zones of small, transverse (subhorizontal) joints. These transverse joint sets probably formed alongside a subvertical fracture which transported meteoric water into the cooling flow. Section near Asifabad, southeastern Deccan Traps. Note also the stubby, horizontal columns with their cross-sections exposed in the vertical face directly above geologist Erika Rader
Photo © *Hetu Sheth*

Fig. 5.51 Joint in the 3.35 Ga Jayachamarajapura (J. C. Pura) komatiite (Western Dharwar craton, India) which allowed the transport of meteoric water, producing small-scale prismatic jointing in the komatitite lava in both joint walls, pointing inwards. Geologists are Mahua Yadav (left) and Samarpita Sarkar (right). Compare Fig. 5.50
Photo © *Kenneth Chakma*

Fig. 5.52 Detail of joint that transported meteoric water in the 3.35 Ga Jayachamarajapura (J. C. Pura) komatiite, and the small, stubby joint prisms of lava that grew perpendicular to the joint and away from each other
Photo © *Kenneth Chakma*

Fig. 5.53 Polyhedral jointing in the crust of an Archaean komatiite lava flow. Kunikenahalli-Kodihalli section, Banasandra greenstone belt, Western Dharwar craton, southern India. Komatiites are important constituents of Archean flood basalt sequences (e.g., Arndt et al. 2008), and Palaeoarchaean (3.38–3.35 Ga) komatiites from southern India were erupted as high-temperature (~1450 °C), low-viscosity lavas that produced thick and massive, polyhedral-jointed sheet flows with sporadic flow-top breccias. More information: Jayananda et al. (2016)
Photo © *Raymond Duraiswami*

Fig. 5.54 Polyhedral jointing in the upper crust of the Jayachamarajapura (J. C. Pura) komatiite, southwest of Shashivala, Karnataka, southern India. The J.C. Pura belt is one of several 3.35 Ga Sargur Group greenstone belts in the Western Dharwar craton. More information: Jayananda et al. (2008), Prabhakar and Namratha (2014)
Photo © *Kenneth Chakma*

Fig. 5.55 Pervasive jointing in a rhyolite lava flow of the Serra Geral Formation, Paraná CFB province. Geologists are Lucas Magalhães May Rossetti and Carla Joana Santos Barreto
Photo © *Carla Barreto*

Fig. 5.56 Plan view of well-formed joint columns in late-stage Deccan trachyte intrusions at Manori Island, Mumbai
Photo © *Hetu Sheth*

Subaqueous Flood Basalt Volcanism, Volcanosedimentary Associations, and Lava-Sediment Interaction

6

Fig. 6.1 Pillow lavas formed when a basaltic lava flow of the Miocene (16 Ma) Columbia River CFB province reached the Pacific Ocean. Location is Depoe Bay, Oregon, USA. The basalt pillows are present in a matrix of pillow breccia, which forms when pillows emplaced on steep slopes roll down and break. Several well-preserved pillows display glassy chilled margins; the largest pillow is 1 m wide
Photo © *Hervé Bertrand*

H. Sheth, *A Photographic Atlas of Flood Basalt Volcanism*, https://doi.org/10.1007/978-3-319-67705-7_6

Chapter Overview

Subaqueous counterparts of the subaerial flood basalts, whether formed under the sea in an oceanic plateau or along a rifted volcanic margin, or in inland lakes and rivers, are exposed in many places due to erosion or tectonic uplift (e.g. Kerr et al. 2000). Icelandic subglacial eruptions also create lakes of meltwater with deposits of pillow lavas, hyaloclastites and tuffs. Pillow lavas are analogous to small-scale compound pāhoehoe lava flows that form subaerially, and form in the same effusive manner as the latter. Flood basalt lava flows can be interstratified with sedimentary strata (called *intertrappeans* in the Deccan literature). Sills and even lava flows (called invasive flows) may invade such strata. Mingling between lava and soft, unconsolidated, typically wet sediment produces heterogeneous rocks called peperites.

The same pillow lavas that are seen in the Phanerozoic flood basalt provinces are found in Archaean and Proterozoic flood basalts, sometimes in a surprisingly good state of preservation. Chilled pillow margins in the 200 Ma CAMP basalts in Morocco have fresh glass still preserved. The physical features of the subaqueous volcanic deposits, their secondary (alteration) minerals, and their associated sedimentary deposits can provide clues about the palaeogeography and palaeoenvironments (lacustrine, riverine, marine) and emplacement depths, and thus constrain tectonic models.

Pillow lavas in the central part of the huge, Permian/Triassic Siberian Traps indicate large-scale subsidence associated with the flood basalt eruptions. Good exposures of the 200 Ma CAMP pillow lavas are found in northeastern USA, as around Paterson, New Jersey where they are now surrounded by or located under people's homes. The Deccan Traps, dominated by subaerially erupted lava flows, has few localities of pillow lavas throughout its large extent. Among these few is Mumbai City, on the Arabian Sea, with beautifully formed spilitized pillow lavas at several places. These pillowed spilites have been the subject of some commendable early work (e.g., Sukheswala 1974), and several quarries in them have yielded beautiful zeolites and associated minerals (Ottens 2003). All of these pillow lava sections, as of today, are within housing colonies and slums, an information technology park with access restrictions (even photography), and a reserved forest with similar restrictions. Working on these pillowed spilites today, with necessary safety and due official permissions from the concerned authorities, involves such bureaucratic red tape that any investigator will prefer to spend his time and energy elsewhere. It is thus ironic that, in a time when much new sophisticated analytical instrumentation is available to study these fascinating rocks, the very access to them is practically impossible. It is unsurprising therefore that the pillowed spilites of Mumbai have received no attention in recent decades; many researchers abroad who are not familiar with the older literature on the Deccan, or Mumbai geology, may not know that they exist.

Fig. 6.2 Pillow lavas in the Central Atlantic Railway section near Uberlândia city, northeastern part of the Paraná CFB province, Brazil. More information: Moraes and Seer (2017). Geologist is Lucia C. Moraes
Photo © *Hildor J. Seer*

Fig. 6.3 Closely packed and elongated pillows of heavily spilitized Deccan basalt in an abandoned quarry at Bagwada, near Daman, western India. Geologist is Sultan Ali. More information: Sethna and Javeri (1999); see also Sukheswala (1974) for an example from Mumbai, western India
Photo © *Sultan Ali*

Fig. 6.4 Pillow facies of the Palaeogene MacCulloch's Tree Lava, ca. 100 m south of MacCulloch's Tree [UK Ordnance Survey Grid Reference: NM 4027 2772], Ardmeanach Peninsula, Isle of Mull, NW Scotland. A thickness of at least 10 m of pillow- and tube-like lava overlies the basal invasive facies of the lava. The classical colonnade-entablature couplet is absent. Eruption of the flow into water is implied by the development of pillow structures. Person for scale
Photo © *Brian R. Bell*

Fig. 6.5 Stack of large bulbous pillows emplaced in the lacustrine interflow sediments between lava flows of the Deccan Traps at Rajakul, near Chhindwara, Madhya Pradesh (central India). Note the presence of pillow breccia, spallings and sediments in between the pillows. Lacustrine sedimentation and formation of pillow lavas within these lakes were common in parts of the Mandla lobe, northeastern Deccan Traps
Photo © *Raymond Duraiswami*

Fig. 6.6 The Tunguska Syncline region of the central part of the Siberian Traps near Tura settlement (Ivanov et al. 2013). The 30 m high cliff exposes pillow lava and pillow breccia of the lower Nidym Formation. Note geologist in the lower right corner of the photo; the Tunguska River is seen in the background
Photo © *Alexei V. Ivanov*

Fig. 6.7 Basalt pillows in the Ginkgo pillow-palagonite complex at Sand Hollow, Washington, Columbia River flood basalt province (see Fig. 6.13, 6.17). The yellow, fragmental matrix between the pillows is pillow breccia and hyaloclastite, largely converted to palagonite (hydrated basaltic glass)
Photo © *Hetu Sheth*

Fig. 6.8 Pillow lavas embedded in hyaloclastite and underlying the Kirkpatrick Basalt lava sequence at Carapace Nunatak, south Victoria Land, Antarctica. Foreset bedding is inclined down to the left. Backpack at base of cliff for scale
Photo © *David H. Elliot*

Fig. 6.9 Elongated basalt pillows in 3D. Stream bed about 10 m wide in the Sanjay Gandhi National Park, Borivli, Mumbai, western Deccan Traps. Connections between adjacent lava pillows and the budding and bifurcation of pillowed lobes are beautifully seen in this outcrop
Photo © *Nasrrddine Youbi*

Fig. 6.10 Closely packed pillow lavas forming a 22 m high cliff section just south of Tumanyan railway station, northern Armenia. Geologist is Arsen Israyelyan; white patches above him are pillow breccia. More information: Sheth et al. (2015)
Photo © *Hripsime Gevorgyan*

Fig. 6.11 Basalt pillows in the Orange Mountain Basalt, part of the so-called Newark or Watchung flood basalts (CAMP) in New Jersey, USA. Location is New Street Quarry, Paterson, New Jersey. Whitish patch on the left, above the hammer, is pillow breccia. Vertical face, hammer 28 cm long. The rocks have just been washed by a rain shower. More information: Lewis (1915), Faust (1975), Puffer and Student (1992). Thanks to Chris Laskowich for his guidance at this and nearby sites
Photo © *Hetu Sheth*

Fig. 6.12 Basalt pillows in a hyaloclastite matrix at the base of a lava flow from the Intermediate Formation of the CAMP, in the Oued Lhar (Herrissane) section of the central High Atlas, Morocco. Details in El Ghilani et al. (2017)
Photo © *José Madeira*

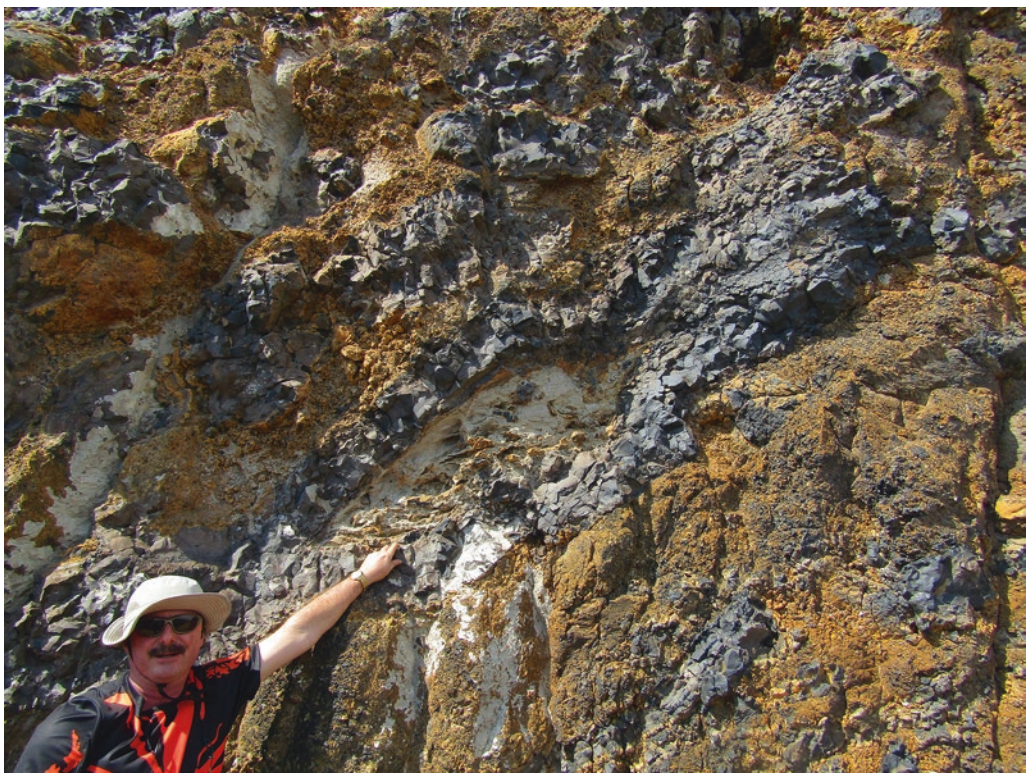

Fig. 6.13 Elongated pillows in the Ginkgo basalt (Frenchman Springs Member) pillow-palagonite complex at Sand Hollow, Washington, Columbia River flood basalt province (see also Fig. 6.7, 6.17). The elongation and dip of the pillows create the equivalent of foreset beds in a delta, indicating the direction of flow of lava (e.g., Tolan and Beeson 1984; Hooper 1997). Geologist Karoly Németh has his hand on a very large pillow, at the photo centre, which incorporated unconsolidated, sandy sediment during its growth, with the development of peperite in its core
Photo © *Hetu Sheth*

Fig. 6.14 Beautifully preserved primary features of basalt pillows at Maradihalli, in the Late Archaean (~2.8 Ga) Chitradurga greenstone belt, Western Dharwar craton, India. Note the convex tops and glassy rinds of the pillows, with chert filling the interpillow spaces. Note also the spherical vesicles under the chilled margin in some of the pillows (e.g., lower right corner of photo), the radially arranged pipe vesicles (and radial fractures) in the pillows, and varioles (dark rounded spots, e.g., above the camera lens). More information: Duraiswami et al. (2016)
Photo © *G. N. Jadhav*

Fig. 6.15 Pillow lava at Sanmenxia, Henan, part of the 1780 Ma Xiong'er volcanic province of the North China craton. More information: Peng (2010)
Photo © *Peng Peng*

Fig. 6.16 Pillow-palagonite complex for the Rosalia flow, Priest Rapids Member, Wanapum Basalt, Columbia River Basalt Group. At this location the flow entered a lake caused by damming of the Columbia River by the Roza flow, Wanapum Basalt. The cliff is 25 m high. Location: The Dalles, Oregon at the intersection of Highways 30 and 197
Photo: *Laszlo Kestay (Keszthelyi), US Geological Survey*

Fig. 6.17 The large pillow-palagonite complex of Ginkgo basalt (Frenchman Springs Member) at Sand Hollow, near Vantage, Washington, Columbia River flood basalt province. The complex is overlain by subaerially emplaced lava. The distinct bright yellow-orange-brown colouration that pervades the pillow-palagonite complex (see also Fig. 6.7, 6.13) is due to the extensive alteration of glass to palagonite. White patches are caliche. Geologist Patrick Hayman provides a scale. More information: Reidel et al. (2003, 2013a, b)
Photo © *Hetu Sheth*

Fig. 6.18 Section in the base of the Intermediate Formation of the CAMP, in the Oued Lhar (Herrissane) section of the central High Atlas, Morocco. The whole section is cut through a single flow whose base is subaqueous and the top subaerial. Divisions 1–4 shown in the photo are (1) densely packed pillows, (2) pillows dispersed in hyaloclastite, (3) transition zone between the subaqueous and subaerial parts, and (4) the subaerial part of the flow. Geologist at the base of the cliff is Idris Ali Ahmadi Bensaid. Details in El Ghilani et al. (2017)
Photo © *Nasrrddine Youbi*

Fig. 6.19 Pillow breccia at the top of the Upper Formation of the CAMP, in the Aït Ourir section of the central High Atlas, Morocco. These breccias form when pillows emplaced on steep slopes detach, roll down and break; locally some well-preserved pillow lavas are found inside the breccia confirming the subaquatic origin of the deposit
Photo © *Nasrrddine Youbi*

Fig. 6.20 Pillow breccia in the 200 Ma Orange Mountain Basalt (CAMP), New Street Quarry, Patterson, New Jersey, USA. Pen is 15 cm long. More information: Puffer and Student (1992) Photo © *Hetu Sheth*

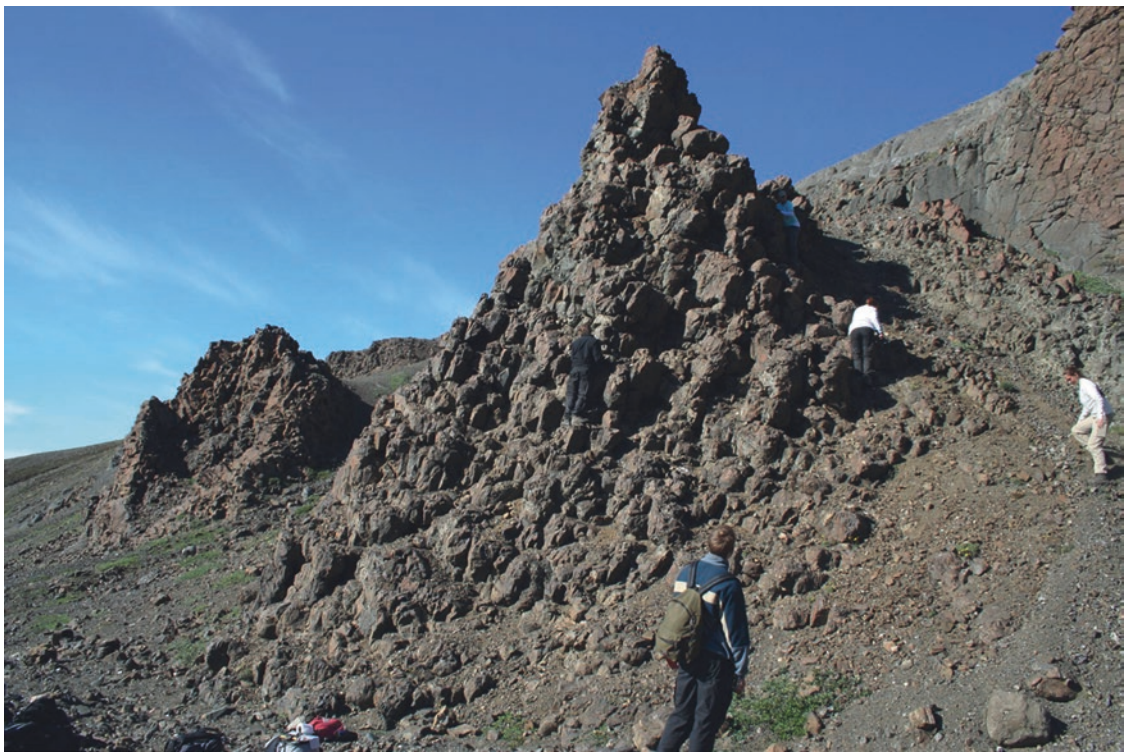

Fig. 6.21 Submarine eruption site in basaltic hyaloclastites. The conical mounds of close-lying pillows are 10–20 m high and appear to be aligned along one or more linear features. They are found over a distance of *c*. 200 m and are interpreted as a submarine eruption site with the mounds reflecting points of magma emission above one or more fissures. The pillow mounds are covered by foreset-bedded hyaloclastites with about 400 m high foresets indicating the water depth at the time. Lower Vaigat Formation, central Nuussuaq, West Greenland Photo: *Lotte Melchior Larsen, Geological Survey of Denmark and Greenland (GEUS)*

Fig. 6.22 Typical hyaloclastite ridge in southwestern Iceland. These ridges are the products of subglacial fissure eruptions during successive Pleistocene glaciations in Iceland, and are more numerous than tuyas (table mountains). Unlike the tuyas, the ridges commonly do not have basal pillow lavas or subaerial lava caps and hyaloclastite deltas at their summits. More information: Schopka et al. (2006), Jarosch et al. (2008)
Photo © *Hetu Sheth*

Fig. 6.23 The table mountain (tuya/stapi) Herðubreið, of the Askja volcanic system in north Iceland. Herðubreið (1686 m above sea level) rises about 1000 m above its surroundings and is generally believed to be a prime example of a construct from a subglacial, central-vent eruption. The pedestal is built of pillow lavas and hyaloclastite breccias and lapilli tuffs, while the tuya is capped by a pāhoehoe lava and associated pillow lava delta emitted from a vent at the very top
Photo © *Thorvaldur Thordarson*

Fig. 6.24 The western Snake River cuts deeply into a Pliocene volcanic province formed by an extensive lava field, associated lava shields and several phreatomagmatic and magmatic explosive eruptive centres. In the canyon walls is exposed a thick succession of relatively thin (meter-scale) pāhoehoe lava flows, forming the main succession. Sinker Butte (the broad pyramid rising from behind the distant cliffs) is a large volcano that grew in a subaqueous environment and then became emergent, and is dominated by volcanism driven by magma-water explosive interaction
Photo © *Karoly Németh*

Fig. 6.25 Exposed lava delta along the Snake River canyon shows that lava flows entered water where pillow lavas and hyaloclastite (brown matrix that hosts irregular blobs of dark lava in the right foreground) formed, and fed volcaniclastic sediments to the lacustrine basin. Cliff is ~120 m high
Photo © *Karoly Németh*

Fig. 6.26 Subaerial thin brown basalt lava flows (at left) pass through a shore zone into a deep marine basin and change facies to form foreset-bedded hyaloclastites. The thin black hyaloclastite horizon can be followed from the palaeoshore to the basin floor and indicates a water depth of close to 500 m. The brown lava flows and hyaloclastites belong to the crustally contaminated Nuuk Killeq Member and are covered by grey picrite flows and hyaloclastites from the Naujánguit Member. Height of field of view 750 m. Vaigat Formation, south coast of Nuussuaq, West Greenland
Photo: *Asger Ken Pedersen, Geological Survey of Denmark and Greenland (GEUS)*

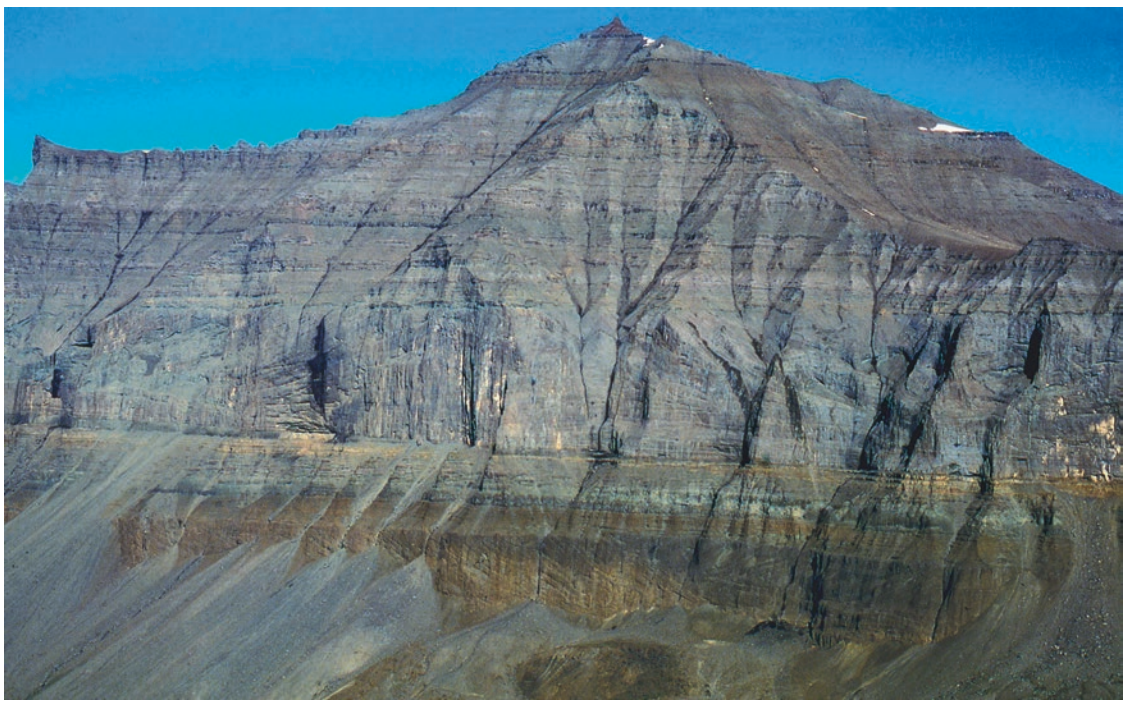

Fig. 6.27 This *c*. 1100 m high mountain wall shows intercalated uncontaminated olivine-rich picrites (grey) and crustally contaminated basalts (rusty brown) in both subaerial flow facies and subaqueous foreset-bedded hyaloclastite facies. The foresets dip in several directions. Vaigat Formation, south coast of Nuussuaq, West Greenland (Larsen and Pedersen 2009; photogrammetric interpretation in Pedersen et al. 1993)
Photo: *Asger Ken Pedersen, Geological Survey of Denmark and Greenland (GEUS)*

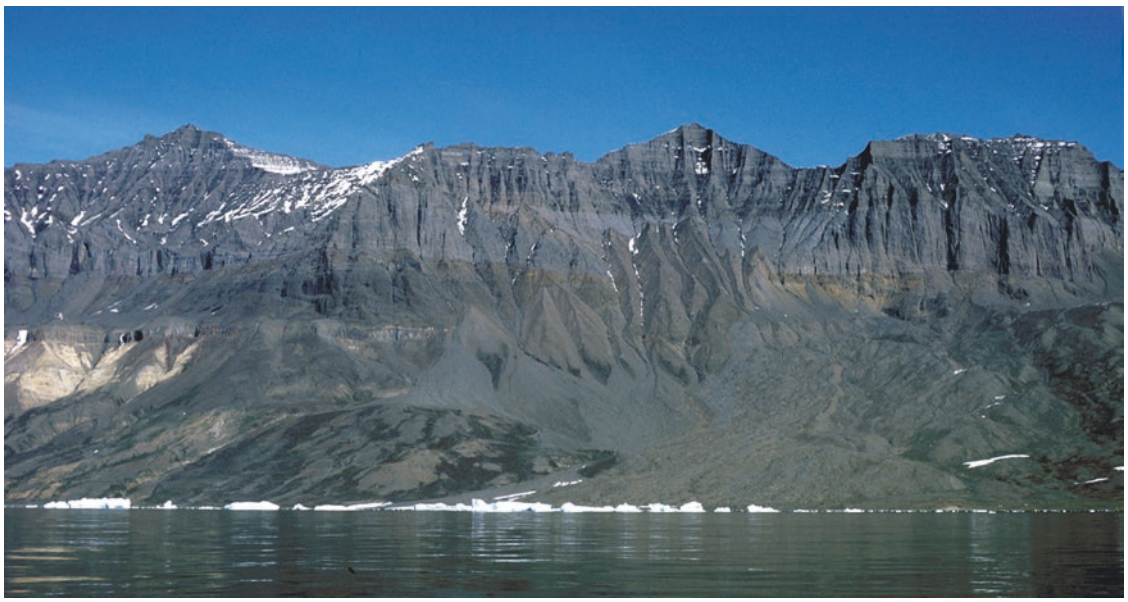

Fig. 6.28 The south coast of Nuussuaq, West Greenland. Light yellow Cretaceous sandstones are overlain by Paleocene volcanic rocks of the Vaigat Formation. Brown, crustally contaminated basaltic to picritic hyaloclastites (massive, foreset-bedded) and associated subaerial lavas (lighter brown) are overlain by grey uncontaminated olivine-rich picrites in both subaqueous (light grey, foreset-bedded) and subaerial (darker grey) facies (photogrammetric interpretation in Pedersen et al. 1993). The peak in the centre-right is 1520 m a.s.l.
Photo: *Asger Ken Pedersen, Geological Survey of Denmark and Greenland (GEUS)*

Fig. 6.29 A 930 m high coastal cliff showing volcanic facies changes with height due to the gradual filling of a lake with volcanic products. From sea level to 160 m there are four subaqueous lava flows with yellowish brown breccia tops; deposits of mudstone have accumulated in the lows on the undulating surface of the lowest flow. These are overlain by a 100 m thick horizon of foreset-bedded hyaloclastites (massive horizon; the foresets dip towards the viewer); the associated overlying subaerial pāhoehoe flows are concealed beneath scree. The following flows are all in subaerial facies with red-oxidised top rubble, indicating that the lake has been obliterated at this locality. Maligât Formation basalts, south coast of Disko, West Greenland
Photo: *Asger Ken Pedersen, Geological Survey of Denmark and Greenland (GEUS)*

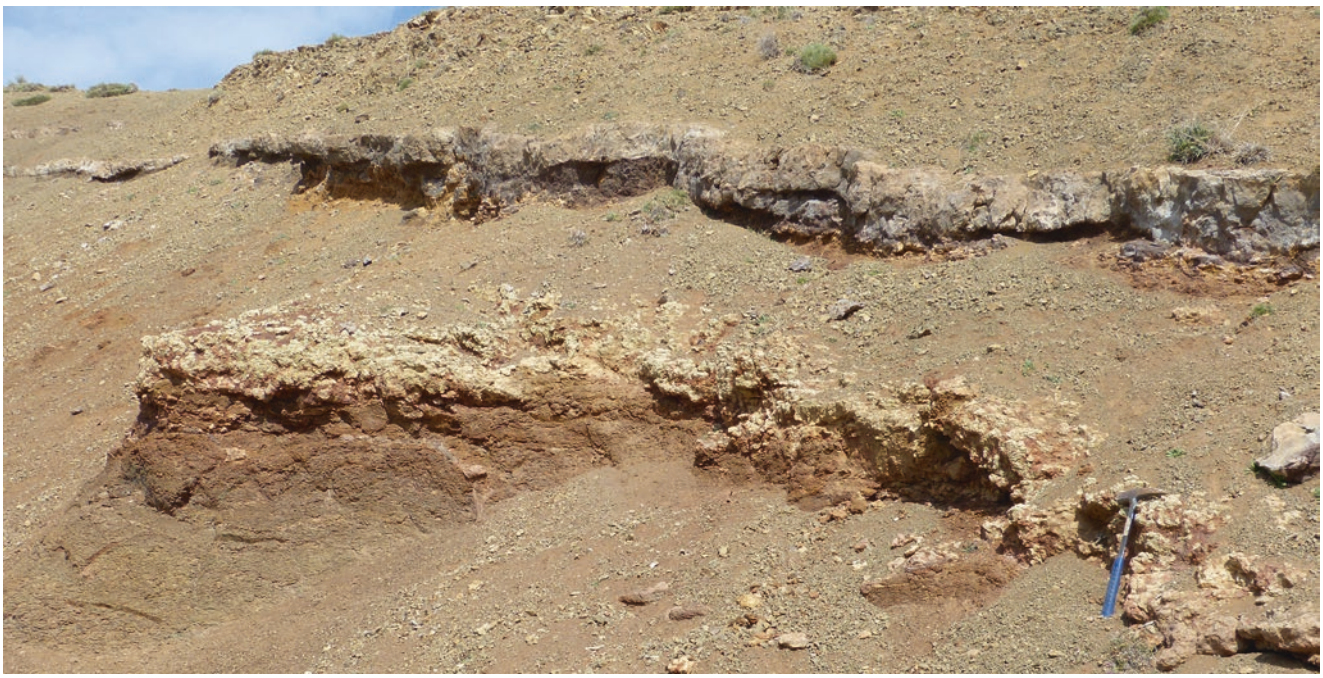

Fig. 6.30 Thin horizon of white limestone between two CAMP basalt flows (dark). Aït Ourir section, High Atlas of Morocco
Photo © *El Hassane Chellai*

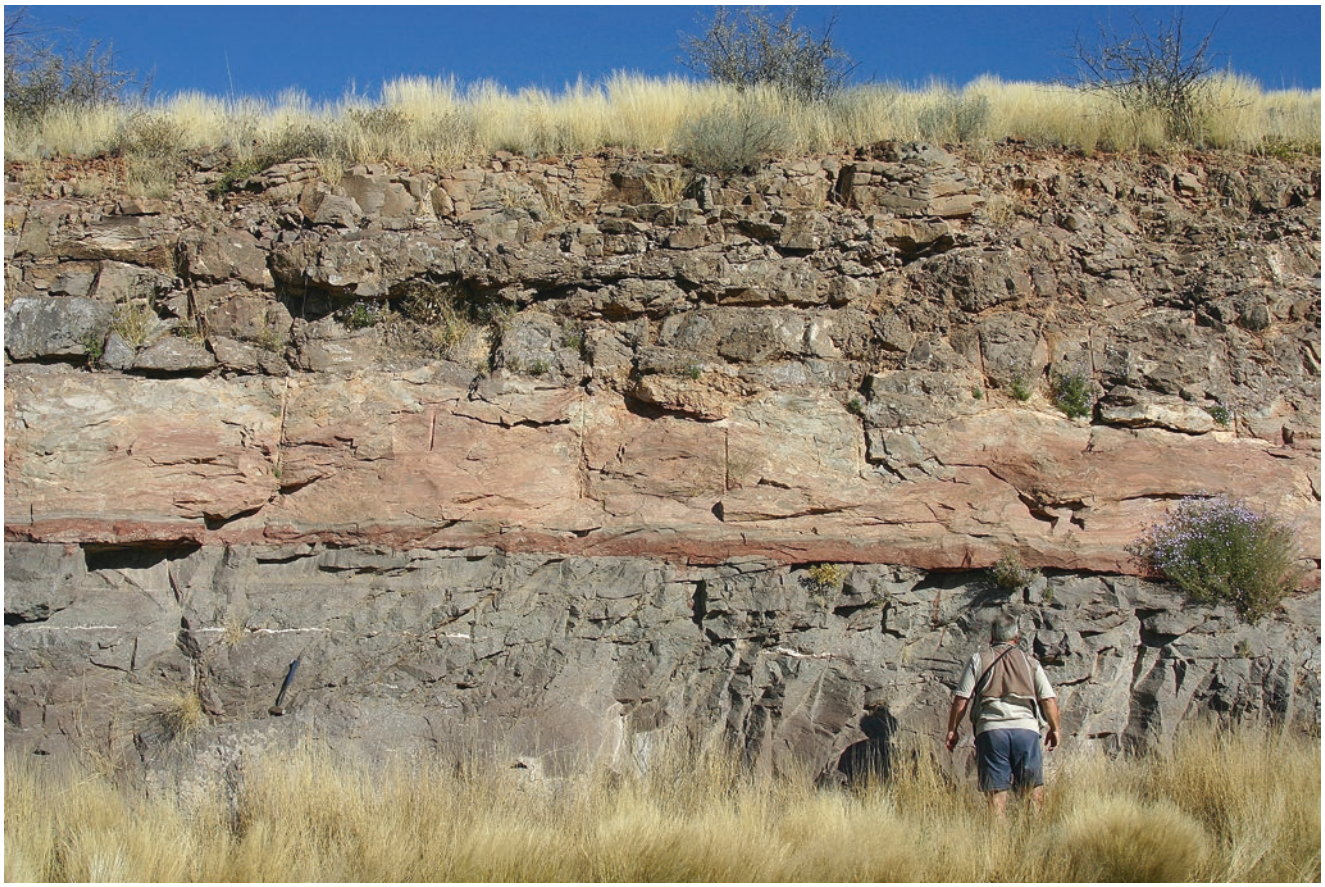

Fig. 6.31 Two Karoo flood basalt lava flows separated by a sandstone bed, Hardap area, Namibia. The geologist is Mike Watkeys
Photo © *Hervé Bertrand*

Fig. 6.32 Sediments between the basalt lava units of the lower (not exposed) and upper Nidym Formation, in the Tunguska Syncline region of the central part of the Siberian Traps (Ivanov et al. 2013). An eruptive hiatus is indicated by the sedimentary interbeds. The vertical distance from the vehicle to the base of the cliff is ~15 m
Photo © *Alexei V. Ivanov*

Fig. 6.33 The contact between the Permian Tungusska coal in an open pit mine in Kaerkan, Siberia, and the overlying Ivakinsky lava, the first lava from the Siberian flood basalts in this area, near 69.33 N, 87.81 E. Little alteration of the coal is observed
Photo © *Linda Elkins-Tanton*

Fig. 6.34 The 135 m thick tachylitic flow at Storm Peak, central Transantarctic Mountains, is glassy to within less than a meter of the upper contact, which is overlain by a sedimentary interbed. The interbed, less than 1 m thick, includes palaeosols containing silicified wood and laminated lacustrine sediments containing fossil conchostracans and fish (Schaeffer 1972; Tasch and Gafford 1984; Stigall et al. 2008). Geologist is Tom Fleming. More information: Elliot and Fleming (2008)
Photo © *David H. Elliot*

Fig. 6.35 Lava flows and pyroclastic deposits from the Central Atlantic Magmatic Province (CAMP) of Algarve (southern Portugal). This photo shows the last lava flow of the ~50 m thick CAMP volcanic pile of the Corcitos section. The interbedded thin layer of red mudstone is affected by normal faults which indicate a horst and graben structure and testify to the CAMP volcanics being part of a syn-rift series. Geologists are Linia Martins, José Munha, José Madeira, Mohamed Khalil Bensalah, Nasrrddine Youbi, Giuliano Bellieni and Angelo De Min
Photo © *Andrea Marzoli*

Fig. 6.36 The Preshal Beg Conglomerate Formation underlying a columnar-jointed, 120 m thick olivine tholeiite lava flow of the Talisker Bay Group, at Preshal Beg, Isle of Skye, Scotland. The conglomerate is immature and dominated by various lava types of local derivation, and indicates local uplift before the eruption of the columnar flow. Ian Norton provides a scale. More information: Williamson and Bell (1994)
Photo © *Hetu Sheth*

Fig. 6.37 Operating quarry in the Rajahmundry Traps, Duddukuru area, Andhra Pradesh, exposing a continuous intertrappean bed of white limestone-marl, underlain by a thick and columnar-jointed lava flow, and overlain by another basalt flow (see Sen and Sabale 2011). The 65 Ma Rajahmundry Traps of southeastern India are contemporaneous with the Deccan Traps of western-central India
Photo: *Bibhas Sen, Geological Survey of India*

Fig. 6.38 Log preserved in lava of the Columbia River Basalt Group at Armour Draw, Washington
Photo: *Laszlo Kestay (Keszthelyi), US Geological Survey*

Fig. 6.39 Tree stump, 50 cm in diameter, enclosed in basalt and rooted in a sedimentary interbed at Mt. Fazio, north Victoria Land, Antarctica. More information: Elliot et al. (1986)
Photo © *David H. Elliot*

Fig. 6.40 Plant mould at the base of a basaltic lava flow (the subhorizontal cylindrical conduit just above pen). Location near Ambajogai, Maharashtra, southeastern Deccan Traps (see Figs. 3.39, 3.40)
Photo © *Erika Rader*

Fig. 6.41 Fossilized tree ("MacCulloch's Tree"), a conifer (*Taxodioxylon*) preserved in a 61 Ma basalt lava flow near the base of the Mull Plateau Group on the coast of the Ardmeanach Peninsula, Isle of Mull, Scotland. Small amounts of charcoal are present along the contacts. Note the change in orientation of the basalt columns, from vertical in the main body of the flow, to inclined and then perpendicular to the tree which acted as a cold inclusion. Geologist is Godfrey Fitton. Linda Kirstein took the photo. More information: Emeleus and Bell (2005)
Photo © *J. Godfrey Fitton*

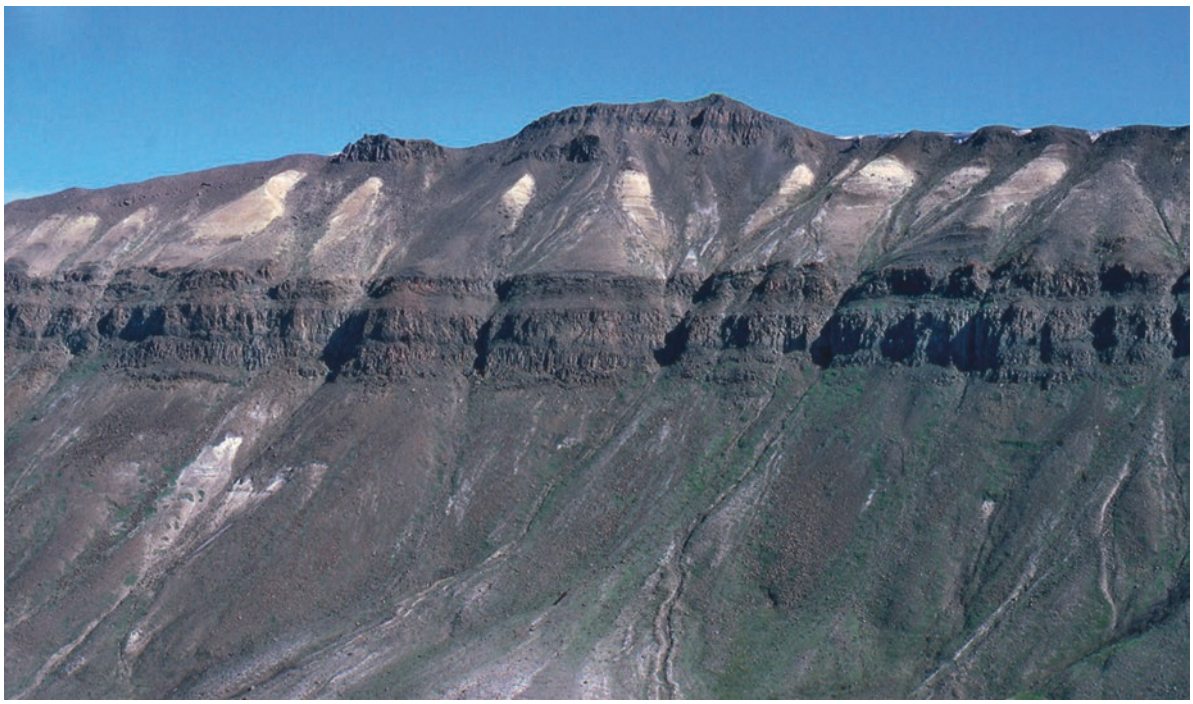

Fig. 6.42 Palaeocene fluvial sandstones with apparent sills that are in fact laterally emplaced invasive basalt lava flows which form normal subaerial flows a few kilometers farther west (to the left). The flows on the skyline are normal subaerial flows. Height of shown section *c*. 400 m. Maligât Formation, south coast of Nuussuaq, West Greenland
Photo: *Asger Ken Pedersen, Geological Survey of Denmark and Greenland (GEUS)*

Fig. 6.43 The Amelal Sill (CAMP) viewed from the Marrakech-Agadir road near Tizi El Hajaj town. The sill intrudes red mudstones of the Aït Hssaine Member, of the Late Triassic Bigoudine Formation, in the Permian to Jurassic Argana Basin of Morocco. The Amelal sill, feeder to the Alemzi Basalt Formation (Upper Argana Basalt), is dated at 201.564 ± 0.054/0.075/0.23 (U-Pb zircon, Blackburn et al. 2013). Cliff is ~100 m in height. More information: El Hachimi et al. (2011)
Photo © *Nasrrddine Youbi*

Fig. 6.44 A dyke of Rajmahal lamproite (tabular body climbing diagonally from behind geologist Ray Kent) passing into a sill between coal seams which show the development of columnar joints. Rocks overlying the coal bed are sandstone and siltstone belonging to the Lower Permian (270–298 Ma) Barakar Formation (Lower Gondwana sequence), a major source of fossil fuel in India. Locality: Ena, 13th seam, OCP-patch A, Kustore, Jharia Coal field, Damodar graben, eastern India
Photo © *Naresh C. Ghose*

Fig. 6.45 Columnar jointing in massive Taylor Group sandstones in contact with a large Ferrar LIP sill capping Terra Cotta Mountain, Antarctica. Host rock in contact with dolerite has also been metamorphosed to quartzite at places near the top of Terra Cotta Mountain
Photo © *Giulia Airoldi*

Fig. 6.46 Columnar Deccan basalt resting over intertrappean sediment (IT) and with a well-developed 30–50 cm thick vesicular zone (VZ) at the base of the flow possibly produced by sediment degassing. Karam river section, Bharudapura, Dhar District, Madhya Pradesh (central India)
Photo © *Dhananjay Mohabey*

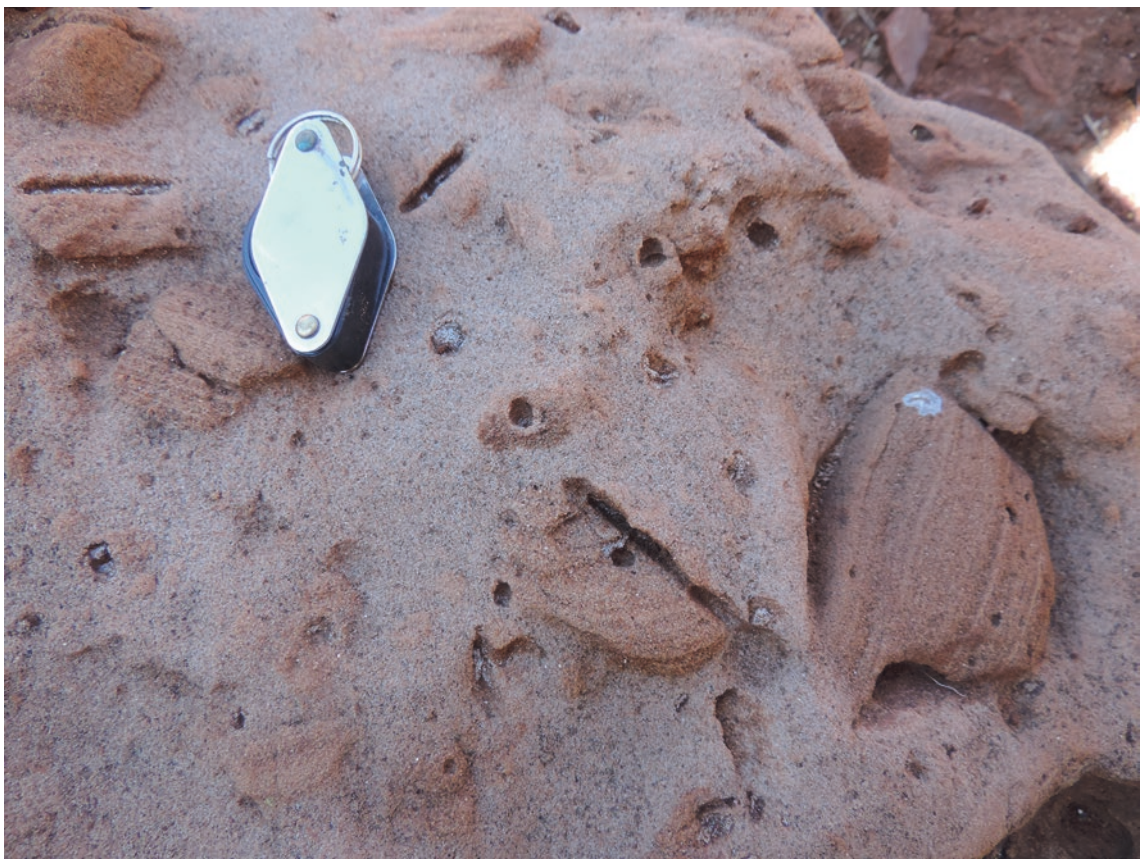

Fig. 6.47 Disrupted Early Cretaceous aeolian sandstone from the Botucatu Formation with abundant degassing pipes formed by lava flow action. Location is in the northeastern part of the Paraná CFB province, Brazil, near Sacramento city
Photo © *Lucia C. Moraes*

Fig. 6.48 Large, slender, clay-filled spiracle exposed in the compound pāhoehoe lavas at Bhuleshwar Ghat, Yewat, Deccan plateau. The spiracle rises from the base of the pāhoehoe lobe (not seen in this photo) and into the vesicular crust. Similar clay-filled spiracles are also exposed at Chekewadi, Ahmednagar. Spiracles are steam injection structures and form when lava flows override sediment-filled puddles. More information: Duraiswami et al. (2003b)
Photo © *Raymond Duraiswami*

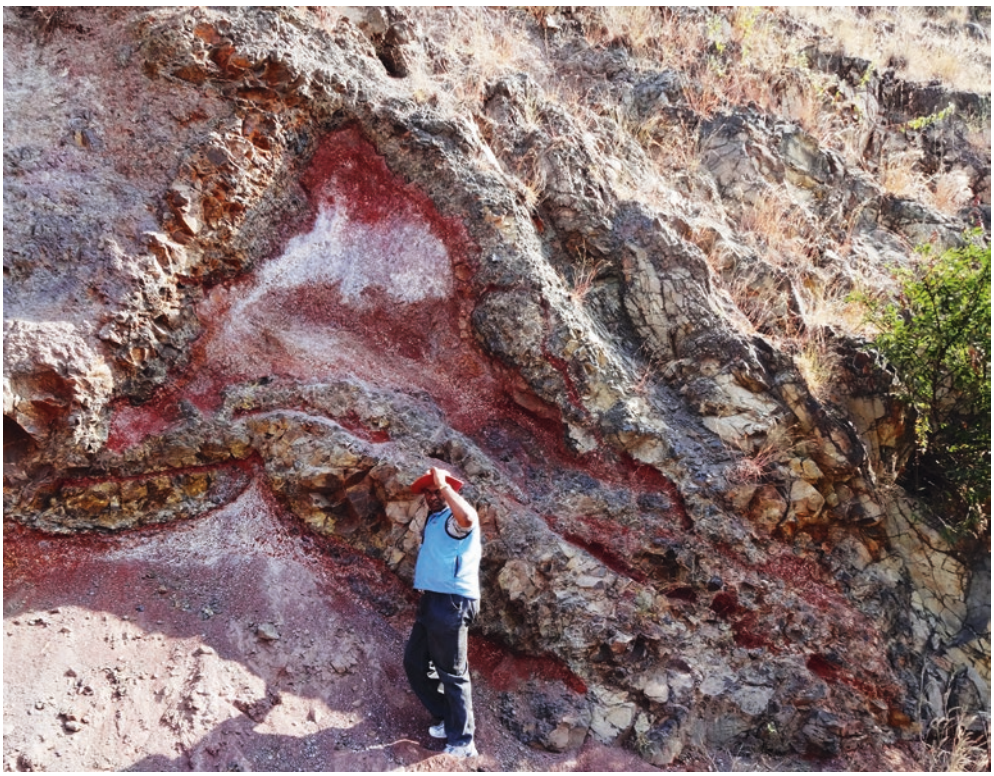

Fig. 6.49 Megaspiracles exposed on the Pune-Bangalore National Highway NH4 near Nipani, southern Deccan Traps. Note the double dome structures of the spiracles. The spiracles are rimmed by blocky peperite. Spiracles like these record lava-sediment interaction within the Deccan Traps (Duraiswami et al. 2003b). Geologist is Raymond Duraiswami
Photo © *Raymond Duraiswami*

Fig. 6.50 A "load cast" at the base of a basaltic lava flow overlying pyroclast-rich clayey sediment, in the Central Atlantic Magmatic Province (CAMP) of Algarve (Corcitos section), southern Portugal. Such "load casts" indicate that the underlying sediments were largely soft and unconsolidated during basalt lava emplacement. Details in Martins et al. (2008)
Photo © *José Madeira*

Fig. 6.51 Peperites at the bottom of the Intermediate Formation of the CAMP Basalts at the Oued Lhar (Herrissane) section of the Central High Atlas. Details in El Ghilani et al. (2017)
Photo © *José Madeira*

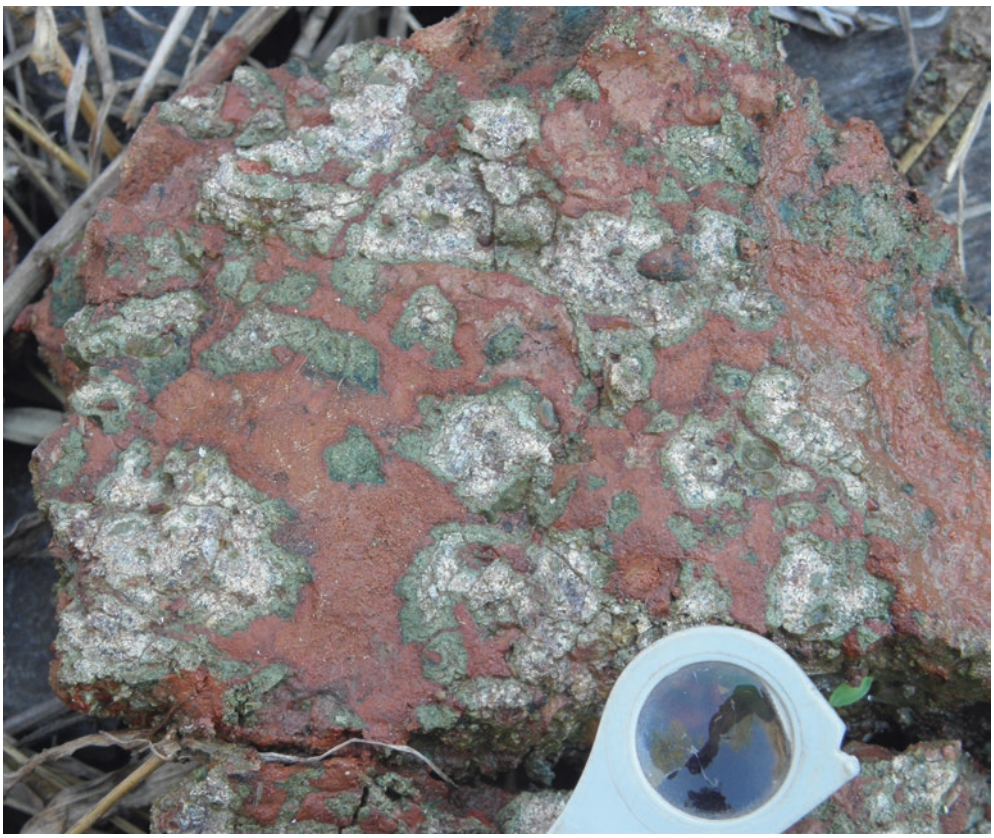

Fig. 6.52 Peperite associated with pillow lavas. Fragments of basalt (white and green) are immersed in a red sandy matrix. Location is the Central Atlantic Railway section near Uberlândia city, northeastern part of the Paraná CFB province, Brazil. More information: Moraes and Seer (2017)
Photo © *Lucia C. Moraes*

Fig. 6.53 Peperite (Skilling et al. 2002) along a dyke margin at Terra Cotta Mountain, Antarctica, showing a chaotic array of angular fragments of chilled Ferrar dolerite entrained in a matrix of medium- to fine-grained sand
Photo © *Giulia Airoldi*

Fig. 6.54 Peperite (Skilling et al. 2002) produced by mingling between flow-bottom breccia of a basalt flow and a caught-up block of red bole. Pen is 15 cm long. Pasarni Ghat between Satara and Mahabaleshwar, western Deccan Traps
Photo © *Nasrrddine Youbi*

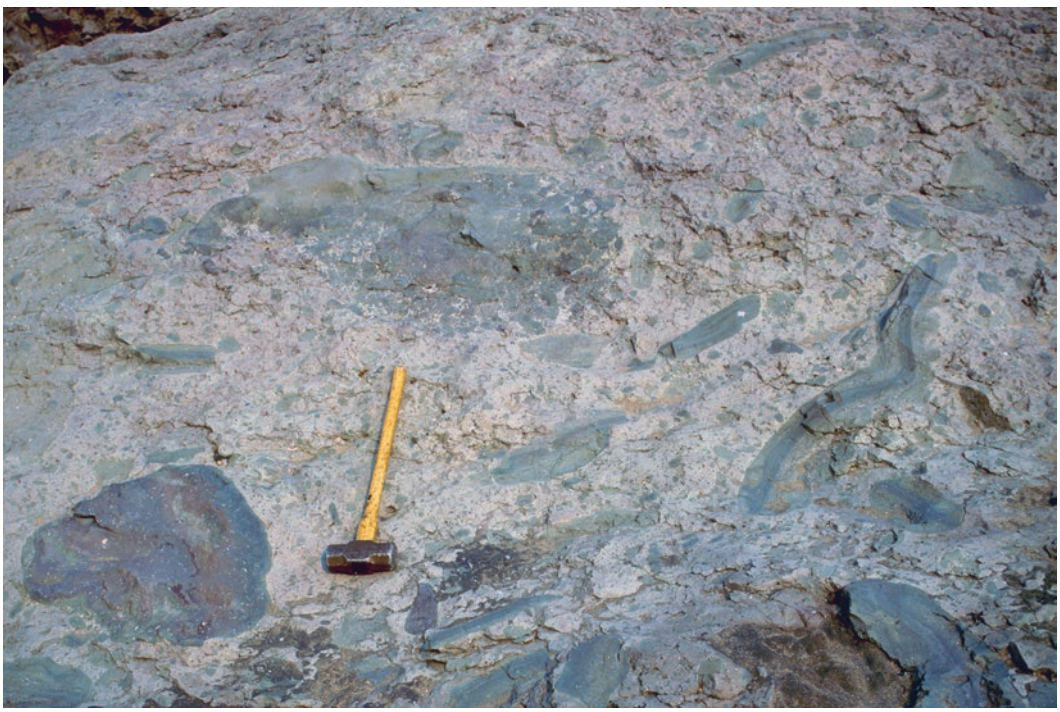

Fig. 6.55 Conglomeratic flow within the Sabie River Basalt Formation of the Karoo Province (Olifants River, South Africa) that is interpreted by Rawlings et al. (1999) as a peperite
Photo © *Martin B. Klausen*

Fig. 6.56 Lava flow of columnar rhyolite overlying "intertrappean" sedimentary deposit, Dongri, Mumbai. Danian-age (post-Cretaceous/Palaeogene boundary) Deccan magmatism is well represented in Mumbai, on the western Indian rifted margin, and the basalts and associated volcanics are separated by many "intertrappean" sedimentary beds, comprising mainly clays and shales, including carbonaceous and tuffaceous shales. The rhyolite flow seen here dips away from the viewer due to the Panvel flexure and is 62.5 Ma in age. Students provide a scale. More information: Singh (2000), Cripps et al. (2005), Sheth and Pande (2014)
Photo © *Hetu Sheth*

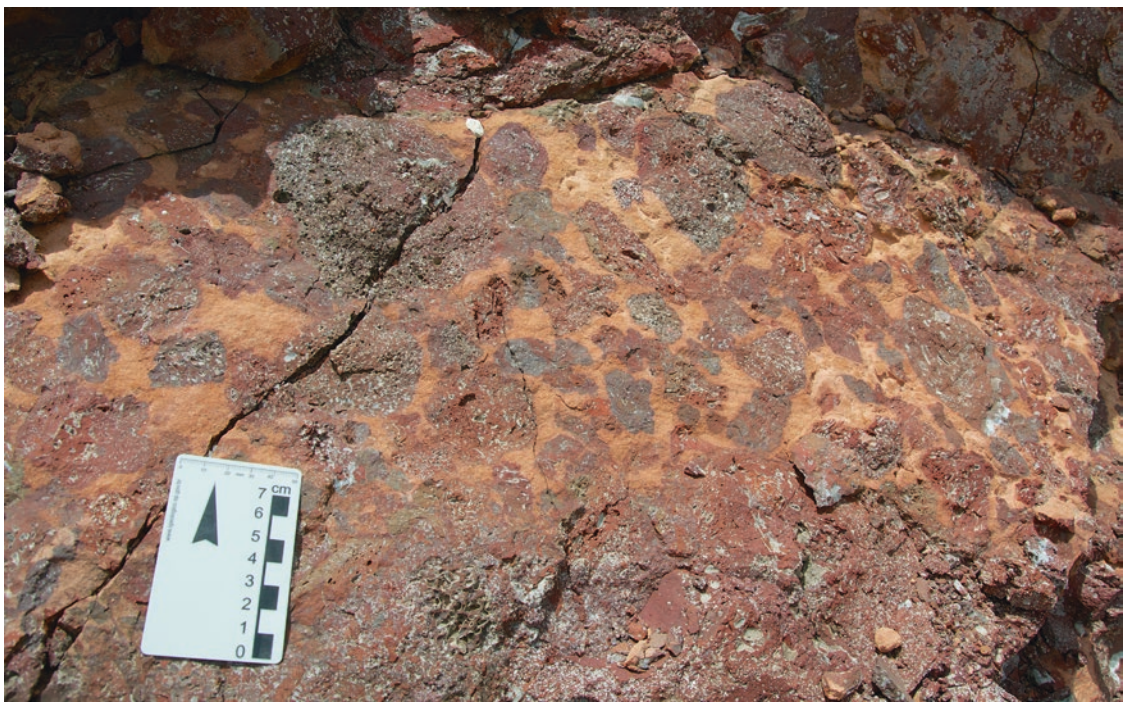

Fig. 6.57 Vesiculated basalt fragments forming the top breccia of a rubbly pāhoehoe flow in the Paraná CFB province, infilled by sand that now forms the matrix. More information: Barreto et al. (2014, 2017)
Photo © *Carla Barreto*

Fig. 6.58 A Neptunian dyke at the top of a Karoo basaltic lava flow, Hardap area, Namibia. As sandstones were deposited over the flow, soft sediments infilled fissures in the top of the flow (note horizontal striations in the dyke). Pen is 15 cm long
Photo © *Hervé Bertrand*

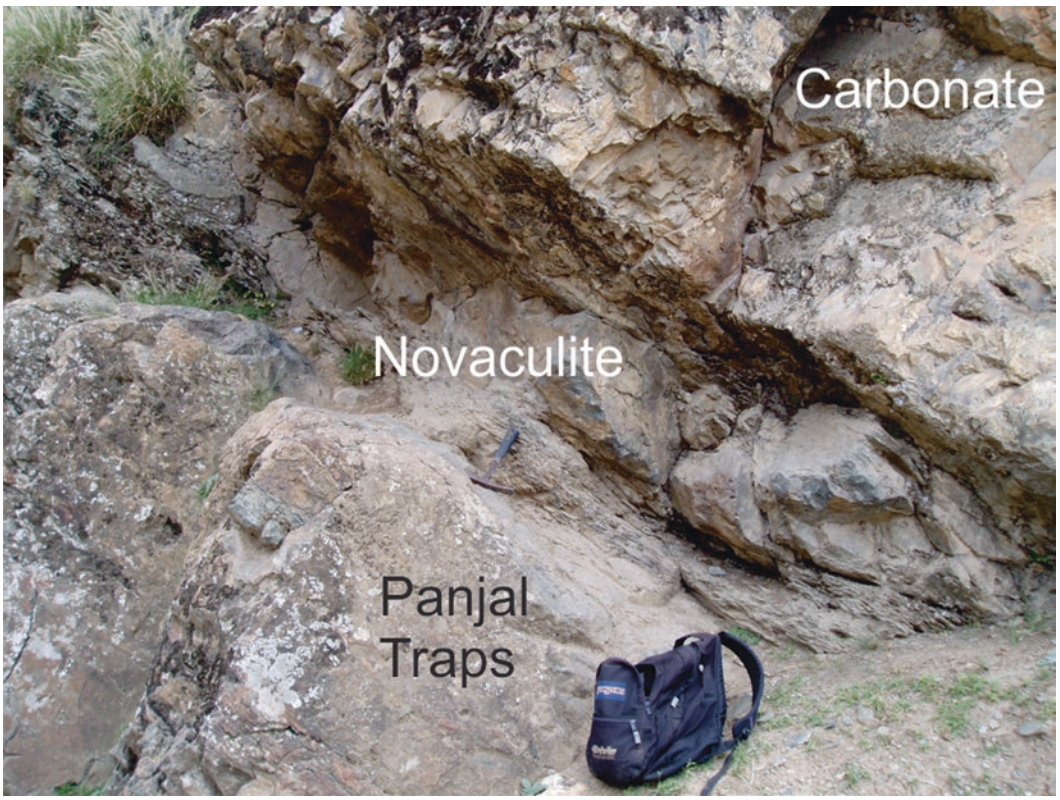

Fig. 6.59 The contact between the uppermost volcanic unit of the Early Permian (290 Ma) Panjal Traps and the novaculite of the Mamal Beds at Guryal Ravine (near Srinagar, Jammu and Kashmir, India). Novaculite is a tough, cherty rock made up of cryptocrystalline quartz, produced by low-grade metamorphism of marine diatomaceous earth. The Panjal Traps and Mamal Beds are overlain by the Zewan Formation (marine limestones). The Mamal Beds contain flora dominated by *Glossopteris*
Photo © *J. Gregory Shellnutt*

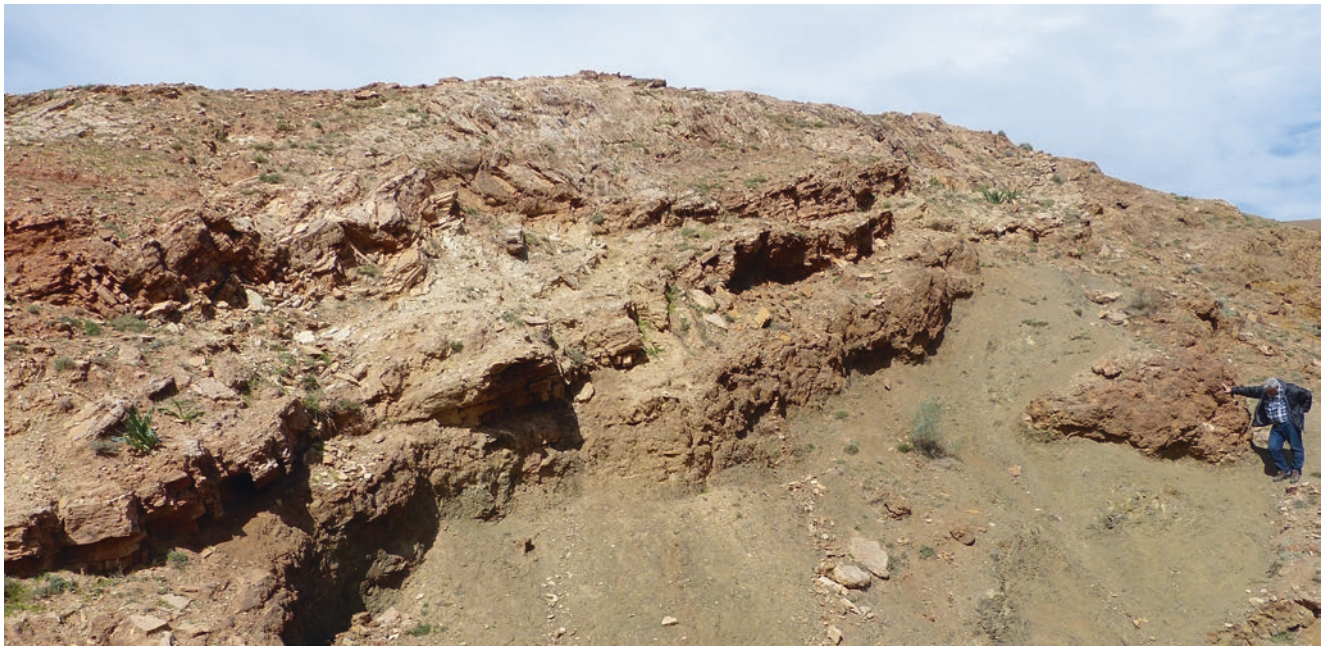

Fig. 6.60 Stromatolitic limestone at the top of the CAMP basalts, Aït Ourir section, High Atlas of Morocco. Geologist is El Hassane Chellai
Photo © *El Hassane Chellai*

Fig. 6.61 The uppermost basaltic simple lava flow (so-called Recurrent flow, dated at 196.6 ± 0.6 Ma, Verati et al. 2007) of the Central Atlantic Magmatic Province (CAMP) at Agouim, southern High Atlas, Morocco. The lava flow is 20 m thick and sits on Rhaetian-Hettangian red clays (exposed base of the section). Pink deposits above the flow are poorly dated Jurassic dolomitic limestones, sandstones and siltstones of the post-rift sequence
Photo © *Hervé Bertrand*

Explosive Volcanism in Flood Basalt Provinces

7

Fig. 7.1 Younger cinder cone on top of flood basalt flows in the southern part of the Afar Triangle, Ethiopia. Note the surface morphology of the lava flows and the well-developed gullies on the scoria cone
Photo © *Anthony R. Philpotts*

H. Sheth, *A Photographic Atlas of Flood Basalt Volcanism*, https://doi.org/10.1007/978-3-319-67705-7_7

Chapter Overview

Flood basalt volcanism, while dominantly effusive, includes explosive volcanism, with provinces such as the Siberian Traps containing substantial pyroclastic deposits (e.g., Black et al. 2015). Explosive volcanism in flood basalt provinces includes processes of purely magmatic volatile-driven fragmentation, such as Hawaiian-style eruptions with fire fountaining (producing spatter cones and clastogenic flows), and Strombolian-style eruptions (producing scoria cones). Many good examples of these are found in the Saudi Arabian *harrats* (Moufti and Németh 2016). Volcanism in Iceland is also unusually diverse (Thordarson and Larsen 2007). The explosive volcanism is important for evaluating flood basalt—mass extinction links. Unconsolidated tephra are easily eroded; they may be potentially under-represented in the preserved geological record on land in many flood basalt provinces, but preserved in the nearby ocean basins.

There are many spatter-scoria cones well exposed in the Miocene Columbia River flood basalt province, marking the sites of long, linear eruptive fissures (e.g., the Roza vent system, Brown et al. 2014, 2015; Camp et al. 2017) similar to the Laki 1783–1784 fissure. Comparable features are practically unknown in the Late Cretaceous Deccan province, despite decades of field work and stratigraphic mapping. Is the absence of near-vent spatter accumulations or scoria deposits in the Deccan simply a preservation issue, as we are now looking at deeper levels of the feeder dykes (say 1 km) than exposed in the Columbia River province? Or did the Deccan lavas break through and raft away these early-formed explosive vents, possibly largely remelting this debris? Again, though the Deccan is poor in pyroclastic deposits overall, Mumbai City would be a good place to study mafic and rhyolitic breccias and ash beds, with all the exposure and access problems due to urbanization already noted.

Explosive volcanism in flood basalt provinces also includes processes of magma fragmentation by external volatiles, producing phreatomagmatic tuff rings, maar-diatremes and larger vent complexes (e.g., Ross et al. 2005), as well as rootless cones. It is of interest that a monogenetic volcanic field, now represented by an eroded maar-diatreme and small intrusive plugs of alkali basalt, basanite and melanephelinite, has been identified in the Kachchh region of the northwestern Deccan Traps (Kshirsagar et al. 2011). Finally, many flood basalt provinces contain significant accumulations of rhyolite, at least some of which represent ignimbrite eruptions. The Karoo and the Paraná provinces are especially notable for their large-volume rhyolites. In the Paraná province for example, rhyolitic ignimbrites form sequences hundreds of meters thick, forming large, flat-topped plateaus that look like typical flood basalt plateaus at first sight. Similar extensive and thick rhyolites, ignimbrites and lava-like, rheomorphic ignimbrites are found in Precambrian flood basalt provinces, such as the 2.06 Ga Rooiberg Group (Bushveld Large Igneous Province).

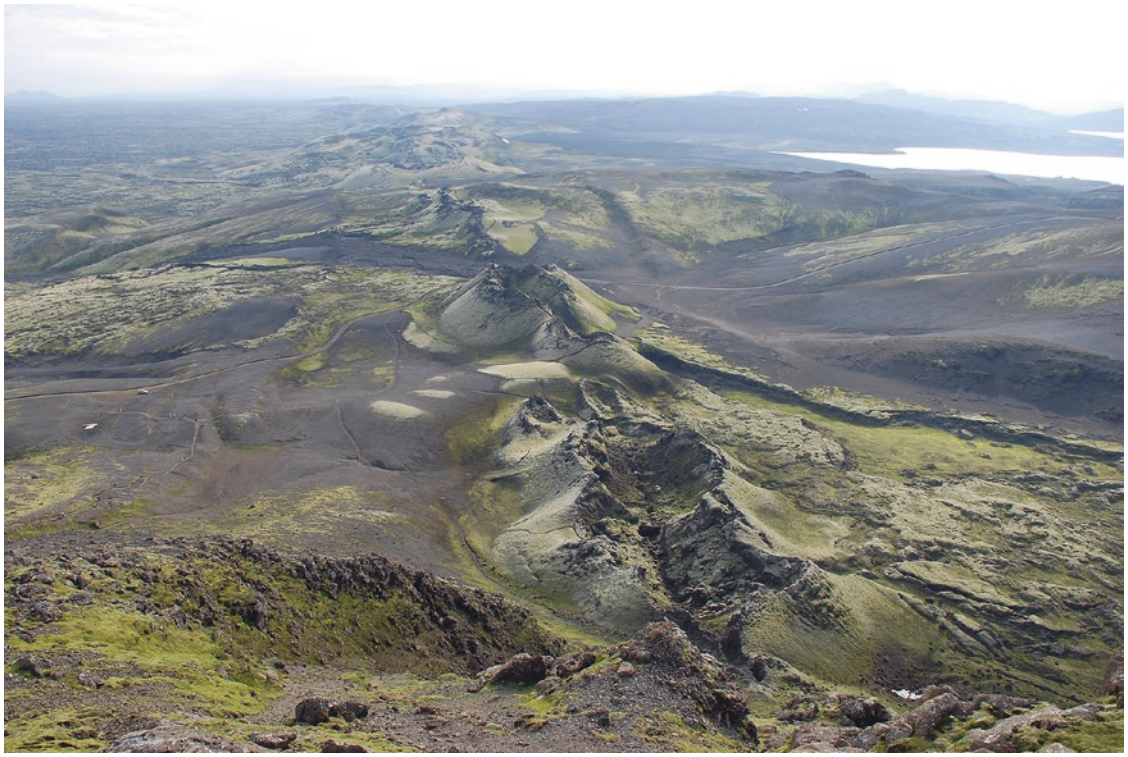

Fig. 7.2 Lakagigar eruptive fissure, Iceland. Up to 140 basaltic spatter and scoria cones are aligned along this 27 km long vent system that produced the 15 km^3 Laki lava flow field in 1783–1784. It is the second largest flood lava eruption on Earth in the last 1200 years. The cones range in height from a few meters to 120 m. On the left, at mid-height, is a car as well as hiking tourists. See Thordarson and Self (1993) for more information
Photo © *Hervé Bertrand*

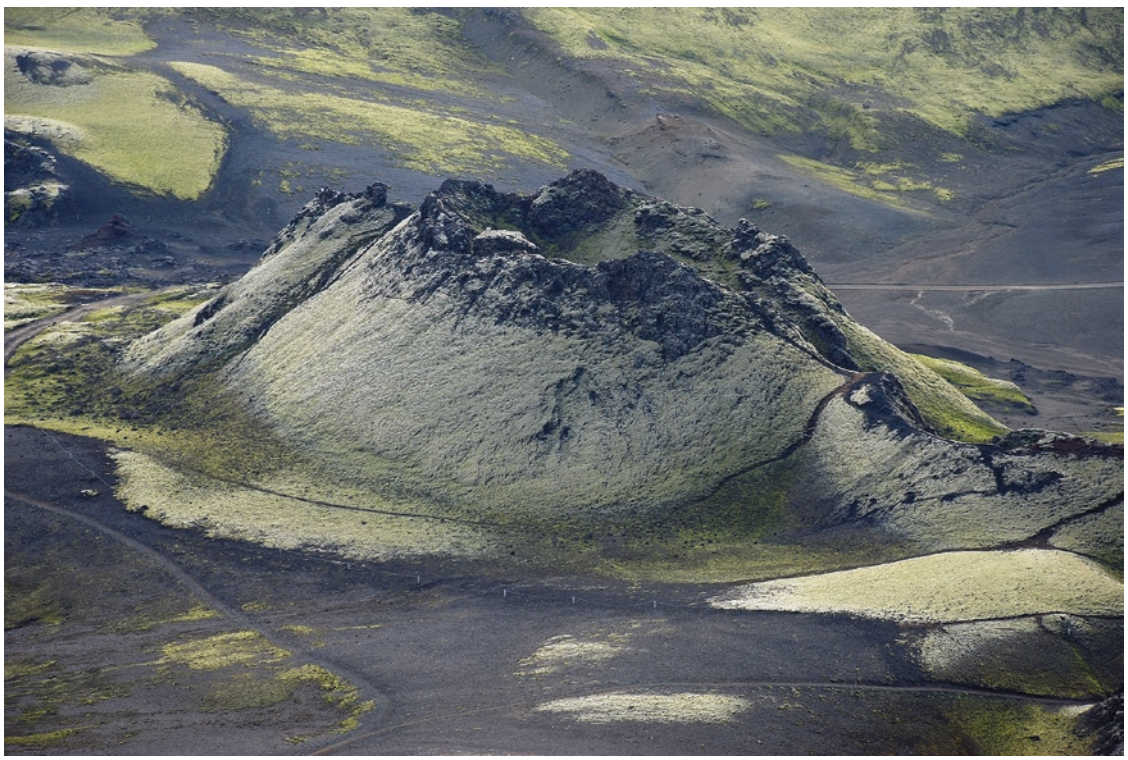

Fig. 7.3 Detail of a basaltic spatter cone (50 m high) on the 1783–1784 Lakagigar eruptive fissure, Iceland. Hiking trail and fence (white posts) at its base provide a sense of scale
Photo © *Hervé Bertrand*

Fig. 7.4 The great Eldgjá fissure or chasm of south Iceland, which hosts part of the vent system that formed the largest flood lava eruption in Iceland's 1200-year recorded history, namely the 934–940 A.D. Eldgjá event. The chasm is 8 km long, and typically 500 m wide and 100 m deep. The chasm itself was not formed in the Eldgjá event and is much older. The upper one-fifth of its walls is composed of fountain-fed Eldgjá lava and tephra; the rest is subglacial hyaloclastite. Dark mound in the left foreground is an Eldgjá spatter mound a few tens of meters in height. More information: Scarth and Tanguy (2001), Thordarson and Larsen (2007)
Photo © *Hervé Bertrand*

Fig. 7.5 Detail of 934–940 A.D. spatter mound within the Eldgjá chasm (ca. A.D. 935), south Iceland. Geologist is Francoise Chalot-Prat
Photo © *Gillian R. Foulger*

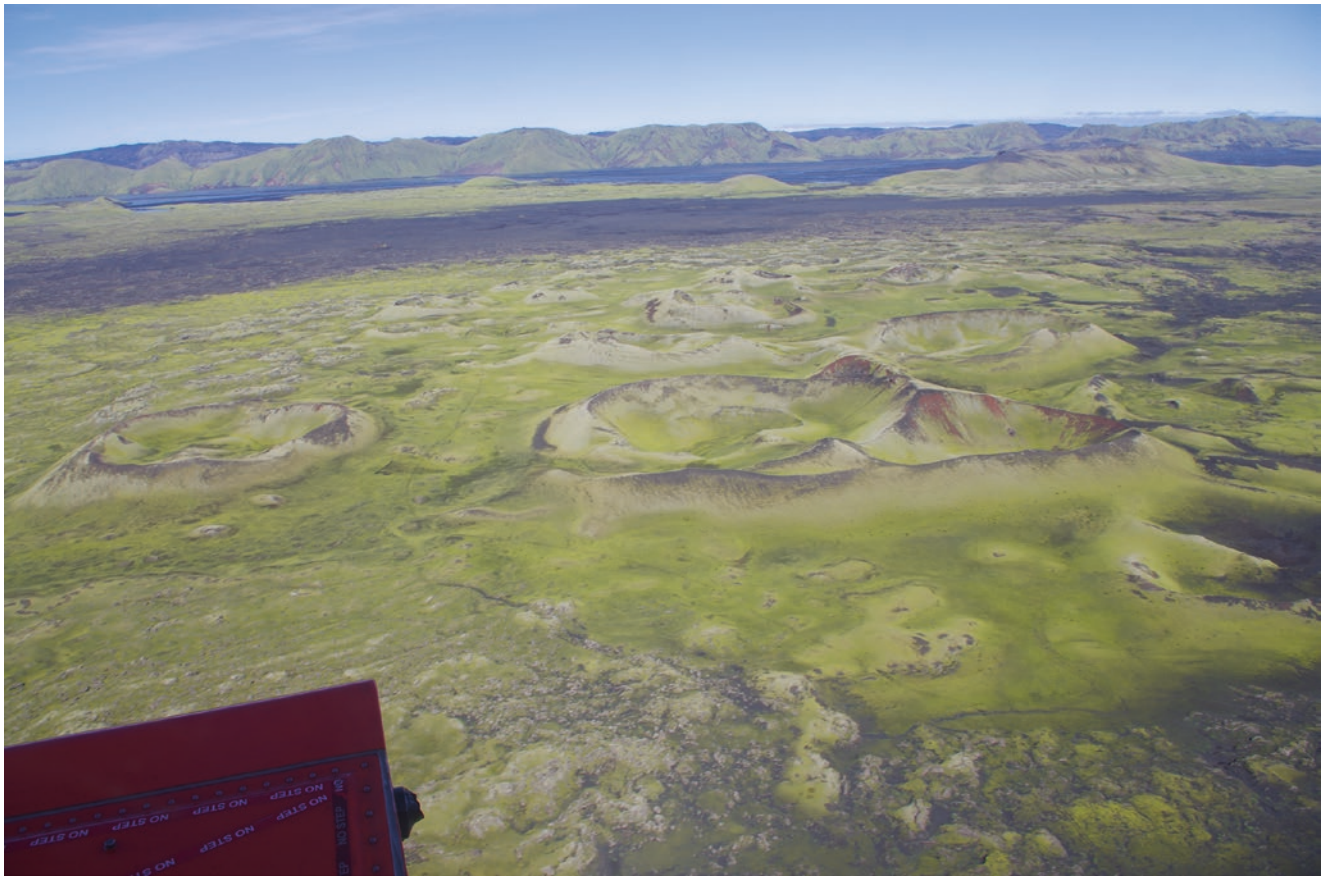

Fig. 7.6 Aerial view of the Innri Eyrar rootless cone group within the 1783–1784 Laki lava flow field. The cone group is located north of the Laki vent system and northwest of Mt. Laki, and was formed in September 1783 by lava emerging from fissure 7 of the Laki vent system. The largest cones (in the foreground) are more than 200 m in diameter and comparable in size to the cones on the Laki vent system
Photo © *Thorvaldur Thordarson*

Fig. 7.7 Rootless cones along the eastern shore of Lake Mývatn, north Iceland. These rootless cones were formed at 2170 ± 38 year BP (the so-called Younger Laxá lava eruption) when the lava emitted from the Lúdentsborgir-Þrengslaborgir fissure (on the east side of the lake) flowed over and interacted with the wetlands and the old lake Mývatn. The Younger Laxá lava flow can be seen in the foreground. Houses provide a scale. See Noguchi et al. (2016) for more information
Photo © *Hervé Bertrand*

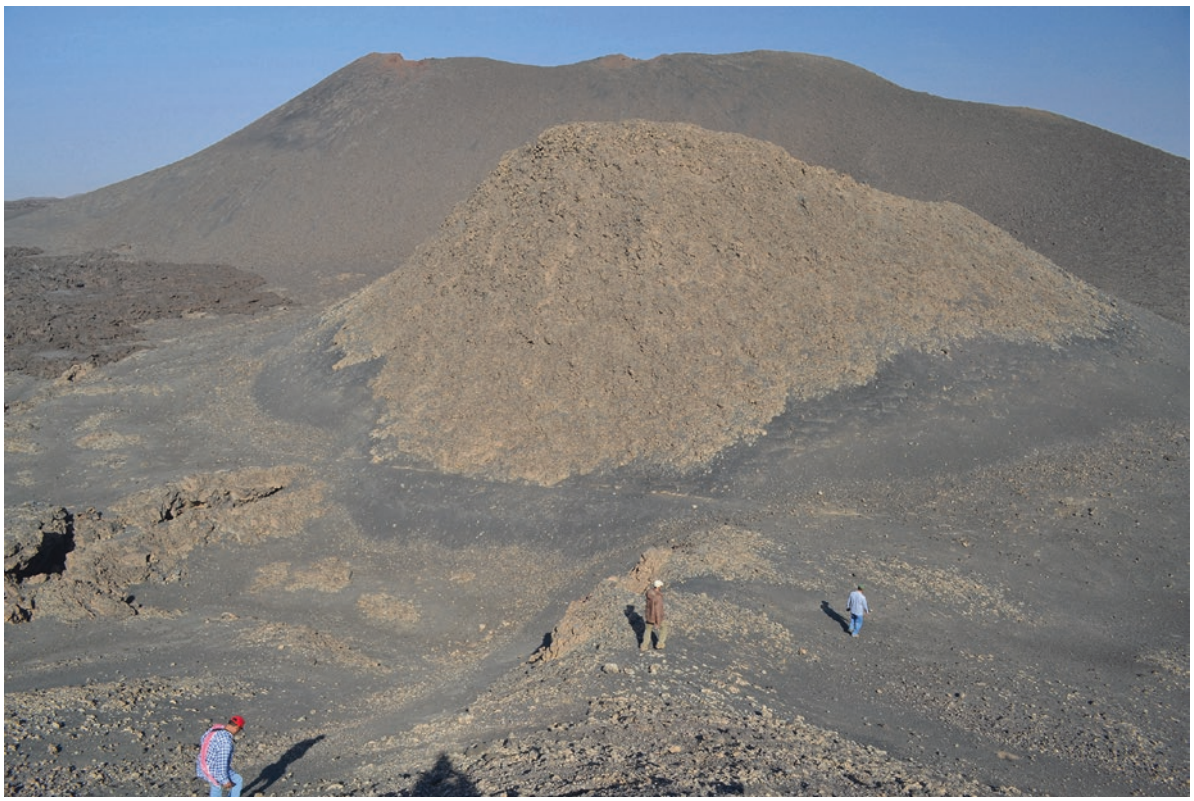

Fig. 7.8 Spatter mound on the axis of the 2.3 km long fissure which produced the A.D. 1256 Al Madinah eruption, Harrat Rahat, Saudi Arabia. In the background is one of the several scoria cones also produced during this fissure eruption
Photo © *Karoly Németh*

Fig. 7.9 Close-up of a lava spatter mound from the A.D. 1256 Al Madinah eruption, composed of 20–30 cm wide, flattened fragments of relatively smooth-surfaced basaltic spatter. Fine, glassy, red ash forms a matrix that is commonly agglutinated to the surface of the spatter fragments
Photo © *Karoly Németh*

Fig. 7.10 Typical scenery of the Al Haruj intracontinental volcanic field in central Libya, a smaller-scale CFB. Note the erosion-modified red desert landscape underlain by multiple Pliocene lava flows, mostly of the pāhoehoe type. In this landscape, scoria cones that commonly form chains along eruptive fissures stand out as landforms preserved by the erosion-resistant collars on their crater rims. The collars result from strong agglutination and welding of lava spatter accumulating rapidly. The cones typically rise 40–80 m above the plains of the lava flows. More information: Németh et al. (2003), Németh (2004)
Photo © *Karoly Németh*

Fig. 7.11 Agglutinate in the edifice-forming pyroclastic successions of scoria and spatter cones of the Miocene to Holocene Al Haruj in Libya. The agglutinate indicates high discharge rate of relatively low-viscosity alkaline basaltic magma which forms many of the extensive lava fields of North Africa. Al Haruj, by its eruptive volume, is probably an order of magnitude smaller than a typical flood basalt province, but is definitely one or two orders of magnitude larger than a typical intracontinental monogenetic volcanic field. In this picture a slide surface (about 4 m across, note hammer in the lower left corner) is shown, indicating that agglutination of lava spatter is a dynamic process and due to the formation of molten material between accumulating agglutinate layers, slow creeping of sections of the edifice can take place, significantly modifying the final volcanic landform we see
Photo © *Karoly Németh*

Fig. 7.12 Eldborg at Geitahlíð, a steep-sided spatter ring on the Reykjanes peninsula, southern Iceland. View is from inside the crater. Person on crater rim provides a scale. Volcano types and eruption styles on Iceland are very diverse. More information: Thordarson and Larsen (2007)
Photo © *Hetu Sheth*

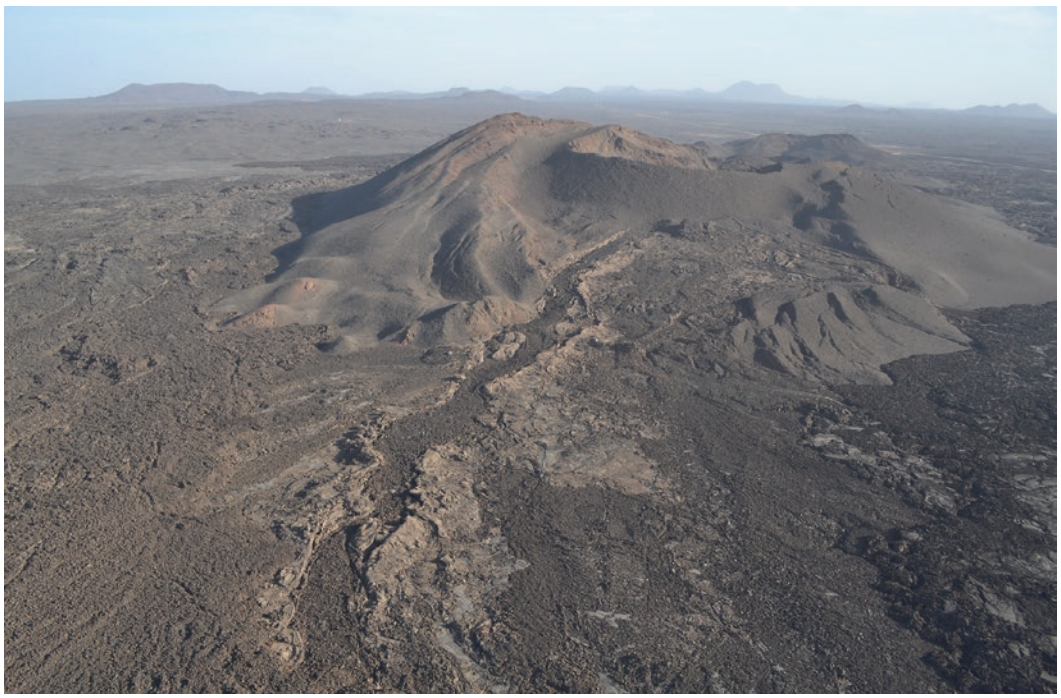

Fig. 7.13 A complex scoria and spatter cone formed along the 2.3 km long fissure which acted as the source of the extensive A.D. 1256 Al Madinah lava flow field in the northern Harrat Rahat. Note the complex architecture of the cone reflecting multiple pit crater formation, rafting, and regrowth of sections of the cone. The cone complex stands about 70 m above the surrounding lava fields
Photo © *Karoly Németh*

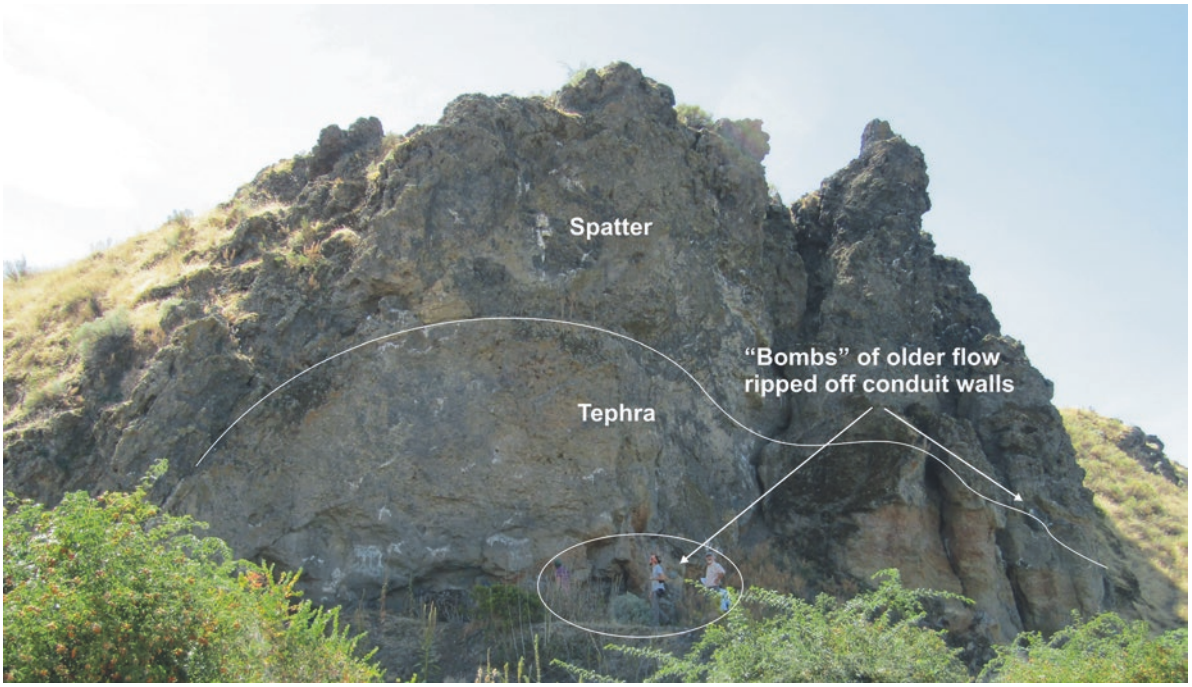

Fig. 7.14 Spatter cone for the 8.5 Ma Martindale flow, Ice Harbor Member, Saddle Mountains Basalt, Columbia River Basalt Group. This is one of several small spatter cones that developed along the dyke. The initial eruption produced a fire fountain depositing tephra. As the eruption progressed, the tephra was covered by spatter (above the thin white line) and the vent was incased by lava. Two of the numerous "bombs" of conduit wall rocks and lithic fragments present in the tephra are indicated. Geologists at the base of the cone, within the elliptical area, are Patrick Hayman, Simone Cogliati and Chris Henry. Location: Snake River at Ice Harbor Dam, Washington. More information: Swanson et al. (1975), Swanson and Wright (1981)
Photo © *Stephen P. Reidel*

Fig. 7.15 Pele's Tears from the 16 Ma Teepee Butte vent, Grande Ronde Basalt, Columbia River Basalt Group. Location: Joseph Canyon, Washington. More information: Reidel and Tolan (1992)
Photo © *Stephen P. Reidel*

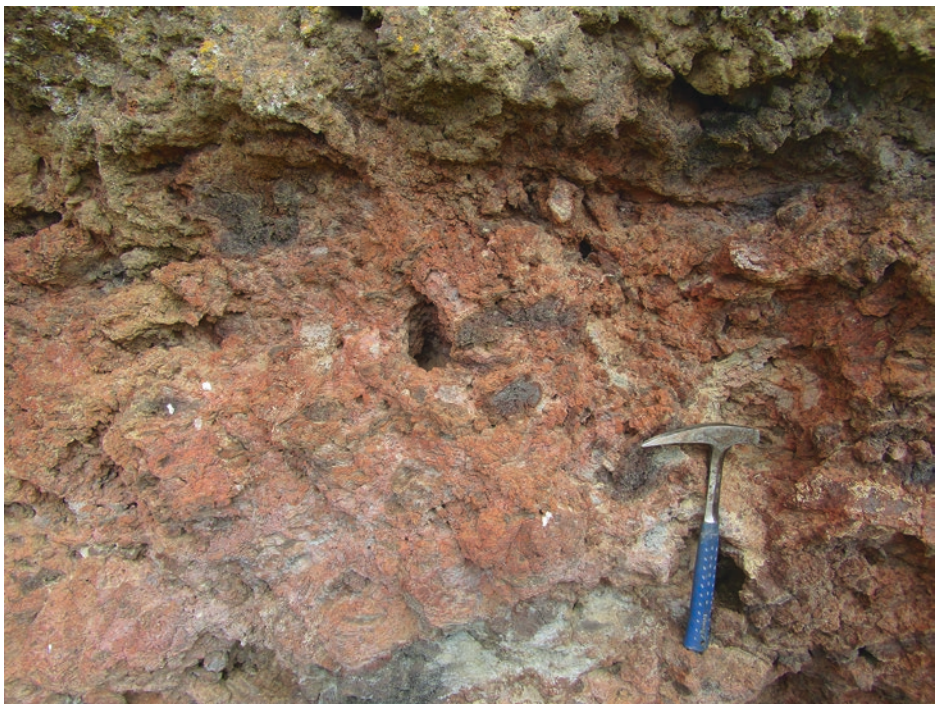

Fig. 7.16 Scoria with bombs (vesicular and dark-coloured), in the Rock Creek vent of the 15.8 Ma, 1300 km^3 Roza Member, Columbia River flood basalt province. The Roza pyroclastic deposits are the best-exposed proximal pyroclastic deposits of any known flood basalt eruption. More information: Brown et al. (2014), Camp et al. (2017)
Photo © *Hetu Sheth*

Fig. 7.17 Basalt bomb (juvenile clast) in a phreatomagmatic deposit in the Central Atlantic Magmatic Province (CAMP) of Algarve (southern Portugal) at the Soidos section. Details in Martins et al. (2008)
Photo © *José Madeira*

Fig. 7.18 Lava rag and spatter in volcaniclastic deposits below the MacCulloch's Tree Lava, Ardmeanach Peninsula, Isle of Mull, NW Scotland [UK Ordnance Survey Grid Reference: NM 4025 2780]. This bed crops out between the high and low water lines of the foreshore from Rubha na-Uamha in the north, to Camas na Fhéidh in the south, and is at least 8 m thick. The base is not seen. Fresh crenulations and folds are preserved on the surfaces of the volcanic fragments. Compass is ca. 10 cm long
Photo © *Brian R. Bell*

Fig. 7.19 Typical mound of tephra in the Roza Member at Winona, Washington, USA. Mound consists of a well-sorted, massive tephra fall deposit and overlies rubbly vesicular pāhoehoe crust in which lapilli fill the voids between slabs and blocks of crust. The mound is draped by welded fall deposits that have welded the clasts on the exterior of the mound. Charlotte Vye-Brown is the geologist. More information: Thordarson and Self (1996) and Brown et al. (2015)
Photo © *Stephen Self*

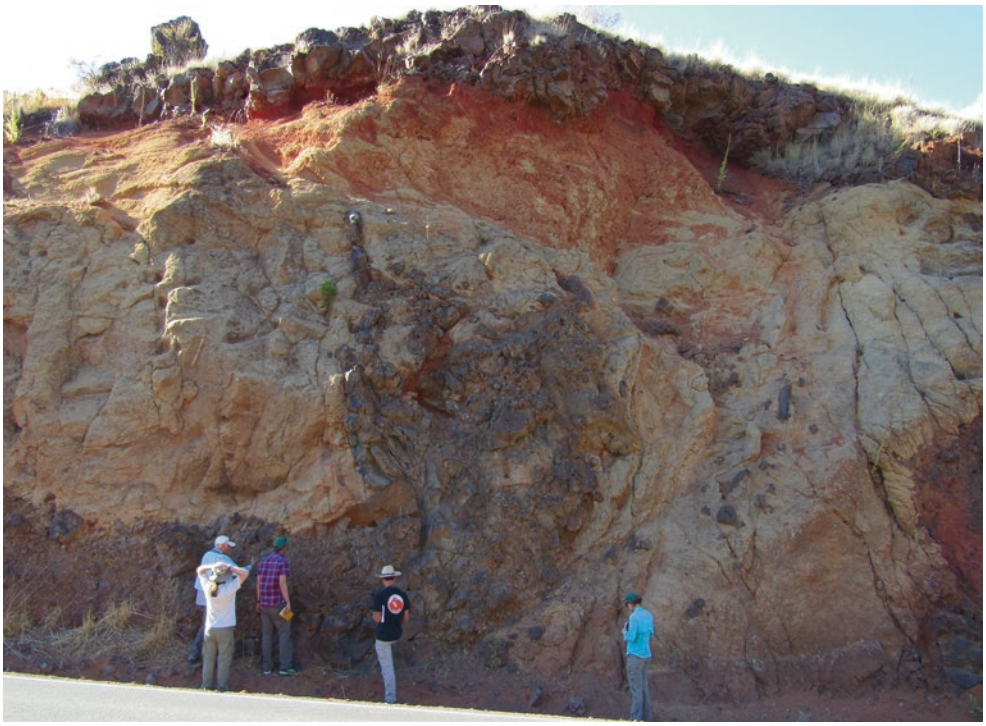

Fig. 7.20 The Little Sheep Creek vent complex of the Grande Ronde Basalt, Columbia River flood basalt province. Here, a flow of Mount Horrible basalt (dark gray) appears to be invasive into the tuff of Wapshilla Ridge (light brown to red), as indicated by cross-cutting relationships and soft sediment deformation. The vent complex is overlain by a Grouse Creek Member flow. More information: Brown et al. (2015), Camp et al. (2017)
Photo © *Hetu Sheth*

Fig. 7.21 Road cut in the Qiaojia section in the intermediate zone of the Emeishan LIP, southwestern China. A thin (30 cm) tuff layer separates a massive plagioclase-phyric lava flow below and a flow of typical high-Ti aphyric Emeishan basalt lava above. See Xu et al. (2004) for the definition of the intermediate zone and the low- and high-Ti Emeishan lava chemistry. Geologist is Alexei Ivanov
Photo © *Alexei V. Ivanov*

Fig. 7.22 The Strombolian scoria cone of Helgafell (5900 BP), viewed from the 1973 scoria cone of Eldfell, on the island of Heimaey in the Vestmannaeyjar (Westman Islands), off the coast of southern Iceland. Helgafell is 120 m high with a basal diameter of 500 m. Person hiking the slopes of Eldfell is Warren Hamilton. More information: Mattsson and Höskuldsson (2003)
Photo © *Hetu Sheth*

Fig. 7.23 Dyke in the cinder cone Biketi, exposed in an old quarry. Javakheti Highland, Lesser Caucasus, Republic of Georgia (Lebedev et al. 2008). Geologist is Vladimir Lebedev
Photo © *Vladimir A. Lebedev*

Fig. 7.24 Pliocene basaltic sequence of the Kars plateau (eastern Turkey) in the Akhurian (Arpaçay) River valley along the Turkish-Armenian border. The view shows ruins of the ancient Armenian city of Ani, now in Turkish territory. The K/Ar age of the lower basalts is 5.6–4.0 Ma, the interlayered tuff ("Ani tuff") ~3 Ma, and the upper basalts ~2.7 Ma (V.A. Lebedev, manuscript submitted). The Ani tuff was the material used for building the ancient city of Ani, and quarries in the tuff on the Armenian side continue to supply this building stone for Armenian buildings
Photo © *Vladimir A. Lebedev*

Fig. 7.25 Permian coal-bearing sedimentary sequence and the lowest Siberian Traps volcaniclastic unit, cut by a 3 m basaltic dyke, near the town of Kayak, Arctic Siberia
Photo © *Benjamin Black*

Fig. 7.26 Coal-bearing Siberian Traps volcaniclastic deposit near the town of Kayak, Arctic Siberia. Coal occurs as 1–50 cm lithic clasts within the deposit. Seth Burgess is the geologist
Photo © *Benjamin Black*

Fig. 7.27 Water-lava interactions within the massive end-Permian volcaniclastics of the Angara River, near 58.90 N, 102.29 E, Siberian Traps. More information: Black et al. (2015)
Photo © *Linda Elkins-Tanton*

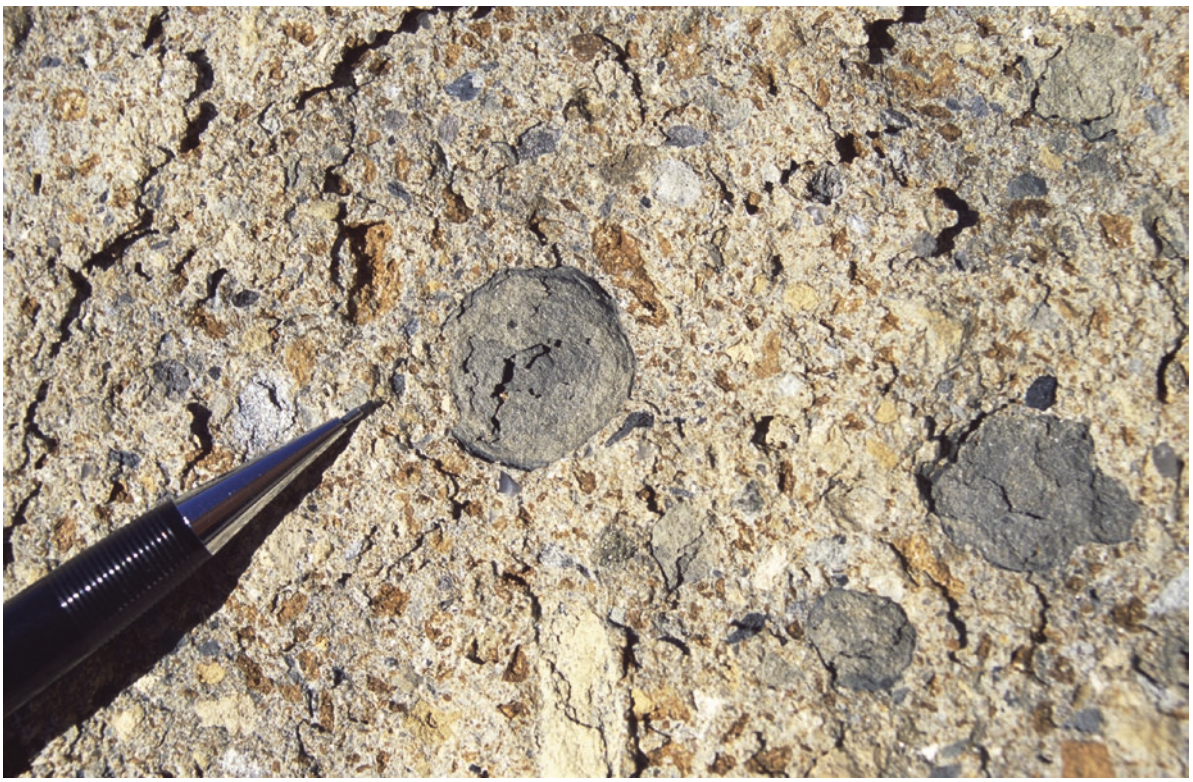

Fig. 7.28 Accretionary lapilli in pyroclastic density-current deposit with matrix of white and grey country rock fragments and brown, altered fluidal basalt pyroclasts. Allan Hills, Antarctica (Ross and White 2005), part of Ferrar Province mafic volcaniclastic deposits (Ross et al. 2005)
Photo © *James White*

Fig. 7.29 Accretionary lapilli in the Daqiao section, Sichuan, Emeishan flood basalt province, China. Field of view is ~50 cm wide
Photo © *Yigang Xu*

Fig. 7.30 Panorama of the Snake River canyon which exposes the proximal section of the Sinker Butte (the broad pyramidal mountain behind the cliff facing the viewer). This is a large emergent volcano, dominated by volcanism driven by magma-water explosive interaction. The gently outward-dipping pyroclastic beds are typical of early subaqueous growth of a hydromagmatic volcano, and the volcano gradually grew above water level, allowing multiple scoria cones to grow in its crater that is seen as a peak in the middle of the image. Lava flows from other sources surrounded and engulfed this volcano, producing a complex stratigraphy
Photo © *Karoly Németh*

Fig. 7.31 The base of one of the largest pyroclastic successions along the Snake River Canyon, USA, exposing the early eruptive products of Sinker Butte, a phreatomagmatic volcano which began under water and became emergent later. Many dykes also cross-cut the pyroclastic succession, often getting arrested within it. Height of cliff seen in photo is ~30 m
Photo © *Karoly Németh*

Fig. 7.32 Jebel Bayda (White Mountain) in Harrat Khaybar is an intact rhyolitic tuff ring of ~100 m height in the middle of a basaltic lava-dominated volcanic field. Basaltic lava emitted from the nearby Jebel Qidr volcano forms beautiful pāhoehoe lava surface textures and partially surrounds the white silicic tuff ring. The pāhoehoe lava pile in the front is about 10 m across and 2 m high. More information: Moufti and Németh (2016)
Photo © *Karoly Németh*

Fig. 7.33 Close-up view of the Sæfell tuff ring on Heimaey, Vestmannaeyjar, southern Iceland. The tuff ring is mostly phreatomagmatic and composed of base surge deposits (proximal areas) with typical cross-bedding (as seen here) and ash fall deposits (distal areas). Geologist is Angelo Peccerillo. More information: Mattsson and Höskuldsson (2003)
Photo © *Gillian R. Foulger*

Fig. 7.34 The Al Wahbah maar crater in the Harrat Kishb, with its nearly 2.5 km wide, scalloped rimmed crater that reaches about 300 m depth. This is one of the largest known maar craters of the Arabian Peninsula and also among the largest on Earth. Its presence is unexpected in the currently dry and arid Saudi Arabia, but as the crater is about 1 Ma in age, this indicates significant changes in the region's hydrogeology. The crater is complex and likely resulted from multiple explosive events along a fissure, which cut deeply into older scoria cones (now forming half section of eroded volcanic edifices exposed in the maar crater rim), multiple lava flows (exposed in the crater wall), and even Neoproterozoic basement rocks
Photo © *Karoly Németh*

Fig. 7.35 Basanite dyke with subhorizontal offshoot (above geologist Badrealam Shaikh), cutting lithic block-rich tuff breccia. The Karinga Dungar maar-diatreme, Kachchh, northwestern Deccan Traps. This is part of an eroded monogenetic volcanic field emplaced in Mesozoic sandstone. More information: Kshirsagar et al. (2011)
Photo © *Hetu Sheth*

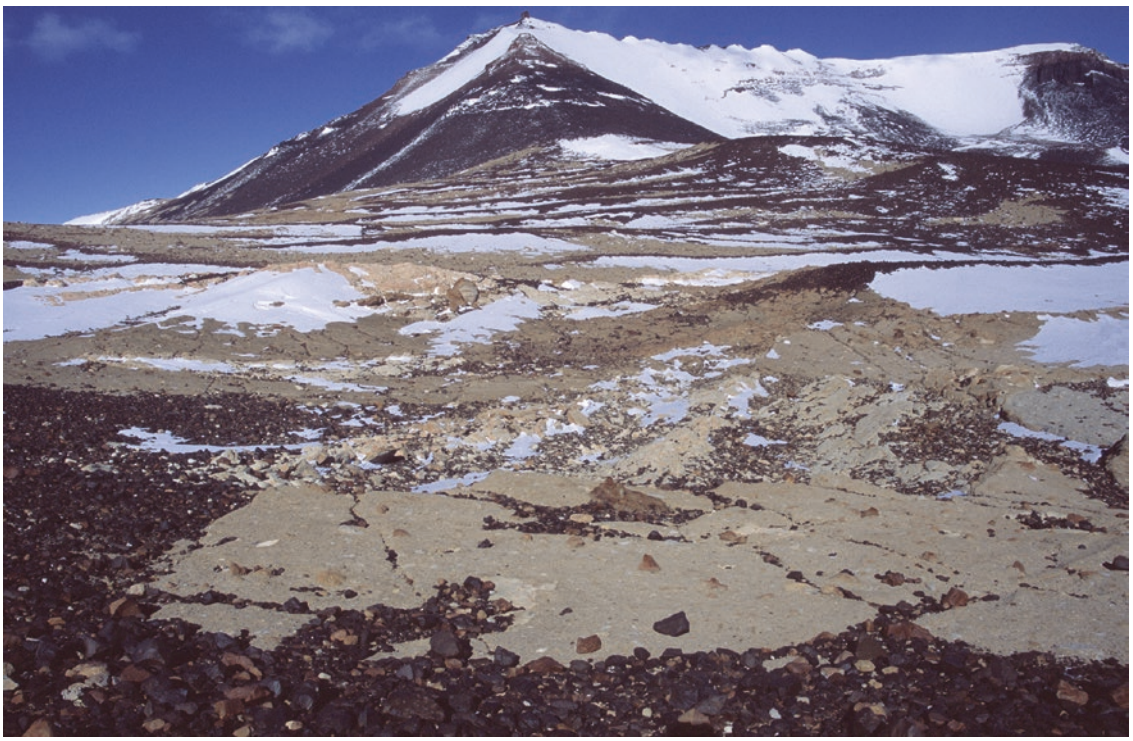

Fig. 7.36 Ferrar Province, Antarctica. Foreground deposits are different domains (colours) of pyroclastic rock, with a block of displaced Beacon sandstone. These are part of the Coombs Hills volcanic complex of overlapping diatreme deposits (White and McClintock 2001; Ross and White 2006). These are overlain by Kirkpatrick flood lavas, forming Mt. Brooke in the background which is 300 m high and reaches 2600 m above sea level
Photo © *James White*

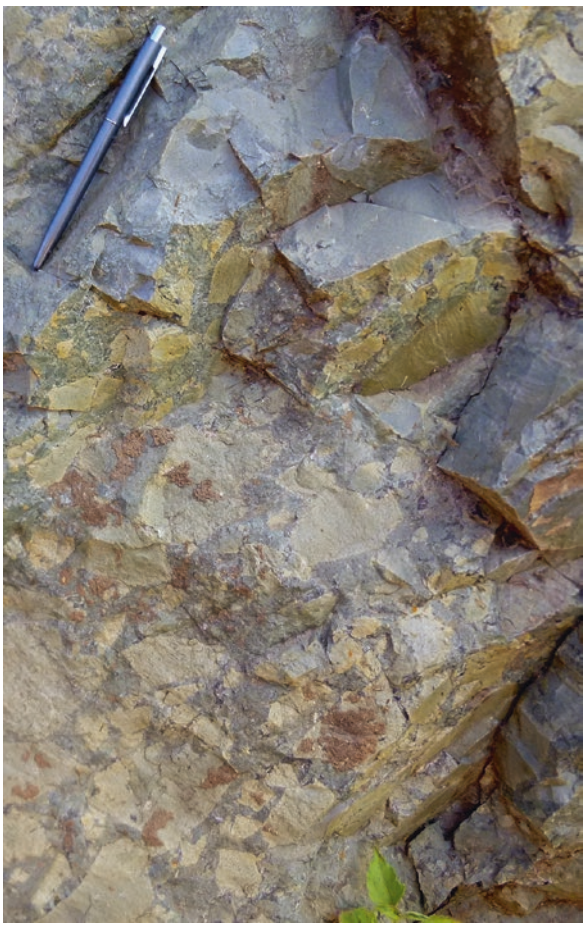

Fig. 7.37 Basaltic tuff breccia at the base of the Chen Pass, in the Song Da rift, northwestern Vietnam. Pen is 15 cm long. This low-Ti basalt and associated low- and high-Ti basalts and picrites represent the Emeishan flood basalt province in Vietnam. More information: Anh et al. (2011), Shellnutt (2014)
Photo © *Hetu Sheth*

Fig. 7.38 Close-up of the volcanic breccia from which the Kanheri Caves (first century B.C. to the ninth century A.D.) in Mumbai have been carved. The breccia appears very heterogeneous, with several rounded fragments of highly vesicular basalt visible. Fragments of non-vesiculated basalt are also present (not seen here). The large angular brown fragment in the lower part contains smaller pieces of basalt. The site (a protected monument of the Archaeological Survey of India) is geologically poorly studied owing to access and sampling problems, but Walker (1971) estimated these Deccan pyroclastic deposits to be within 10 km of the eruptive vent
Photo © *Nasrrddine Youbi*

Fig. 7.39 "Agglomerate" from the Deccan Traps, composed of angular to subrounded rock fragments and a tuffaceous matrix. The rock is poorly size-sorted. Location north of Baladgam, Taluka Kawant, District Chhota Udaipur, Gujarat. At least some of the Deccan "agglomerates" may be flow-top breccias
Photo: *Dhananjai Verma, Geological Survey of India*

Fig. 7.40 Rhyolitic pumice deposit from the 1875 Plinian eruption of Askja volcano, covering a lava flow in the Ódáðahraun highland desert, Iceland. A tumulus (2 m high) of a former basaltic flow is seen. The shield volcano in the background is Kollóttadyngja
Photo © *Hervé Bertrand*

Fig. 7.41 Detail of the rhyolitic pumice deposit from the 1875 Plinian eruption of Askja volcano, in the Ódáðahraun highland desert. The large pumice is 50 cm long. More information: Carey et al. (2010)
Photo © *Hervé Bertrand*

Fig. 7.42 The ca. 20 cm thick Palaeogene Port Mor Mudstone [UK Ordnance Survey Grid Reference: NM 4230 7940] crops out along the southeastern coast of the island of Muck, NW Scotland. It is a fragmental rock containing fresh crystals of sanidine, Na-rich clinopyroxene, plagioclase, biotite and titanite, together with lithic fragments of trachyte and basalt, set in a clay-silt matrix. It is interpreted as a highly oxidized pyroclastic bed. It fills in irregularities in the top surface of the underlying pāhoehoe basaltic lava, and lobes of the overlying basaltic hawaiite lava extend down into the mudstone Photo © *Brian R. Bell*

Fig. 7.43 Rheomorphic ignimbrite (rhyolitic) of the Schrikkloof Formation (Rooiberg Group) near Modimolle, Limpopo Province, South Africa. The Palaeoproterozoic Rooiberg Group comprises basaltic to intermediate and rhyolitic volcanic rocks (lavas and welded ignimbrites) 2061 ± 2 Ma in age (Walraven 1997), and belongs to the Bushveld LIP. Present exposures of the Rooiberg volcanic rocks cover an area of ca. 50,000 km^2 and are 3–5 km thick Photo © *Nils Lenhardt*

Fig. 7.44 Rheomorphic flow folds in high-grade rhyolitic ignimbrite from the upper sequence of the Paraná CFB province, Rio Grande do Sul, Brazil
Photo © *José Madeira*

Fig. 7.45 Landscape developed on the upper sequence (mostly high-grade dacitic to rhyolitic ignimbrites) of the Paraná CFB province. Extensive horizontal sheets of welded ignimbrites have produced flat-topped plateaus with stepped topography. Individual units can be followed for tens of kilometers. Rio Grande do Sul, Brazil
Photo © *José Madeira*

The Intrusive Substructure of Flood Basalt Provinces

8

Fig. 8.1 Arch created by marine erosion in fine-grained and jointed Tasmanian dolerite sheet (most likely part of a larger sill) near Mars Bluff, Bruny Island, Tasmania, Australia. Person is 1.67 m tall
Photo © *Trevor J. Falloon*

H. Sheth, *A Photographic Atlas of Flood Basalt Volcanism*, https://doi.org/10.1007/978-3-319-67705-7_8

Chapter Overview

Intrusions constitute the plumbing system and the "substructure" of flood basalts, consisting of extensive and complex networks of dykes, sills and sheets, and plugs and larger plutonic bodies. Owing to the low viscosity of basaltic magma it can be transported in veins and dykelets that are millimeters to centimeters thick, whereas large dykes and sills that are tens of meters to >100 m thick transport very large magma volumes and may produce considerable thermal erosion in their wall rocks. Whereas some provinces contain few sills and contain large swarms of preferentially oriented dykes (e.g., Deccan, Columbia River province), sills reach extensive and magnificent development in other provinces (e.g., Siberia, Karoo-Ferrar-Tasmania). It is possible that the dyke-dominant flood basalt provinces are those associated with large-scale crustal or lithospheric extension or transtension, whereas the sill-dominant flood basalt provinces are those associated with large-scale crustal compression or transpression. If so, there would be two fundamentally opposed tectonic environments in which to form the same end-product, flood basalt provinces. The cone sheets of Ardnamurchan in Scotland are famous but are not yet identified from many other flood basalt provinces which do otherwise have exposed plutonic foci.

The intrusive bodies in flood basalt provinces are very important in that they are greatly more voluminous than the surface eruptives (estimated by some as constituting 90% of the total magma volume produced), and they provide insights into crustal-lithospheric structure, tectonic stresses, geodynamics and even continental reconstructions, they transport mantle-derived magma within the crust and to the surface, and in them operate many igneous processes which govern the compositions of the final erupted products.

Dykes and sills may show similar physical features as the surface flood basalts, particularly columnar jointing, and frequently show multiple magma injections that cooled against each other, not dissimilar to the "dyke-in-dyke" injections in oceanic crust at spreading centres. Multiple magma injections in the same feeder intrusion may explain some thick flood basalt lava flows that are internally geochemically heterogeneous, and also provide for an interesting conceptual volcanological discussion regarding the monogenetic or polygenetic nature of flood basalt provinces (Sheth and Cañón-Tapia 2015). Physical tracing of a dyke or a sill into a lava flow is the best way of identifying feeder dykes (keeping in mind complications such as lava drainback into a fissure creating pseudodykes). However, because feeder dykes are covered by their own lava flows, and because exposures showing feeder relationships are few or rare even in old and deeply eroded provinces like the Deccan, the identification of feeder dykes to flood basalt lavas depends on correlations based on radiometric age, geochemical-isotopic composition, and magnetic polarity. Giant mafic dyke swarms found in the Precambrian cratons arguably are feeders of flood basalts now lost to erosion (Ernst et al. 2001).

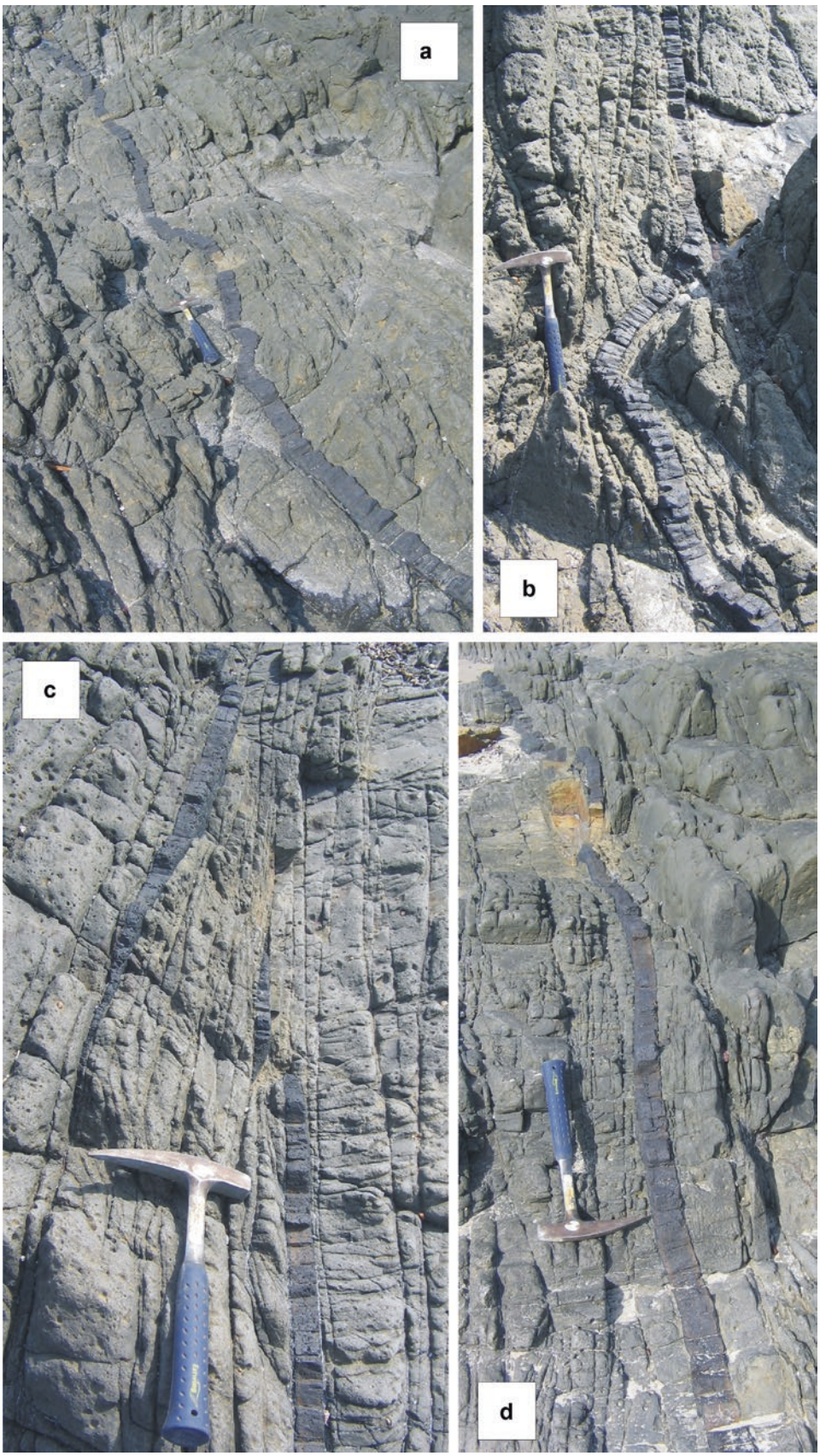

Fig. 8.2 (**a–d**) Basaltic dykelets cutting a basalt flow, exposed on the wave-cut platform at Borlai-Korlai, on the Konkan coast south of Mumbai, western Deccan Traps
Photos © *Hetu Sheth*

Fig. 8.3 One of many basic and ultrabasic, tholeiitic and alkaline dykes of the Coastal dyke swarm of the Deccan Traps. The dyke cuts flow-top breccia forming the wave-cut platform on the Konkan coast south of Mumbai. Geologist is T. K. Biswal. More information: Vanderkluysen et al. (2011)
Photo © *Hetu Sheth*

Fig. 8.4 Small *en echelon* Deccan basalt dykes cutting weathered basalt flow, Borlai-Korlai, Konkan coast south of Mumbai. Note the sharp margins and transverse jointing in both dykes, and how the lateral terminations of the dykes rotate towards each other in their area of overlap. Area in between them has been filled by beach sand, and pen (white) at photo centre is 15 cm long
Photo © *Hetu Sheth*

Fig. 8.5 Basaltic dyke and associated dykelet (a few centimeters thick) cross-cutting the gabbroic layered complex of Freetown, Sierra Leone, Central Atlantic Magmatic Province (CAMP) Photo © *Hervé Bertrand*

Fig. 8.6 Mafic dykes in the Keping area, Tarim LIP, northwestern China (Xu et al. 2014b) Photo © *Yigang Xu*

Fig. 8.7 Basalt dyke, subvertical, with subhorizontal cooling columns, within an extremely weathered Deccan basalt flow. The dyke has resisted the weathering much more than the host. Note the finer scale of jointing at dyke contacts. Near Igatpuri, Western Ghats. Geologist is Loÿc Vanderkluysen
Photo © *Hetu Sheth*

Fig. 8.8 Dyke belonging to the Roza Member dyke complex exposed at Rattlesnake Grade, Columbia River flood basalt province. Most of these dykes are about 2 m in thickness, and cut the Grande Ronde Basalt flows. The roadcut in the photo is through and parallel to the Roza dyke, so that the undulatory margins of the dyke with its transverse cooling columns exposed in cross-section are visible. Geologist party includes, from left to right, Richard Brown, Leif Karlstrom, Simon Martin, Stephen Hernandez, Loÿc Vanderkluysen, Chris Henry, Elise Rumpf, and Nicole Moore
Photo © *Hetu Sheth*

Fig. 8.9 Basaltic dyke ~3 m wide, crosscutting a Permian coal-bearing sedimentary sequence and the lowest Siberian Traps volcaniclastic unit near the town of Kayak, Arctic Siberia
Photo © *Benjamin Black*

Fig. 8.10 Picritic dykes, with a screen of highly weathered compound pāhoehoe host flow in between. Wave-cut platform, Elephanta Island, Mumbai harbour, western Deccan Traps. The ~N-S-striking dykes dip steeply left (east), with the host flows dipping ~12° WNW, due to the Panvel flexure. The dykes are therefore pre-flexure. Geologist is Hrishikesh Samant
Photo © *Hetu Sheth*

Fig. 8.11 This photo, taken from the road between Foum Zguid and Tissinnt towns, shows a NE-trending dolerite dyke (satellite dyke of the famous Great Foum Zguid dyke, CAMP) cross-cutting the Devonian sedimentary cover of the Anti-Atlas (Morocco) and feeding one sill of the Draa Valley/Zemoul sill complexes. Geologists are Sara Callegaro and Hervé Bertrand
Photo © *Nasrrddine Youbi*

Fig. 8.12 A particularly well-exposed tholeiitic dyke in an abandoned quarry pit, Dive Ghat, Pune, western Deccan Traps. The dyke shows cooling columns perpendicular to its margins, both of which are characterized by much closer-spaced cooling joints, owing to steeper thermal gradient and faster cooling. The host rock is a highly weathered compound flow. Geologist is El Hassane Chellai
Photo © *Nasrrddine Youbi*

Fig. 8.13 E-W-trending dolerite dyke near Saitale, Nandurbar area, central Deccan Traps. Dyke is 23.3 km long and 7 m wide, with both margins (shown by arrows) well exposed. The rest of the topographic ridge is composed of the host Deccan basalt. Geologist is Hetu Sheth. More information: Ray et al. (2007)
Photo © *Hetu Sheth*

Fig. 8.14 Prominent dyke-formed ridge in the Nandurbar area, central Deccan Traps, extending for many kilometers and rising several tens of meters above the surrounding plains of highly weathered basalt. Houses on the left provide a scale. The Nandurbar dykes are part of the Narmada-Tapi giant dyke swarm. Note that the dykes usually form only the axial, crestal parts of these ridges, the ridge slopes being made up of the intruded basalt flows (Ray et al. 2007)
Photo: *Bibhas Sen, Geological Survey of India*

Fig. 8.15 A >20 m thick Ferrar LIP dyke intruding Taylor Group sedimentary rocks on the northern side of Mt. Kuipers, Antarctica. Geologist is Murray McClintock
Photo © *James White*

Fig. 8.16 The Satdhara ("seven streams") dyke, a Deccan dolerite dyke exposed in the Denwa River near Pachmarhi, central India. The dyke produces waterfalls on the downstream side of the river. The dyke strikes ~E-W and dips 85° N, and is 28–34 m thick. It cuts through a thick sequence of Lower Triassic Gondwana sandstone. The geologists provide a scale. More information: Sheth et al. (2009)
Photo © *Hetu Sheth*

Fig. 8.17 Geologists measuring a 35 m wide dyke of the 1680 Ma Laiwu dyke swarm, Laiwu, Shandong, North China craton. The country rocks are Archaean (2.7–2.5 Ga) TTG gneisses
Photo © *Peng Peng*

Fig. 8.18 A 50 m wide dyke of the 925 Ma Dashigou dyke swarm, Fengzhen, Neimenggu, North China craton. The host rocks are Palaeoproterozoic aluminium-rich paragneisses of the Fengzhen khondalite series. More information: Peng et al. (2011)
Photo © *Peng Peng*

Fig. 8.19 The Higganum dyke along Route 9 near Higganum, Connecticut, USA. This is a CAMP feeder dyke exposed in southern New England for 250 km. The car provides a scale. More information: Philpotts and Martello (1986)
Photo © *Loÿc Vanderkluysen*

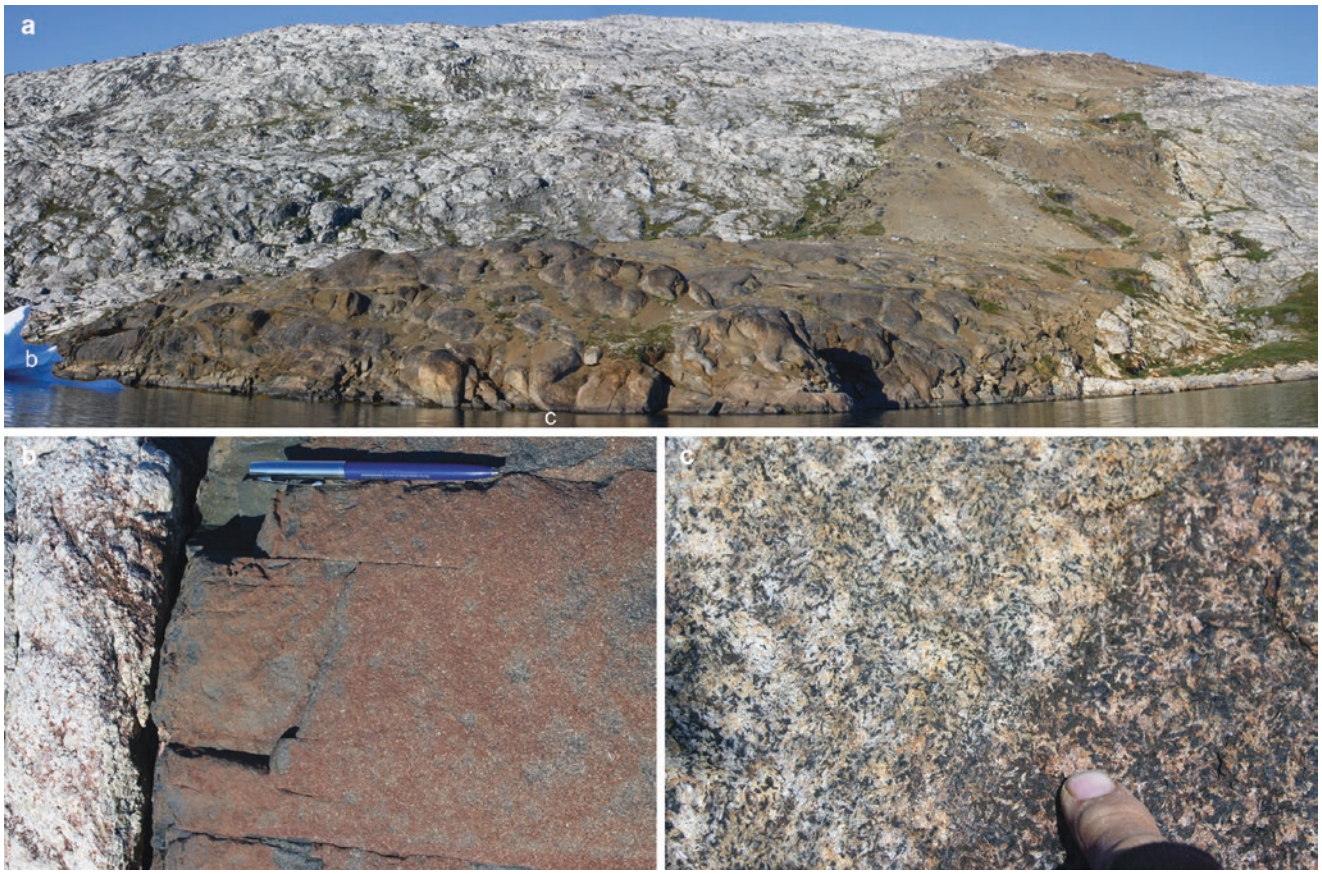

Fig. 8.20 The Mesoproterozoic (1.35–1.14 Ga) Gardar province, southern Greenland. (**a**) ~100 m wide, E-W trending, 1275 Ma mafic dyke cutting Archaean gneiss in the Timmiarmiit area (southern SE Greenland), looking east. (**b**) Basaltic chilled northern margin of the dyke. (**c**) Gabbroic centre of the dyke with internal mingling of more or less mafic parts. More information in Bartels et al. (2016)
Photo © *Martin B. Klausen*

Fig. 8.21 The NE-SW-trending and gabbroic Foum Zguid dyke, in the Draa valley, at Tansikht, Anti-Atlas, Morocco. The dyke ridge is 80 m high. This major, 200 km long dyke of the Central Atlantic Magmatic Province (CAMP) is dated at 201.111 ± 0.071 Ma (Davies et al. 2017) Photo © *Hervé Bertrand*

Fig. 8.22 The famous 200 km long Great Foum Zguid dyke (CAMP, 201 Ma) cross-cutting the Ordovician sedimentary cover of the Anti-Atlas in a ridge beside the road between Agdez city and Nkob town, Morocco. The dyke with a lighter colour than the Ordovician rocks forms the ridge crest
Photo © *Nasrrddine Youbi*

Fig. 8.23 Miocene basaltic lava pile (200 m thick) cut by a dyke. Höfn area, Iceland
Photo © *Hervé Bertrand*

Fig. 8.24 Miocene basaltic lava pile (500 m thick) cut by two dykes, Reyðarfjörður, Iceland
Photo © *Hervé Bertrand*

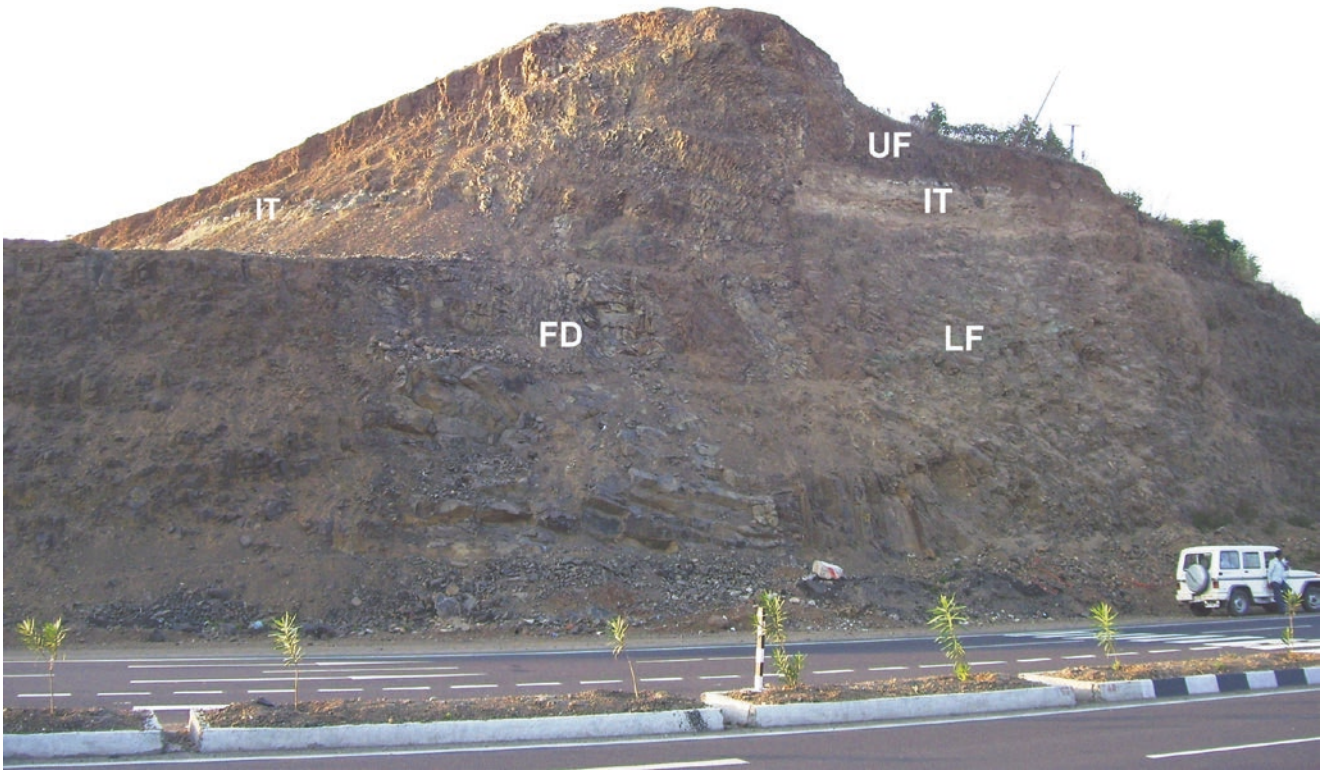

Fig. 8.25 Jointed feeder dyke (FD) cutting across the a lower basalt flow (LF) and overlying lake sediment (IT, "intertrappean", white layer) to feed an upper basalt flow (UF). Mumbai-Agra National Highway 3, Khakrapar, Dhar district, Madhya Pradesh (central India) Photo © *Dhananjay Mohabey*

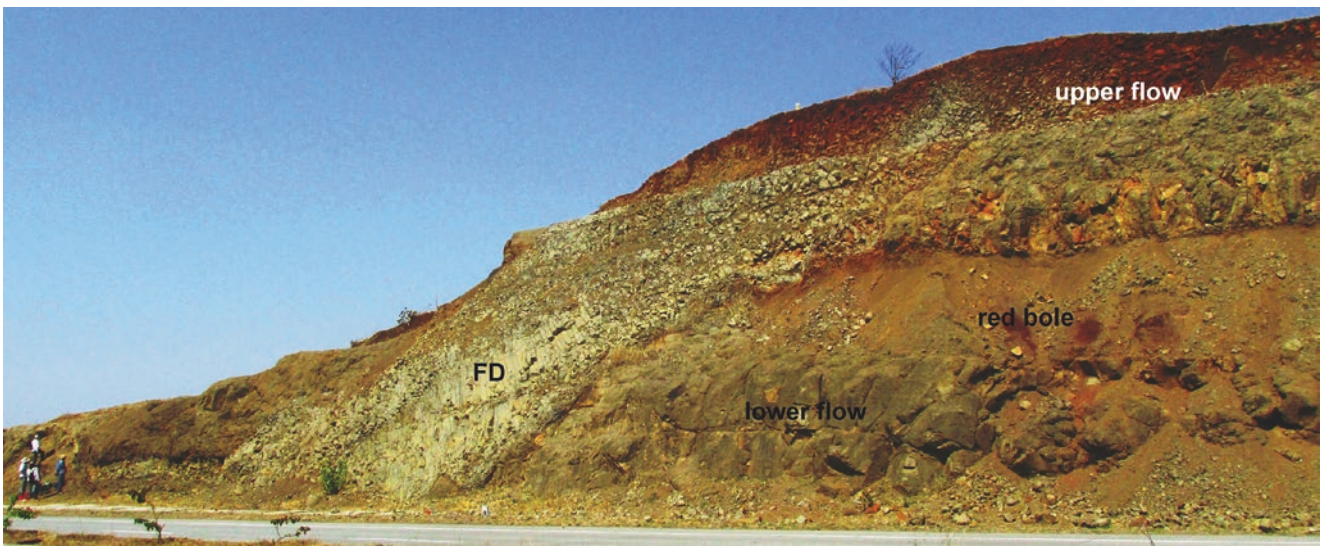

Fig. 8.26 Feeder dyke (FD) cutting across a lower Deccan basalt flow with sharp contact and feeding an overlying flow. A red bole separates the two flows. Amarkantak Group. Multai-Betul road section at Tejgaon, Betul district, Madhya Pradesh (central India). Geologists in the lower left corner provide a scale
Photo © *Dhananjay Mohabey*

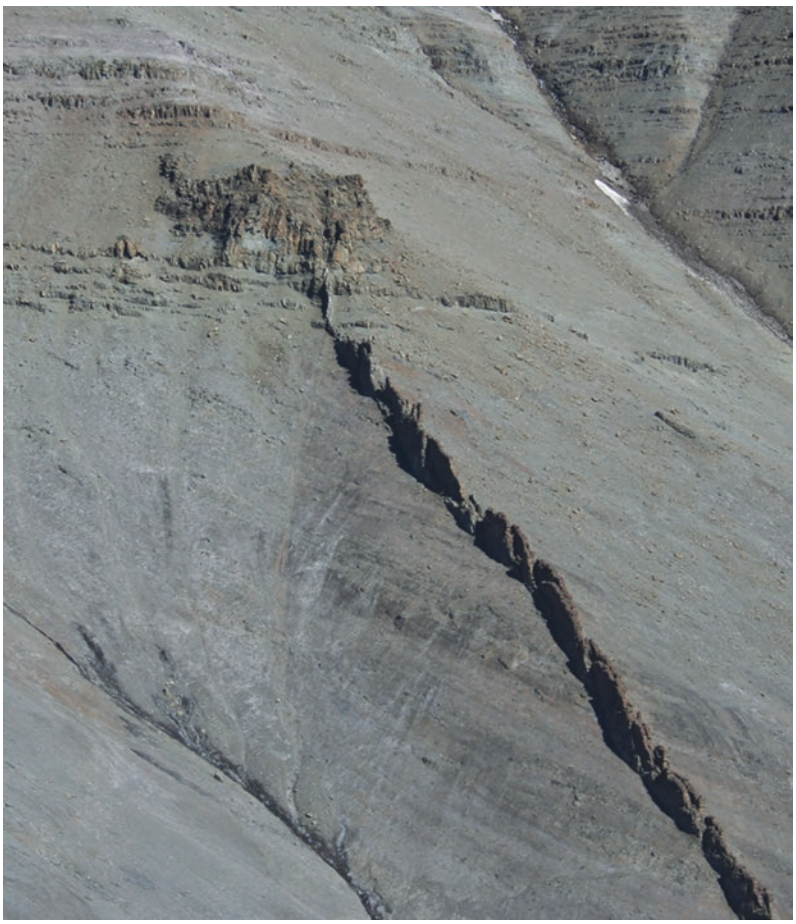

Fig. 8.27 Subaerial picrite eruption site. A thin feeder dyke cuts vertically through picritic hyaloclastites and lava flows and terminates within subaerial lavas in an irregular mass of columnar-jointed picrite. The picrite mass is about 20 m in width and height. Vaigat Formation, central Nuussuaq, West Greenland Photo: *Asger Ken Pedersen, Geological Survey of Denmark and Greenland (GEUS)*

Fig. 8.28 Feeder dyke. A basaltic dyke (~10 m wide) passes through a number of crudely columnar-jointed lava flows and feeds a scoria cone at Hafragilsfoss in Jökulsárgljúfur, north Iceland. Height of the cliff is ~80 m. More information: Reynolds et al. (2016) Photo © *Hervé Bertrand*

Fig. 8.29 Multiple-injection Deccan dolerite dyke in a road cut near Pandherwadi, ~25 km south of Satara, with at least three columnar rows (numbered) exposed. The cross-sections of the subhorizontal joint columns are well visible in the subvertical exposed faces. Vilas Bhonsle provides a scale. See Sheth and Cañón-Tapia (2015) for a discussion
Photo © *Hetu Sheth*

Fig. 8.30 Exceptionally well-exposed multiple-injection dyke, with four distinct, columnar-jointed magma injections and narrow chilled margins of the two outermost injections against a basalt flow. Dyke trends north-south and has a total width of 4.8 m. The flow stands weathered much more than the dyke. Geologist is Rajiv Sharma. Location: Shatabdinaga, Manjuhills, Aurangabad, central Deccan Traps. More information: Sangode et al. (2017)
Photo © *Satish J. Sangode*

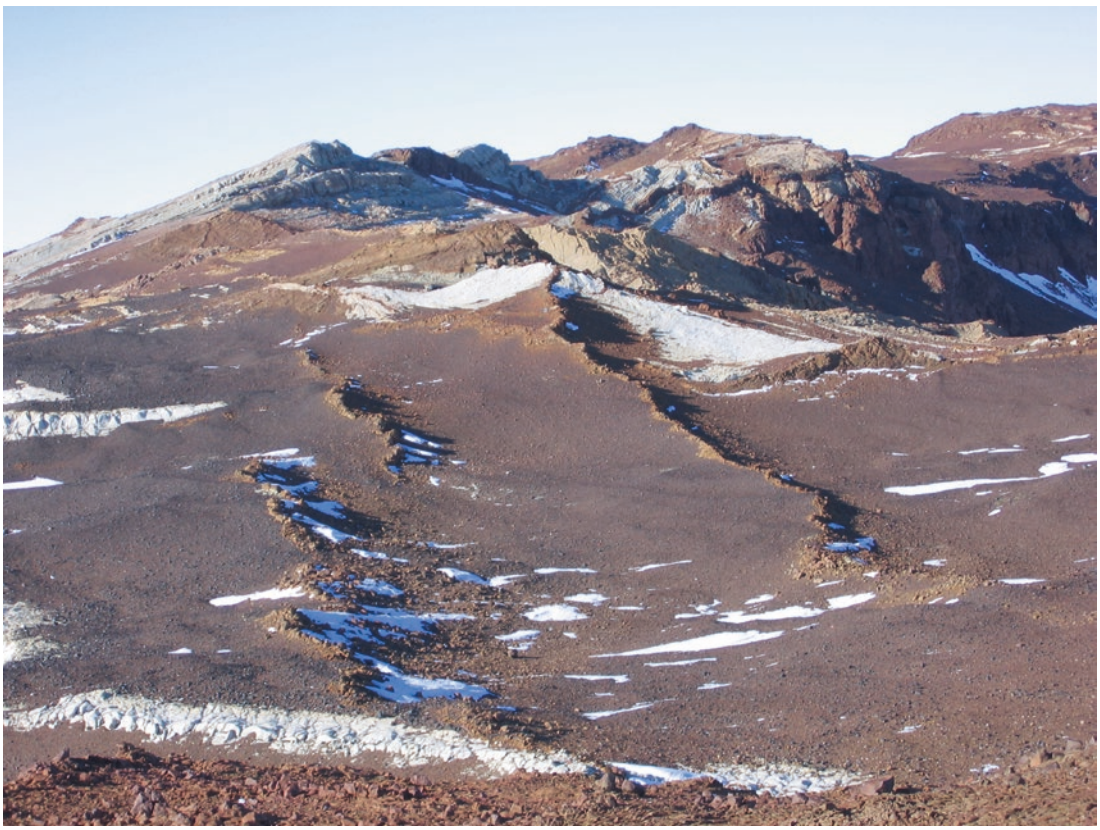

Fig. 8.31 Ferrar Province dykes (foreground) and sills break up the Beacon Supergroup sandstones at Coombs Hills, Antarctica. Regional dip here is subhorizontal; tilting results from Ferrar intrusions (White et al. 2009; Muirhead et al. 2014). The foreground dykes are ~0.5 m wide, and the mid-ground sill ~1.5 m thick
Photo © *James White*

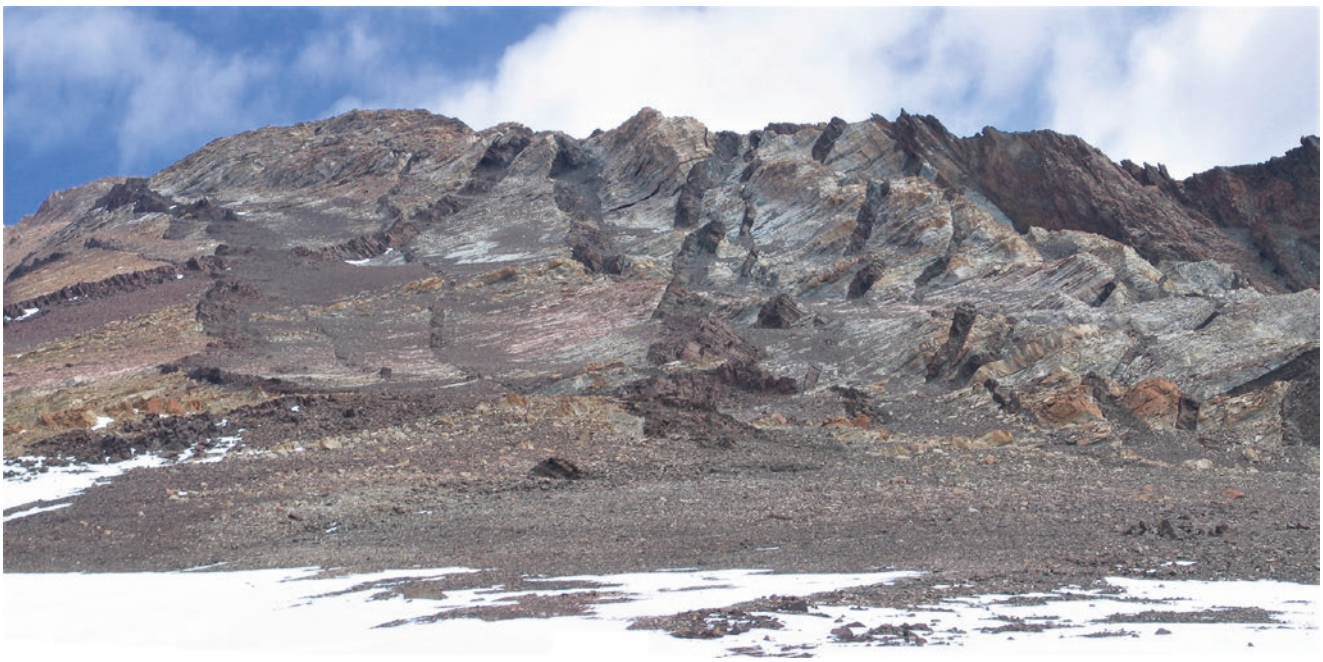

Fig. 8.32 The northern face of Terra Cotta Mountain, Antarctica, exposing a swarm of southeast-dipping dykes intruding Taylor Group sedimentary rocks. The dykes range in thickness between ~3 and ~20 m. The width of the image is ~450 m at its centre
Photo © *James White*

Fig. 8.33 Three dykes of Grande Ronde Basalt exposed on the banks of the Grande Ronde river, Columbia River flood basalt province. The dykes are up to about 5 m thick and columnar-jointed, and form relatively erosion-resistant walls. Truck on the road provides a scale. More information: Camp et al. (2017)
Photo © *Hetu Sheth*

Fig. 8.34 The southernmost exposed part of the Blosseville Basalt Group, with the lava package dipping towards the sea. The seemingly "fractured" area closest to the sea is where the Coast Parallel Flexure of East Greenland and the coast-parallel dyke swarm is exposed. The Skaergaard Intrusion is seen in the lower left foreground
Photo © C. *Kent Brooks*

Fig. 8.35 A major feature along the East Greenland coast is the coastal dyke swarm. The swarm is coast-parallel and very dense, in essence a sheeted dyke complex. It has been intruded in several stages during the flexuring of the continental margin when the continent broke up (Nielsen and Brooks 1981). South of Kangerlussuaq it cuts the Precambrian gneisses, and north of Kangerlussuaq it cuts the Tertiary basalts. In this picture the coast-parallel basaltic dyke swarm cuts the gneisses on the island Fladø in the foreground; the section is ~1 km across. In the background the swarm cuts the flood basalts and the Kap Edvard Holm gabbro complex. The snow-covered peak in the far background (left) is Kangerdlugssuaqs Tinde (2200 m), and further left are the Andrups Tårne (Towers)
Photo © *C. Kent Brooks*

Fig. 8.36 The coastal dyke swarm in East Greenland at Hængefjeldet, just north of Kangerlussuaq. The dykes here cut tuffs and volcaniclastic sediments of the Hængefjeldet Formation (Nielsen et al. 1981). The cliff in the foreground is ca. 70–100 m high from left to right. The light colour of the dykes in the photo reflects their composition and their greenschist facies mineralogy. These dykes relate to the later alkaline (Alk-1, Alk-2) and the late transitional dykes (Trans-1, Nielsen 1978). It is to be remembered that in some regions of the coast-parallel dyke swarm, transitional to mildly alkaline and often evolved compositions (to trachyte) constitute 30–50% of all dyke material, and that the dyke swarm developed possibly over 20 million years. It is not a simple analogy to the dyke injection at a mid-oceanic ridge under constant extension such as Iceland, but includes swarms of dykes related to highly evolved volcanic centres along the continental margin. The mountain in the background and across the glacier is Tinden, about 1044 m in height
Photo: *Troels F.D. Nielsen, Geological Survey of Denmark and Greenland (GEUS)*

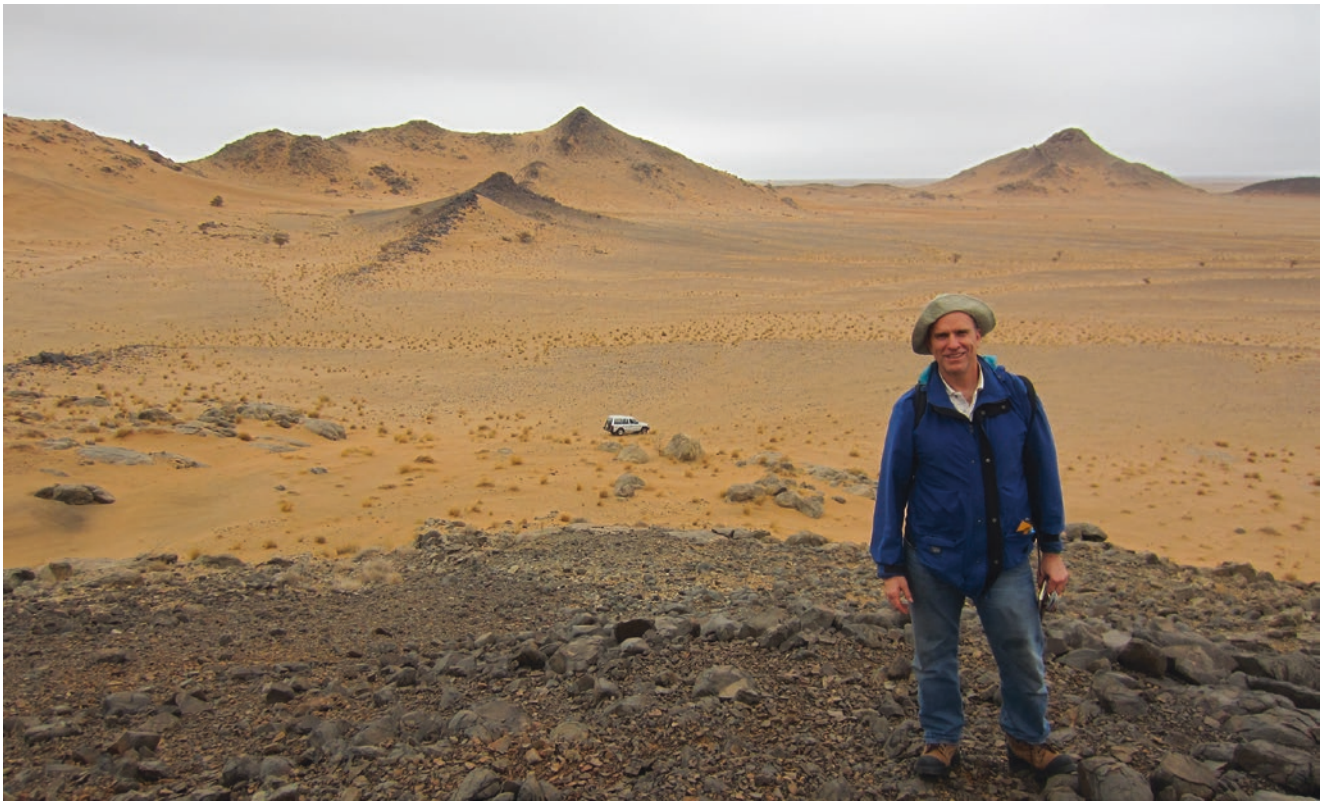

Fig. 8.37 Dykes in the Sahara desert, in Moroccan Sahara (Western Sahara). Several dolerite dykes are present including one that extends into the distance along two hills, seen on the left of the geologist Richard Ernst, who is standing on another dyke. The dykes are Late Archaean or Proterozoic
Photo © *Richard E. Ernst*

Fig. 8.38 Outcrop and semi-outcrop marks the surface trace of a dolerite dyke in the Sahara desert, in Moroccan Sahara (Western Sahara). The dyke is likely Precambrian in age, though undated. Geologists are Nasrrddine Youbi and Ech-Cherki Rjimati
Photo © *Richard E. Ernst*

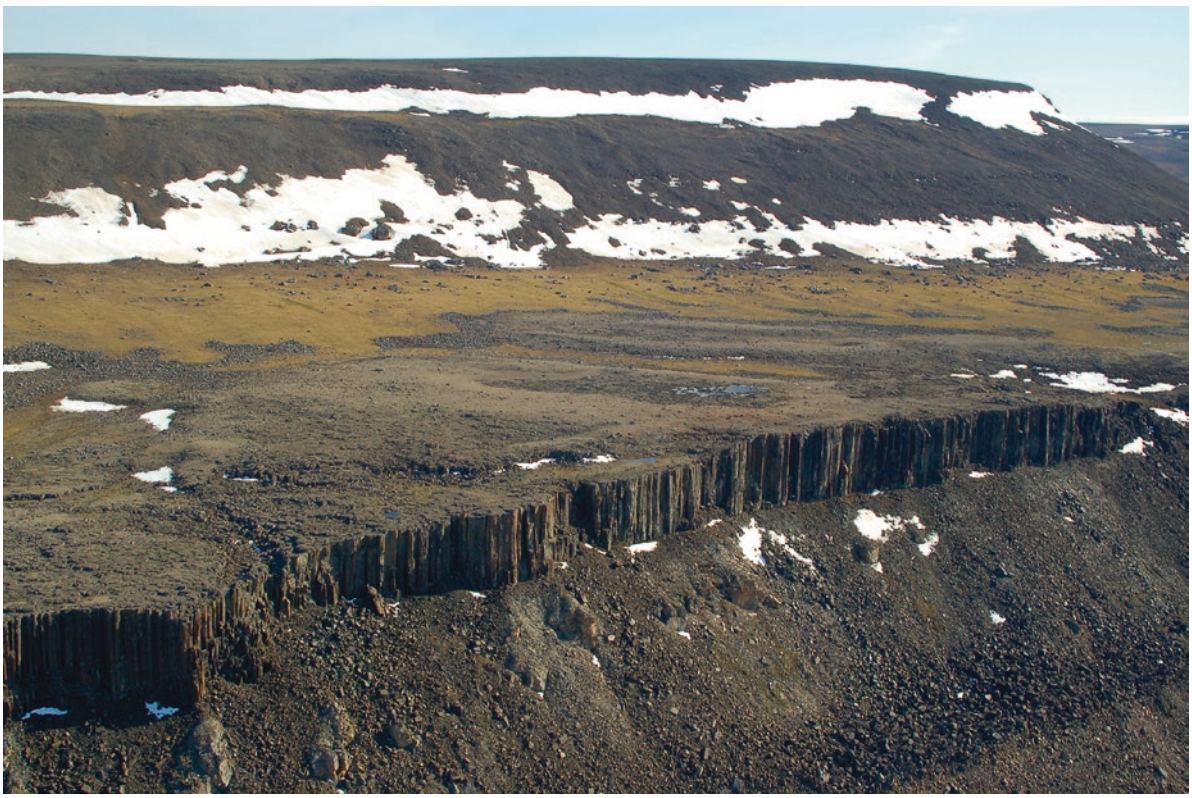

Fig. 8.39 A cliff-forming Natkusiak flood basalt sill (a few tens of meters thick) with prominent columnar jointing, Victoria Island, Canadian Arctic. View is to the south on GSC Mapsheet 104 (Rainbird et al. 2013). There is a thin sandstone layer beneath the sill and also hidden in the rubble above. The cliffs in the background are formed by the Natkusiak lavas, part of the 725 Ma Franklin LIP Photo © *Dominique Weis*

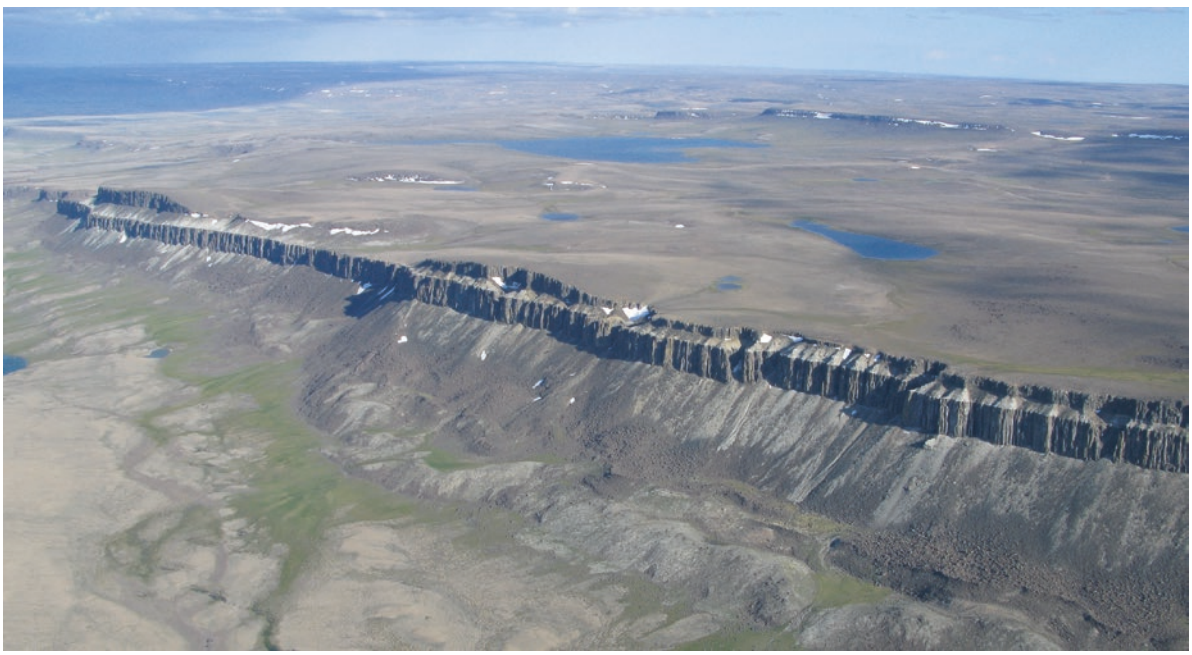

Fig. 8.40 Two tholeiitic sills of the 725 Ma Natkusiak flood basalts, with a thin sedimentary layer in between, on Victoria Island, Arctic Canada. These flood basalts are part of the Franklin LIP. View is looking ESE on GSC Mapsheet 199 (Bédard and Rainbird 2015). The resistant upper sill extends to the cliffs in the far distance such that the entire flat surface is a diabase plain. The distant cliffs are formed by higher sills
Photo: *Jean Bédard, Geological Survey of Canada*

Fig. 8.41 Doleritic sill referred to as the 'Kilt Rock' within the Little Minch Sill Complex that crops out in the eastern part of the Trotternish Peninsula of the Isle of Skye, NW Scotland. This Palaeogene sill has been intruded into the Middle Jurassic Valtos Sandstone Formation. Note another sill at sea level. Height of the cliff is ca. 75 m
Photo © *Brian R. Bell*

Fig. 8.42 Scott Simper photographs Seth Burgess on a lichen-covered columnar basaltic sill on an island in the Angara River near 58.38 N, 102.85 E. Note well-developed chiesel marks on the columns
Photo © *Linda Elkins-Tanton*

Fig. 8.43 Sverre Planke stands by the Bratsk Sill, a dolerite intrusion of the Siberian Traps flood basalt province, near 56.29 N, 101.79 E
Photo © *Linda Elkins-Tanton*

Fig. 8.44 A sill of the Draa Valley/Zemoul sill complexes (CAMP) intruding the Devonian sedimentary cover of the Anti-Atlas (Morocco). Photo was taken from the road between the towns of Foum Zguid and Tissinnt near Mrimnna at Oued Tissinnt. Note geologists in the left foreground for scale
Photo © *Nasrrddine Youbi*

Fig. 8.45 Columnar-jointed Karoo sill forming vertical cliffs near the summit of a 580 m high mountain of the Karoo flood basalts reaching 2040 above sea level. Location is about 150 km west of Durban
Photo © *Saumitra Misra & Kreesan Palan*

Fig. 8.46 Two Karoo dolerite sills connected by a dyke and intruding Permian sedimentary rocks, east of Williston, South Africa. Note a finger of the upper sill into the underlying sedimentary rocks (near hammer)
Photo © *Hervé Bertrand*

Fig. 8.47 Tasmanian Jurassic dolerite sill exposed in sea cliffs (height ~170 m) at Fluted Cape, South Bruny National Park, Bruny Island, Australia
Photo © *Trevor J. Falloon*

Fig. 8.48 Organ Pipes: a columnar-jointed sill of Tasmanian dolerite that forms the top of Mount Wellington, 1271 m above sea level and the city of Hobart in the foreground. The columns are 2–6 m wide and 20–60 m high
Photo © *Alexei V. Ivanov*

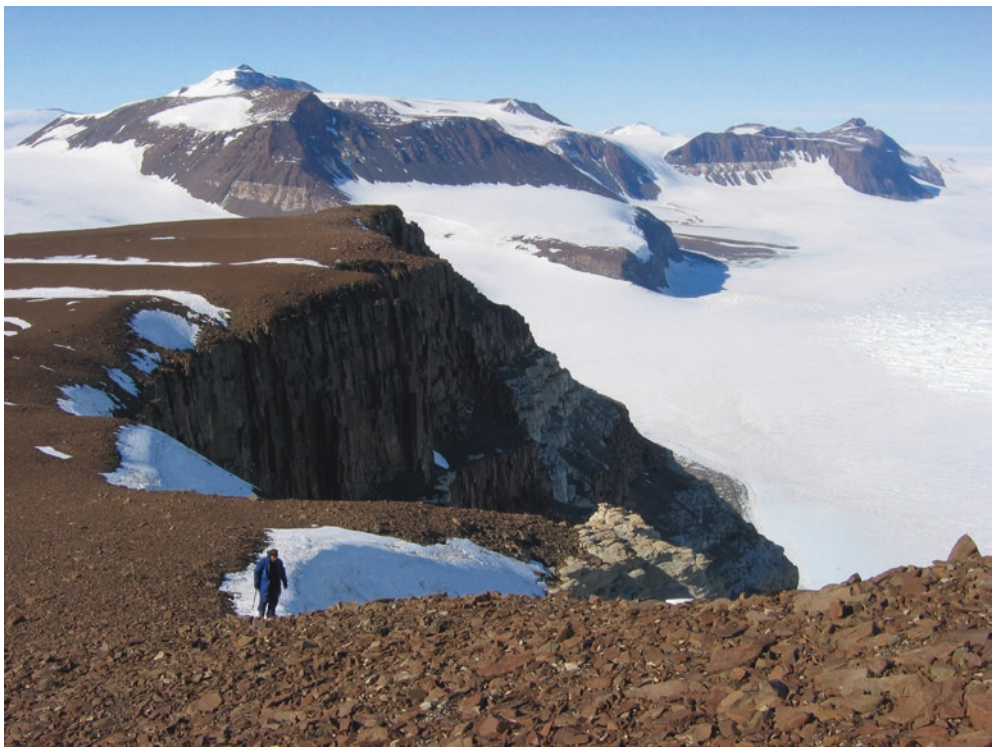

Fig. 8.49 Ferrar Province sills intruding sandstone of the Beacon Supergroup, Mt. Gran, Antarctica, with Thor Thordarson traversing above an 800 m cliff exposure (White et al. 2009; Airoldi et al. 2016)
Photo © *James White*

Fig. 8.50 Photo to the north from Friis Hills in the McMurdo Dry Valleys, Antarctica. The lower half of the ~250 m thick Basement Sill (part of the Ferrar LIP) intrudes granite basement on the valley floor, which is covered in glacial till. In the background, the Asgard Range exposes sills and a sheet swarm. Geologist Rob Dunn is standing on the Peneplain Sill
Photo © *James Muirhead*

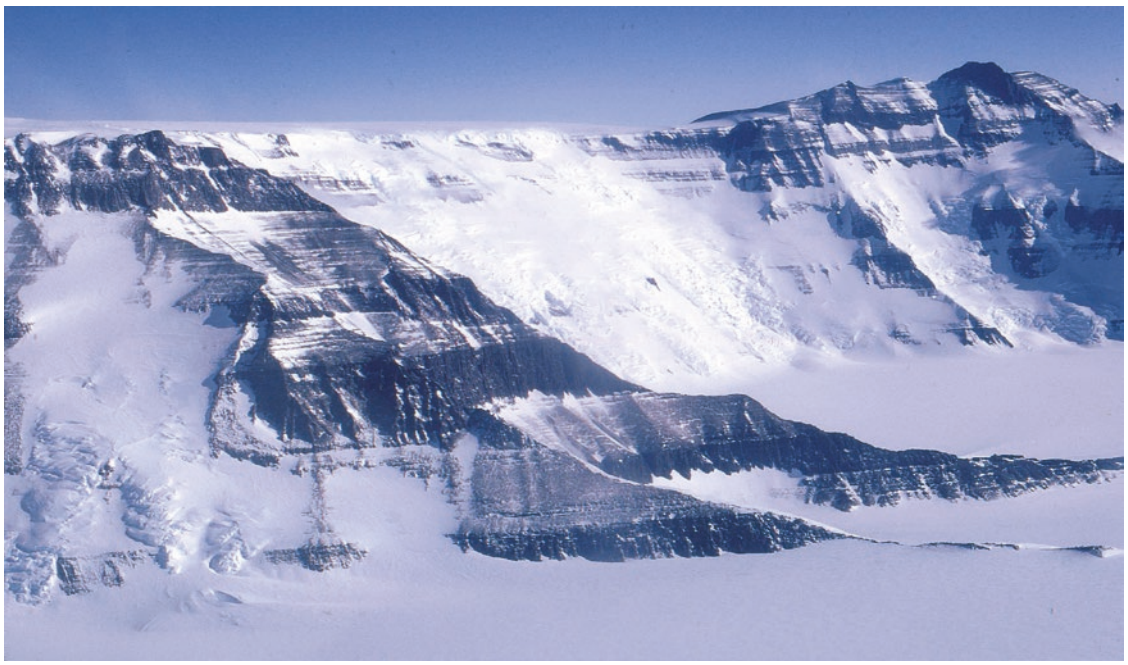

Fig. 8.51 Five Ferrar Dolerite sills, each 100–200 m thick, intruded into Permian non-marine clastic strata in a 1500 m section at Mt. Mackellar, central Transantarctic Mountains. More information: Elliot and Fleming (2004)
Photo © *David H. Elliot*

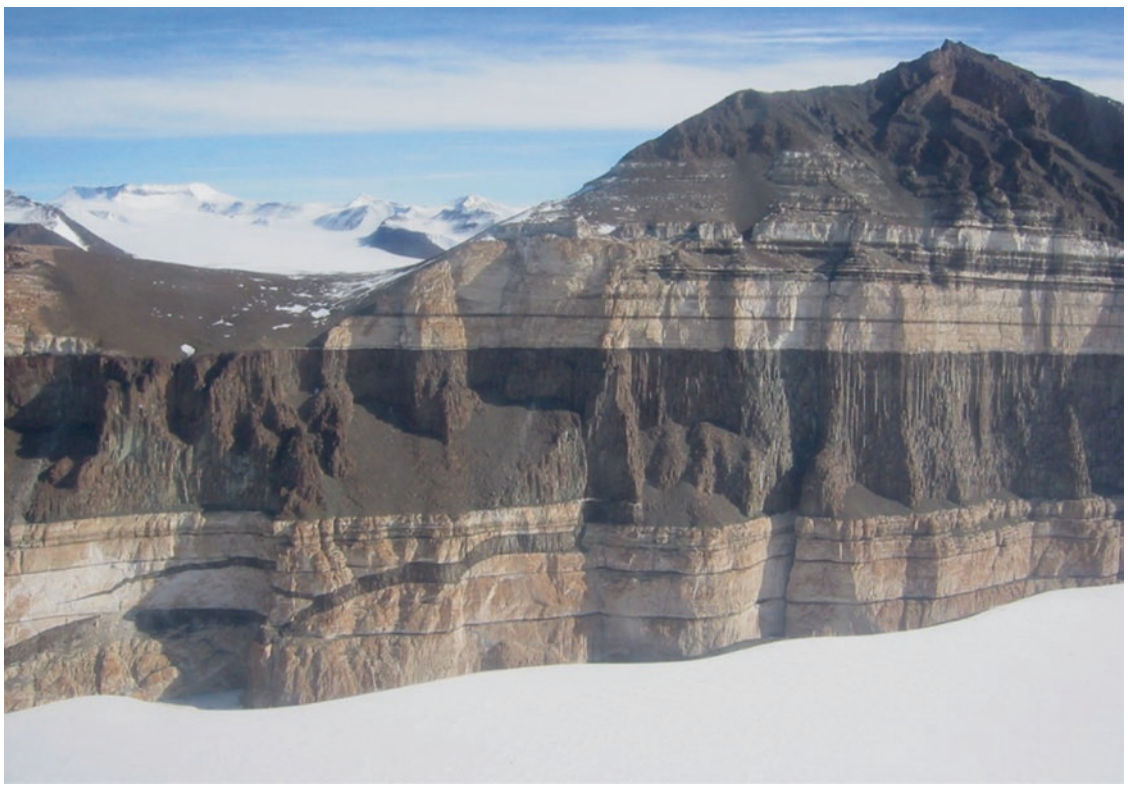

Fig. 8.52 Sills of Jurassic Ferrar dolerite intruded into the Beacon Sandstone, at Finger Mountain, Victoria Land and McMurdo Dry Valleys, Antarctica. The middle, columnar-jointed sill, sending fingers into the sandstone, is ~300 m thick, and the height of the mountain above the snowy plain is ~1100 m
Photo: *Jean Bédard, Geological Survey of Canada*

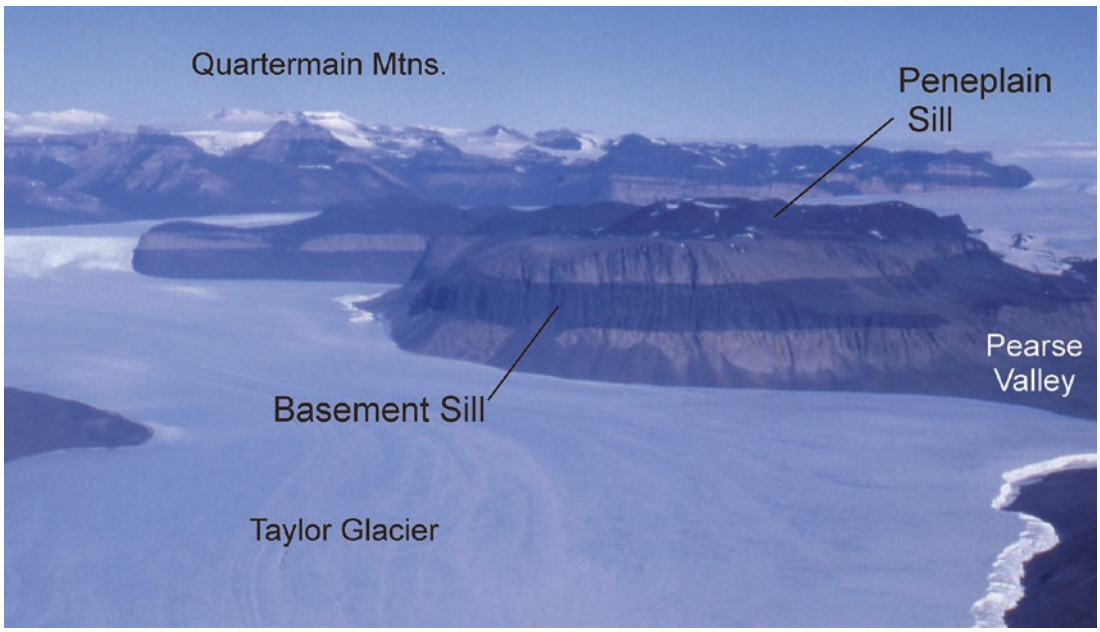

Fig. 8.53 Ferrar Dolerite, Taylor Glacier, South Victoria Land. The stratigraphically lowest Basement Sill (ca. 250 m thick) and Peneplain Sill (ca. 300 m thick) are exposed in the foreground at Friis Hills and Solitary Rocks (Hamilton 1965; Gunn 1966; Marsh 2004). In the distance stratigraphically higher, dark-coloured sills intrude Devonian Beacon strata in the Quartermain Mountains
Photo © *Thomas H. Fleming*

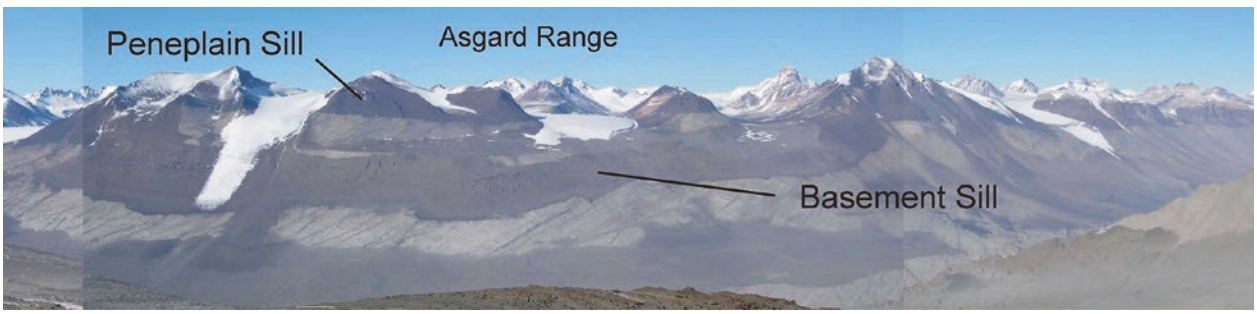

Fig. 8.54 Wright Valley, South Victoria Land, Antarctica. Outcrops of Ferrar Dolerite sills are exposed in the southern wall of Wright Valley (Asgard Range). The Basement Sill (ca. 350 m thick) intrudes Lower Palaeozoic granitoids and forms a series of interconnected lobes (Gunn 1966; Marsh 2004). Higher elevations of the Asgard Range consist of remnants of the Peneplain Sill that is intruded at or near the regional unconformity (Marsh 2004) between Devonian strata and Lower Palaeozoic granitoids
Photo © *Thomas H. Fleming*

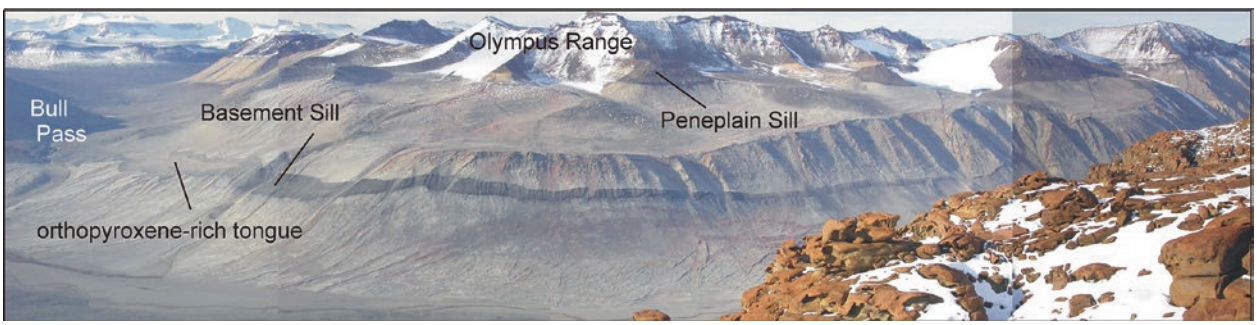

Fig. 8.55 Wright Valley, South Victoria Land, Antarctica. Ferrar Dolerite sills are exposed in the northern wall of Wright Valley (Olympus Range). The lowermost sill (Basement Sill) occupies Bull Pass and to the west is ca. 380 m thick. It contains a thick and prominent tongue enriched in orthopyroxene phenocrysts and forms sandy talus slopes in the vicinity of Bull Pass (Bédard et al. 2007). The sill thins dramatically eastward (to the right) in the photo and eventually turns upward into a thin dyke which penetrates the overlying sill. Adjacent to the prominent gulley on the left hand side of the image, it is about 80 m thick (B.D. Marsh, pers. comm., 2017). Dark rocks at higher elevations of the Olympus Range are remnants of the Peneplain Sill (Gunn 1966; Marsh 2004)
Photo © *Thomas H. Fleming*

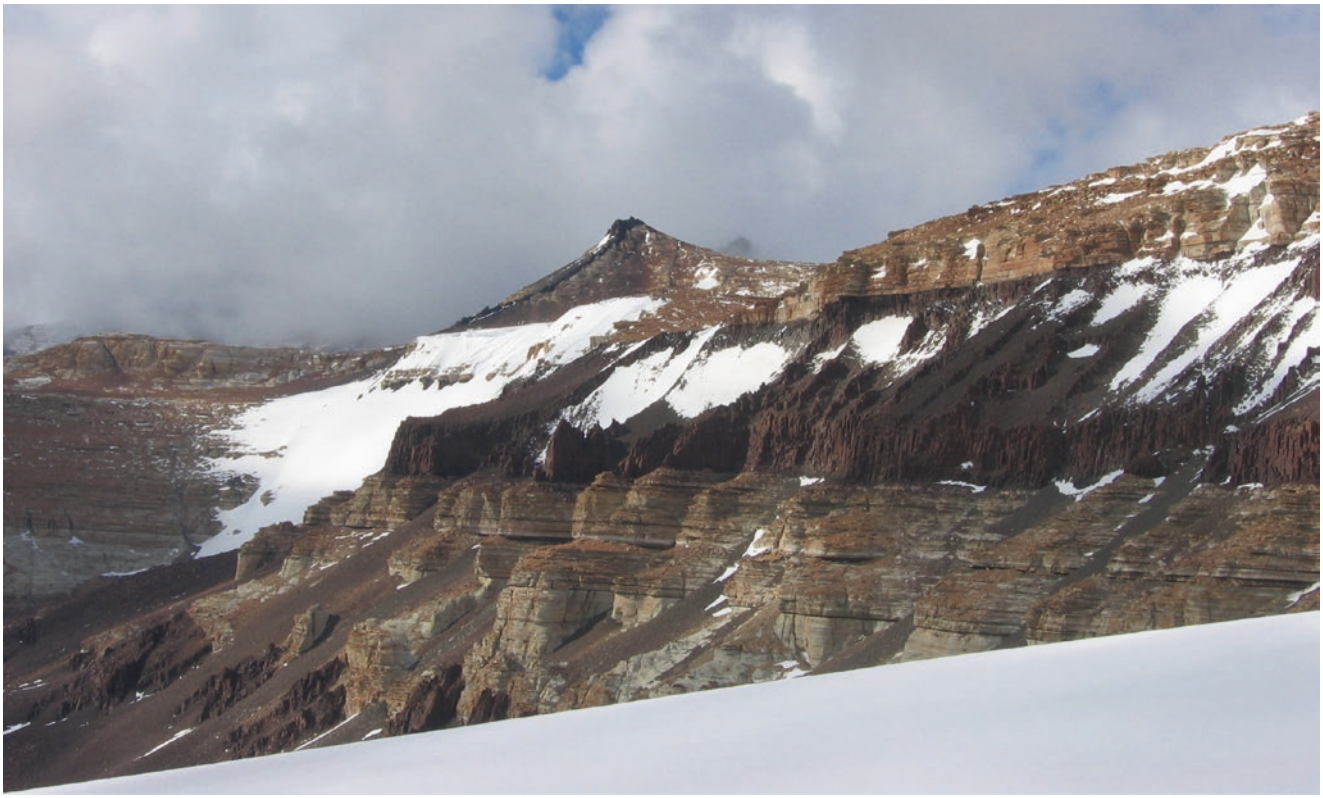

Fig. 8.56 Twenty-meter thick columnar-jointed Ferrar Dolerite sill in Beacon Supergroup sandstones, Mt. Kuiper, Antarctica (e.g., Muirhead et al. 2014). Glacier is in foreground; the dyke ascends the stratigraphy to dolerite-capped hill on the horizon
Photo © *James White*

Fig. 8.57 Photo taken on the northern side of the Friis Hills, McMurdo Dry Valleys, Antarctica. A small sill segment (~2 m thick) departs from the top margin of the ~250 m thick Basement Sill of the Ferrar LIP. Geologist is Rob Dunn
Photo © *Giulia Airoldi*

Fig. 8.58 A picritic multiple sill on the Trotternish peninsula, Isle of Skye, NW Scotland. The sills are part of the British Palaeogene igneous province. More information: Emeleus and Bell (2005)
Photo © *Hetu Sheth*

Fig. 8.59 The Palisades dolerite sill, part of the 200 Ma CAMP in the northeastern USA, is up to 300 m thick and typically columnar-jointed. Photograph is from an operating quarry in West Nyack, southern New York State, and shows only the lowest two of the ten or so benches cut through the sill. Mine geologist and the vehicle provide a scale. The Palisades Sill is multiple and was formed by several magma injections, which can be correlated with erupted lava flows of the Newark Basin, New Jersey. More information: Puffer et al. (2009)
Photo © *Hetu Sheth*

Fig. 8.60 The Gettysburg Sill, one of many dolerite sheet intrusions of the ~200 Ma Central Atlantic Magmatic Province (CAMP), here in an operating quarry near Gettysburg, Pennsylvania, USA. The sill is the red layer near the top of the quarry, and has baked underlying and overlying sediments to a tough hornfels. Digger and truck at a lower level provide a scale
Photo © *Loÿc Vanderkluysen*

Fig. 8.61 Karoo doleritic sill (30–40 m thick) intruding Permian sedimentary rocks near Noordoewer, Namibia
Photo © *Hervé Bertrand*

Fig. 8.62 The 22 m thick, columnar-jointed Mahad sill exposed on the Mumbai-Goa Highway near Mahad, Konkan Plain, western Deccan Traps, and here photographed after a rain shower. Geologist is Hetu Sheth. This sill is a saucer-shaped tholeiitic sill emplaced into the Deccan basalt sequence. More information: Duraiswami and Shaikh (2013)
Photo © *Nasrrddine Youbi*

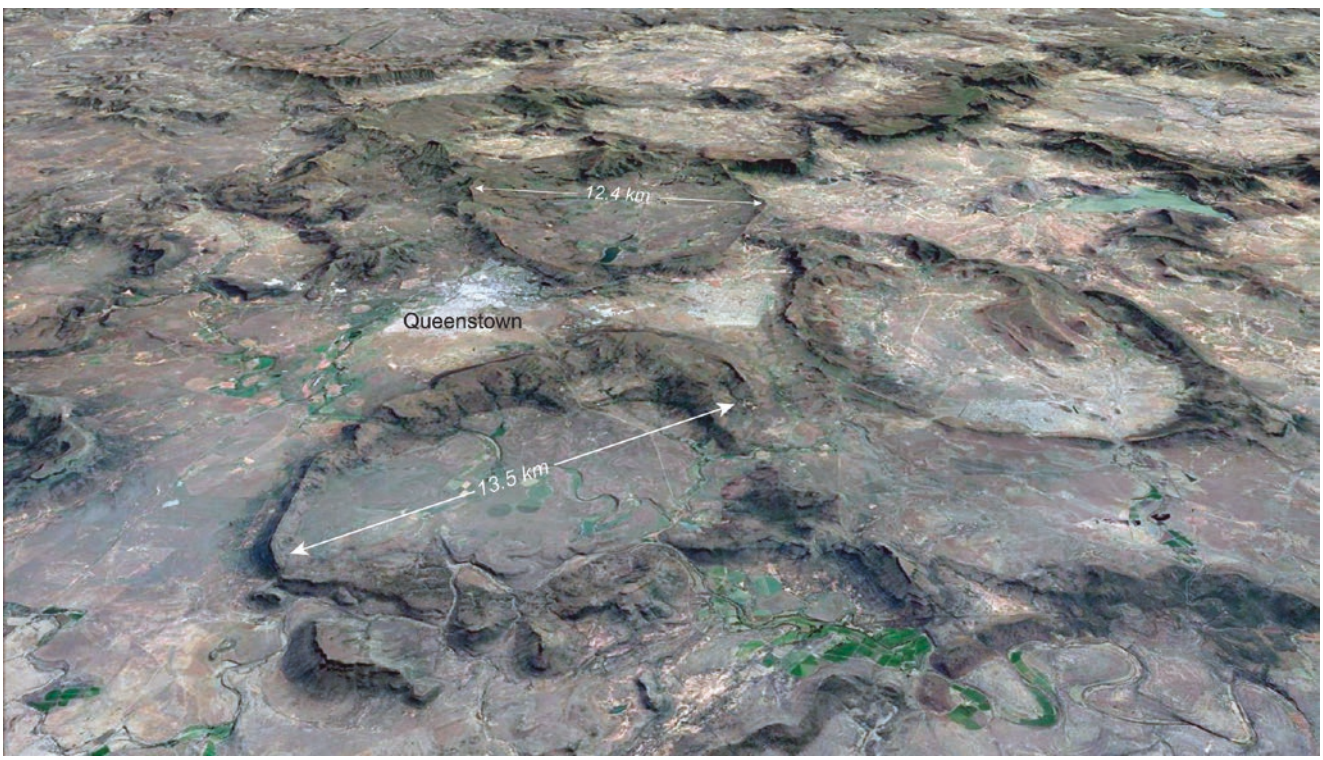

Fig. 8.63 Saucer-shaped sills in the Karoo Supergroup, as viewed obliquely north in Google Earth
Image capture © *Martin B. Klausen*

Fig. 8.64 The Gilbert Hill columnar basalt in Andheri, a late-Deccan (60.5 Ma) mafic sheet intrusion in the Mumbai sequence. The hill, originally much more extensive and about the height of a ten-storeyed building, is now largely destroyed and almost completely surrounded by buildings
Photo © *Hrishikesh P. Samant*

Fig. 8.65 Anton Latyshev and Roman Veselovskiy at the Daldykan Intrusion near Noril'sk, at 69.35 N, 88.08 E, Siberian Traps. A zircon from this intrusion was dated at 251.376 Ma (Burgess and Bowring 2015)
Photo © *Linda Elkins-Tanton*

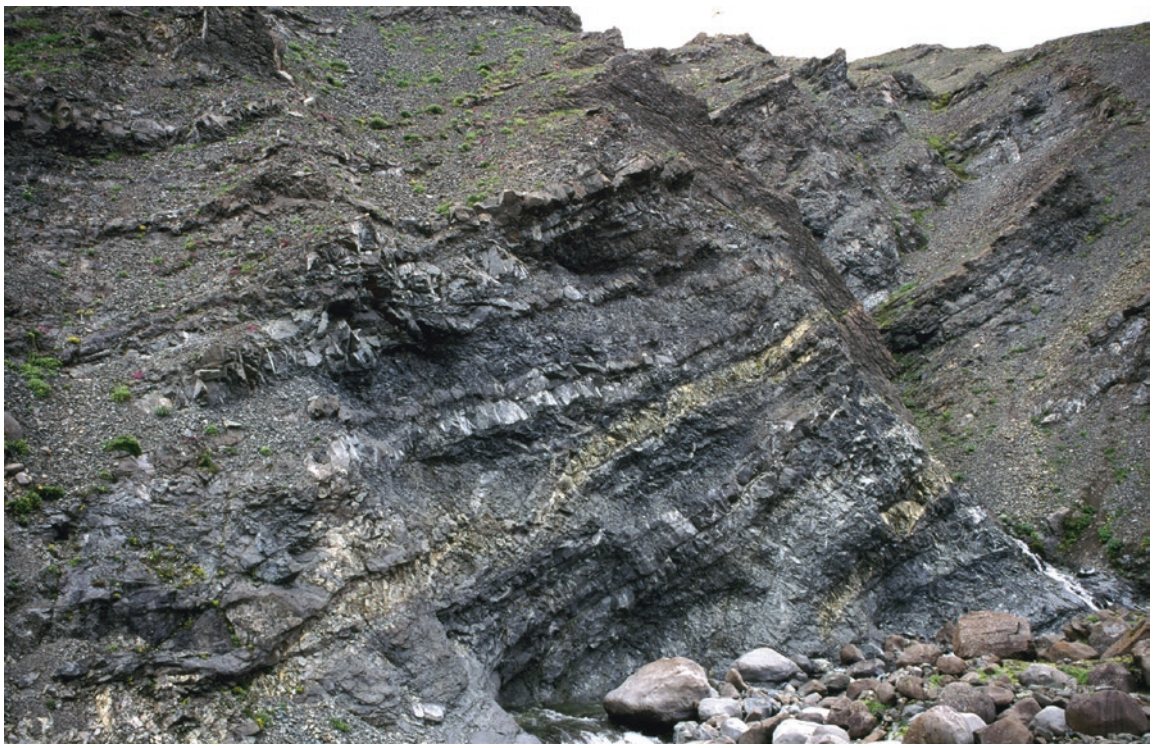

Fig. 8.66 Less than 1 m thick and inclined (cone) sheets, of varied compositions, at the Geitafell central volcano (SE Iceland; cf. Fig. 3d in Klausen 2004)
Photo © *Martin B. Klausen*

Fig. 8.67 Basaltic sheet on the southern wave-cut platform of Elephanta Island, Mumbai harbour, western Deccan Traps. Sheet shows pervasive, spectacular prismatic jointing (see also Fig. 5.5), and dips ~45° E in basalt flows (smooth surfaced) which dip 12° WNW. Geologist is Joseph D'Souza. On the left horizon are the hills of Uran
Photo © *Hetu Sheth*

Fig. 8.68 Palaeogene cone sheets of dolerite within metasedimentary host rocks (psammites) of the Moine Supergroup, Ardnamurchan, NW Scotland. These cone sheets belong to the Ardnamurchan Intrusive Complex, and are typically up to 3 m thick, with a common focal point at depth. Note houses in the left background
Photo © *Brian R. Bell*

Fig. 8.69 Cone sheets of tholeiitic dolerite cutting Outer Bytownite Gabbros near the Scavaig River, Cuillin Central Complex, Skye. Three cone sheets (numbered) are visible, with narrow screens of host rock in between. Brian Bell is seated on cone sheet 1. More information: Emeleus and Bell (2005)
Photo © *Hetu Sheth*

Fig. 8.70 Photo of a hybrid, dyke-sill intrusion of the Ferrar LIP at Allan Hills, Antarctica. Here a ~2 m-thick, moderately dipping (~55°) dyke transitions up section into a sill before breaking out again into a dyke. The host rocks are sandstones of the Victoria Group
Photo © *Julie Rowland*

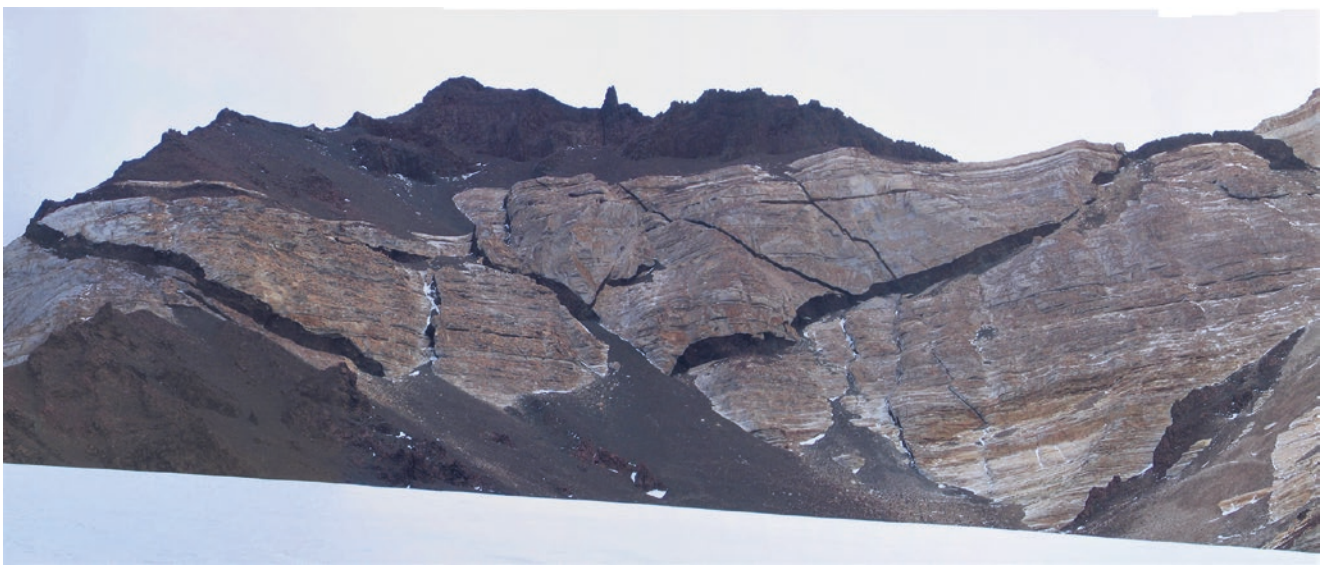

Fig. 8.71 The southeastern face of Terra Cotta Mountain, Antarctica. Here a swarm of moderately dipping Ferrar LIP dykes ascend a 200 m high cliff and merge with a sill on the mountain's summit
Photo © *James White*

Fig. 8.72 A 180 m high cliff face exposing a swarm of sills (~30 m thick) interconnected by inclined sheets at Mt. Gran, Antarctica
Photo © *James White*

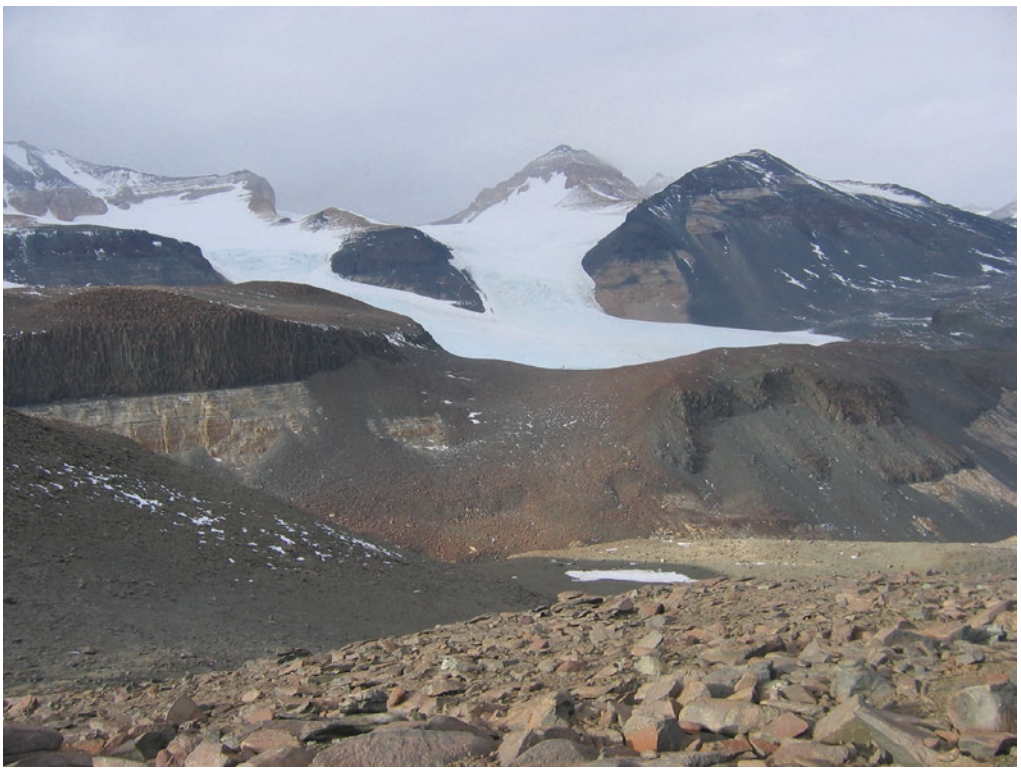

Fig. 8.73 Columnar-jointed Ferrar Dolerite sill (~40 m thick at left) in Beacon Supergroup sandstones, Friis Hills, Antarctica. Note thick inclined sheet stepping up to right toward higher-level sill in right background. Country rock below lowest sill, to the right, is granitic basement (Airoldi et al. 2016)
Photo © *James White*

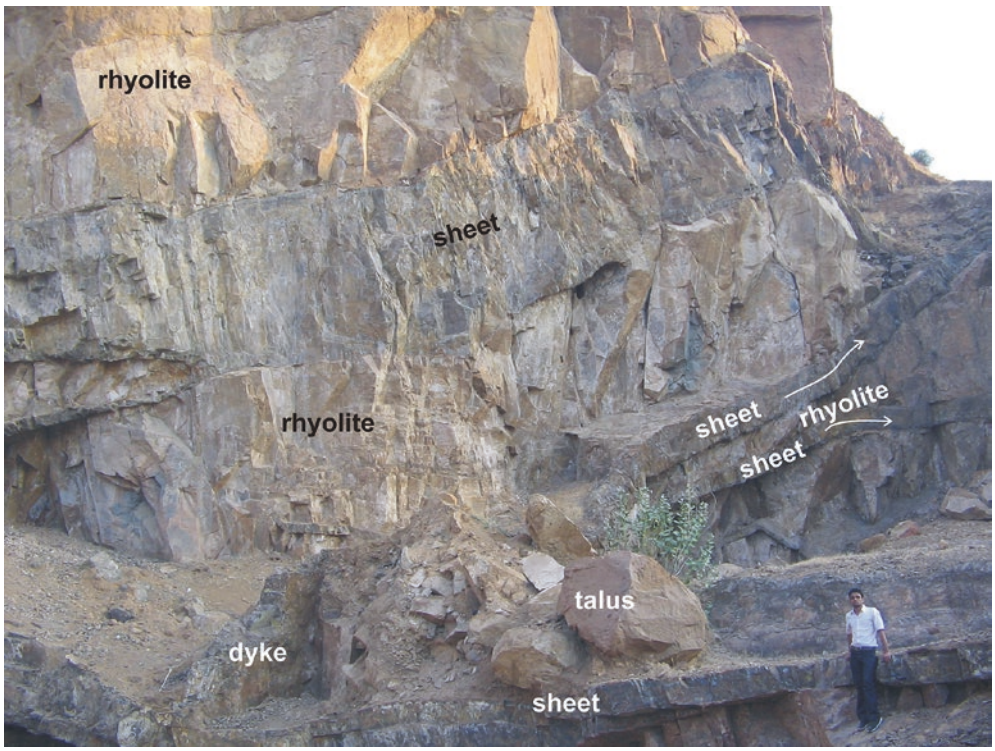

Fig. 8.74 Inclined sheets and dyke, of unknown composition, cutting a subvolcanic rhyolite plug (golden brown). White arrows show the upward divergence of two nearby sheets with a screen of the rhyolite in between. Exposure is in an abandoned quarry pit in the town of Sihor, Saurashtra, northwestern Deccan Traps, and has not been studied. Geologist is Badrealam Shaikh
Photo © *Hetu Sheth*

Fig. 8.75 Unroofed mid-Miocene basaltic plug aptly named Chocolate Mountain, Santa Rosa-Calico volcanic field, northern Nevada, USA. The feature is ~0.6 km across at exposed base. See Brueseke and Hart (2008) for more information
Photo © *William K. Hart*

Fig. 8.76 Modally layered Outer Bytownite Gabbros of the Cuillin Intrusive Complex, Isle of Skye. Height of hill in centre of view is ca. 145 m
Photo © *Brian R. Bell*

Fig. 8.77 Isle of Skye, NW Scotland. The foreground cliffs are composed of pale brown Elgol Sandstone Formation, of the Middle Jurassic Great Estuarine Group. Beyond are younger formations of the Great Estuarine Group. Note people at the base of the cliffs for scale, and sheep (white specks) on the grassy slope above the cliffs. The imposing pyramid in the background is the 926 m high Bla Bheinn (Blaven), composed of the Outer Bytownite Gabbros of the Skye Central Complex, cut by cone sheets
Photo © *Hetu Sheth*

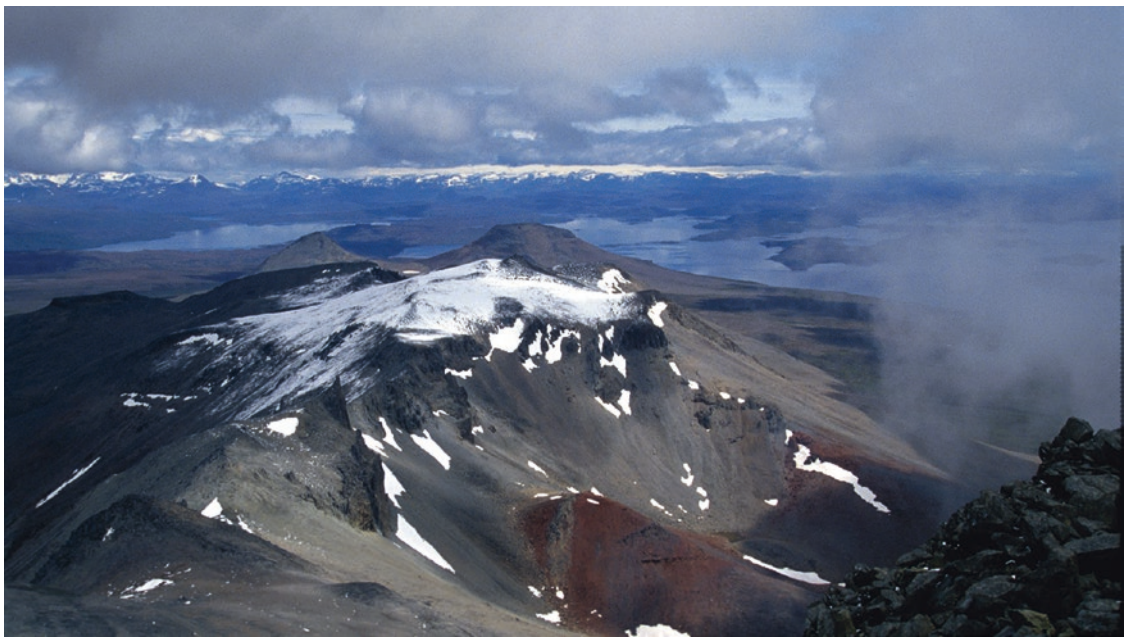

Fig. 8.78 The summit of Mt. Wyville Thomson (937 m), formed of alkaline plugs intruding flood basalts of the southeast Kerguelen province. In the background, the large development of Kerguelen alkaline flood basalts on the Crozet peninsula is visible
Photo © *Dominique Weis*

Fig. 8.79 The Skaergaard Intrusion: Gabbrofjeld peak (1200 m) seen from across Uttental Sund. To the right is the snout of Forbindelsegletscher. Note the three noticeable leucogabbro layers of the Triple Group below the top of Gabbrofjeld. The lower two leucogabbro layers host the Skaergaard PGE-Au mineralization. Geologist in the boat is C. Kent Brooks
Photo: *Bjørn Thomassen, Geological Survey of Denmark and Greenland (GEUS)*

Fig. 8.80 Mount Girnar (1117 m, centre of photo) in Saurashtra, composed of layered gabbro below and diorite above, is the largest intrusion in the Deccan Traps, and has domed up basaltic flows (rising to >800 m) which are here seen to dip radially away from it. Relief is >1 km
Photo © *Hetu Sheth*

Fig. 8.81 Mount Girnar (1117 m) in Saurashtra, the largest intrusion in the Deccan Traps. The mountain is composed of gabbro and layered gabbro in the lower and peripheral parts, and diorite and monzonite in the upper part, and has domed up overlying basaltic flows, imparting them radial dips (not seen in this photo). The chain of hills in the foreground, composed of light-coloured rock, is a nearly complete ring dyke of granophyre which cuts the outward-dipping basalt flows (Mathur et al. 1926). Relief is >1 km, and the actual summit is beyond (east of) and higher than the top seen in this photograph
Photo © *Hetu Sheth*

Igneous Processes and Magmatic Diversity in Flood Basalt Provinces

9

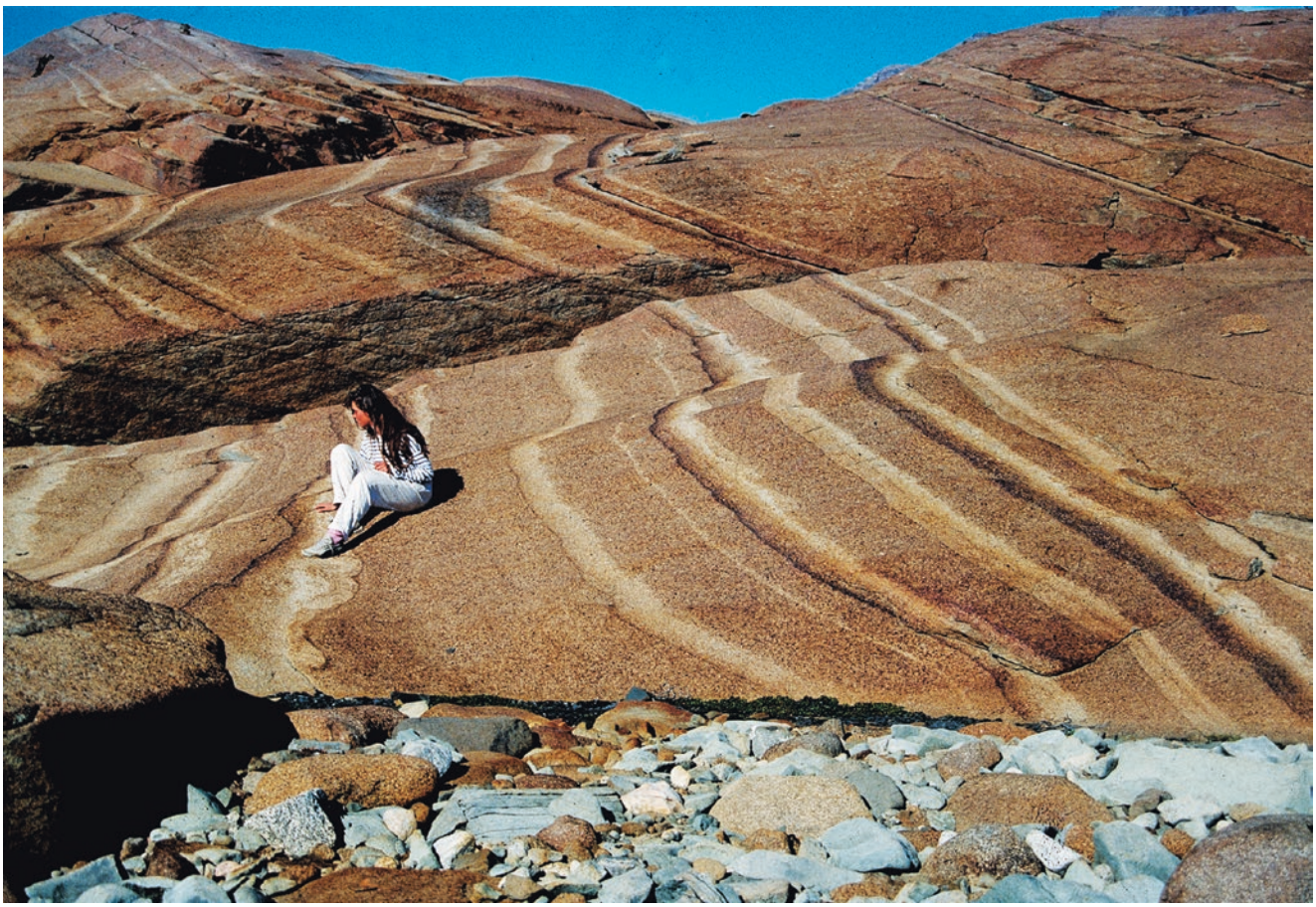

Fig. 9.1 Igneous layering in the Skaergaard Intrusion, East Greenland. Layered gabbros of Upper Zone A (UZa) inland from Hjemmebugt (Home Bay). The liquidus paragenesis of the gabbro is plagioclase, Fe-rich olivine, clinopyroxene, magnetite and ilmenite. The geologist is Karen Bollingberg
Photo © *C. Kent Brooks*

H. Sheth, *A Photographic Atlas of Flood Basalt Volcanism*, https://doi.org/10.1007/978-3-319-67705-7_9

Chapter Overview

Flood basalt provinces, though dominated by tholeiitic basalt and basaltic andesite, in fact contain a great variety of rock types, both subalkalic and alkalic, and ultramafic to silicic. Rhyolites are voluminous in provinces like the Karoo and Paraná provinces, and in the Yellowstone "hotspot track" associated with the Columbia River province. Though volumetrically minor in the Deccan province taken as a whole, rhyolites are important or even dominant in parts of the western and northwestern Deccan situated along the western Indian rifted margin (e.g., Sheth and Pande 2014). Alkalic rock types such as basanites, nephelinites, syenites, trachytes and lamprophyres, along with carbonatites, are found in all or most provinces. Komatiites were important associates of Archaean flood basalts.

Such non-basaltic rocks in flood basalt provinces are the products of many magmatic processes including crystal settling, transport of early-formed crystal loads in unrelated magmas, partial melting of older crustal rocks and contemporaneous, hydrothermally altered intrusions or lava flows, and mingling and mixing between mafic and felsic magmas. Direct field evidence for such processes having occurred can be found in the plutonic bodies exposed in flood basalt provinces, including the huge Precambrian layered mafic intrusions which host significant economic mineral deposits like chromium and platinum, and younger intrusions such as the Skaergaard where many of the current ideas in igneous petrology were first developed and tested (e.g., Wager and Deer 1939; Wager et al. 1960).

The spectacular giant plagioclase basalt (GPB) lava flows found throughout the Deccan have been recently interpreted (Sheth 2016) as accidental mixtures between plagioclase flotation cumulates in deep crustal or Moho-level mafic sills and new tholeiitic magmas. An interesting corollary of this model is that anorthosites, which reached important development in the Archaean and especially during the Proterozoic, have continued to form during Phanerozoic time, and that continental flood basalt provinces should be viewed as sites of anorthosite formation in the deep continental crust. An interesting further question to be answered is why GPBs, abundant in the Deccan, and not uncommon in the Columbia River and Emeishan provinces, or indeed Iceland (with its thick crust), are notably rare or absent in other provinces such as Siberia, Karoo, or Indo-Madagascar. Is this because the continental crusts under these provinces were too thick for underplated mafic sills to crystallize plagioclase in the first place? Another interesting broader question is why there are archetypal flood basalt provinces, such as the British Palaeogene Igneous Province, where mildly alkalic compositions like hawaiites and mugearites are common (indeed, the type localities for some of these rock types are in this province), whereas others like the Deccan or Columbia River have minor volumes of such rocks? One thing is certain: flood basalt provinces are by no means just "monotonous tholeiitic basalt".

Fig. 9.2 Contact between the Grande Ronde Basalt (above) and the Imnaha Basalt (below) at the confluence of Grande Ronde and Snake Rivers, Columbia River flood basalt province. The contact represents a major compositional and physical change from the more primitive and plagioclase-phyric Imnaha Basalt to the typically aphyric and compositionally evolved Grande Ronde Basalt. The absence of significant weathering or sediment deposition at the contact suggests very little time between the two major formations of the Columbia River Basalt Group. Anita Ho is the geologist
Photo © *Stephen P. Reidel*

Fig. 9.3 Giant plagioclase basalt (GPB) flow between two basalt flows. Shivneri Fort near Junnar, western Deccan Traps. The GPB flow (Manchar GPB, 975 m above sea level) is extremely rich in plagioclase megacrysts (up to 3 cm in length, but 5 cm megacrysts are common in the Deccan GPBs). Photo shows why the GPBs have been valuable field marker horizons in working out the lava stratigraphy of the western Deccan Traps. Note also that the boundaries of the GPB with the underlying and overlying flows are quite irregular. Geologist is Shubhankar Majhi
Photo © *Ishita Pal*

Fig. 9.4 Succession of picrite lava flows consisting of alternating flow groups of thin and thick flows. The part shown is 300 m thick. Through the gap is a view to yellow sandstones overlain by picrite flows in central Nuussuaq. Vaigat Formation, south coast of Nuussuaq, West Greenland
Photo: *Asger Ken Pedersen, Geological Survey of Denmark and Greenland (GEUS)*

Fig. 9.5 Bifurcations in the UG-1 chromitite layer and its spectacular layering with anorthosite (footwall) in the 2.06 Ga Bushveld Complex in South Africa, world's largest layered mafic intrusion (e.g., Cawthorn 2015). Photograph is from the world-famous Dwars River area in the Eastern Bushveld that hosts the best surface exposure of the UG-1 chromitite; the Dwars River Heritage Site monument is seen in the background of the exposure
Photo © *Ria Mukherjee*

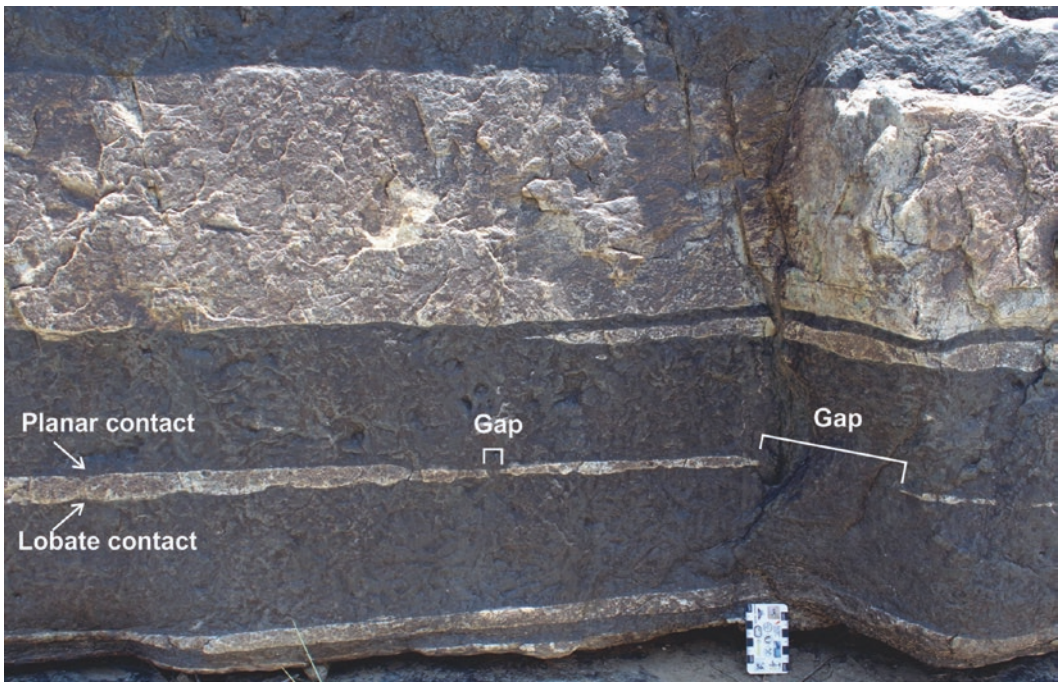

Fig. 9.6 Anorthosite layers and lenses that thin and wedge out laterally in massive chromitites. Note anorthosite layer with a planar upper contact and scalloped lower contact with underlying chromitite and a 1 cm-wide gap between adjacent lenses, and a 10 cm gap which terminates in a discontinuous tail at the same stratigraphic horizon. Dwars River Locality, Eastern Bushveld Complex, South Africa. See a detailed discussion in Pebane and Latypov (2017)
Photo © *Rais Latypov*

Fig. 9.7 Thin chromitite layers that show the fritted contacts with anorthosite and the numerous small anorthosite inclusions that appear to be connected both to each other and adjacent anorthosites. Dwars River Locality, Eastern Bushveld Complex, South Africa. See a detailed discussion in Pebane and Latypov (2017)
Photo © *Rais Latypov*

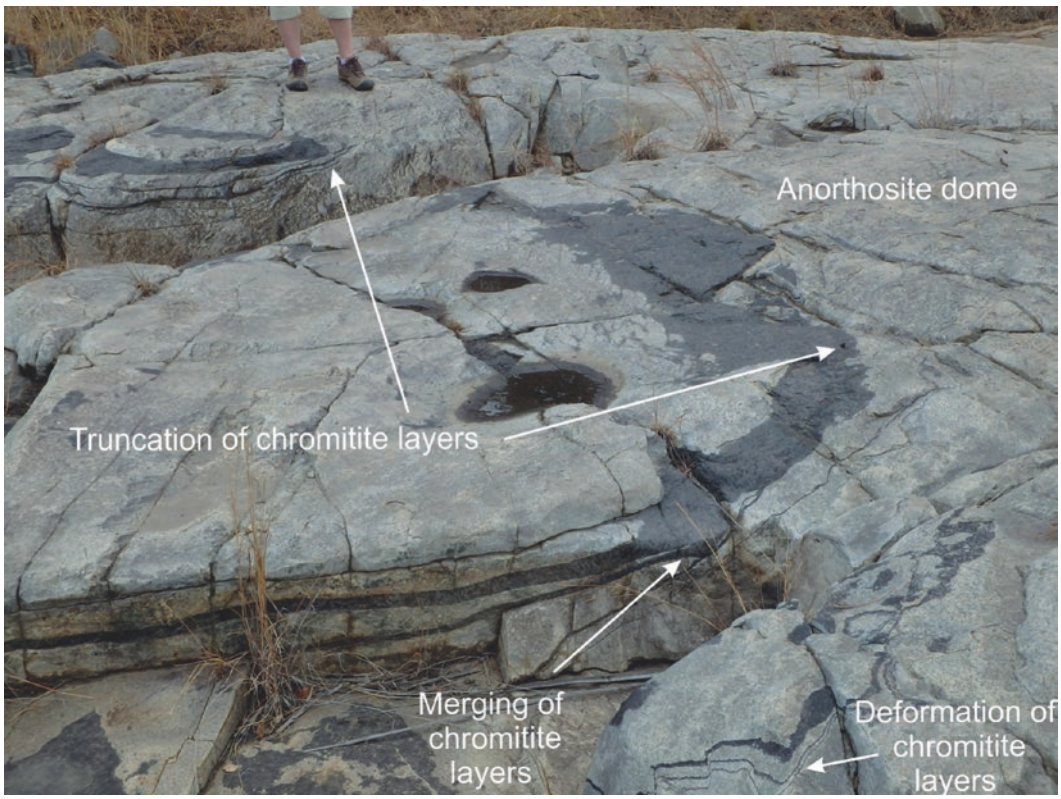

Fig. 9.8 The merging, truncation and deformation of chromitite layers at the margin of an anorthosite dome. Dwars River Locality, Eastern Bushveld Complex, South Africa. Person for scale. See a detailed discussion in Pebane and Latypov (2017)
Photo © *Rais Latypov*

Fig. 9.9 Chromitite layers affected by brittle deformation within mobilized plagioclase cumulate. Magnifying lens provides a scale. Dwars River Locality, Eastern Bushveld Complex, South Africa. See a detailed discussion in Pebane and Latypov (2017)
Photo © *Rais Latypov*

Fig. 9.10 Photograph of large oikocrysts of orthopyroxene that branch downwards within host mottled anorthosite. Dwars River Locality, Eastern Bushveld Complex, South Africa. Person on left, with notebook and shoes partly visible. See a detailed discussion in Pebane and Latypov (2017)
Photo © *Rais Latypov*

Fig. 9.11 Spectacular inch-scale "doublets" comprising rhythmic layering of pyroxene layers (dark) within anorthosite in the Lower Banded Series of the 2.7 Ga Stillwater Complex (Montana, USA). The layering is vertical because of tectonic tilting. Geologist is Ria Mukherjee. More information: Boudreau (2016)
Photo © *Ria Mukherjee*

Fig. 9.12 Igneous layering in the gabbroic Freetown Intrusion, Sierra Leone, Central Atlantic Magmatic Province (CAMP). The modal layering is marked by a variable ratio of plagioclase to ferromagnesian minerals. More information: Callegaro et al. (2017)
Photo © *Hervé Bertrand*

Fig. 9.13 Igneous layering and cross-bedding in the gabbroic Freetown Intrusion, Sierra Leone, Central Atlantic Magmatic Province (CAMP). More information: Callegaro et al. (2017)
Photo © *Hervé Bertrand*

Fig. 9.14 The Skaergaard Intrusion. Layered gabbros of the Upper Zone A (UZa) inland from Hjemmebugt (Home Bay). The liquidus paragenesis of the gabbro is plagioclase, Fe-rich olivine, clinopyroxene, magnetite and ilmenite. Geologists are Kent Brooks (blue anorak) and student T. S. Petersen
Photo: *Troels F.D. Nielsen, Geological Survey of Denmark and Greenland (GEUS)*

Fig. 9.15 Inch-scale layering in gabbro of the Kap Edvard Holm Complex, East Greenland. Exposures by the lake down from Willow Ridge. The volume of inch-scale layered gabbro is truncated by magma and mush during deformation of semi-consolidated gabbro. Hammer is 60 cm long
Photo: *Troels F.D. Nielsen, Geological Survey of Denmark and Greenland (GEUS)*

Fig. 9.16 Layered Outer Bytownite Gabbros of the Palaeogene Cuillin Intrusive Complex, Isle of Skye, NW Scotland. These modally layered gabbros crop out east of the Scavaig River (visible in top left of view). Pole is 1 m long
Photo © *Brian R. Bell*

Fig. 9.17 The Outer Bytownite Gabbros of the Skye Central Complex just west of the Scavaig River, with Meall na Cuilce in the background. Photograph shows autoliths of coarse-grained gabbro, gabbroic pegmatite and troctolite. The slight fabric detectable trending across the outcrop in the foreground is more of glacial striae than igneous layering. Bruce Julian provides a scale
Photo © *Hetu Sheth*

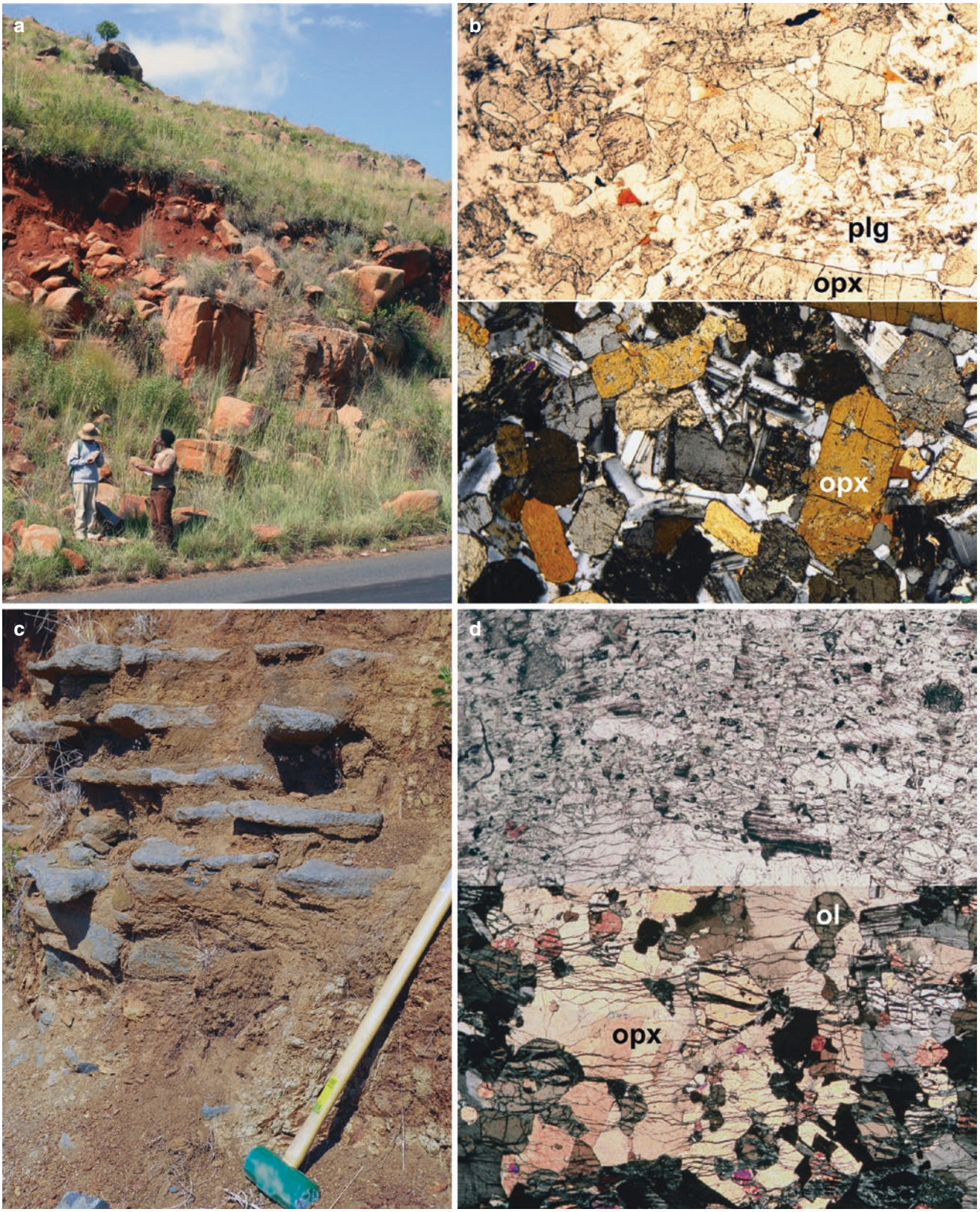

Fig. 9.18 Marginal sills of the 2.06 Ga Bushveld Igneous Complex. (**a**, **b**) Noritic sill outcrop and thin section image (cf. BCS1-02/HWS in Wabo et al. 2016). (**c**, **d**) Harzburgitic cumulates along the base of a Bushveld marginal sill, primarily exhibiting partly resorbed and serpentinized olivines (ol) inside orthopyroxene (opx) oikocrysts. *Plg* plagioclase. Thin section images (width of view = 3 mm) subdivided into upper plane and lower crossed polar halves
Photos © *Martin B. Klausen*

Fig. 9.19 Igneous layering within the Vesturhorn central volcano in eastern Iceland. From bottom (right) to top (left): Thin, rhythmic banding (note cross-bedding near lens cap indicated by white arrow), sharply overlain by an ultramafic layer that is more gradually overlain by homogenous melagabbro
Photo © *Martin B. Klausen*

Fig. 9.20 (**a**) Members of a 2000 km long and ~1630 Ma old Melville Bugt Dyke Swarm across Greenland (Halls et al. 2011). (**a**) An 8 m thick, NNW trending dyke in SE Greenland "bulges" (B), where it cuts an E-W-trending Palaeoproterozoic dyke. (**b**) Trough-like layering within another thick dyke exposed as faint and centimeter-scale rhythmic banding (RB). Hammer shaft end is 4 cm wide. More information in Klausen et al. (2016a)
Photos © *Martin B. Klausen*

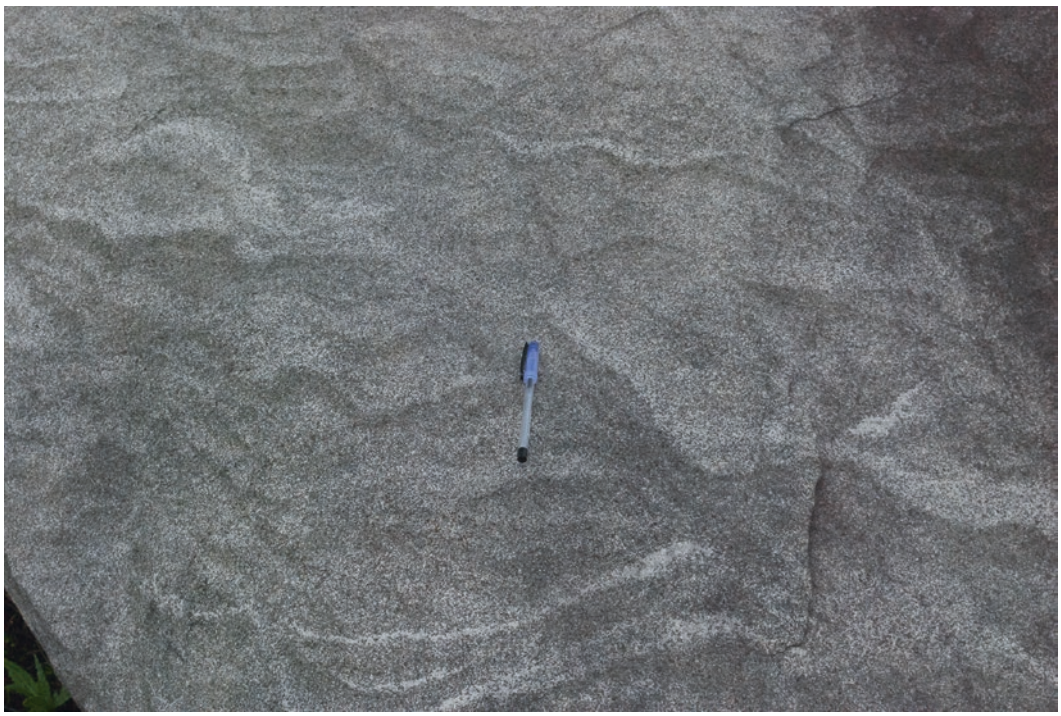

Fig. 9.21 Locally developed anorthositic and mafic-rich layers, many distinctly wavy, in the York Haven diabase sheet (part of the 200 Ma Central Atlantic Magmatic Province, CAMP). Photo is from the Gettysburg National Military Park (Pennsylvania, USA), where the diabase is generally texturally uniform and such segregations few. Pen is 15 cm long
Photo © *Loÿc Vanderkluysen*

Fig. 9.22 Layered gabbro with millimeter-thick layers in the Mer Mundwara alkaline plutonic complex, Rajasthan, western India. Coin diameter is 2 cm. The complex is now recognized as polychronous, with magmatic events at 102–110, 84–80 and 68–64 Ma (Deccan magmatism). More information: Pande et al. (2017a)
Photo © *Hetu Sheth*

Fig. 9.23 A patch of gabbro-pegmatite within the gabbroic Freetown Intrusion, Sierra Leone, Central Atlantic Magmatic Province (CAMP). More information: Callegaro et al. (2017)
Photo © *Hervé Bertrand*

Fig. 9.24 The central part of the 200 m-thick Holyoke basalt flow (of the 200 Ma Central Atlantic Magmatic Province, CAMP), here exposed in the east face of the North Branford quarry, Connecticut. The quarry face is 40 m high and >4.7 km long, and one of the longest Trap-rock quarry faces in the world. The light-coloured layer dipping gently to the right is a sheet of coarse-grained ferrodiorite in the fine-grained basalt, formed from interstitial liquid that was expelled from compacting crystal mush in the lower part of the flow. This layer, and several others like it, can be traced along the entire length of the quarry
Photo © *Anthony R. Philpotts*

Fig. 9.25 Segregations of coarse-grained ferrodiorite (dark layers and veins dipping towards the right) in the columnar-jointed Holyoke Basalt (CAMP), Tariffville gorge, Connecticut, USA. Geologists are Tony Philpotts and Loÿc Vanderkluysen. More information: Philpotts et al. (1996)
Photo © *Hetu Sheth*

Fig. 9.26 Close-up of a coarse-grained ferrodiorite segregation (dark and drilled) in the colonnade of the Holyoke Basalt (CAMP), Tariffville gorge, Connecticut, USA. View is of a nearly vertical face. Hammer is 28 cm long. More information: Philpotts et al. (1996)
Photo © *Hetu Sheth*

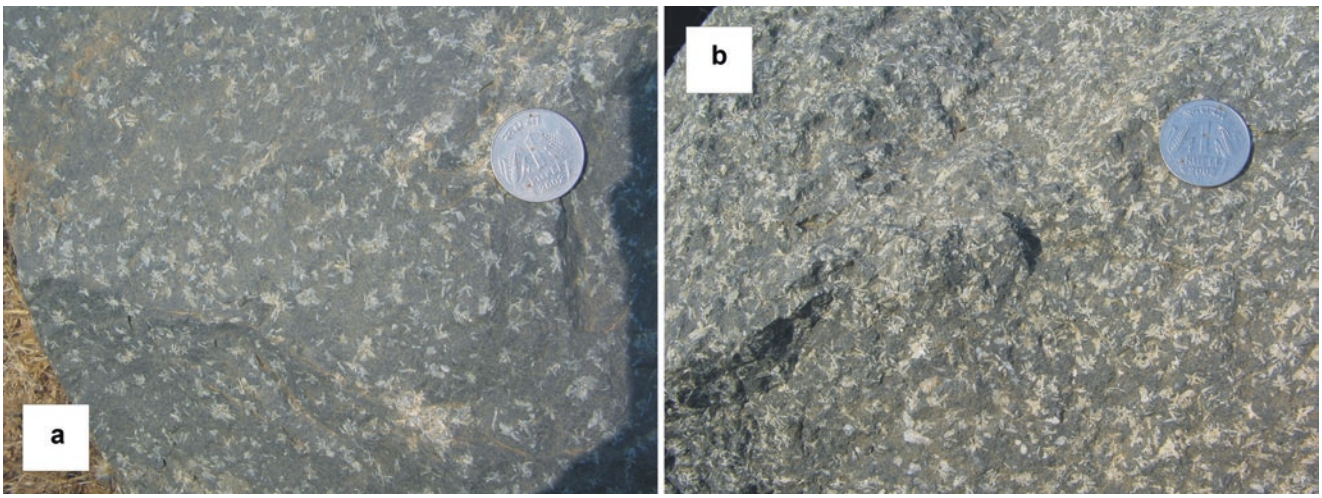

Fig. 9.27 (**a**, **b**) Outcrop-scale igneous differentiation. Plagioclase phenocrysts (up to 1 cm in length) form abundant star-like glomerocrysts on two near-perpendicular faces of a dyke boulder (**a**). On lower faces of the same boulder (**b**), the glomerocrysts are extremely abundant, with the rock becoming a crystal mush and even a cumulate in small patches. Note that this is not simply a sectioning effect, as several faces of very different orientations are involved. Note also the same scale of both photographs (coin diameter 2.5 cm). Location is Varal, Saurashtra, northwestern Deccan Traps. More information: Sheth et al. (2013)
Photos © *Hetu Sheth*

Fig. 9.28 Vertical section through a thin, plagioclase-phyric basaltic dyke, with plagioclase phenocrysts concentrated along its median plane, possibly due to flowage (flow differentiation). Hiran river bed at Rangpur, near Kawant, Gujarat, Deccan Traps. Pen is 14 cm long
Photo © *Hetu Sheth*

Fig. 9.29 The Thalghat giant plagioclase basalt (GPB), near Igatpuri, Western Ghats, Deccan Traps. Lath-shaped crystals are plagioclase megacrysts and spherical and rounded objects are secondary infillings of vesicles. Sheth (2016) interprets GPB flows and dykes widespread in the Deccan Traps (Karmarkar et al. 1971; Hooper et al. 1988; Higgins and Chandrasekharam 2007), and comparable examples found in other flood basalt provinces, as produced by the remobilization and transport of anorthositic mushes in lower crustal sill complexes by genetically unrelated tholeiitic magmas piercing through the sills
Photo © *Hetu Sheth*

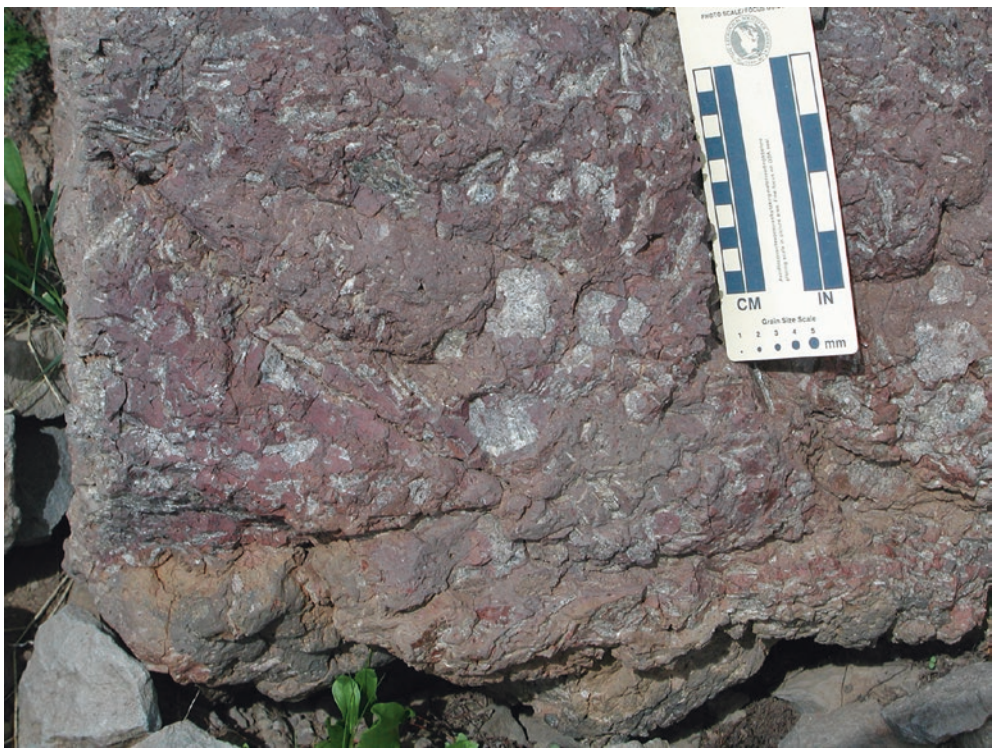

Fig. 9.30 Oxidized portion of a plagioclase-megacrystic flow common to the mid-Miocene Steens Basalt of SE Oregon, USA. See Bondre and Hart (2008) for additional information
Photo © *William K. Hart*

Fig. 9.31 Giant plagioclase basalt in the Emeishan flood basalt province, Daqiao section, Sichuan, China. More information: Cheng et al. (2014)
Photo © *Yigang Xu*

Fig. 9.32 The Bijasan Ghat giant plagioclase basalt (GPB), Deccan Traps, showing its spectacularly megacryst-packed nature
Photo © *Priyanka Shandilya*

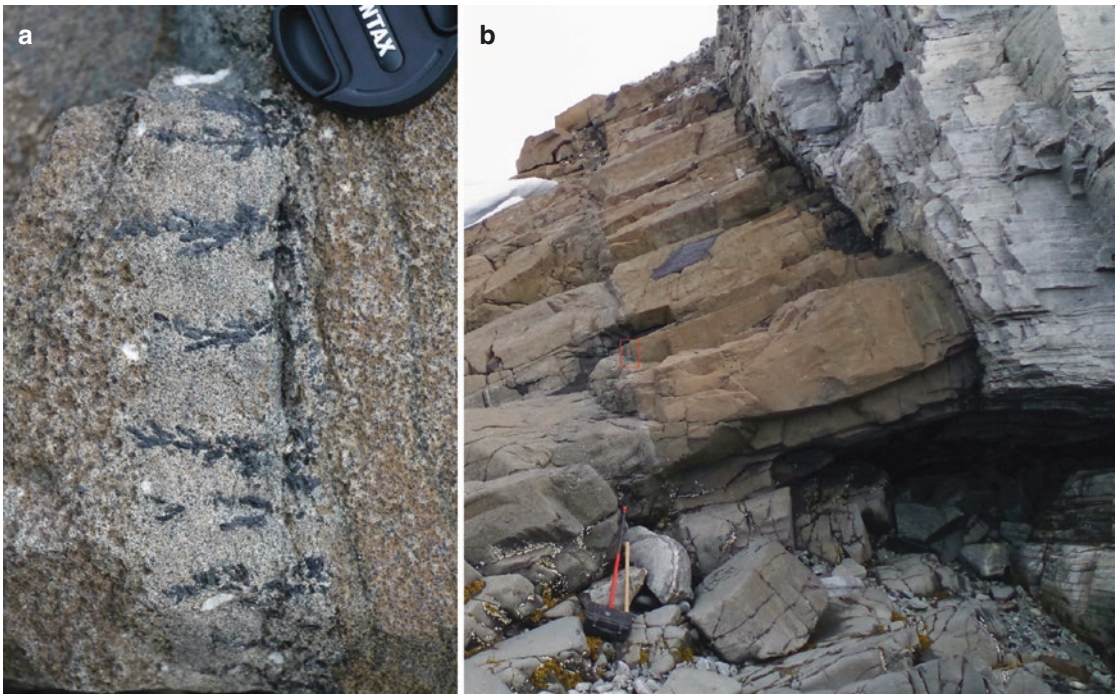

Fig. 9.33 A presumed Tertiary coast-parallel dyke in SE Greenland that is located ~500 km south of the proto-Icelandic hotspot track, and has an unusual internal E-contact. (**a**) Close-up showing centimeter-size dentritic augites that grew into a molten dyke interior, epitaxially from (**b**) a ~2 m-thick chilled marginal zone. More information in Weatherley et al. (2016). Black camera box below hammer shaft is 32 cm wide. Country rock to the right is banded orthogneiss
Photo © *Martin B. Klausen*

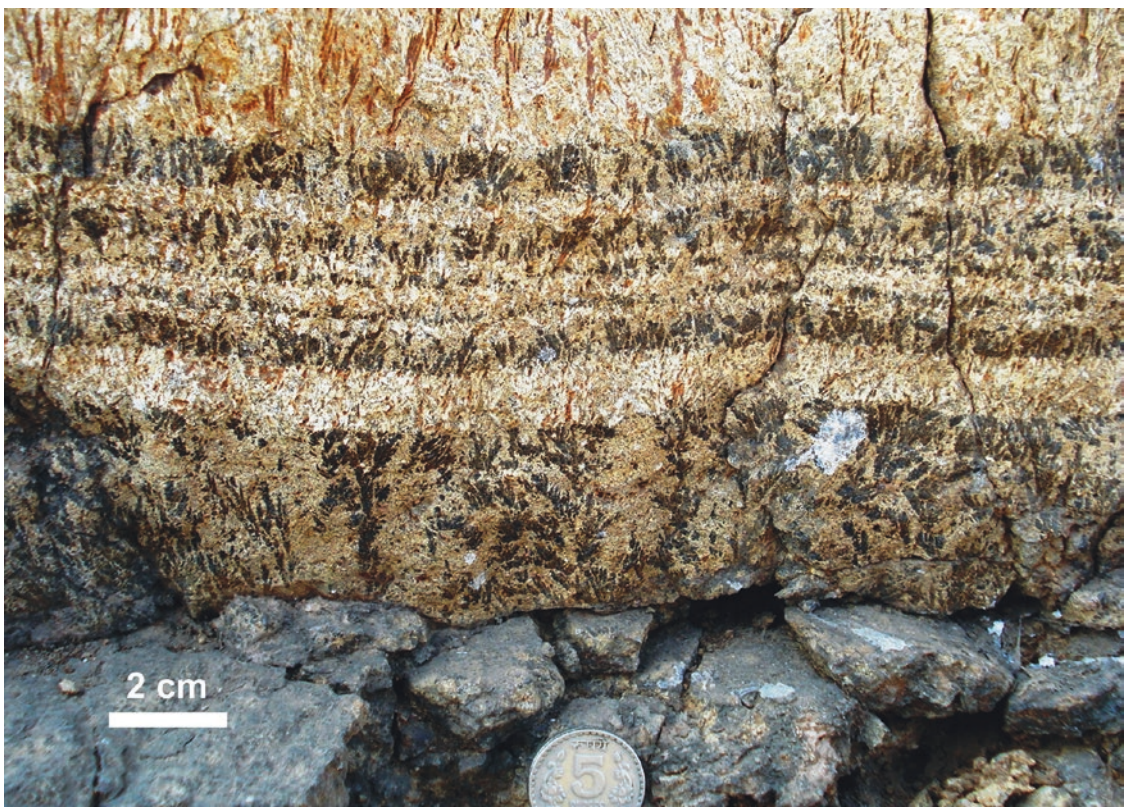

Fig. 9.34 Comb-layering in Deccan basalt, Nasik area, Maharashtra. The dark and light layers are dominated by elongate, curved and branching crystals of pyroxene alternating with plagioclase. This comb layering forms lava channel linings and fills (Sen et al. 2012). Coin is ~2 cm wide
Photo: *Bibhas Sen, Geological Survey of India*

Fig. 9.35 Spinifex texture in the Ghattihosahalli komatiite, part of the 3.35 Ga Sargur Group greenstone belts in the Western Dharwar craton, southern India. More information: Jayananda et al. (2008), Maya et al. (2017)
Photo © *Mahua Yadav*

Fig. 9.36 Acicular plates of olivine forming the spinifex texture in the A2 zone (Arndt et al. 2008) of an Archaean komatite lava flow in the Western Dharwar craton, southern India. Kunikenahalli-Kodihalli section, Banasandra greenstone belt. Coin is 2.5 cm in diameter. The texture is produced by quench crystallization promoted by very rapid cooling of melt, with low nucleation rate and high crystal growth rate at a high degree of supercooling (Donaldson 1982; see also Arndt and Fowler 2004). More information: Jayananda et al. (2016)
Photo © *Raymond Duraiswami*

Fig. 9.37 Centimeter-thick vein of granophyre in a fallen block of ferrodiorite, on the bank of the Farmington River in the Tariffville gorge, Connecticut, USA. Pen is 15 cm long. The top left corner shows the colonnade tier of the host Holyoke Basalt flow (CAMP). Geologist is Tony Philpotts. More information: Philpotts et al. (1996)
Photo © *Hetu Sheth*

Fig. 9.38 Karoo gabbroic intrusion cross-cut by two small granophyric dykes, Mount Ayliff, South Africa
Photo © *Hervé Bertrand*

Fig. 9.39 Silicic magmatism in a CFB province. Imposing landscape of the Barda Hills in western Saurashtra, rising 627 m above the Arabian Sea only a few kilometers away, and formed of overlapping stocks of Deccan granophyre and microgranite which remain little studied. Note person walking in the foreground
Photo © *Hetu Sheth*

Fig. 9.40 Silicic magmatism in a CFB province. The Red Hills on the Isle of Skye, NW Scotland, with smooth, rounded topography, and made up of the Skye granites emplaced as bosses or ring dykes. More information: Emeleus and Bell (2005)
Photo © *Hetu Sheth*

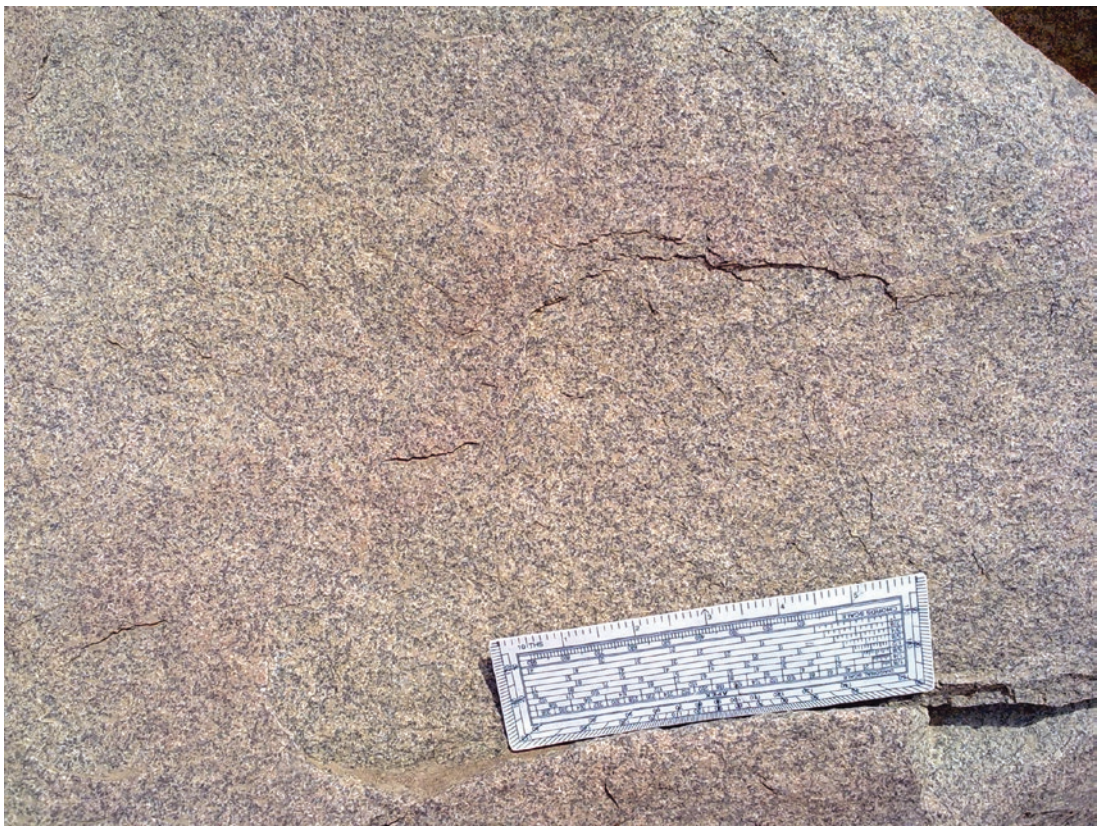

Fig. 9.41 Granophyre in the Phenai Mata alkaline igneous complex, Gujarat, western Deccan Traps. Ruler is 6 in. long
Photo: *Dhananjai Verma, Geological Survey of India*

Fig. 9.42 Brecciated flow-top of a rubbly pāhoehoe flow of the Paraná CFB province, overlain by rhyolitic lavas that record the final stage of volcanism in the Serra Geral Formation. Geologists are Lucas Magalhães May Rossetti and Carla Joana Santos Barreto
Photo © *Carla Barreto*

Fig. 9.43 Silicic volcanism is a common phenomenon associated with the western Saudi Arabian post-Miocene intraplate volcanic provinces. In the Harrat Khaybar, thick but short obsidian lava flows emitted from silicic lava domes of potash-rich rhyolites are commonly seen, and are suspected to have been important for early human communities developing and trading with these materials. More information: Moufti and Németh (2016)
Photo © *Karoly Németh*

Fig. 9.44 Historical (1477) obsidian flow of Námshraun reaching the Frostastadavatn lake, Iceland. The flow is 450 m wide at the lake shore
Photo © *Hervé Bertrand*

Fig. 9.45 Historical (1477) obsidian flow of Laugahraun, Iceland. Note the arcuate flow ridges convex towards the front of the flow. The flow is ~25 m thick at the flow front and 1200 m wide. Note houses, tents and cars near the right edge of the photo at mid-height
Photo © *Hervé Bertrand*

Fig. 9.46 Detail of the historical (1477) obsidian flow of Laugahraun, Iceland. Note the ramp structures and flow folding in this very high-viscosity silicic lava
Photo © *Hervé Bertrand*

Fig. 9.47 Dyke of Deccan lamprophyre cutting basalt flows, Borlai-Korlai, western Indian rifted margin. The wave-cut platform provides nice views of the dyke in both section and plan. Geologist is T. K. Biswal
Photo © *Hetu Sheth*

Fig. 9.48 Thin dyke of Deccan lamprophyre cutting basalt flows, Borlai-Korlai. The dyke exposed on the wave-cut platform bends several times along its short length, but maintains its overall trend
Photo © *Hetu Sheth*

Fig. 9.49 A lensoidal sill of Rajmahal lamproite (brown, photo centre) intruding the coaliferous Lower Gondwana sedimentary sequence, Jharia coal field, eastern India. Adjoining coal seams (dark grey) on the left and at the bottom are indurated and hardened and have developed columnar joints. A thin coal seam is above the sill and is overlain by the Barakar Sandstone. The contacts of the sill with the coal are marked by thin white carbonate veins. Geologists are Ray Kent and Bryan Storey. Locality: Ena, 13th seam, OCP-patch A, Damodar graben
Photo © *Naresh C. Ghose*

Fig. 9.50 Nephelinite dyke intruding syenite pluton, Sarnu-Dandali, Rajasthan, northwestern India. The syenite also contains many mafic enclaves of earlier syn-plutonic dykes. The rocks are a part of the Indo-Madagascar flood basalt province. More information: Sheth et al. (2017d)
Photo © *Hetu Sheth*

Fig. 9.51 Phonolite dyke (adjacent to geologists) in a syenite pluton, Sarnu-Dandali area near Barmer, Rajasthan, northwestern India. These alkaline rocks are 89–86 Ma in age and part of the Indo-Madagascar flood basalt province. Note the characteristic "granite-like" erosion of the syenite. See Sheth et al. (2017d) for more information
Photo © *Kamal Kant Sharma*

Fig. 9.52 Centimeters-thick vein of carbonatite intruding syenite, Sarnu-Dandali, Rajasthan, northwestern India. The vein shows offsets at places, due to shearing. The rocks are part of the ~88 Ma Indo-Madagascar flood basalt province. More information: Sheth et al. (2017d)
Photo © *Hetu Sheth*

Fig. 9.53 Roman Veselovskiy holds an Explorer's Club Flag and stands atop the northern carbonatite stock in the alkaline Guli complex, near 70.93N, 101.29E, Siberian Traps
Photo © *Linda Elkins-Tanton*

Fig. 9.54 Bradford Hager stands on carbonatite layers in the alkaline Guli complex, near 70.88N, 101.30E
Photo © *Linda Elkins-Tanton*

Fig. 9.55 Magnetite-bearing carbonatite from the alkaline Guli complex, Siberian Traps, near 70.88N, 101.30E
Photo © *Linda Elkins-Tanton*

Fig. 9.56 Piqiang intrusive complex with V-Ti-Fe deposits, Tarim LIP. Lighter bands are dioritic and dark bands gabbroic in composition. More information: Zhang et al. (2010), Cao et al. (2017)
Photo © *Yigang Xu*

Fig. 9.57 Enclaves of alkali basalt in Deccan trachyte, Essel World Naka, Mumbai. Darkening of trachyte fracture faces is due to rain and weathering; dark globular bodies are the enclaves. Bikashkali Jana is the geologist. More information: Zellmer et al. (2012)
Photo © *Hetu Sheth*

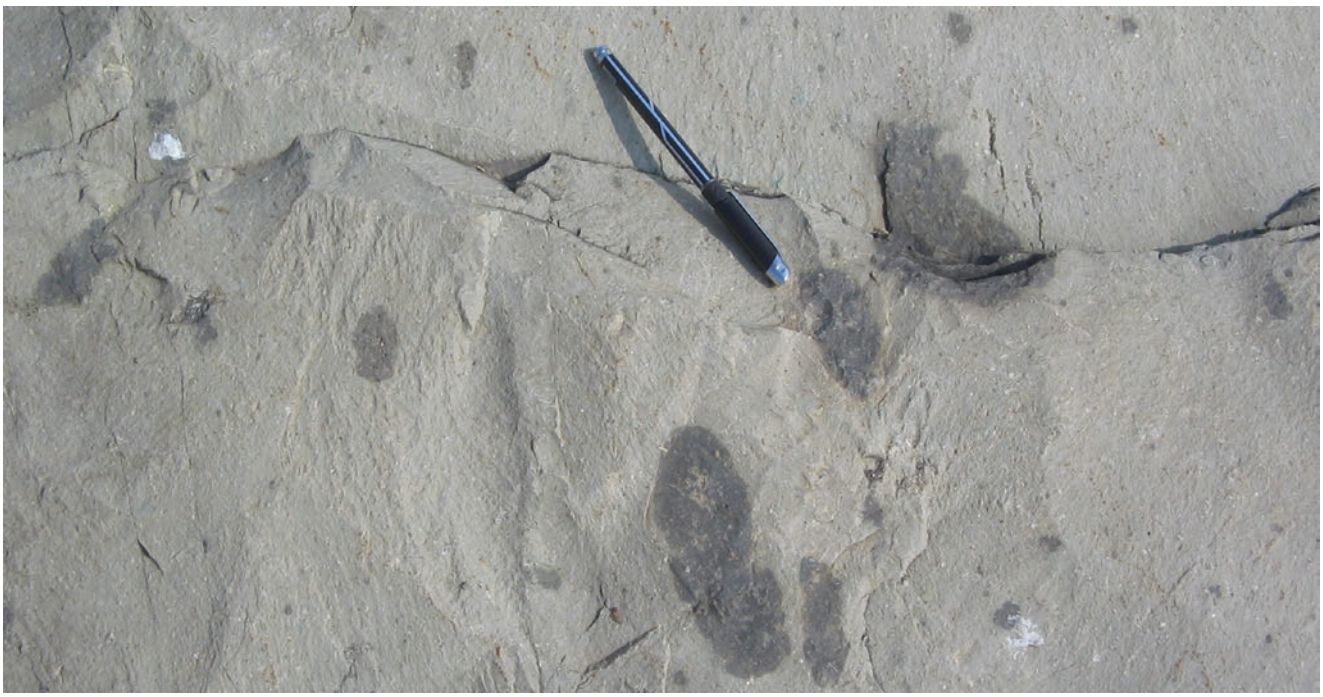

Fig. 9.58 Close-up of enclaves of alkali basalt in Deccan trachyte, Essel World Naka, Mumbai. The larger mafic enclave at the bottom centre contains a patch of the host trachyte melt. Pen is 15 cm long. More information: Zellmer et al. (2012)
Photo © *Hetu Sheth*

Fig. 9.59 Mafic pillows in the Mount Girnar (NW Deccan) diorite, indicating recharge of a largely liquid dioritic magma chamber. Note the large variation in pillow size and the pillows' lobate and cuspate boundaries. The boulder is ~2 m across, and the occurrence hitherto unstudied
Photo © *Hetu Sheth*

Fig. 9.60 Palaeogene igneous breccia formed by the mingling of mafic (basaltic) magma and silicic (rhyolitic) magma. The dark mafic component, typically dolerite or basalt, comprises angular fragments as well as pillow-like forms, and is set in a pale microgranite matrix. The microgranite also occurs as veins within the dolerite and basalt clasts, and in the coherent mafic body in the shadow. Eilean Carrach, Ardnamurchan, NW Scotland. Pole is 1 m long
Photo © *Brian R. Bell*

Fig. 9.61 Gabbro-granite magma mingling, in the net-veined complex of Eystra-horn at exposures near Hvalnes, Iceland. Hammer for scale
Photo © *Hervé Bertrand*

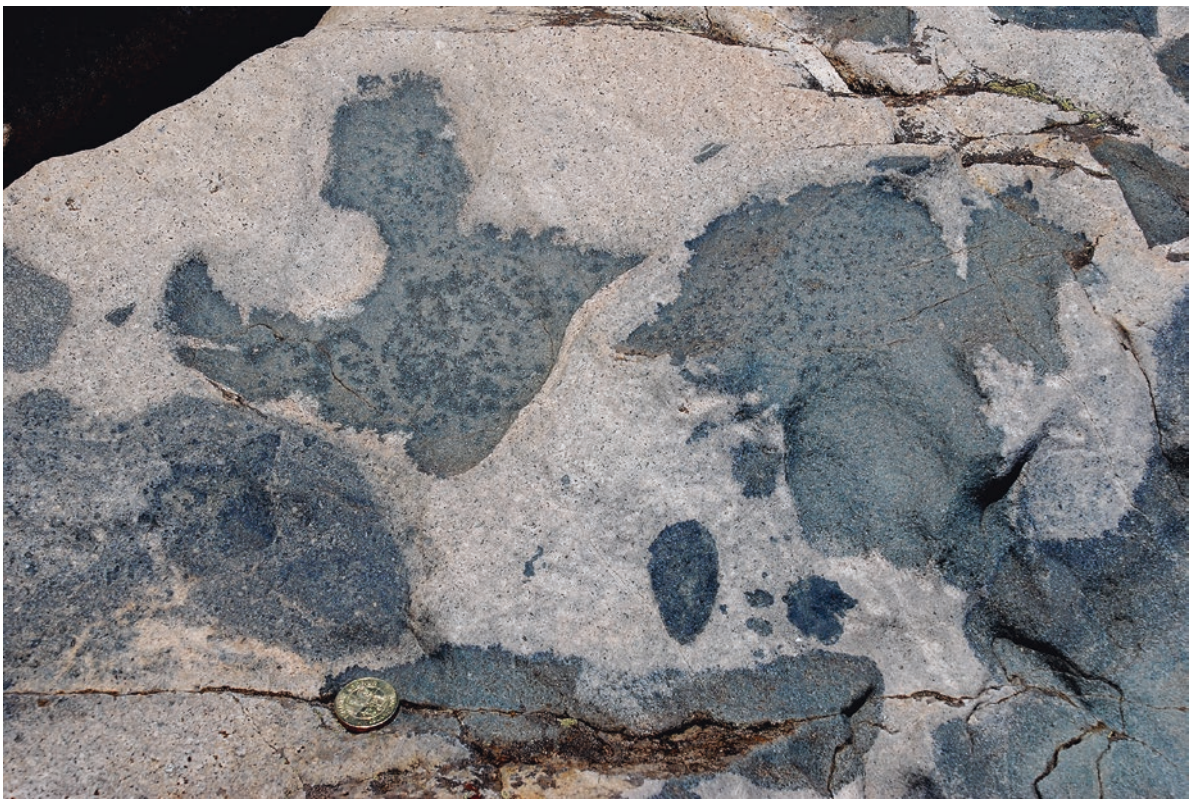

Fig. 9.62 Close-up of gabbro-granite magma mingling showing the detail of their mutual contacts. Note the cuspate shape of the gabbroic enclaves and their smooth to finely crenulated margins against the granite. Eystra-horn near Hvalnes, Iceland. Coin for scale
Photo © *Hervé Bertrand*

Fig. 9.63 Magma mingling in a rhyolite dyke at Moti Vadal village, about halfway between the towns of Savarkundla and Mahuva, in Saurashtra, northwestern Deccan Traps. The small enclave of basalt shows phenocrysts of plagioclase several millimeters long, and sharp but crenulated margins with the host rhyolite. Pen is 15 cm long
Photo © *Vivek Ghule*

Fig. 9.64 Columnar rhyolite on Coconut Island, in the St. Mary's Islands off the southwestern Indian coast. The rhyolite is 85.7 Ma in age ($^{40}Ar/^{39}Ar$) and part of the Indo-Madagascar flood basalt province. Small mafic enclaves indicating magma mingling are found in the rhyolite. Kanchan Pande is the geologist. More information: Pande et al. (2001), Melluso et al. (2009)
Photo © *Hetu Sheth*

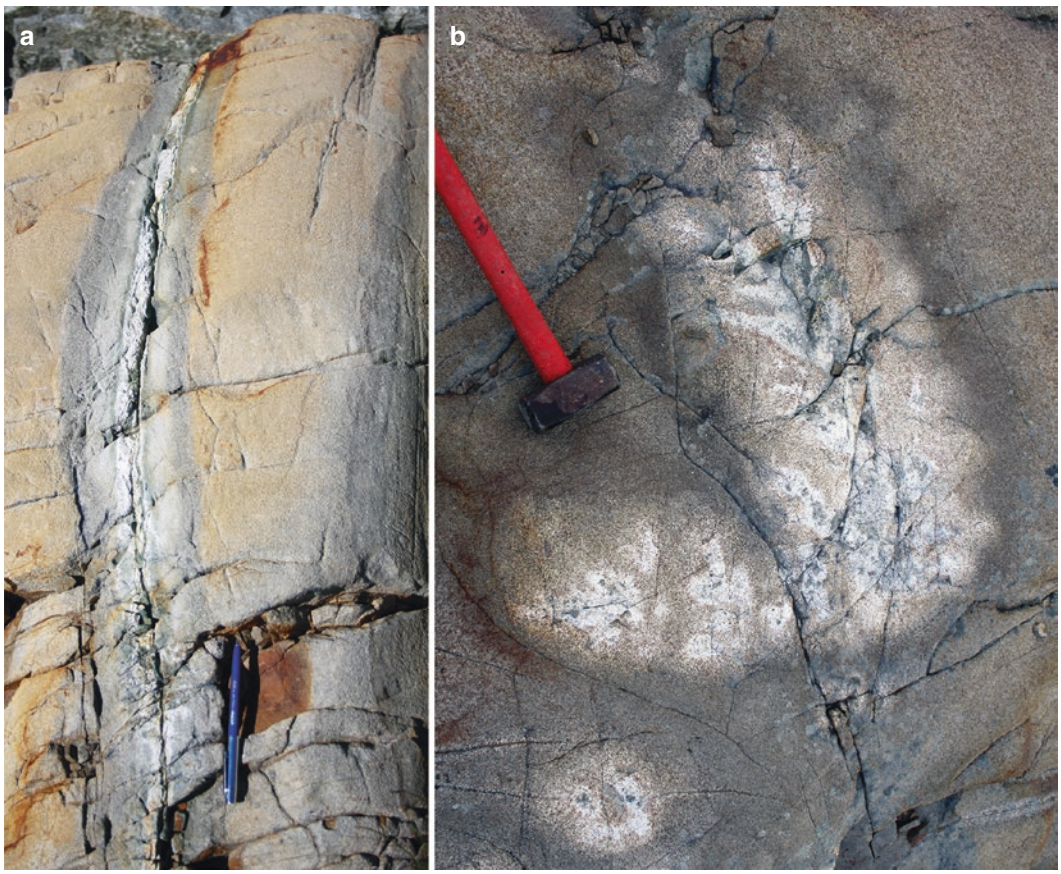

Fig. 9.65 As members of a 2000 km long and ~1630 Ma old Melville Bugt Dyke Swarm across Greenland (Halls et al. 2011), dykes across southern SE Greenland often exhibit evidence of partial host rock melting. (**a**) Back-veining of felsic melts, injected orthogonally from the dyke margin. Pen for scale. (**b**) Partially melted gneissic host-rock xenolith
Photos © *Martin B. Klausen*

Fig. 9.66 The Rajmane dyke in the central Deccan Traps, several kilometers long. It is one of two nearby and parallel dykes profusely laden with lithologically divese xenoliths of the underlying Precambrian crust, which are seen as the whitish patches in the dyke. Geologist is Ranjini Ray. More information: Ray et al. (2008)
Photo © *Hetu Sheth*

Fig. 9.67 Some curiosities from the Deccan. Small lithophysae in altered Deccan rhyolite, Bhaguda hill, SE Saurashtra. Coin is 2 cm in diameter. More information: Misra (1999), Kshirsagar et al. (2012)
Photo © *Hetu Sheth*

Fig. 9.68 Curiosities from the Deccan. Hand specimens of Deccan lithophysae from Bhaguda-Longdi, SE Saurashtra, sliced through their centres and polished to enhance the contrast between the host glass and the central voids (star-shaped and filled by banded agate). Ruler is in centimeters. More information: Kshirsagar et al. (2012), Breitkreuz (2013)
Photo © *Hetu Sheth*

Fig. 9.69 Variolitic lava flow of the Hekpoort Formation, possibly indicating devitrification of once-glassy basalt (akin to spherulitic rhyolitic lavas, see Arndt and Fowler 2004). The 300–830 m thick Hekpoort Formation (2224 ± 21 Ma; Walraven and Martini 1995) in the Transvaal basin of South Africa crops out over an area of ca. 100,000 km^2 (Lenhardt et al. 2012). It is characterized by a complex interplay of subaerial lava flows of predominantly basaltic composition, pyroclastic deposits, and their reworked counterparts (Lenhardt et al. 2012 and references therein)
Photo © *Nils Lenhardt*

Fig. 9.70 More curiosities from the Deccan. Spectacular giant pseudoleucites (up to 8 cm in size) embedded in a tinguaitic groundmass. Locality Ghori, Taluka Kawant, District Chhota Udaipur, part of the Panwad-Kawant carbonatite-alkaline complex in southeastern Gujarat, Deccan Traps. More information: Sukheswala and Sethna (1967), Viladkar (2010)
Photo: *Dhananjai Verma, Geological Survey of India*

Tectonic Deformation of Flood Basalt Provinces

10

Fig. 10.1 Large road cut at Pangin near Pasighat, Arunachal Pradesh, northeastern India, showing mafic dykes of the Early Permian, poorly studied Abor flood basalt province (Bhat 1984; Ali et al. 2012). The host rocks (Gondwana Supergroup sandstones) and the dykes are strongly folded and sheared, being part of the actively deforming and rapidly uplifting Lesser Himayalan Duplex. Geologist Dnyanada Salvi, standing on the road, provides a scale Photo © *George Mathew*

H. Sheth, *A Photographic Atlas of Flood Basalt Volcanism*, https://doi.org/10.1007/978-3-319-67705-7_10

Chapter Overview

Tectonic deformation of flood basalt provinces can occur at various times and on different size scales. Extensional faulting and graben formation occurs contemporaneously with volcanism, as at Iceland. The Thingvellir graben in southwestern Iceland is the current plate boundary between the North American and Eurasian plates. In many flood basalts at rifting continental margins, large-scale monoclinal flexures have formed, with massive oriented dyking, during the late stages of volcanism. Good examples are the Lebombo monocline of the Karoo, the Torres flexure of the Paraná, the Panvel flexure of the Deccan, and the West Greenland and East Greenland coastal flexures. Models suggested for these coastal monoclinal flexures include compressional folding, step faulting, and listric faulting (see Klausen and Larsen 2002; Samant et al. 2017 and references therein).

Many oceanic plateaus have been thrust up on land due to plate convergence and compressive tectonics, examples being the Wrangellia terrane in Alaska, the Siletzia terrane in the Pacific northwest USA, and the Ontong Java oceanic plateau in the western Pacific (the world's largest) whose southwestern edge is tectonically exposed in the Solomon Islands. Flood basalt provinces originally formed on new rifted continental margins have later become incorporated into fold-and-thrust belts, examples being the Early Permian Abor and Panjal flood basalts now forming high elevations in the Himalayan orogenic belt. Similar is the case with many Precambrian giant dyke swarms (frequently metamorphosed to amphibolite) which are now exposed in deeply eroded orogenic belts, with their original flood basalt cover lost.

One does not normally thick of a flood basalt sequence when asked to imagine folded strata: few (if any) textbooks on structural geology and tectonics have chosen flood basalts to depict features of folding. However, striking regional-scale compressive deformation is seen in the Miocene-age Columbia River flood basalt province, a large part of which is folded into more or less regularly spaced anticlines (with wavelengths of tens of kilometers) associated with thrusts (Reidel et al. 2003, 2013a, b, c). What is more, the compressive deformation here occurred along with eruptions over a long time period. There are indications that the Deccan basalts forming sequences as much as 1 km thick, in the Satpura mountain range in central India, are undergoing large-scale, Columbia River-type compressional folding over an area several hundred kilometers wide: evidence includes strong tectonic dips with local reversals, folding of the underlying Gondwana sedimentary rocks, angular unconformities reported within Quaternary alluvial horizons overlying the basalts, and some compressional earthquakes, all consistent with the current NNE-SSW compressive tectonic stress regime in the Indian shield actively pushing into Tibet. Finally, the process of impact cratering, which produces high and near-instantaneous tectonic deformation, and which is seen widely on the Moon and other planetary bodies, is evidenced very well at the 50 kyr old, ~1.9 km diameter Lonar Crater, in the arid central Deccan Traps, India (Senthil Kumar 2005; Maloof et al. 2010; Senthil Kumar et al. 2014).

Fig. 10.2 The Þingvellir graben, Iceland, marking the plate boundary between the Eurasian and the North American plates. The graben contains numerous NE-SW-trending fissures and normal faults. The fault in the far distance is the Hrafnagjá fault, the eastern margin of the graben
Photo © *Hervé Bertrand*

Fig. 10.3 The Almannagjá fault, the western boundary fault of the Þingvellir graben, southwestern Iceland. The graben marks the boundary between the Eurasian and North American Plates. The Almannagjá fault has produced downthrow and tilting of blocks. The opening of the fault is as much as 40 m and the total vertical displacement ~35 m (Gudmundsson 2005). Houses (shown by arrows) on the downfaulted block provide a scale. Lake Þingvallavatn, in the background, is Iceland's largest natural lake
Photo © *Hetu Sheth*

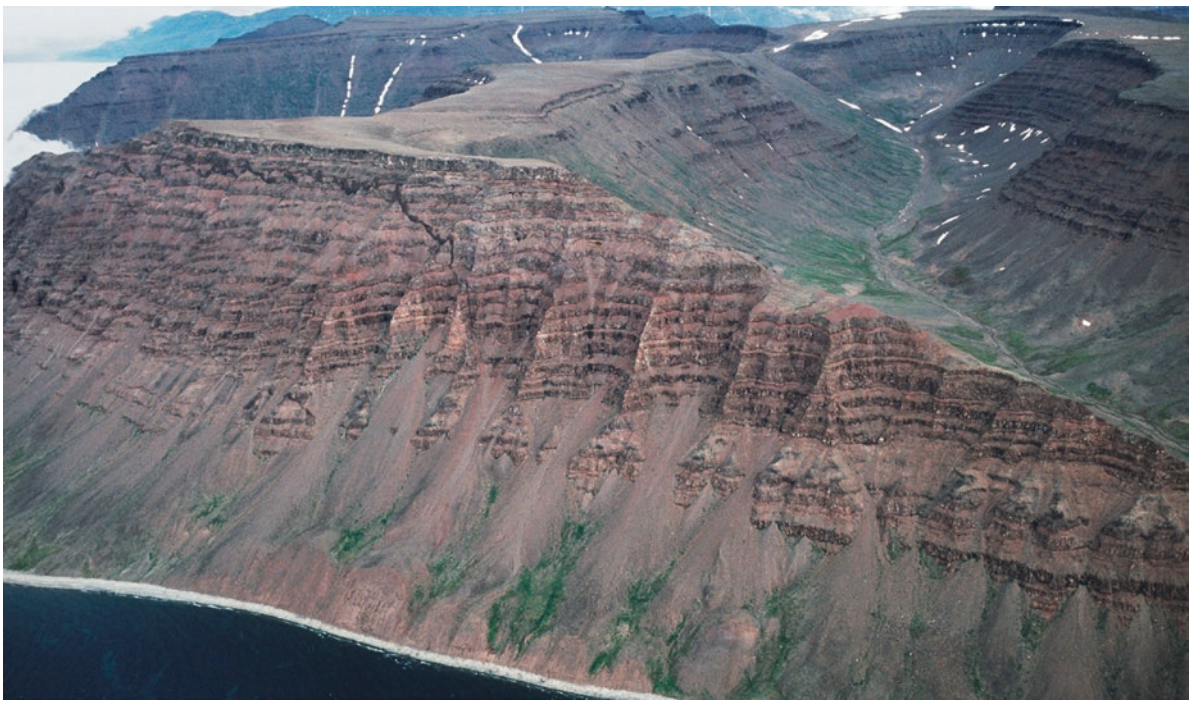

Fig. 10.4 The lava succession in western Disko (West Greenland) is tilted and dips towards the sea in the west (to the left). The top flows here are the youngest flows preserved of the Maligât Formation (Larsen and Pedersen 2009). The top plateau in the foreground is at around 600 m altitude
Photo: *Asger Ken Pedersen, Geological Survey of Denmark and Greenland (GEUS)*

Fig. 10.5 Coastal monoclinal flexures in rifted-margin flood basalt provinces: The East Greenland Flexure exposed as a seaward-dipping contact between Precambrian gneissic basement and overlying basal flood basalts, just south of the Imilik gabbroic complex in the background. Note that thicker tholeiitic feeder dykes are tectonically tilted to the same degree as the 40°-dipping lavas, whereas cross-cutting, paler grey and 'syn-flexural' transitional dykes are steeper (c.f. Figs. 2d-e & 4a in Klausen and Larsen 2002). The peak of the foreground ridge is ~800 m above sea level
Photo © *Martin B. Klausen*

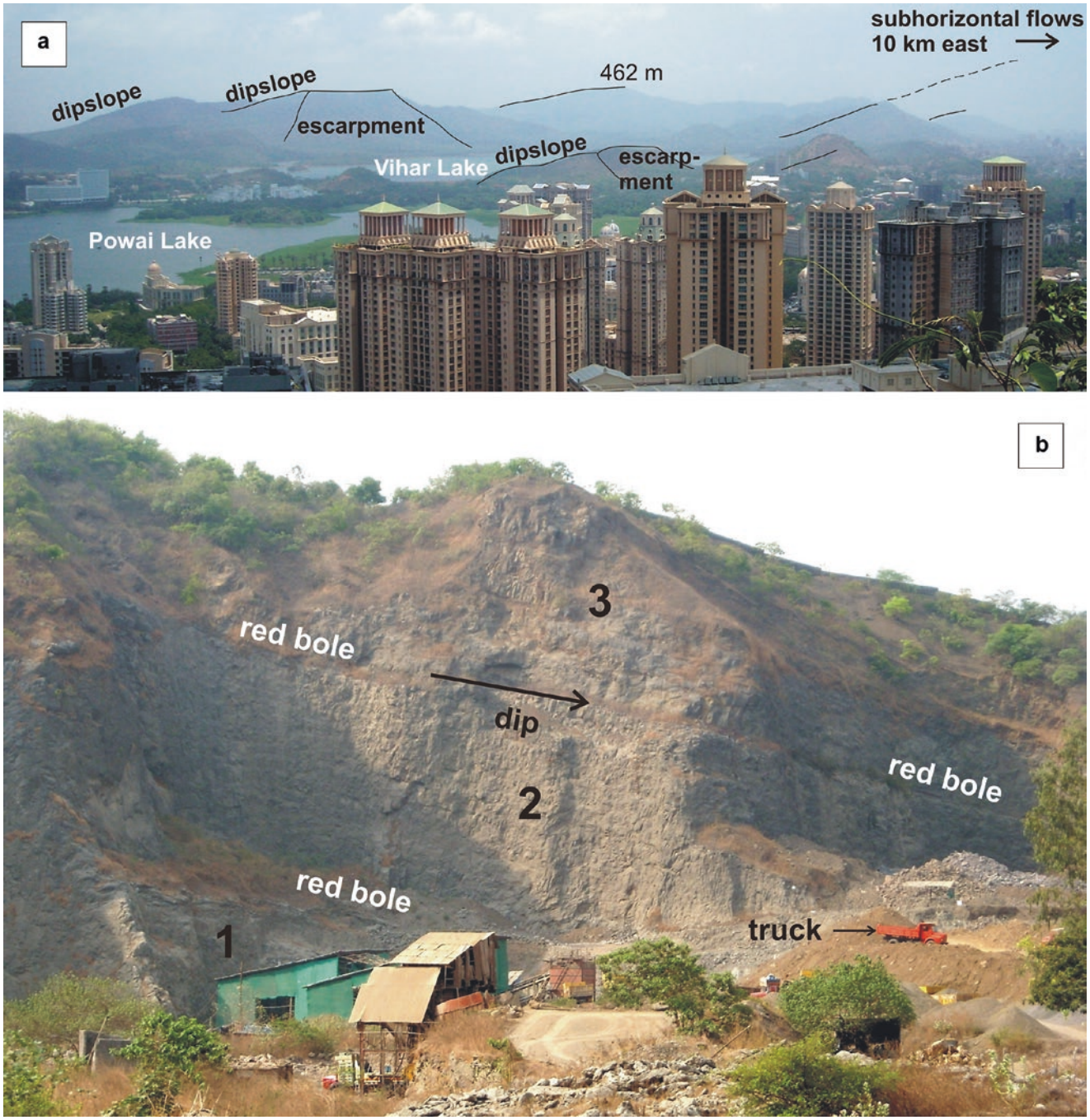

Fig. 10.6 The Panvel flexure of the Deccan Traps is a 150 km long tectonic zone along the western Indian rifted margin where the otherwise horizontal flood basalt sequence acquires significant dips towards the Arabian Sea. These photos are from the Mumbai metropolis (20 million people) where the flexure is both beautifully exposed and sadly destroyed, and convey a sense of the regional scale of the flexure. Panel (**a**) shows a view (looking roughly north-northwest) of the suburb of Powai and surrounding hilly areas obtained from the top of Ghatkopar Hill, 209 m above sea level and nearly the same height above the lakes. Skyscrapers of the Hiranandani complex in the foreground are nearly as high as the Ghatkopar Hill. The hills seen in the photo are cuestas with steep east-facing escarpments and long, gentler dipslopes, owing to the westerly-northwesterly dip (~17°) of the basalts, which are shown by black lines. The dashed line to the right is simply the dip projected upwards, and 10 km to the east, in New Mumbai, the basalts are subhorizontal flows. In between is the low-lying area of the Thane Creek, connected with the Arabian Sea and possibly a tectonic graben, so no physical continuity exists. (**b**) View (roughly south) of a large rock face cut through the dipslope, being worked for road metal in a quarry in the suburb of Vikhroli nearby. Three lava flows distinctly dipping west-northwest by 17° are well exposed, each separated from the other by a distinct red bole bed. Shacks in the foreground and truck in the background provide a scale. Numerous dykes are also present in the Ghatkopar-Vikhroli-Powai areas. More information: Sheth et al. (2014), Pande et al. (2017b) Photos © *Hetu Sheth*

Fig. 10.7 Lateral view of normal fault with well-developed slickensides (white striations) in the Deccan basalts of Elephanta Island, Mumbai harbour, Panvel flexure zone. The basalts dip 12° WNW (to the left), and the floor of the abandoned quarry is 40 m below geologists Vanit Patel and Hrishikesh Samant. This is the western of two normal faults. The white striations are due to secondary fibrous zeolite and calcite which grew during slippage on the fault. Slip was oblique. More information: Samant et al. (2017)
Photo © *Hetu Sheth*

Fig. 10.8 Detail of slickensides on a normal fault in Deccan basalt, Elephanta Island, Mumbai harbour, Panvel flexure zone. This is the eastern of two normal faults. The white striations are due to secondary fibrous zeolite and calcite which arguably grew during slippage on the fault. Slip was oblique. More information: Samant et al. (2017)
Photo © *Hetu Sheth*

Fig. 10.9 Slickensides with steps on a hand specimen of Deccan red bole from Elephanta Island, Mumbai harbour, India. Secondary zeolite mineralization is represented by the white patches. A normal fault runs through this outcrop, and the area is in the Panvel flexure zone. More information: Samant et al. (2017)
Photo © *Hrishikesh P. Samant*

Fig. 10.10 Slickensides on a normal fault through a Deccan dolerite dyke, southern Saurashtra. Geologist is Vivek Ghule
Photo © *Hetu Sheth*

Fig. 10.11 Drag-folded lava-hyaloclastite bedding along the northern exposed caldera fault of the Mélakolli central volcano (eastern Iceland). Dashed line traces one folded lava bed whereas dotted line traces the fold axis. Depth of the gully is ~40 m
Photo © *Martin B. Klausen*

Fig. 10.12 The Lonar Crater, a young (50 ka), hypervelocity impact crater in basalt in the central Deccan Traps. The crater is 1.8 km in diameter and its raised rims are 20–80 m above the pre-impact ground surface which is at 530 m above sea level. More information: Senthil Kumar (2005), Maloof et al. (2010), Senthil Kumar et al. (2014)
Photo © *Hetu Sheth*

Fig. 10.13 Many older flood basalt provinces are now parts of fold-thrust belts. The Early Permian (290 Ma) Panjal Traps, here exposed in the Pir Panjal Range in the Kashmir Himalaya, form the backdrop to the beautiful Moghul gardens of Nishat Bagh in the capital city of Srinagar. Tourists include Chaitali and Shikhar Sheth. The cliffs in the background rise 400 m above the gardens and, outside the photo, more than 1200 m above the Kashmir valley. More information: Bhat et al. (1981), Shellnutt et al. (2011, 2014) Photo © *Hetu Sheth*

Fig. 10.14 The structural contact between the uppermost Panjal Traps basalt (Early Permian, green, on the left) and Triassic carbonates (brown) near Chandanwadi (Pahalgam, Jammu and Kashmir, India). The contact is a thrust and the basalt within the fault zone has developed a prominent schistosity
Photo © *J. Greogory Shellnutt*

Fig. 10.15 Red, green and black clays separating episodic CAMP volcanism, in a road cut exposure. Prominent dark red clay band is ~6 m in height. Aït Ourir section, High Atlas of Morocco. Beds are near-vertical because of Atlasic tectonics
Photo © *El Hassane Chellai*

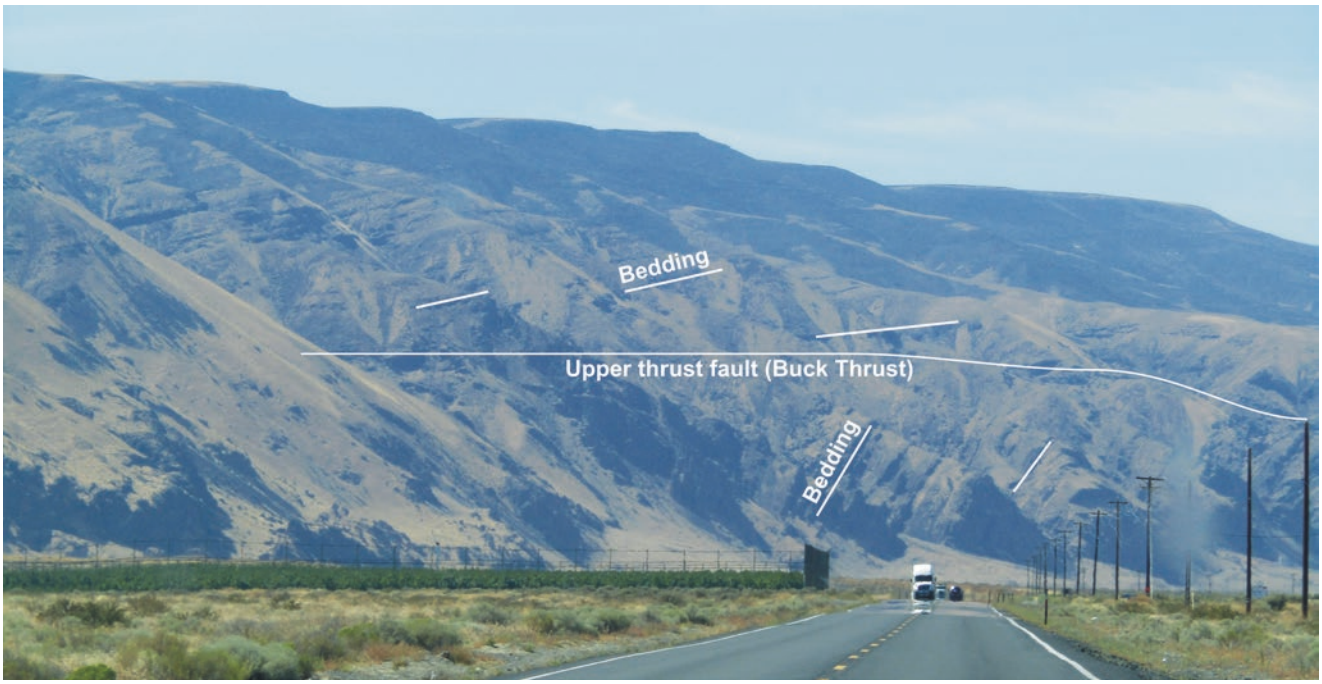

Fig. 10.16 The northern side of the Umtanum Ridge, an anticlinal ridge like many others in the Yakima Fold Belt and the Pasco Basin, Columbia River flood basalt province (Price and Watkinson 1989; Watters 1989; Reidel et al. 2003, 2013c). Short white lines indicate the trace of bedding. The gently dipping basalts to the south (higher elevations on the ridge) are separated from the overturned and steeply dipping basalts at the front by a thrust, called the Upper (Buck) Thrust. A lower thrust is not exposed, but covered by the Columbia River at this locality (behind the fence and at the base of the mountain). Trucks on the highway provide a sense of scale; photo taken through the windshield of a moving car
Photo © *Stephen P. Reidel*

Fig. 10.17 The Lewiston Structure: a huge anticline bounded to the north by a thrust. It is one of many such anticlinal ridges in the Yakima Fold Belt and the Pasco Basin, Columbia River flood basalt province (Price and Watkinson 1989; Watters 1989; Reidel et al. 2003, 2013c; Alloway et al. 2013). Late evening photo from the Rooster's waterfront restaurant in Clarkston (Washington State), on the south bank of the Snake River, 230 m above sea level. View is to the north, the river is 600 m wide, and the anticlinal ridge rises 600 m above it. Buildings on the north shore of the river (white objects) provide an approximate scale
Photo © *Hetu Sheth*

Fig. 10.18 Large anticline in the Columbia River flood basalts, in the Columbia Hills. View is looking roughly south, from the Washington (north) side of the Columbia River towards Oregon. The anticlinal ridge rises several hundred meters above the river; truck on the opposite side of the river, about one third of the way from the left, provides a rough scale. For more information on the folding and deformation of the Columbia River flood basalts, see Price and Watkinson (1989), Watters (1989), and Reidel et al. (2003, 2013c)
Photo © *Hetu Sheth*

Fig. 10.19 The Columbia Hills fault zone, Columbia River flood basalt province. Here, the basalts are cut by vertical fractures and faults, with the Grande Ronde basalt flow behind the geologists rotated to vertical, with its constituent columnar joints horizontal. Vertical outcrops on the hill, giving the false impression of erosion-resistant dykes, are basalt flows cut by fractures that have produced cataclastic flow in the basalts. Geologists are, from left to right, Ernst Hegner, Steve Reidel, and Vic Camp. More information: Price and Watkinson (1989), Watters (1989), Reidel et al. (2003, 2013c), and Camp et al. (2017)
Photo © *Hetu Sheth*

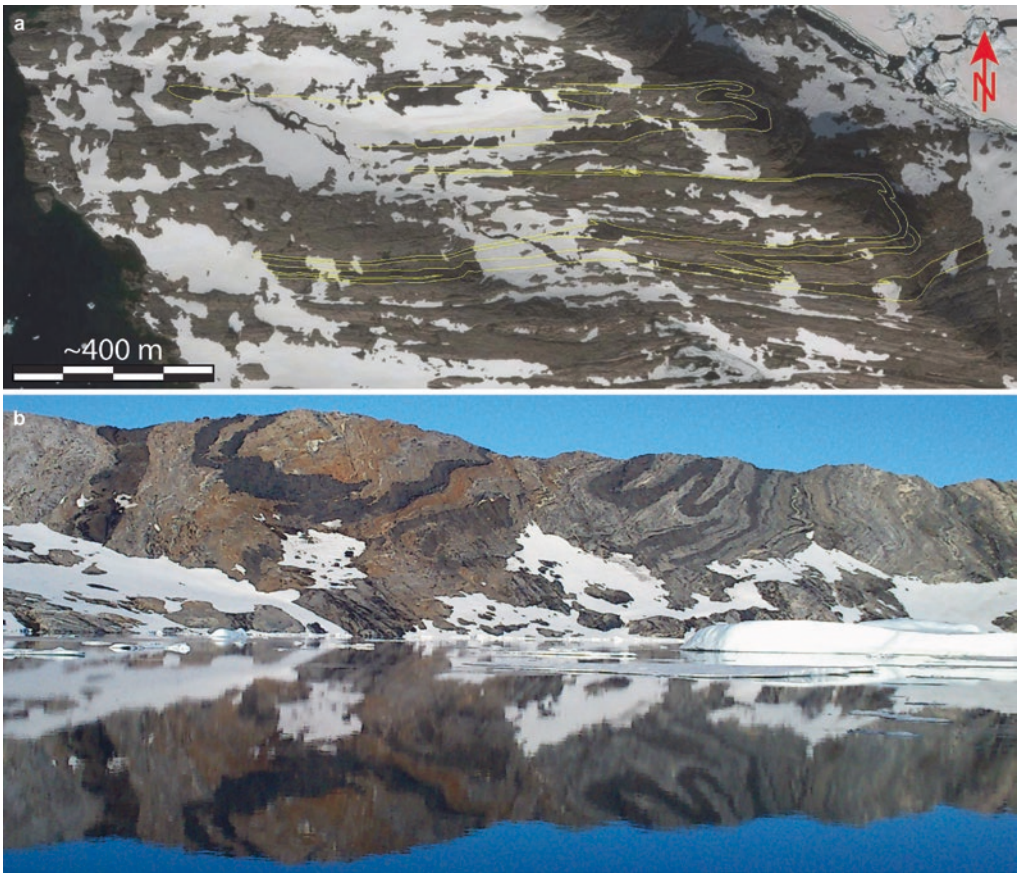

Fig. 10.20
Palaeoproterozoic mafic dykes folded within the Nagssugtoqidian orogen, on the western flank of Hornemann Island, SE Greenland. (**a**) Google Earth map. (**b**) NE side of island section in (**a**). Figure 6–8 in Klausen et al. (2016b). These dykes are of uncertain provenance, but link up with the Scourie Swarm in Scotland, made up of many 2.37–2.42 Ga dykes (cf. Davies & Heaman 2014) that are coeval with dykes across SW Greenland (Nilsson et al. 2013), as well as across the Dharwar, Baltic, Yilgarn and Zimbabwe Cratons (i.e., the supercontinent of Superia)
Photo © *Martin B. Klausen*

Secondary Mineralization in Flood Basalts

11

Fig. 11.1 The Námafjall fumarole field south of the Krafla volcano, in north Iceland. In the background is the table mountain (stapi/tuya) of Búrfell and the largely subglacial formation of Heilagsdagsfjall (up to 1000 m above sea level and 500 m above the surroundings) Photo © *Dominique Weis*

H. Sheth, *A Photographic Atlas of Flood Basalt Volcanism*, https://doi.org/10.1007/978-3-319-67705-7_11

Chapter Overview

Amethyst, the violet, purple or pink, semiprecious variety of the mineral quartz, has been prized for thousands of years in Egypt and Greece. It is only one of a large group of secondary minerals that are found in flood basalts, deposited by late-stage or post-volcanic hydrothermal solutions in cavities, or formed during low-grade metamorphism of the lower part of a sinking flood basalt pile loaded by new lavas at the top.

Brazilian amethyst from the Paraná flood basalts is world-famous, much of the production coming from the municipality of Ametista do Sul, in the state of Rio Grande do Sul. Amethyst is sold by weight here. Indian agates, products of the Deccan Traps, have been traded for millenia. (The most famous early gem product of India is, of course, diamond, sourced from Precambrian-age kimberlites.) Some flood basalt lavas and associated intrusions contain economic mineralization such as copper and even gold. However, the much more common and abundant secondary minerals in flood basalts are the many silica minerals, zeolites, calcite, and apophyllite, among others. Most of them make beautiful semiprecious stones and many of these adore the shelves of world museums, like the magnificent Terra Mineralia museum in Freiberg, Germany, and the pages of this book.

Much Indian agate has come from a Tertiary Trap-conglomerate in the Ratanpur area near Rajpipla in the western Deccan (Wadia 1975), highly prized green apophyllite from the Pune area of the Deccan plateau, and beautiful zeolites (including exquisitely formed mesolite, scolecite and natrolite) from Pune, the pillowed spilites of Mumbai, and other areas of the western Deccan. Tourists can easily buy beautiful amethyst (in particular), zeolite and apophyllite specimens from roadside vendors in the British-colonial tourist area of southern Mumbai, or at the Elephanta Caves in the Mumbai harbour and the Ajanta and Ellora Caves in the central Deccan, all of which are UNESCO World Heritage sites. However, the prices are typically greatly inflated, calling for careful haggling with the often-aggressive vendors, and authentic information on the source areas and geological occurrences of the minerals is generally unavailable if someone is collecting for a proper museum exhibit. Ottens (2003) provides an excellent, detailed and beautifully illustrated description of Deccan zeolites and the Deccan secondary mineral industry. An even bigger source of information on Deccan and Indian secondary minerals and gemstones, again with beautiful photographs, is Ottens (2011), albeit in German. Götze (2011) similarly provides a lengthy and detailed scientific essay and many beautiful photographs of agates of the world.

Fig. 11.2 Spilitized pillowed basalt in an abandoned quarry at Bagwada, near Daman, Gujarat, western Deccan Traps (see Fig. 6.3). Vertical section. Spilitization involves the transformation of the primary basalt minerals (calcic plagioclase and clinopyroxene) into albite (sodic plagioclase) and chlorite. Note radially arranged pipe vesicles filled by zeolites. Black patches and spots in the cores of some pillows (left of the hammer and top right corner of the photo) are of the original basalt which escaped transformation into spilite. More information: Sethna and Javeri (1999)
Photo © *Hetu Sheth*

Fig. 11.3 Fumarolic alteration of a rhyolitic dome, Bláhnúkur, in the Torfajökull area, south-central Iceland. The rhyolite is transformed into mixed clay minerals, chlorite, and hydroxides
Photo © *Hervé Bertrand*

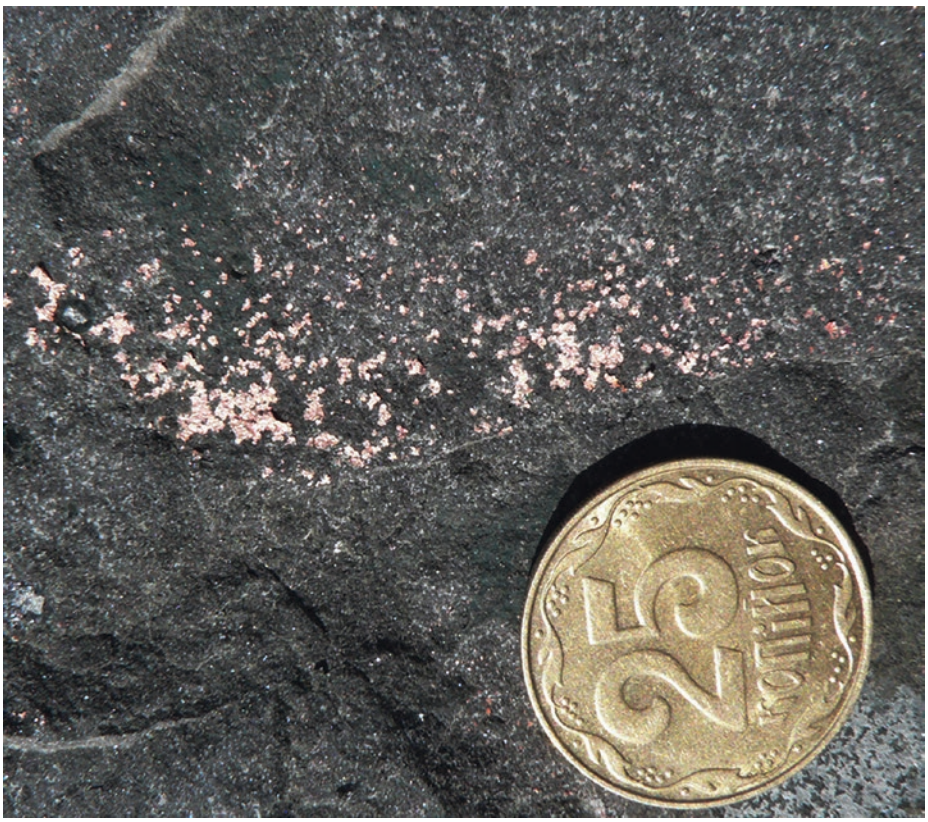

Fig. 11.4 This photo from the Rafalivka quarry (51.23 N, 26.04 E) shows native copper mineralization in chlorite-filled thin veinlets in the 570 Ma Volyn continental flood basalts, in the southwestern part of the East European craton. The Volyn flood basalts are relatively heavily altered by post-magmatic hydrothermal processes. Late-magmatic and post-magmatic mineralization is very variable, and is represented by chlorite, zeolites, carbonates, silica minerals, etc., besides subeconomic deposits of native copper and native silver
Photo © *Leonid Shumlyanskyy*

Fig. 11.5 Epidote and copper mineralization in altered Emeishan basalt
Photo © *Yigang Xu*

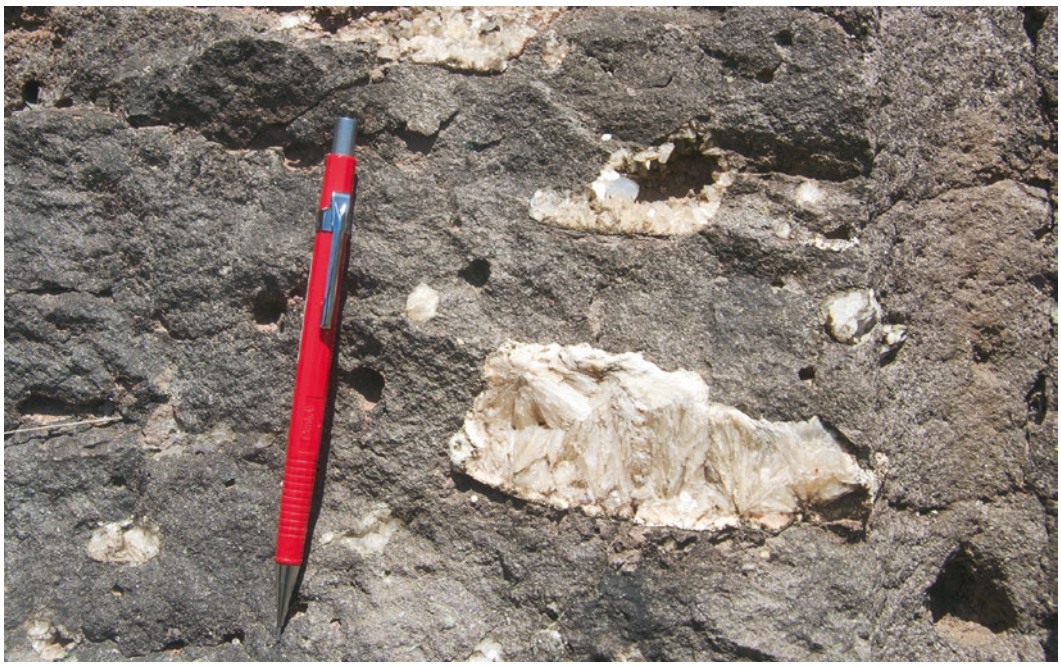

Fig. 11.6 Large amygdules filled by stilbite and quartz in the upper half of a simple pāhoehoe flow of the Paraná CFB province. Note also cavities not mineralized. Pen is 15 cm long
Photo © *Carla Barreto*

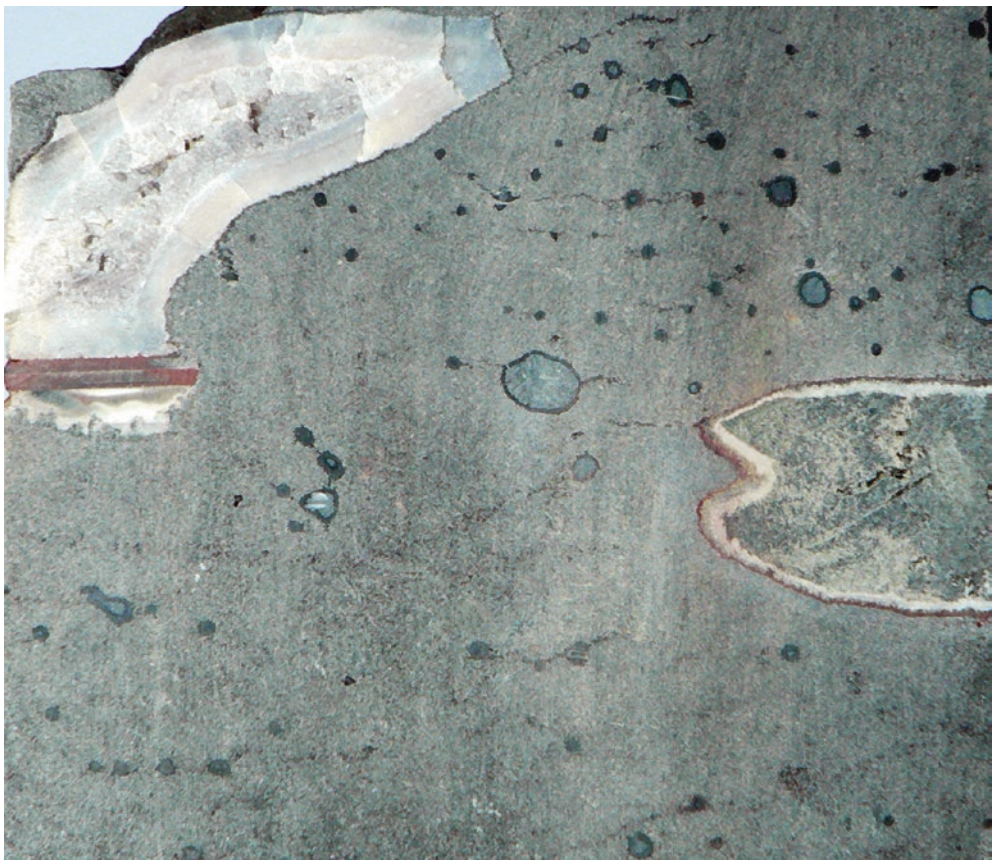

Fig. 11.7 Cut (not polished) surface (5 cm wide) of an amygdaloidal basalt of the Volyn flood basalt province. Amygdules are filled mainly with chlorite (grey to black in small amygdules). The large zoned amygdule to the right is filled with chlorite (centre) which is rimmed by zeolite (light grey) and haematite (brown). An amygdule in the upper left corner of the photo is filled with agate partly crystallized to quartz in the central part. In the lower part this amygdule contains 2 mm-thick layers of haematite. These layers may serve as mineralogical levels as they indicate the horizontal plane at the time of crystallization
Photo © *Leonid Shumlyanskyy*

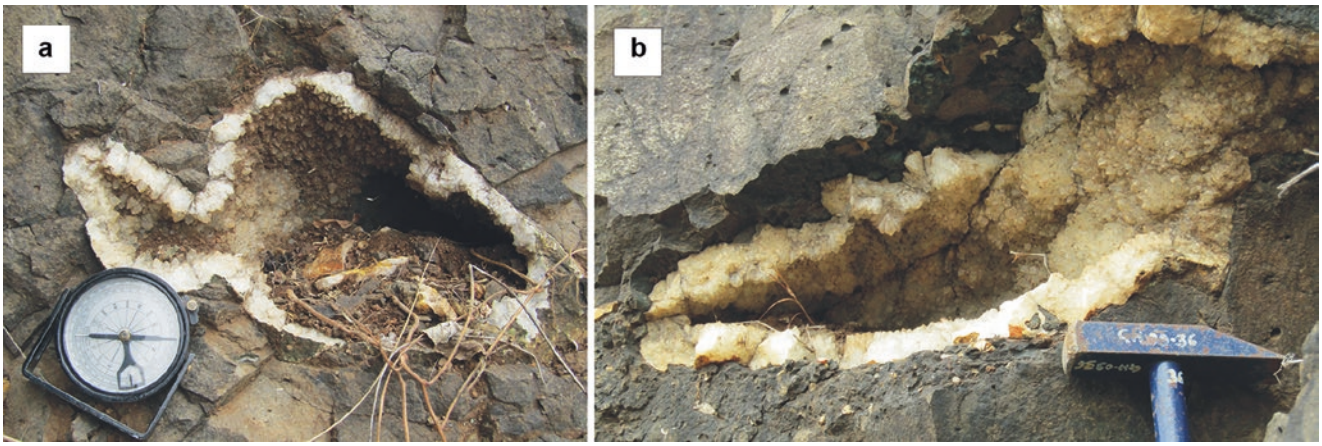

Fig. 11.8 (**a**, **b**) Quartz-lined geodes in a Deccan basalt flow. Ganesh Ghat section, east of Malshej Ghat, Western Ghats
Photos © *Hetu Sheth*

Fig. 11.9 Lithophysa in glassy Deccan trachyte at Gandhi Smriti Memorial, Sanjay Gandhi National Park, Borivli, Mumbai. The central cavity of the lithophysa is filled by secondary quartz. Coin is 2 cm wide. More information: Kshirsagar et al. (2012)
Photo © *Hetu Sheth*

Fig. 11.10 Mine gallery exposing a large amethyst geode in a lava flow from the basaltic sequence of the Paraná CFB Province. The notebook at the base of the geode is 15 cm long. Ametista do Sul, Rio Grande do Sul, Brazil. More information: Gilg et al. (2003)
Photo © *José Madeira*

Fig. 11.11 Large geode with amethyst, ~1.5 m high, at a hotel reception in Hualien, eastern Taiwan. Most probably from the town of Ametista do Sul, in the State of Rio Grande do Sul, Brazil (B. Ottens, pers. comm., 2017). More information: Gilg et al. (2003)
Photo © *Hetu Sheth*

Fig. 11.12 Calcite nailhead spar and scalenohedra, on a bed of drusy quartz crystals, found in spilite pillows at the Pathanwadi quarry, Kandivli (East), Mumbai, western Deccan Traps. Specimen is 3 cm high and 5 cm wide
Photo © *Arnav H. Samant*

Fig. 11.13 Apophyllite and brown heulandite on quartz, Jalgaon, central Deccan Traps. Size 2 cm × 2 cm
Photo © *Arnav H. Samant*

Fig. 11.14 Secondary minerals of the Deccan Traps: Calcite with stilbite on chalcedony, 12 cm high. Savda Quarry, Jalgaon, Maharashtra, India. See Sukheswala et al. (1974), and Ottens (2003, 2011) for many photos and extensive descriptions of secondary minerals of the Deccan Traps
Photo © *Berthold Ottens*

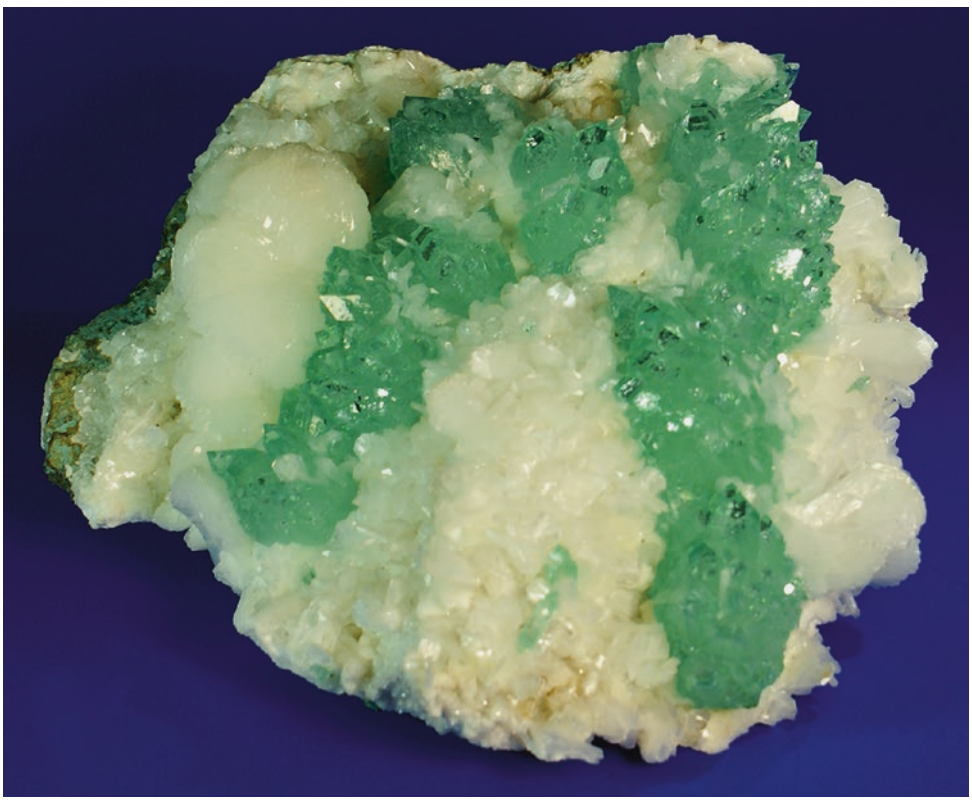

Fig. 11.15 Green apophyllite on stilbite, 22 × 21 × 10 cm. Pashan quarry, Pune, Maharashtra, India
Photo © *Berthold Ottens*

Fig. 11.16 Mordenite on chalcedony filaments, 6 × 4 × 3 cm. Chinchvad, Maharashtra, India
Photo © *Berthold Ottens*

Fig. 11.17 Okenite and gyrolite on laumontite, 8 cm high. Kurar quarry, Malad, Mumbai, India
Photo © *Berthold Ottens*

Fig. 11.18 Scolecite, 12 × 9 × 12 cm. Junnar, Maharashtra, India. The yellow mineral underneath is stilbite
Photo © *Berthold Ottens*

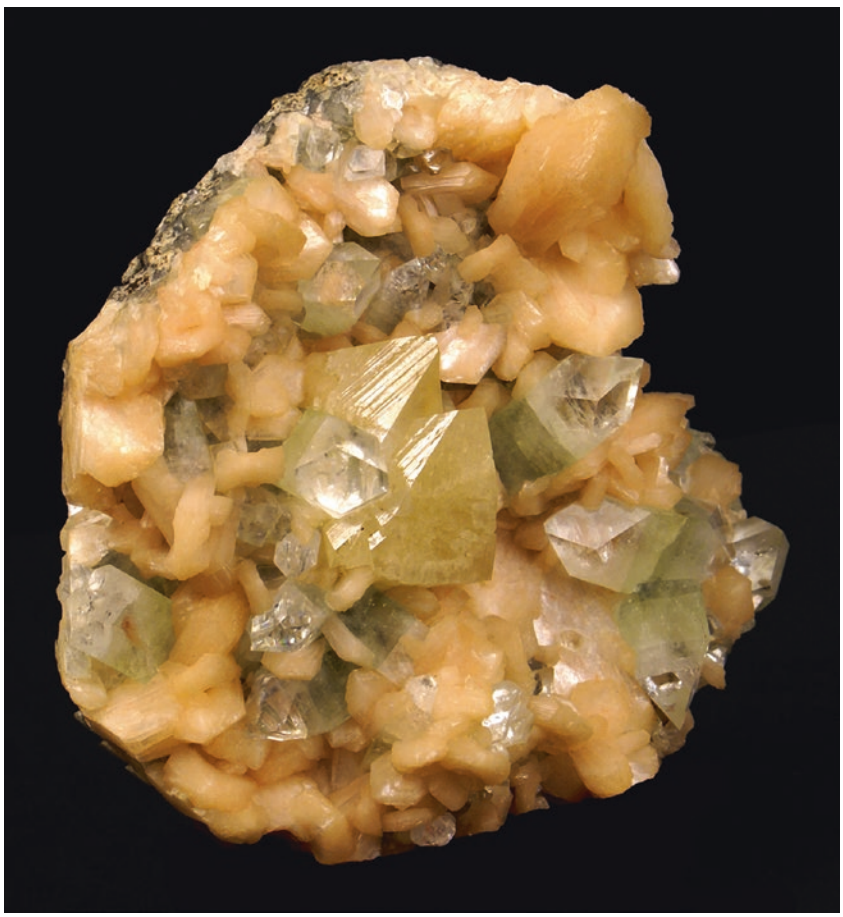

Fig. 11.19 Powellite with apophyllite on stilbite, 12 × 10 × 5 cm. Savda Quarry, Jalgaon, Maharashtra, India
Photo © *Berthold Ottens*

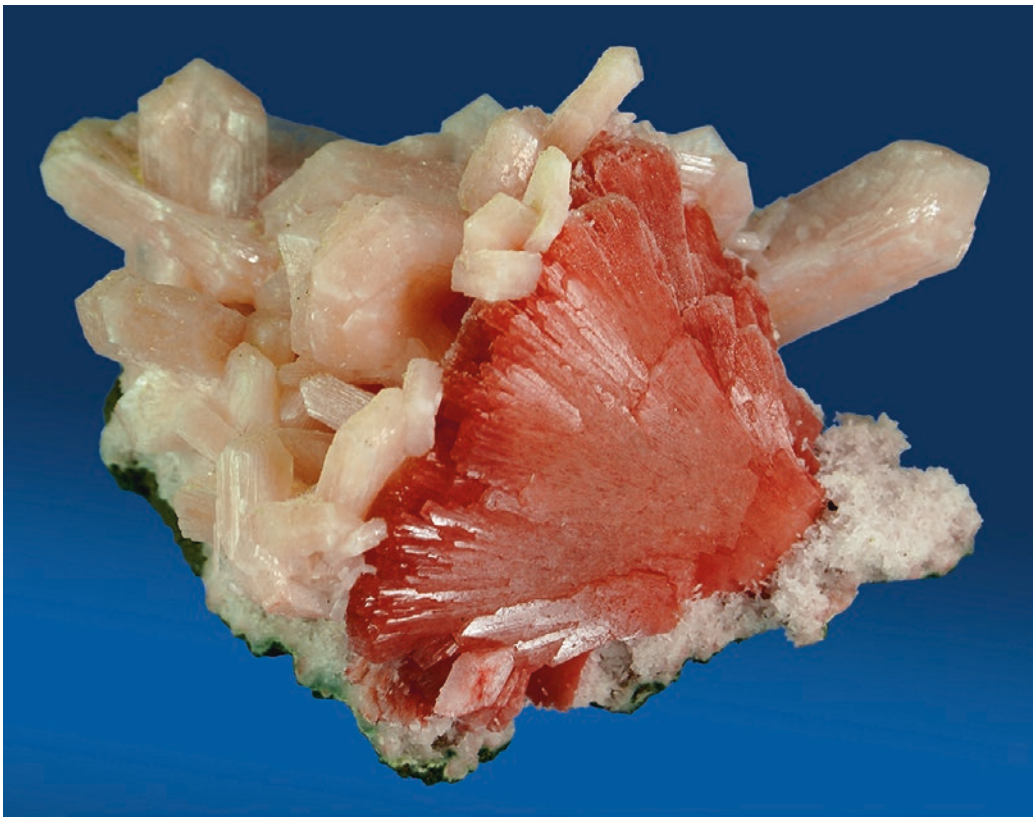

Fig. 11.20 Red heulandite with salmon pink stilbite, 10 × 6 × 6 cm. Savda Quarry, Jalgaon, Maharashtra, India
Photo © *Berthold Ottens*

Fig. 11.21 Salmon pink chabazite with calcite, 14 × 7 × 8 cm. Kurar quarry, Malad, Mumbai, India
Photo © *Berthold Ottens*

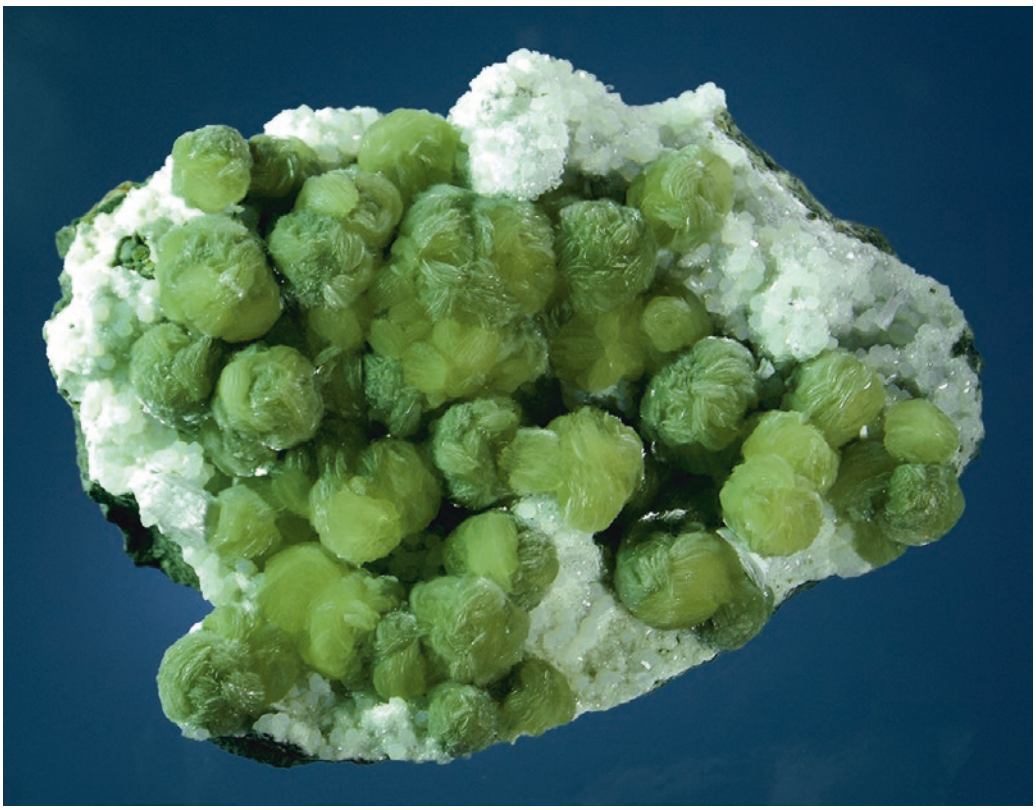

Fig. 11.22 Green gyrolite, 11 × 9 × 5 cm. Kurar quarry, Malad, Mumbai, India
Photo © *Berthold Ottens*

Fig. 11.23 Natrolite with prehnite, 10 × 8 × 5 cm. Kurar quarry, Malad, Mumbai, India
Photo © *Berthold Ottens*

Fig. 11.24 Apophyllite with stilbite, 5 cm high. Savda Quarry, Jalgaon, Maharashtra, India
Photo © *Berthold Ottens*

Fig. 11.25 Stellerite on fibrous mordenite, 7 x 5.5 x 4 cm. Aurangabad, Maharashtra, India
Photo © *Berthold Ottens*

Fig. 11.26 Prehnite cast after laumontite, 16 × 12 × 7 cm. Kurar quarry, Malad, Mumbai, Maharashtra, India
Photo © *Berthold Ottens*

Fig. 11.27 Mesolite with green apophyllite, 14 cm high. Pashan quarry, Pune, Maharashtra, India
Photo © *Berthold Ottens*

Fig. 11.28 Laumontite with little gyrolite spheres, 12 × 9 cm. Kurar quarry, Malad, Mumbai, Maharashtra, India
Photo © *Berthold Ottens*

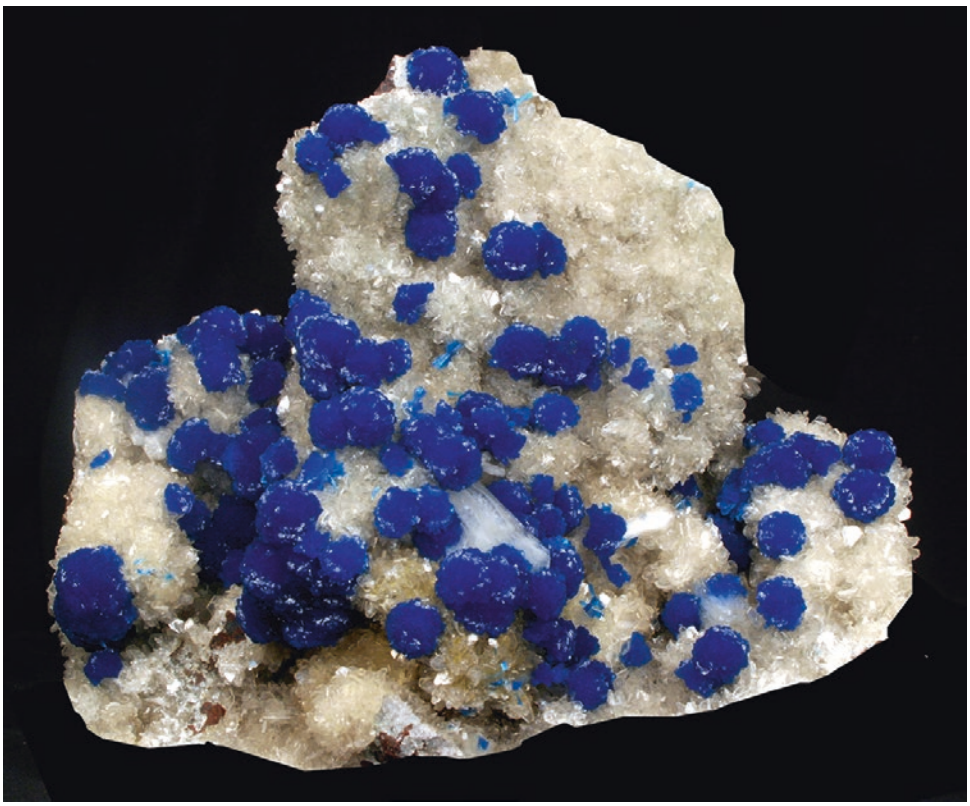

Fig. 11.29 Cavansite with stilbite on heulandite, 7 × 6 × 3 cm. Wagholi quarry, Pune, Maharashtra, India
Photo © *Berthold Ottens*

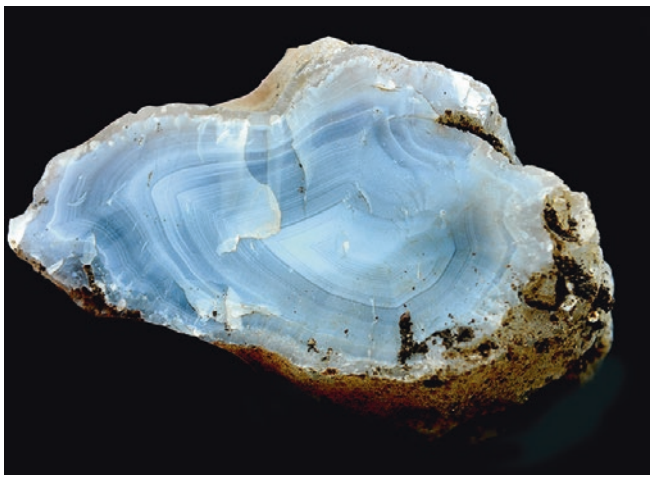

Fig. 11.30 Cryptocrystalline silica. Banded chalcedony-agate from the Deccan. Kalagwani, Burhanpur district, Madhya Pradesh (central India). 11 × 6 cm
Photo © *Berthold Ottens*

Fig. 11.31 "Eye agate", Jalna, Deccan. 23 × 15 cm
Photo © *Berthold Ottens*

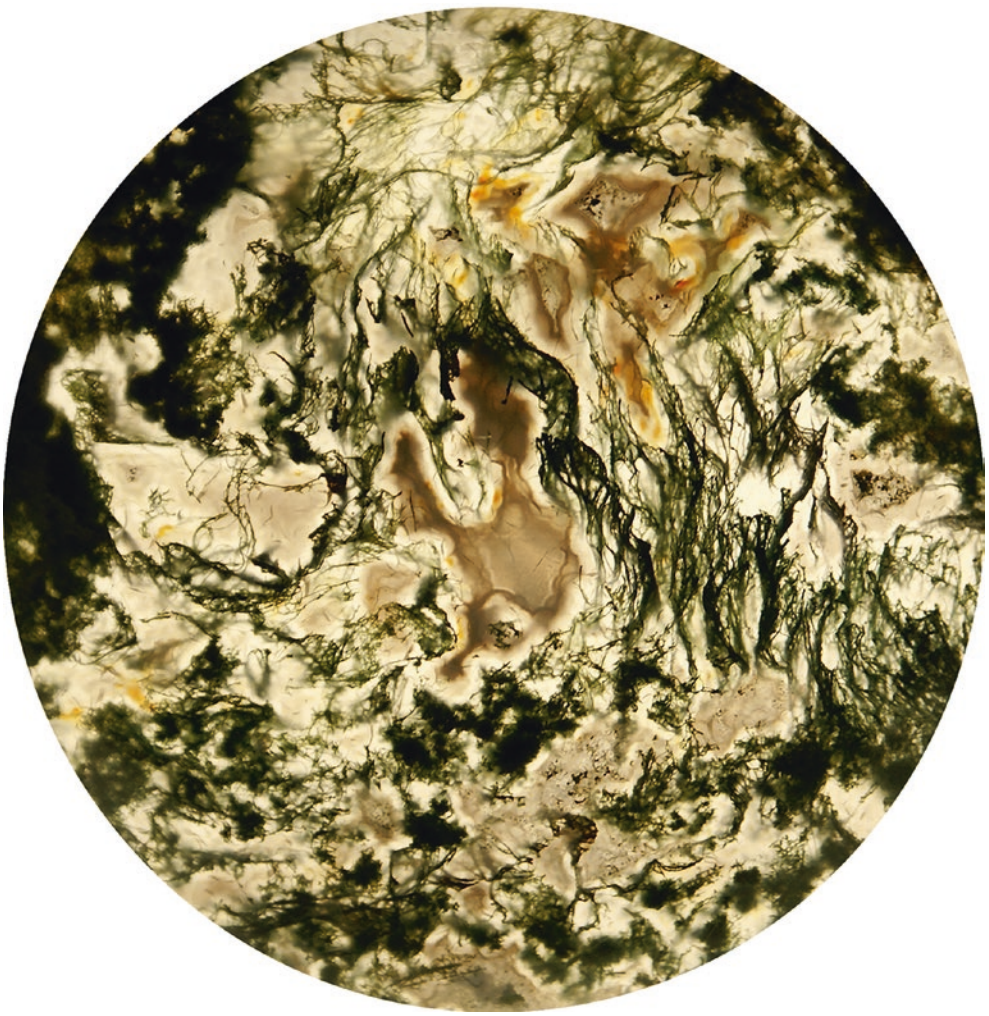

Fig. 11.32 Moss agate, Jalna, Deccan. 3 cm diameter
Photo © *Berthold Ottens*

Weathering and Erosion of Flood Basalt Provinces

12

Fig. 12.1 Residual mountains rising from the flat Deccan plateau (and forming substantial ranges) at Malshej Ghat, Maharashtra. The pyramidal mountain in this photo rises 300 m above the plateau (which is at 700 m above sea level), and ends at the top in three distinct conical peaks which are hidden behind the monsoon clouds. White objects at photo centre are farmers
Photo © *Hetu Sheth*

H. Sheth, *A Photographic Atlas of Flood Basalt Volcanism*, https://doi.org/10.1007/978-3-319-67705-7_12

Chapter Overview

The weathering and erosion of flood basalt provinces are phenomena not directly related to the volcanism itself, but they together give rise to the landscapes and appearance of flood basalt provinces as observed today. In this way, this final chapter "completes the cycle" and brings the reader back to Chap. 1.

Weathering products of flood basalts include clays and clayey "bole" beds (most commonly red, but also brown, green, and even black), laterites (more appropriately called ferricretes), and bauxites. Ferricretes and bauxites are academically important, in discussions of geomorphology, climate, hydrogeology and tectonics. They are also commercially important, for building stone and aluminium ore, and similarly in civil engineering (regarding landslides and associated hazards, particularly in flood basalts like the Deccan which receive extensive rainfall). Ferricretes capping the Deccan highlands of the Western Ghats have been interpreted as the erosional remnants of a once-continuous weathering blanket (e.g., Widdowson 1997) and alternatively as formed in a palaeoriver valley system now exposed in inverted relief (Ollier and Sheth 2008). In Iceland, alteration of glassy basalt produces palagonite. Terracettes (produced by small mass movements) and spheroidal weathering (a type of exfoliation, formed due to volume expansion on ingress of meteoric water) are universal features of global flood basalts and their intrusive equivalents. Wave erosion at rocky beaches produces pedestal rocks, whereas natural bridges and imposing pillars are left by advanced erosion of flood basalts like the Deccan.

Whereas very advanced erosion and planation will produce a flat terrain out of anything, leaving no surface irregularities (except a few monadnocks), moderately high degrees of erosion tend to emphasize and bring out the internal rock structure and rock fabric. This is what explains the continued persistence of even the smallest outcrop-scale features in older flood basalts, such as pipe vesicles, chiesel marks on joint columns, and delicate but beautifully preserved ropy pāhoehoe surfaces, illustrated in this book. The record of small-scale magmatic processes that ocurred hundreds of millions of years before human beings is still not completely erased from the rocks. This record is available for anyone going to the field to read and marvel at. Whatever be the fate of the human race, flood basalts will continue to form, to affect the lithosphere, hydrosphere, atmosphere and biosphere, and to leave a geological record of all this far into the Earth's future.

Fig. 12.2 Highly vesicular, oxidized and reddened top of a flow of the Grande Ronde Basalt (Sentinel Bluffs Member), overlain by the basalt flow of Palouse Falls (Frenchman Springs Member, Wanapum Basalt). Location: Lower Monumental Dam on the Snake River, Washington, Columbia River flood basalt province. Geologist is Elise Rumpf
Photo © *Hetu Sheth*

Fig. 12.3 Small spheroidal boulders in highly weathered Deccan basalt near Sadavaghapur-Borgewadi in the Bamnoli Range, ~25 km SSW of Satara, Western Ghats, India. Vertical face
Photo © *Hetu Sheth*

Fig. 12.4 Spheroidal weathering of a Karoo basaltic lava flow, Hardap area, Namibia. The former columnar jointing of the flow is still recognizable
Photo © *Hervé Bertrand*

Fig. 12.5 Spheroidal weathering in progress, in the Late Pliocene to Early Pleistocene South Caucasus flood basalts, here in northern Armenia. More information: Sheth et al. (2015)
Photo © *Arsen Israyelyan*

Fig. 12.6 Intense tropical spheroidal weathering of the gabbroic Freetown layered intrusion, Sierra Leone (CAMP). The gabbro is transformed into mixed clay minerals and iron hydroxides; note the many concentric shells of weathered material surrounding relatively fresh gabbro
Photo © *Hervé Bertrand*

Fig. 12.7 Differential weathering producing pitted and patterned surfaces in troctolites of the Cuillin Central Complex, Skye, NW Scotland. Geologist is Yigang Xu
Photo © *Hetu Sheth*

Fig. 12.8 Very large, adjacent spheroidal boulders, each with tens of thin "onion shells" enclosing a relatively dense core, exposed in the Bamnoli Range in the Satara region of the Western Ghats, Deccan Traps. Vertical face. The compass at the photo centre is ~10 cm in size
Photo © *Nasrrddine Youbi*

Fig. 12.9 Large-scale spheroidal weathering in Paraná flood basalt, Brazil. Geologist is Carla Joana Santos Barreto
Photo © *Carla Barreto*

Fig. 12.10 Clayey "red bed" horizon between two basalt flows, Isle of Skye, Scotland. Many would term this "red bole", while others restrict that term to palaeosols. At least some of these are ash beds, besides other possible origins (e.g., Srivastava et al. 2012)
Photo © *Hetu Sheth*

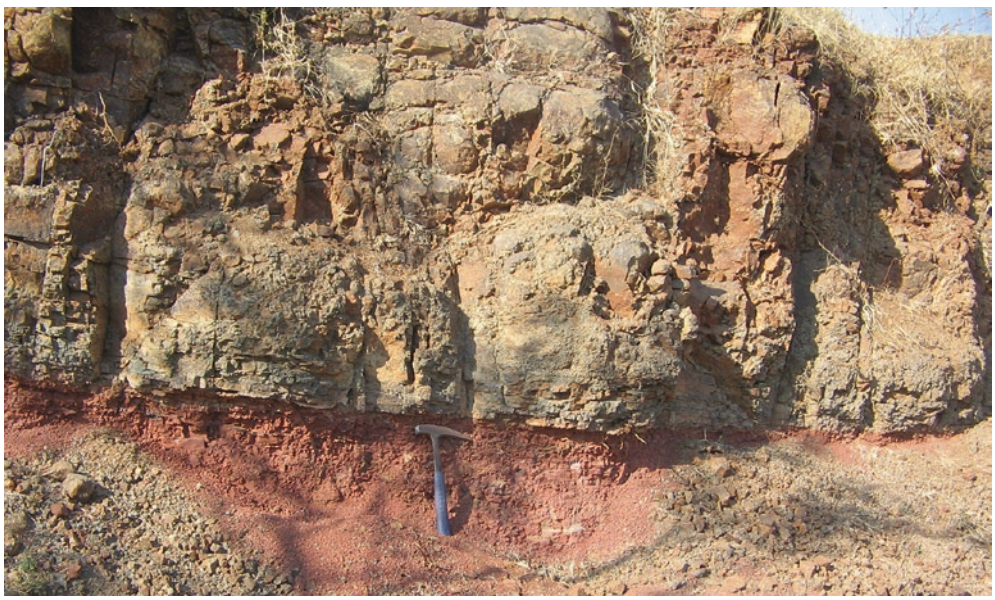

Fig. 12.11 Typical red bole bed underlying a jointed and spheroidally weathered basalt flow near Shirpur, central Deccan Traps. Note small-scale cubical jointing in the red bole. The basalt and the bole dip gently north (*right*). The red boles have various possible origins. Some are palaeosols, others are altered glassy margins of basalt flows, some are sedimentary, and Wilkins et al. (1994) consider still others as altered ash beds
Photo © *Hetu Sheth*

Fig. 12.12 Well-developed red bole horizon (bright orange) underlying the irregular columns of the entablature of a Deccan basalt flow. No colonnade exists. The red bole contains many highly weathered basalt fragments and may originally have been flow-top breccia, among several other possible origins. El Hassane Chellai is the geologist. Satara area, Western Ghats
Photo © *Nasrrddine Youbi*

Fig. 12.13 Thin and highly compacted layer of dark red bole separating two extremely altered basalt flows in the Shevade-Saitale area, ~30 km northeast of Sakri, central Deccan Traps. Geologist is Jyotirmoy Mallik
Photo © *Hetu Sheth*

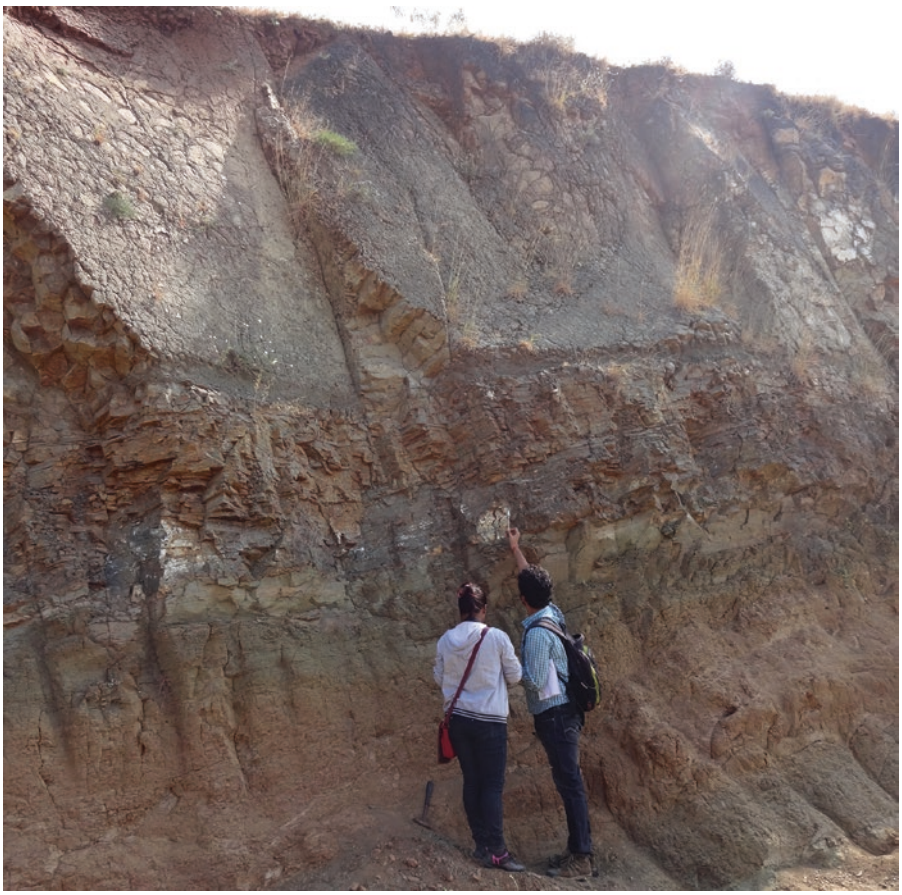

Fig. 12.14 Pāhoehoe sheet lobe with an entablature containing many randomly oriented, small-scale columnar sets (upper part of photo), underlain by a tier of distinctly platy, centimeter-scale horizontal jointing (middle part of photo), underlain by a brown bole (2 m exposed). No disturbance of the bole by the lava flowing over it took place. See also Fig. 3.33, 5.45. Location 3 km southwest of Talaja on the road to Mahuva, Saurashtra, northwestern Deccan Traps. Geologists are Tarulata Das and Vivek Ghule
Photo © *Raymond Duraiswami*

Fig. 12.15 Subaerial basalt lava flows with thick lateritic sediment horizons developed between flows. The shown succession is 130 m thick. Maligât Formation, east Disko, West Greenland
Photo: *Asger Ken Pedersen, Geological Survey of Denmark and Greenland (GEUS)*

Fig. 12.16 Highly weathered basaltic lava flows forming a 80 m high section in the Central Atlantic Magmatic Province (CAMP), Agourai, Middle Atlas, Morocco. Most of the basalt is transformed into clay minerals, except for a few preserved layers
Photo © *Hervé Bertrand*

Fig. 12.17 Hyaloclastites transformed into yellow-brown palagonite, Reykjanes peninsula, Iceland. The blocks are about 1 m in height
Photo © *Hervé Bertrand*

Fig. 12.18 Freshly exposed surfaces of ferricrete ("laterite") capping the Deccan basalts in the Koyna-Satara region, Western Ghats. Pen is 15 cm long. The local people call these rocks "jambha" (purple) in the Marathi language. More information: Ollier and Sheth (2008)
Photo © *Hetu Sheth*

Fig. 12.19 Panoramic view, in evening sunlight, of some of the many ferricrete-capped Deccan basalt mesas around Panchgani, near Mahabaleshwar, Western Ghats. Note people seated at the edge of the ferricrete cliff, against the brightly lit white buildings. More information: Ollier and Sheth (2008)
Photo © *Hetu Sheth*

Fig. 12.20 The tableland of Matheran east of Mumbai rises from the Konkan plain to 803 m above sea level. Originally a spur of the Western Ghats escarpment further east, Matheran is now isolated from it. The tropical climate and abundant monsoon rain has produced a ferricrete cap several tens of meters thick over the Deccan basalt (Ollier and Sheth 2008), and the deep weathering supports a dense jungle which in fact gives Matheran ("jungle on the head") its name. The photo shows a typical monsoon view when numerous streams plunge over the tableland. Though the skies are dark, the cool breezes, greenery, and great views make this whole region a favourite with trekkers
Photo © *Eraiyoli Sankaran*

Fig. 12.21 View of Deccan basalt cliffs forming the western edge of the Matheran tableland, 803 m above sea level. The view is from Echo Point, where Chandrahas Halai is standing clicking his camera, towards Louisa Point, with the pinnacle below. Louisa Point is ~1 km away as the crow flies and tourists on it can just be seen as tiny dots against the sky. The dense jungle at the top is supported by a thick ferricrete cap
Photo © *Eraiyoli Sankaran*

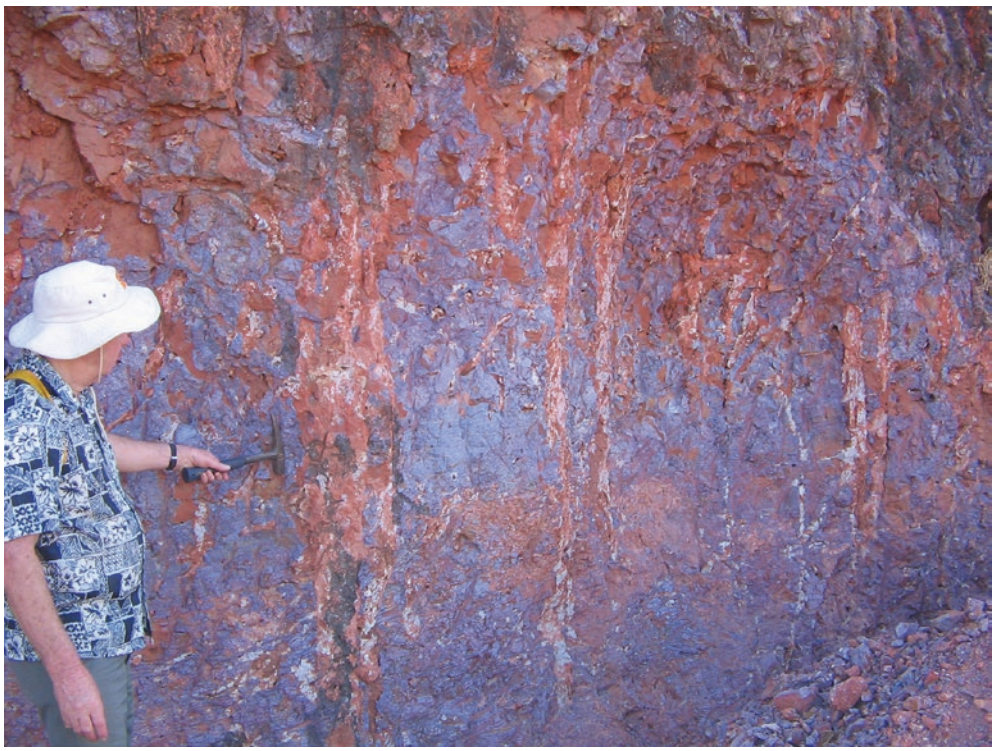

Fig. 12.22 "Mega-mottles" in a brilliantly and variously coloured saprolite profile at the top of the Deccan basalt plateau in the Koyna-Satara region. Between Sadavaghapur and Borgewadi villages, Bamnoli Range, Western Ghats. Geologist is Cliff Ollier. More information: Ollier and Sheth (2008)
Photo © *Hetu Sheth*

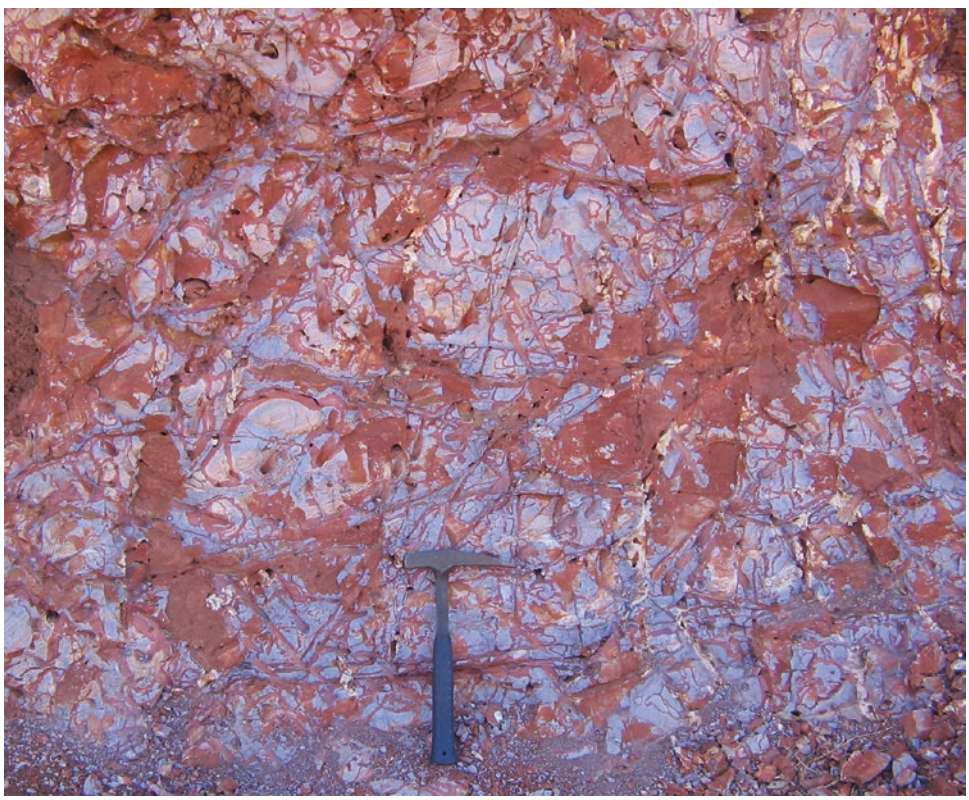

Fig. 12.23 Not a modern art painting illustrating confusion in the world and the painter's mind, but a brilliantly coloured vertical face in a saprolite profile at the top of the Deccan basalt plateau. Outcrop between Sadavaghapur and Borgewadi villages, Bamnoli Range, Koyna-Satara region, Western Ghats. More information: Ollier and Sheth (2008)
Photo © *Hetu Sheth*

Fig. 12.24 Deccan basalt mesa with erosion-resistant ferricrete cap, at Pittri village on the Satara-Kas road, Western Ghats. Note good development of terracettes on the mesa slope. Persons provide a scale. More information: Ollier and Sheth (2008)
Photo © *Hetu Sheth*

Fig. 12.25 Large-scale block collapse with rotation, northern Skye, NW Scotland. Sheep in the foreground and in the far distance (white dots) provide a scale. The hills on the right are composed of lava flows that dip steeply into the high mountain behind, showing subhorizontal to gently dipping lava flows. More information: Emeleus and Bell (2005)
Photo © *Hetu Sheth*

Fig. 12.26 Reduction of the surface area of the ferricrete cap on the Deccan basalt, as seen here at Sadavaghapur in the Koyna-Satara region of the Western Ghats. This proceeds in jumps, by mass movements of loosened ferricrete blocks, sometimes on villages located at the base of the cliff. Geologist is Cliff Ollier. More information: Ollier and Sheth (2008)
Photo © *Hetu Sheth*

Fig. 12.27 Detached blocks of laterite crust near Morewadi, located between Sajjangad and Thoseghar in the Bamnoli Range, Western Ghats. These large blocks provide evidence of mechanical disintegration of the ~20 m thick, erosion-resistant laterite caprock overlying the Deccan basalt flows
Photo © *Vishwas S. Kale*

Fig. 12.28 A natural bridge in Deccan basalt near Gulunchwadi, in the Ane Ghat, about 18 km from Ale Phata, Pune district. An ephemeral stream has cut through a spur, creating the natural bridge. The bridge is 10–12 m wide at the base Photo © *Vishwas S. Kale*

Fig. 12.29 Small pedestal rocks formed by wave erosion in Deccan basalt on the southern shore of Elephanta Island, Mumbai harbour Photo © *Hetu Sheth*

Fig. 12.30 Arnala, with a prominent pinnacle at its top, forms one of the residual mountains of Deccan basalt on the Konkan Plain, between the Western Ghats escarpment and the Arabian Sea. The pinnacle rises ~380 m above the foreground. Both extensive erosion and deep weathering (as indicated by the dense jungle) are observed Photo © *Hetu Sheth*

Glossary[1]

'A'ā Hawaiian term for a fundamental and widespread basaltic lava type with a rough, jagged, spinose, and generally clinkery surface (Macdonald 1953). More information: Rowland and Walker (1990), Harris et al. (2017).

Accretionary lapilli Aggregates of fine ash, commonly with a concentric structure and formed by accretion of damp ash in eruption clouds (White and Houghton 2000).

Agglomerate Older term more or less equivalent to *breccia* (volcanic breccia), which denotes a deposit of angular volcanic rock fragments with considerable size variation.

Agglutinate Deposit produced by instantaneous flattening of hot, soft pyroclasts upon landing (Wolff and Sumner 2000); the term is more or less equivalent to *spatter*.

Alkaline Magma with relatively high proportion of alkalis to silica, such that in rocks like granite with high silica and free quartz, the excess alkalis enter pyroxenes and amphiboles, and in silica-poor rocks like basalt, silica-undersaturated minerals such as the feldspathoids appear.

Amygdules Vesicles of a lava now filled by secondary minerals such as zeolites. Also spelt *amygdales*.

Amygdaloidal A vesicular lava with the vesicles now filled by secondary minerals (amygules).

Anorthosite Cumulate rock made up of >90% plagioclase (typically labradorite), found in large Precambrian-age massifs, layered mafic intrusions, and ophiolites.

Aphanitic Rock with constituent mineral grains too small to be distinguished with the naked eye (so $\ll$1 mm).

Ash Fine explosive ejecta <2 mm in diameter (Bardintzeff and McBirney 2000).

Basanite A silica-undersaturated volcanic or shallow intrusive rock with plagioclase feldspar, clinopyroxene, olivine and nepheline. Equivalent to the older term *alkali olivine basalt* (Kearey 1996).

Basalt Aphanitic basic rock (45–52 wt.% silica, <5 wt.% total alkalis) made up of subequal amounts of calcic plagioclase (typically labradorite) and clinopyroxene, with accessory olivine and Fe-Ti oxides (Best 2003). The most abundant volcanic rock on the Earth and the terrestrial planets (Basaltic Volcanism Study Project 1981).

Basaltic andesite Intermediate rock (52–57 wt.% silica, <5 wt.% total alkalis) transitional between basalt and andesite (Best 2003). Many flood "basalt" lavas, dykes and sills of the world are technically basaltic andesite.

Block An erupted fragment of pre-existing solid country rock, >64 mm in size, and typically angular in form.

Bole An inter-flow weathering horizon with clayey sediment, common in flood basalt provinces such as the Deccan. Bole beds may

[1]What follows is a compilation of the definitions of technical terms used in this atlas, particularly for flood basalt nonspecialists, though specialists may also find the definitions and accompanying notes useful. The definitions are taken from several sources, and have been suitably edited in many cases. Additional sources which provide further information or clarification are also indicated. Note that some terms, such as "large igneous province", have definitions that are highly debated, and such controversies are best kept beyond the scope of this atlas, but ample reading material is indicated.

H. Sheth, *A Photographic Atlas of Flood Basalt Volcanism*, https://doi.org/10.1007/978-3-319-67705-7

be red, green, brown or black depending on the chemical and mineral composition, and may have different origins, including palaeosols, fine-grained detrital sediments, altered glassy bases of the flows themselves, and altered ash beds.

Bomb An erupted fragment of lava, >64 mm in size, typically rounded in form and representing juvenile (new) magma, not pre-existing rocks around the volcanic conduit.

Breakout A mass of lava that flows out at the surface from underneath a solidified or partially solidified mass of lava, as by lifting or fracturing of the solidified crust of the latter.

Breccia A mass of angular fragments of volcanic rock, normally with a wide range of sizes (Bardintzeff and McBirney 2000).

Carbonatite Magma or lava made up of at least 50% carbonate minerals (most commonly calcium, magnesium and sodium carbonate). Carbonatite lava flows have very low eruption temperatures of ~500 °C and erupt today only at Oldoinyo Lengai volcano in Tanzania (Schmincke 2004).

Chiesel marks Horizontal striations on the face of a joint column in lava, produced by periodic propagation of the bounding columnar joints.

Chromitite Monomineralic cumulate rock made up of the mineral chromite ($FeO{\cdot}Cr_2O_3$), found in layered mafic intrusions and ophiolites, and particularly abundant in the Bushveld Complex of South Africa, world's largest layered mafic intrusion.

Clinker Loose, exceedingly rough, irregular, and spiny fragments that cover the surface of an 'a'ā lava flow (Macdonald 1953).

Colonnade A tier in a thick *simple* lava flow or *sheet lobe* which is characterized by a regular arrangement of well-formed columns, and solidified by slow, conductive cooling (Tomkeieff 1940; Long and Wood 1986; Lyle 2000).

Columnar joints Joints which develop in solidifying lava flows and intrusions due to thermal contraction and which, by linking up laterally and propagating downwards from the top and upwards from the base, divide the igneous body into columnar units with five, six or seven sides.

Columnar rosette A structure in which joint columns have a radial disposition, with the columns diverging from a central zone. These are often mistakenly interpreted as solidified lava tubes.

Compound flow Lava flow composed of many individual flow-units or lobes (Walker 1971).

Cone sheets Tabular sheet intrusions formed where magma invades a conical fracture system whose apex lies near the top of the underlying central intrusion (Best 2003).

Continental flood basalt (CFB) A flood basalt province formed on a continent, and contrasted with *oceanic plateau*, a flood basalt province formed on the seafloor.

Cumulate Igneous rock formed by mechanical accumulation of crystals from a magma, such that there never was a magma of the composition of the cumulate rock.

Diabase A mafic dyke rock that is appreciably altered (but not metamorphosed) from an originally fresh dolerite (McHone 1992).

Diktytaxitic Texture in some coarse-grained basaltic lava flows or sheet intrusions in which small angular voids are dispersed in a network of plagioclase and pyroxene grains (Best 2003).

Diorite Phaneritic intrusive igneous rock containing plagioclase (more sodic than the labradorite found in gabbros) and amphibole (unlike the clinopyroxene in gabbro), with accessory pyroxenes and quartz. The plutonic equivalent of andesite (Kearey 1996).

Dolerite Medium-grained (1–5 mm) rock of basaltic composition, made up of the minerals plagioclase and clinpyroxene, with some accessory olivine and Fe-Ti oxides, and commonly forming dykes and sills.

Dyke A tabular (sheet-like) magma intrusion, typically vertical or subvertical, that is discordant with (cuts across) the structure of the surrounding rocks.

Dykelet A small dyke, millimeters to centimeters thick and a few meters long.

Enclave Patch or blob of one magma inside another of a different composition, left over without complete mixing with the host.

Entablature A tier in a thick *simple* lava flow or *sheet lobe* which is characterized by thin (<10 cm), chaotically arranged columns. In simple situations, the entablature overlies the colonnade in a flow, and the entablature solidifies rapidly downward by convective cooling,

due to the entry of meteoric water into the cooling flow, while the colonnade solidifies much more slowly upward (Tomkeieff 1940; Long and Wood 1986; Lyle 2000). A flow may have several of the entablature and colonnade tiers formed over several years of alternate dry and wet seasons.

Feeder dyke A dyke (magma-filled fracture) that transports magma from a magma chamber to the surface of the Earth, feeding an eruption. A dyke that is unable to reach the surface is called an *arrested* or *non-feeder* dyke.

Felsic Rock made up of light-coloured minerals rich in silica and alumina, such as quartz, alkali feldspars, and feldspathoids. Contrasted with *mafic*.

Ferricrete A term preferable over *laterite*, applied to the iron-cemented, hard, weathered materials (duricrusts) found on plateau remnants, whatever their mode of origin (e.g., Ollier and Pain 1996). See also Widdowson (2004) and Ollier and Sheth (2008).

Ferrodiorite Medium- to coarse-grained rock, more evolved (with lower MgO and higher silica) than gabbro, found as segregations in basaltic lava flows and intrusions, and also forming intrusions in the Proterozoic anorthosite massifs. The latter ferrodiorites are low in silica, MgO, alkalis, and europium, but rich in total iron (up to 38 wt.%), TiO_2 (up to 10.5 wt.%), P_2O_5 (up to 2.3 wt.%), Sr, Ba, Zr, and the light rare earth elements (e.g., Ashwal 1993).

Fissure eruption An eruption occurring from an elongated fissure, instead of a central vent.

Flood basalt A voluminous and laterally extensive lava flow, normally erupted from a fissure, which inundates pre-existing topography and produces a flat-topped landscape owing to its large volume and high fluidity. Stacks of many flood basalt lava flows erupted rapidly from fissures produce a flood basalt province.

Flow-unit A small constituent unit of a compound lava flow, each flow-unit being a separate cooling and vesiculation unit and bounded by a chilled margin (Nichols 1936; Walker 1971). The term is more or less equivalent to *lobe* or *lava lobe*.

Flow-top breccia The fragmental top of a lava flow, common in basaltic through rhyolitic lava flows, and characteristic of the flood basalt morphological type called rubbly pāhoehoe.

Flow-bottom breccia The fragmental base of a lava flow, characteristically an 'a'ā flow, formed by the continuous recycling of flow-top breccia or clinker into the front of the advancing flow.

Fractional crystallization Separation of crystals from melt in a magma, by a range of possible mechanisms including gravity settling, convection currents, etc.

Gabbro Coarse-grained (>5 mm) rock of basaltic composition, made up of the minerals plagioclase and clinopyroxene, with some accessory olivine and Fe-Ti oxides, and commonly forming large plutonic intrusions. A related rock with roughly equal amounts of plagioclase and orthopyroxene is termed *norite*.

Gas blister Large cavity typically several meters in diameter, left by a large escaping gas bubble which formed by coalescence of many smaller bubbles within a flood basalt flow. Frequently lined with secondary minerals.

Geode A cavity in volcanic rock, centimeters to meters in size, lined with secondary minerals.

Giant dyke swarm Dyke swarms that are several hundred kilometers to as much as a few thousand kilometers in length. See Ernst et al. (1995) and Ernst (2014), and references therein, for examples.

Giant plagioclase basalt Highly porphyritic basalts widespread in some flood basalt provinces like the Deccan of India, in which large megacrysts (2–5 cm) of plagioclase make up 35% or more of the rock volume. They commonly form lava flows, but dykes are also known. More information: Sheth (2016).

Granophyre Fine- to medium-grained granitic rock forming shallow-level plutons, and characterized by a granophyric texture (intergrowth between quartz and K-feldspar in which K-feldspar is the host and quartz forms irregularly shaped patches within it). A larger-scale version of this texture in which quartz forms areas with polygonal outlines, producing an appearance of Egyptian hieroglyphics, is called *graphic* texture.

Hyaloclastite Glassy volcanic fragments, typically of basaltic lava, resulting from sudden quenching and nonexplosive shattering in water (Batiza and

White 2000; Bardintzeff and McBirney 2000). Schopka et al. (2006) use the term hyaloclastite synonymously with the Icelandic term *móberg*, to describe all unconsolidated and consolidated volcaniclastic rocks which consist chiefly of variably palagonitized sideromelane fragments dominantly in the ash (<2 mm) but extending into the lapilli (2–64 mm) size range. Rhyolitic hyaloclastites also occur.

Hydrovolcanic Indicating explosive interaction between magma and surface water.

Hydrothermal Related to phenomena involving water heated by a magmatic source at depth.

Hyp-abyssal Located at depths between the Earth's surface and the deeper crust; term used for dykes, sills and shallow-level plutons.

Hummocky pāhoehoe A pāhoehoe flow that contains tumuli (Swanson 1973; Walker 1991; Self et al. 1997, 1998).

Igneous layering Compositional layering produced in an igneous body, typically a pluton, by high-temperature igneous processes such as crystal settling.

Inflation The thickening of an already emplaced lava flow-unit or lava flow by the injection of additional lava under a solidified crust (Self et al. 1997, 1998). The term goes back at least to Macdonald (1953).

Inflation cleft Tension crack formed at the top of a tumulus. Lava may extrude from the inflation cleft as a *squeeze-up*.

Intracanyon A lava flow that was erupted in (or flowed along) a pre-existing canyon in older rocks, and often able to cover long distances.

Intrusion A subsurface igneous rock body formed when molten magma forces its way into surrounding host rocks and then cools (Lipman 2000).

Komatiite High-temperature lava of highly magnesian composition (MgO >18% and frequently >30%), with estimated eruption temperatures of ~1600 °C, found in Archaean (and Proterozoic) greenstone belts and very rare in the Phanerozoic rock record.

Lamproite A group of peralkaline, volatile-rich, ultrapotassic, volcanic to hypabyssal rocks. The mineralogy is variable, but lamproites typically contain phenocrysts of olivine + phlogopite ± leucite ± K-richterite ± clinopyroxene ± sanidine (Winter 2001).

Lamprophyre A diverse group of dark, porphyritic, mafic to ultramafic, generally highly potassic and hypabyssal rocks, forming small shallow-level intrusions. They are normally rich in alkalis, volatiles, Sr, Ba and Ti, with biotite-phlogopite and/or amphibole phenocrysts (Winter 2001).

Lapilli Fragmental volcanic ejecta between 2 and 64 mm in diameter.

Large Igneous Province (LIP) A term which has been and remains the subject of considerable controversy and is unsatisfactorily defined. *Large Igneous Provinces* (LIPs) were initially defined (Coffin and Eldholm 1992, 1993, 1994) as massive crustal emplacements of predominantly mafic extrusive and intrusive rock, which originated via processes other than "normal" seafloor spreading, and which have areal extents >0.1 million km^2. Sheth (2007) argued that the term LIP should include many more igneous phenomena, such as granitic batholiths and volcanic rift zones, and proposed a minimum area of 50,000 km^2 so as to permit these features to be included among LIPs. He argued that tectonic setting should not be a part of the LIP definition, and "flood basalt provinces" was a better term to represent the provinces typically described as LIPs. Bryan and Ernst (2008) proposed a revised definition as follows: "*Large Igneous Provinces* are magmatic provinces with areal extents >0.1 million km^2, igneous volumes >0.1 million km^3 and maximum lifespans of ~50 million years that have intraplate tectonic settings or geochemical affinities, and are characterised by igneous pulse(s) of short duration (~1–5 million years), during which a large proportion (>75%) of the total igneous volume has been emplaced." As discussed by Cañón-Tapia (2010) and Sheth and Cañón-Tapia (2015), this revised definition continues to have problems, such as the imposition of a particular (intraplate) setting, difficulties of defining "normal" seafloor spreading, and the vagueness of "intraplate geochemical affinities".

Laterite Tropical, yellow-brown-purple, iron-rich weathering product, of basalts and many other rock types including metamorphic rocks (e.g., Widdowson 1997; Widdowson and Gunnell 1999), which has had highly variable and confusing definitions. See discussions in, e.g., Ollier (1991), Bourman and Ollier (2001), and Ollier and Sheth (2008).

Lava Molten rock material above the surface of the Earth, largely liquid, with suspended solid crystals and escaping volatiles, and capable of flowage.

Lava channel Pathway along which a stream of lava moves, open to the atmosphere, and typically confined by levees along the channel margins.

Lava dome A steep-sided, more or less round extrusion of viscous lava, typically rhyolite, dacite, or trachyte.

Lava flow A discrete body of lava emplaced as a dynamically continuous unit (Kilburn 2000). Also defined as the product of a single continuous outpouring of lava, roughly corresponding to one episode of an eruption, whereas a *flow field* is the aggregate product of a single eruption or vent and built of up one or more lava flows (Self et al. 1997). As stated in Self et al. (1997), "In simplest terms, a flow field is a field of lava flows and each lava flow is made up of a number of lobes". However, distinguishing eruptive units exposed only in vertical section, in older flood basalt provinces, as *flows* or *flow fields* is very difficult or impossible, and the terms must be applied carefully.

Lava tube Enclosed pathway, typically with a circular or elliptical cross-section, along which lava is transported, with a thick and solidified roof and walls around it which prevent significant heat loss. Also called *lava tunnel*, but Lockwood and Hazlett (2010) advocate the term *pyroduct*.

Lithophysa Subspherical masses (plural, *lithophysae*) in rhyolitic lava flows and compacted tuffs, generally a few centimeters in diameter and composed of concentric onion-like shells of fine-grained quartz and alkali feldspar separated by empty spaces. Their origin may involve rhythmic exsolution and expansion of volatiles during crystallization, and vapour-phase precipitates including quartz commonly occur in them (Best 2003). Lithophysae are often filled with secondary silica, in which case they are known as thundereggs, geodes, and agates (Shaub 1979). More information: Breitkreuz (2013).

Lobe A coherent package of lava that is surrounded by a chilled glassy crust, and ranging in size from small *toes* to large *sheet lobes* (Self et al. 1997, 1998; Thordarson and Self 1998).

Maar A low-rimmed explosion crater formed by a phreatomagmatic eruption, and commonly subsequently filled by a lake. The underlying pipe-like, breccia-filled structure of a maar is called a *maar-diatreme* (Vespermann and Schmincke 2000).

Mafic Rock made up of dark-coloured minerals rich in iron and magnesium, such as olivines, pyroxenes, amphiboles, and Fe-Ti oxides. Contrasted with *felsic*.

Mafic dyke swarm Group of mafic dykes emplaced in the same igneous episode, or dykes that show similar trends or radial or fanning patterns (Halls 1982; Ernst et al. 1995).

Magma Molten rock material under the surface of the Earth; commonly a mixture of liquid (melt) in large part with some suspended crystals and dissolved volatiles.

Magma mingling Two magmas of different composition coming in contact without complete mixing or hybridization (at a given scale of observation), so that blobs or *enclaves* of one magma remain suspended within the other up to and after complete solidification.

Magma mixing Two magmas of different composition coming in contact and producing a third homogeneous magma of intermediate composition.

Microgranite A granite (phaneritic rock with essential quartz and alkali feldspar, and accessory biotite, hornblende, etc.), which is fine-grained (<1 mm) to medium-grained (1–5 mm).

Modal layering Layering in an igneous body, characterized by different modal proportions of various minerals in the different layers. Different from *cryptic layering*, which involves mineral compositional variations invisible to the naked eye.

Multiple-injection dyke Dyke fracture which is repeatedly and periodically used to transport magma of similar composition from a magma chamber to higher levels of the Earth, identifiable by internal chilled margins and other features (e.g., cooling columns) of the distinct magma batches solidified against each other. Many sills of this kind are also known. If the distinct magma batches differ substantially in composition, the term *composite* is used.

Nephelinite Silica-undersaturated mafic volcanic or shallow intrusive rock containing subequal amounts of clinopyroxene and nepheline.

Neptunian dyke A sheet-like sand body cutting through overlying rocks, as a result of liquefaction and upward injection of sand through a fissure, during an earthquake.

Obsidian Glassy lava of rhyolitic composition, with high silica content, vitreous lustre and conchoidal fracture. Commonly of deep black colour.

Pāhoehoe A fundamental and widespread type of low-viscosity basalt lava consisting of thin sheets, tongues and lobes, commonly overlapping one another and fed from distributary tubes, with subspherical vesicles and a smooth and sometimes rope-like surface (Best 2003).

Palagonite Hydrated basaltic glass, made up of clay minerals and usually with an orange brown colour, associated with subaqueous or subglacial eruptions (e.g., Schopka et al. 2006). Fresh basaltic glass is called *sideromelane* if translucent and *tachylite* if opaque due to microlites (Smellie 2000; Schmidt and Schmincke 2000; White and Houghton 2000).

Pele's tears Small droplets of shiny black basaltic glass, generally a few millimeters to a few centimeters in size and with spherical, dumbbell or tadpole shapes acquired during ballistic flight (Vergniolle and Mangan 2000).

Peperite Heterogeneous mixtures formed by mingling between magma and unconsolidated, typically wet, sediment (Skilling et al. 2002). The sediment may be unconsolidated without necessarily being wet (see Jerram and Stollhofen 2002).

Peralkaline With molar ($Na_2O + K_2O$) > Al_2O_3 (Winter 2001).

Phaneritic Rock with individual grains large enough to be distinguished by the naked eye.

Phenocrysts Large crystals in an igneous rock, contained in a fine-grained matrix called the *groundmass*.

Phonolite Alkaline volcanic or dyke rock, made up of alkali feldspar and nepheline, and the fine-grained equivalent of nepheline syenite.

Phreatomagmatic An explosive eruption produced by the interaction between magma and near-surface groundwater.

Picrite Ultrabasic rock with >12% MgO, with plagioclase, clinopyroxene and abundant olivine, formed either as a relatively high-temperature picritic liquid or by simple accumulation of olivine in a basaltic magma.

Pillow lava Interconnected bulbous, bolster-like or tube-like forms of basaltic lava, formed by subaqueous eruptions. Cross-sections commonly show a convex upper surface and a flat or concave lower surface, with radial fractures inside, and a chilled glassy margin (rind) outside (Schmidt and Schmincke 2000).

Pillow breccia A mixture of large, typically glassy fragments and pieces of pillow lava formed by the shattering of pillow lava crusts or by breakage of newly formed pillows rolling down steep submarine slopes (Batiza and White 2000).

Pipe vesicles Tubular gas cavities usually less than a centimeter in diameter and several centimeters long that are found at the bases of many pāhoehoe flows (Lockwood and Hazlett 2010). They are often vertical but also often plunging or bent, and are one of the universal but still poorly understood features. More information: Walker (1987), Philpotts and Lewis (1987), Godinot (1988).

Pit crater A circular crater formed by the sinking of the ground due to loss of support from below, as by collapse of the roof of a large underground lava tube system (Hazlett and Hyndman 1996; Lockwood and Hazlett 2010).

Pitchstone Hydrated rhyolitic glass, black in colour like obsidian, but with a duller lustre than obsidian.

Plateau basalt Term equivalent to flood basalt, though referring to their final, characteristic

landscape form, unrelated to their processes of formation (see a discussion in Sheth 2007). Interestingly, Tyrrell (1932) distinguished the two terms in another sense, defining flood basalts as silica-saturated basalt eruptions from fissures, and plateau basalts as silica-undersaturated basalt eruptions from central edifices such as scoria cones. The topic is worthy of future analysis.

Plug Small and shallow-level pluton with a roughly circular cross-section, emplaced within country rocks or in a volcanic conduit.

Plumose markings Feather-like patterns of striations on joint surfaces, radiating away from the origin of the joint in the direction of joint opening (Davis and Reynolds 1996).

Pluton General term for any igneous intrusion.

Pseudoleucite An intergrowth of orthoclase and nepheline pseudomorphic after leucite.

P-type pāhoehoe Pipe vesicle-bearing pāhoehoe, meaning a common type of pāhoehoe with pipe vesicles at the base of individual flow-units or lobes (Wilmoth and Walker 1993). Forms by inflation, as contrasted with *S-type* pāhoehoe which does not undergo inflation (Self et al. 1998).

Porphyritic Inequigranular igneous texture with two grain sizes, and with large *phenocrysts* surrounded in a fine-grained matrix called the *groundmass* (Best 2003).

Pyroclastic Volcanic material formed by explosive volcanism.

Pyroclastic flow A pyroclastic density current in which most of the material and momentum are contained in a basal concentrated particulate dispersion (Wilson and Houghton 2000).

Rheomorphic ignimbrite A volcanic deposit of high-temperature pyroclastic material (ash and pumice) laid down by a pyroclastic flow, and undergoing intricate internal structural deformation after deposition due to flowage under gravity.

Rhyolite High-silica (>66 wt.%) volcanic rock, made up of the minerals quartz and alkali feldspar, with accessory minerals such as biotite or hornblende, and the volcanic equivalent of granite.

Rubbly pāhoehoe A basaltic lava flow type transitional between pāhoehoe and ‘a’ā, with a zone of fragmental flow-top breccia in its upper part, common and abundant in flood basalt provinces.

Rootless cone These hydrovolcanic cones form in and rest directly on tube-fed, inflated pāhoehoe lava flows when the lava interacts with surface or near-surface water, ice, or wet ground, and the resulting mild explosions produce scoria and spatter that accumulate to form small cones around the explosion spots (Thorarinsson 1953). They do not represent primary vents connected by vertical conduits to a subsurface magma source. However, their alternative name *pseudocraters* is inappropriate, inasmuch as the craters themselves are real. More information: Greeley and Fagents (2001), Fagents and Thordarson (2007), Reynolds et al. (2015).

Ropy lava Pāhoehoe lava breakouts with rope-like and corded forms, produced by the pulling of the thin viscoelastic surface crust by underlying lava whose terminus has come to a rest, and the resultant folding of this crust (Fink and Fletcher 1978). The convexity of ropes indicates the movement direction of the lava forming that breakout. Ropy lava is always found in pāhoehoe lava flows, though much pāhoehoe is not ropy.

Saucer-shaped sill Sheet-like intrusions with a saucer-shaped geometry, typically made up of a subhorizontal inner sill forming the base, a steeply dipping inclined sheet cross-cutting the host-rock stratification, and a subhorizontal outer sill (Chevallier and Woodford 1999; Polteau et al. 2008).

Scoria Highly vesicular and low-density pyroclastic ejecta, most commonly of basaltic to andesitic composition.

Scoria cone A cone made up of scoria accumulated around an eruptive vent, with or without associated lava flows (Németh and Martin 2007). Also called *cinder cone*, and typical of Strombolian eruptions.

Secondary minerals Minerals such as quartz, calcite, apophyllite, and numerous zeolites that do not form from flood basalt magma, but much later during the movement of hydrothermal solutions through the lava pile, and get deposited in vesicles and cavities of the basalts.

Segregation features Vesicle cylinders and sheets found in pāhoehoe lava, made up of lava significantly more bubble-rich than the rest of the lava unit. More information: Goff (1996), Caroff et al. (2000), Costa et al. (2006).

Sheet A tabular intrusion which dips at an angle of ~45° to the horizontal, and is thus neither a dyke nor a sill.

Sheet lobe A large pāhoehoe lava lobe, tens of meters thick and many kilometers long (Self et al. 1997, 1998; Thordarson and Self 1998), typically columnar-jointed. The term is more or less equivalent to, and preferable over, the older term *simple flow*.

Sill A tabular (sheet-like) magma intrusion, typically horizontal or nearly so, that is concordant with (parallel to) the structure of the surrounding rocks.

Simple flow A thick (up to tens of meters) and laterally extensive (kilometers to many kilometers) lava flow which is not divisible into constituent flow-units or lobes, and thus contrasted with a *compound flow* (Walker 1971). Simple flows are typically columnar-jointed throughout their thickness; the term is more or less equivalent to *sheet lobe*.

Slabby pāhoehoe Pāhoehoe lava with its upper crust broken into distinct slabs, which may undergo rotations, collisions and breakage while the flow moves. With intense brecciation of the slabs, flow-top breccia is produced and the lava flow is now rubbly pāhoehoe.

Spatter Pyroclasts, typically produced during basaltic fire fountains, that are plastic when they hit the ground and undergo flattening. Equivalent to *agglutinate* (Wolff and Sumner 2000). A cone or mound produced by spatter accumulating around an eruptive vent is called a *spatter cone* or mound.

Spheroidal weathering A type of chemical weathering common in humid, tropical climates that affects highly jointed rock and produces many spherical and concentric layers or shells of highly weathered rock, with relatively unaltered rock forming the cores of these spheroids.

Spherulite Rounded or spherical polycrystalline growths, made up of radiating, microscopic fibres of quartz and alkali feldspar, formed by nucleation in highly supercooled and viscous rhyolitic melt, or by devitrification of rhyolitic glass (obsidians, pitchstones and vitrophyres). More information: Marshall (1961), Lofgren (1971), Smith et al. (2001), Watkins et al. (2009).

Spilite Basaltic rock hydrated and altered in contact with seawater or hydrothermal solutions, such that clay minerals and chlorite develop from pyroxenes and sodic plagioclase (albite) from calcic plagioclase (labradorite). Spilite is greenish in colour, and a view also exists that the albite and chlorite may crystallize directly from a hydrous spilite magma, rather than being alteration products of basaltic minerals (see Amstutz 1974).

Spinifex Texture characteristic of the surfaces and upper chilled crusts of komatiite lava flows in which long blades and feathers of quench olivine criss-cross.

Spiracle Irregular cylindrical cavity within a lava flow, up to a few centimeters in diameter and meters in length, formed by a steam explosion during the passage of the lava over a pool of shallow water, or water-saturated unconsolidated sediment. The sediment can be mobilized and be injected into the flow along with the steam (Lockwood and Hazlett 2010).

Squeeze-up Extrusions of lava that come out of the inflation clefts of tumuli or between the flow-units of a compound pāhoehoe flow (Nichols 1939). They may superficially resemble dykes and dykelets when seen on an eroded surface.

S-type pāhoehoe Spongy pāhoehoe, with large numbers of close-spaced, rounded vesicles throughout its thickness (Walker 1989; Wilmoth and Walker 1993), unlike *P-type* pāhoehoe which has rounded vesicles in the upper crust and pipe vesicles at the base and a nearly non-vesicular core.

Strombolian Style of eruptions, characteristically of basalt and basaltic andesite, which is somewhat more explosive than Hawaiian eruptions, and in which discrete blasts produce large amounts of scoria and ash around the eruptive vent, building a scoria cone (syn. cinder cone). Lava flows may also be erupted.

Syenite Coarse-grained felsic rock made up of alkali feldspars and accessory quartz or nepheline. The plutonic equivalent of trachyte.

Tephra A collective term for all pyroclastic deposits.

Toe A small lava lobe up to 50 cm in thickness and 100 cm in the long dimension (Self et al. 1997, 1998; Thordarson and Self 1998).

Toothpaste lava A type of basaltic lava flow transitional between pāhoehoe and 'a'ā in terms of viscosity and flow velocity. It typically extrudes from rootless openings (boccas) on other flows, usually late in an eruption, and has a surface characterized by longitudinal grooves and ridges oriented parallel to lava movement, caused by irregularities in the shape of the feeding bocca. More information: Bullard (1947), Krauskopf (1948), Rowland and Walker (1987), Sheth et al. (2011b).

Tholeiite Defined variously as basaltic magma or rock which is subalkalic, silica-saturated, hypersthene-normative, and iron-rich. The term *tholeiitic* when applied to other rock types indicates the same characteristics.

Trachyte Alkaline felsic volcanic or subvolcanic rock with alkali feldspar, with or without some quartz. The fine-grained equivalent of syenite. Grades into phonolite with nepheline present.

Tuff Consolidated volcanic ash.

Tuff breccia A deposit with subequal proportions of fine-grained tuff (<2 mm) and large angular fragments (>64 mm).

Tuff ring Small explosive volcano formed by magma-water interaction, with a crater surrounded by an ejecta ring. It differs from a maar in having its floor above the surrounding ground surface (Németh and Martin 2007).

Tumulus Structure produced by the localized domal uplift of the crust of a lava flow due to the build-up of lava pressure underneath, as can happen due to the blockage of an underlying lava tube further downstream (Walker 1991; Rossi and Gudmundsson 1996). *Tumuli* (the plural form) commonly have a pronounced axial cleft through their middle, formed by extension of the crust, as well as radial cracks. Tumuli generally have a circular or elliptical planform, though many elongated tumuli are also known, and are to be distinguished from *pressure ridges*, elongated ridges produced by lateral compression within a lava flow (Walker 1991).

Tuya Subglacial volcanic table mountain, with flat top and steep sides. These table mountains form by eruption of pillow lavas and hyaloclastite in a lake of meltwater under an ice cap, followed upward by tuffs, and finally subaerial lava and associated hyaloclastite deltas (Bardintzeff and McBirney 2000; Schopka et al. 2006). They are common in British Columbia, from where the name comes (Matthews 1947), and in Iceland, where they are called *stapi*. They are different from the *hyaloclastite ridges* of Iceland (called *tindars* by Jones 1969) which also represent subglacial fissure eruptions, but commonly lack basal pillow lavas and summit subaerial lava or hyaloclastite deltas (Schopka et al. 2006; Jarosch et al. 2008).

Ultrapotassic With molar K/Na ratio >3 (Winter 2001).

Vesicle A small, rounded, smooth-surfaced void in solidified lava or pyroclast, formerly occupied by gas. The term *bubble* denotes the same in molten lava (Wilmoth and Walker 1993; Cashman et al. 1994).

Vesicle banding Horizontal banding, defined by horizontal trains of amygdules commonly found in the upper crusts of pāhoehoe lava units. Forms due to the periodic uprise of gas bubbles from the molten interior and their arrest in the progressively downward-solidifying crust.

Vesicle cylinder A type of segregation feature: cylindrical upwellings of bubble-rich lava that rise vertically from the top of a diktytaxitic crystal mush zone at the base of a solidifying pāhoehoe flow, and are commonly found preserved within the flow core. They are typically a few centimeters in diameter, with circular or elliptical cross-sections, and tens of centimeters to meters in length. Many cylinders are reported from the Paraná flood basalts, for example (Barreto et al. 2014, 2017). To vertical trails of vesicles found in these flows, having indistinct boundaries with host basalt and irregular shapes, these authors apply the term *proto-cylinders*.

War bonnets Large rosettes of cooling columns found in lava flows of the Columbia River flood basalt province, USA, and interpreted by some as solidified lava tubes.

Xenoliths Fragments of the rocks (crustal and mantle) under a volcano, brought to the surface during a volcanic eruption, or to shallower depth levels by magma intrusions.

Zeolites A group of numerous hydrated aluminosilicate minerals with framework structures. The structures are porous and the cavities are occupied by large ions and water molecules, both with considerable mobility, permitting ion exchange and reversible dehydration. Zeolites are found as amygules in basaltic rocks, as authigenic minerals in sedimentary rocks, and in low-grade metamorphic and hydrothermally altered rocks (Kearey 1996).

References

Airoldi GM, Muirhead JD, Long SM, Zanella E, White JDL (2016) Flow dynamics in mid-Jurassic dykes and sills of the Ferrar large igneous province and implications for long-distance magma transport. Tectonophysics 683:182–199

Ali JR, Aitchison JC, Chik SYS, Baxter AT, Bryan SE (2012) Palaeomagnetic data support Early Permian age for the Abor Volcanics in the lower Siang valley, NE India: significance for Gondwana-related break-up models. J Asian Earth Sci 50:105–115

Alloway MR, Watkinson AJ, Reidel SP (2013) A serial cross-section analysis of the Lewiston Structure, Clarkston, Washington, and implications for the evolution of the Lewiston Basin, *in* Reidel SP, Camp VE, Ross ME, Wolff JA, Martin BS, Tolan TL, Wells RE (eds) The Columbia River Flood Basalt Province. Geol Soc Am Spec Pap 497:349–361

Altermann W, Lenhardt N (2012) The volcano-sedimentary succession of the Archean Sodium Group, Ventersdorp Supergroup, South Africa: volcanology, sedimentology and geochemistry. Precamb Res 214-215: 60–81

Amstutz GC (1974) Spilites and Spilitic Rocks. Springer, 426 p

Anh TV, Pang K-N, Chung S-L, Lin H-M, Hoa TT, Anh TT, Yang H-J (2011) The Song Da magmatic suite revisited : a petrologic, geochemical and Sr-Nd isotopic study on picrites, flood basalts and silicic volcanic rocks. J Asian Earth Sci 42 :1341–1355

Arndt NT, Fowler A (2004) Textures in komatiites and variolitic basalts, in Eriksson PG, Altermann W, Nelson DR, Mueller WU, Catuneanu (eds) The Precambrian Earth: Tempos and Events, Elsevier, 298–311

Arndt NT, Lesher CM, Barnes SJ (2008) Komatiite. Cambridge Univ Press, 488 p

Ashwal LD (1993) Anorthosites. Springer-Verlag Berlin, 422 p

Aydin A, DeGraff JM (1988) Evolution of polygonal fracture patterns in lava flows. Science 239:471–476

Bardintzeff, J-M, McBirney AR (2000) Volcanology. 2nd Edn. Jones and Bartlett, 268 p

Barreto CJS, Lima EF, Scherer CM, Rossetti LMM (2014) Lithofacies analysis of basic lava flows of the Paraná igneous province in the south hinge of Torres Syncline, Southern Brazil. J. Volcanol Geotherm Res 285:81–99

Barreto CJS, Lima EF, Goldberg K (2017) Primary vesicles, vesicle-rich segregation structures and recognition of primary and secondary porosities in lava flows from the Paraná igneous province, southern Brazil. Bull Volcanol 79:31, doi: 10.1007/s00445-017-1116-x

Bartels A, Nilsson MKM, Klausen MB, Söderlund U (2016) Meso-Proterozoic dykes in the Timmiarmiit area, southeast Greenland: evidence for a continuous Gardar dyke swarm across Greenland's North Atlantic Craton. GFF 138:255–275

Basaltic Volcanism Study Project (1981) Basaltic Volcanism on the Terrestrial Planets. Pergamon Press, New York, 1286 p

Batiza R, White JDL (2000) Submarine lavas and hyaloclastite, *in* Sigurdsson H, Houghton BF, McNutt SR, Rymer H, Stix J (eds) Encyclopedia of Volcanoes. Academic Press, 361–382

Bédard JH, Rainbird RH (2015) Geology, Iglulik, Victoria Island, Northwest Territories. Geol. Surv. Canada, Can Geosci Map 199 (prelim. ed.) 1:50,000 scale, NTS 87/G08, 1 sheet, doi:10.4095/297283

Bédard JH, Marsh BD, Hersum TG, Naslund HR, Mukasa SB (2007) Large-scale

H. Sheth, *A Photographic Atlas of Flood Basalt Volcanism*, https://doi.org/10.1007/978-3-319-67705-7

mechanical redistribution of orthopyroxene and plagioclase in the Basement Sill, Ferrar Dolerites, McMurdo Dry Valleys, Antarctica: petrological, mineral-chemical and field evidence for channelized movement of crystals and melt. J Petrol 48:2289–2326

Bertrand H (1991) The Mesozoic tholeiitic province of northwest Africa: a volcano-tectonic record of the early opening of Central Atlantic, *in* Kampunzu AB (ed) Magmatism in Extensional Structural Settings, Springer Verlag, 147–188

Bertrand H, Dostal J, Dupuy C (1982) Geochemistry of early Mesozoic tholeiites from Morocco. Earth Planet Sci Lett 58:225–239

Best MG (2003) Igneous and Metamorphic Petrology. 2nd ed. Blackwell Publ, 729 p

Bhat MI (1984) Abor volcanics: further evidence for the birth of the Tethys Ocean in the Himalayan segment. J Geol Soc Lond 141:763–775

Bhat MI, Zainuddin SM, Rais A (1981) Panjal Trap chemistry and the birth of Tethys. Geol Mag 118:367–375

Black BA, Weiss BP, Elkins-Tanton LT, Veselovskiy RV, Latyshev A (2015) Siberian Traps volcaniclastic rocks and the role of magma-water interactions. Geol Soc Am Bull 127:1437–1452

Blackburn TJ, Olsen PE, Bowring SA, McLean NM, Kent DV, Puffer J, McHone G, Rusbury ET, Et-Touhami M (2013) Zircon U–Pb geochronology links the end-Triassic extinction with the Central Atlantic Magmatic Province. Science 340: 941–945

Bondre NR, Hart WK (2008) Morphological and textural diversity of the Steens Basalt lava flows, southeastern Oregon, USA: implications for emplacement style and nature of eruptive episodes. Bull Volcanol 70:999–1019

Bondre NR, Duraiswami RA, Dole G (2004a) Morphology and emplacement of flows from the Deccan volcanic province, India. Bull Volcanol 66:29–45

Bondre NR, Duraiswami RA, Dole G (2004b) A brief comparison of lava flows from the Deccan volcanic province and the Columbia-Oregon Plateau flood basalts: implications for models of flood basalt emplacement, *in* Sheth HC, Pande K (eds) Magmatism in India through Time. Proc Ind Acad Sci (Earth Planet Sci) 113:809–817

Boudreau AE (2016) The Stillwater Complex, Montana – overview and the significance of volatiles. Min Mag 80:585–637

Bourman RP, Ollier CD (2001) A critique of the Schellmann definition and classification of 'laterite'. Catena 47:117–131

Breitkreuz C (2013) Spherulites and lithophysae – 200 years of investigation on high-temperature crystallization domains in silica-rich volcanic rocks. Bull Volcanol 75:705, doi: 10.1007/s00445-013-0705-6

Brooks CK (2011) The East Greenland Rifted Volcanic Margin. Geol Surv Denmark Greenland Bull 24, 96 p

Brown RJ, Blake S, Bondre NR, Phadnis VM, Self S (2011) 'A'ā lava flows in the Deccan volcanic province, India, and their significance for the nature of continental flood basalt eruptions. Bull Volcanol 73:737–752

Brown RJ, Blake S, Thordarson T, Self S (2014) Pyroclastic edifices record vigorous lava fountains during the emplacement of a flood basalt flow field, Roza Member, Columbia River Basalt Province, USA. Geol Soc Am Bull 126:875–891

Brown RJ, Thordarson T, Self S, Blake S (2015) Disruption of tephra fall deposits caused by lava flows during basaltic eruptions. Bull Volcanol 77:90, doi: 10.1007/s00445-015-0974-3

Brueseke ME, Hart WK (2008) Geology and Petrology of the mid-Miocene Santa Rosa – Calico Volcanic Field, northern Nevada. Nevada Bur. Mines Geol. Bull. 113 (online publication http://www.nbmg.unr.edu/dox/dox.htm), 82 p

Bryan SE, Ernst RE (2008) Revised definition of large igneous provinces (LIPs). Earth-Sci Rev 86:175–202

Bryan SE, Ukstins-Peate I, Peate DW, Self S, Jerram DA, Mawby MR, Marsh JS, Miller JA (2010) The largest volcanic eruptions on Earth. Earth-Sci Rev 102:207–229

Bullard FM (1947) Studies on Paricutin volcano, Michoacán, Mexico. Geol Soc Am Bull 58:443–450

Burgess SD, Bowring SA (2015) High-precision geochronology confirms voluminous magmatism before, during and after Earth's most severe extinction. Science Adv 1:e1500470, doi: 10.1126/sciadv.1500470

Callegaro S, Marzoli A, Bertrand H, Blichert-Toft J, Reisberg L, Cavazzini G, Jourdan F, Davies J, Parisio L, Bouchet R, Paul A, Schaltegger U, Chiradia M (2017) Geochemical constraints provided by the Freetown layered complex (Sierra Leone) on the origin of high-Ti tholeiitic CAMP magmas. J Petrol, doi: 10.1093/petrology/egx073

Camp VE, Roobol MJ, Hooper PR (1991) The Arabian continental alkali basalt province: Part II, Evolution of Harrats Kura, Khaybar, and Ithnayn, Kingdom of Saudi Arabia. Geol Soc Am Bull 103:363–391

Camp VE, Ross ME, Duncan RA, Jarboe NA, Coe RS, Hanan BB, Johnson JA (2013) The Steens Basalt: earliest lavas of the Columbia River Basalt Group, *in* Reidel SP, Camp VE, Ross ME, Wolff JA, Martin BS, Tolan TL, Wells RE (eds) The Columbia River Flood Basalt Province. Geol Soc Am Spec Pap 497:87–116

Camp VE, Reidel SP, Ross ME, Brown RJ, Self S (2017) Field-trip Guide to the Vents, Dykes, Stratigraphy, and Structure of the Columbia River Basalt Group, Eastern Oregon and Southeastern Washington. US Geol Surv Sci Invest Rep 2017-5022-N, 88 p, https://doi.org/10.3133/sir20175022N

Cañón-Tapia E (2010) Origin of large igneous provinces: the importance of a definition, *in* Cañón-Tapia E, Szakács A (eds) What is a volcano? Geol Soc Am Spec Pap 470:77–101

Cao J, Wang CY, Xu Y-G, Xing CM, Wei X, Sun YL, Li J (2017) Triggers on sulfide saturation in Fe-Ti oxide-bearing, mafic-ultramafic layered intrusions in the Tarim large igneous province, NW China. Mineral Dep 52: 471–494

Carey RJ, Houghton BF, Thordarson T (2010) Tephra dispersal and eruption dynamics of wet and dry phases of the 1875 eruption of Askja volcano, Iceland. Bull Volcanol 72:259–278

Caroff M, Maury RC, Cotten J, Clément J-P (2000) Segregation structures in vapour-differentiated basaltic flows. Bull Volcanol 62:171–187

Cashman K, Mangan M, Newman S (1994) Surface degassing and modifications to vesicle size distributions in active basalt flows. J Volcanol Geotherm Res 61:45–68

Cawthorn RG (2015) The Bushveld Complex, South Africa, *in* Charlier B, Namur O, Latypov R, Teigner C (eds) Layered Intrusions, Springer, 517–587

Cheng L-L, Yang Z-F, Zeng L, Wang Y, Luo Z-H (2014) Giant plagioclase growth during storage of basaltic magma in Emeishan large igneous province, SW China. Contrib Mineral Petrol 167:971, doi: 10.1007/s00410-014-0971-0

Chevallier L, Woodford A (1999) Morphotectonics and mechanism of emplacement of the dolerite rings and sills of the western Karoo, South Africa. S Afr J Geol 102:43–54

Coffin MF, Eldholm O (1992) Volcanism and continental break-up: a global compilation of large igneous provinces, *in* Storey BC, Alabaster T, Pankhurst RJ (eds) Magmatism and the Causes of Continental Break-up. Geol Soc Lond Spec Publ 68:17–30

Coffin MF, Eldholm O (1993) Scratching the surface: estimating dimensions of large igneous provinces. Geology 21:515–518

Coffin MF, Eldholm O (1994) Large igneous provinces: crustal structure, dimensions, and external consequences. Rev Geophys 32:1–36.

Costa A, Blake S, Self S (2006) Segregation processes in vesiculating crystallizing magmas. J Volcanol Geotherm Res 153:287–300

Cripps JA, Widdowson M, Spicer RA, Jolley DW (2005) Coastal ecosystem responses to late stage Deccan Trap volcanism: the post K/T boundary (Danian) palynofacies of Mumbai (Bombay), west India. Palaeogeogr Palaeoclimatol Palaeoecol 216:303–332

Cucciniello C, Demonterova EI, Sheth H, Pande K, Vijayan A (2015) $^{40}Ar/^{39}Ar$ geochronology and geochemistry of the Central Saurashtra mafic dyke swarm: insights into magmatic evolution, magma transport, and dyke-flow relationships in the northwestern Deccan Traps. Bull Volcanol 77:45, doi: 10.1007/s00445-015-0932-0

Davies JHFL, Heaman LM (2014) New U-Pb baddeleyite and zircon ages for the Scourie dyke swarm: a long-lived large igneous province with implications for the Palaeoproterozoic evolution of NW Scotland. Precamb Res 249:180–198

Davies JHFL, Marzoli A, Bertrand H, Youbi N, Ernesto M, Schaltegger U (2017) End-Triassic mass extinction started by intrusive CAMP activity. Nature Comm 8:15596, doi: 10.1038/ncomms15596

Davis GH, Reynolds SJ (1996) Structural Geology of Rocks and Regions. 2nd ed. John Wiley, 776 p

Deshmukh SS, Nair KKK (eds) (1996) Deccan Basalts. Gondwana Geol Soc (Nagpur) Sp Vol 2, 543 p

Donaldson CH (1982) Spinifex-textured komatiites: a review of textures, mineral compositions, and layering, *in* Arndt NT, Nisbet EG (eds) Komatiites, 211–244. George Allen and Unwin, London

Duraiswami RA, Shaikh TN (2013) Geology of the saucer-shaped sill near Mahad, western Deccan Traps, India, and its significance to the flood basalt model. Bull Volcanol 75:731, doi: 10.1007/s00445-013-0731-4

Duraiswami RA, Bondre NR, Dole G, Phadnis VM, Kale VS (2001) Tumuli and associated features from the western Deccan volcanic province, India. Bull Volcanol 63:435–442

Duraiswami RA, Bondre NR, Dole G, Phadnis VM (2002) Morphology and structure of flow-lobe tumuli from Pune and Dhule areas, western Deccan volcanic province. J Geol Soc Ind 60:57–65

Duraiswami RA, Dole G, Bondre N (2003a) Slabby pāhoehoe from the western Deccan volcanic province: evidence for incipient pāhoehoe-'a'ā transitions. J Volcanol Geotherm Res 121:195–217

Duraiswami RA, Bondre N, Dole G (2003b) Enigmatic spiracle-like structures from a basaltic flow near Chekewadi, western Deccan volcanic province. Current Sci 85:1267–1269

Duraiswami RA, Bondre NR, Dole G (2004) Possible lava tube system in a hummocky lava flow at Daund, western Deccan volcanic province, India, *in* Sheth HC, Pande K (eds) Magmatism in India through Time. Proc Ind Acad Sci (Earth Planet Sci) 113:819–830

Duraiswami RA, Bondre NR, Managave S (2008) Morphology of rubbly pāhoehoe (simple) flows from the Deccan volcanic province: implications for style of emplacement. J Volcanol Geotherm Res 177:822–836

Duraiswami RA, Gadpallu P, Shaikh TN, Cardin N (2014) Pāhoehoe-'a'ā transitions in the lava flow fields of the western Deccan Traps, India – implications for emplacement dynamics, flood basalt architecture and volcanic stratigraphy, *in* Sheth HC, Vanderkluysen L (eds) Flood Basalts of Asia. J Asian Earth Sci 84:146–166

Duraiswami RA, Inamdar MM, Shaikh TN (2016) Emplacement of pillow lavas from the ~2.8 Ga Chitradurga greenstone belt, south India: a physical volcanological, morphometric and geochemical perspective. J Volcanol Geotherm Res 264:134–149

Dutton CE (1883) Hawaiian Volcanoes, 2005 ed. Univ Hawaii Press, Honolulu, 235 p

El Ghilani S, Youbi N, Madeira J, Chellai EH, López-Galindo A, Martins L, Mata J (2017) Environmental implication of subaqueous lava flows from a continental large igneous province: examples from the Moroccan Central Atlantic Magmatic Province (CAMP). J Afr Earth Sci 127:211–221

El Hachimi H, Youbi N, Madeira J, Bensalah MK, Martins L, Mata J, Medina P, Bertrand H, Marzoli A, Munhá J, Bellieni G, Mahmoudi A, Ben Abbou M, Assafar H (2011) Morphology, internal architecture and emplacement mechanisms of lava flows from the Central Atlantic Magmatic Province (CAMP) of Argana Basin (Morocco), *in* Van Hinsbergen DJJ, Buiter SJH, Torsvik TH, Gaina C, Webb CJ (eds) The Formation and Evolution of Africa: A Synopsis of 3.8 Ga of Earth History. Geol Soc Lond Spec Publ 357:167–193

Elliot DH, Fleming TH (2004) Occurrence and dispersal of magmas in the Jurassic Ferrar large igneous province, Antarctica. Gondwana Res 7:223–237

Elliot DH, Fleming TH (2008) Physical volcanology and geological relationships of the Jurassic Ferrar large igneous province, Antarctica. J Volcanol Geotherm Res 172:20–37

Elliot DH, Siders MA, Haban MA (1986) Jurassic tholeiites in the region of the upper Rennick glacier, North Victoria Land, *in* Stump E (ed) Geological Investigations in Northern Victoria Land. Antarctic Resarch Series, Am Geophys Union 46:249–265

Emeleus CH, Bell BR (2005) The Palaeogene Volcanic Districts of Scotland. 4th Edn. British Geol Surv, Nottingham, 212 p

Ernst RE (2014) Large Igneous Provinces. Cambridge Univ. Press, 653 p

Ernst RE, Jowitt SM (2013) Large Igneous Provinces (LIPs) and metallogeny, *in* Soc Econ Geol Spec Publ 17:17–51

Ernst RE, Youbi N (2017) How large igneous provinces affect global climate, sometimes cause mass extinctions, and represent natural markers in the geological record. Palaeogeogr, Palaeoclimatol, Palaeoecol 478:30–52

Ernst RE, Head JW, Parfitt E, Grosfils E, Wilson L (1995) Giant radiating dyke swarms on Earth and Venus. Earth-Sci Rev 39:1–58

Ernst RE, Grosfils EB, Mege D (2001) Giant dyke swarms on Earth, Venus, and Mars. Ann Rev Earth Planet Sci 29:489–534

Fagents SA, Thordarson T (2007) Rootless volcanic cones in Iceland and on Mars, *in* Chapman M (ed) The Geology of Mars: Evidence from Earth-based Analogs, Cambridge Univ Press, 151–177

Farooqui MY, Hou H, Li G, Machin N, Neville T, Pal A, Shrivastava C, Wang Y, Yang F, Yin C, Zhao J, Yang X (2009) Evaluating volcanic reservoirs. Oilfield Review (Schlumberger) 21:36–47

Faust GT (1975) A Review and Interpretation of the Geologic Setting of the Watchung Basalt Flows, New Jersey. US Geol Surv Prof Pap 864-A, 42 p

Ferrari L, Conticelli S, Vaggelli G, Petrone CM, Manetti P (2000) Late Miocene volcanism and intra-arc tectonics during the early development of the Trans-Mexican Volcanic Belt. Tectonophysics 318:161–185

Fink JH, Fletcher RC (1978) Ropy pāhoehoe: surface folding of a viscous fluid. J Volcanol Geotherm Res 4:151–170

Fitton JG, Mahoney JJ, Wallace PJ, Saunders AD (eds) (2004) Origin and Evolution of the Ontong Java Plateau. Geol. Soc. Lond. Spec. Publ. 229, 369 p

Foulger GR, Jurdy DM (eds) (2007) Plates, Plumes, and Planetary Processes. Geol Soc Am Spec Pap 430, 974 p

Foulger GR, Natland JH, Presnall DC, Anderson DL (eds) (2005) Plates, Plumes, and Paradigms. Geol Soc Am Spec Pap 388, 861 p

Garland FE, Hawkesworth CJ, Mantovani MSM (1995) Description and petrogenesis of the Paraná rhyolites. J Petrol 36:1193–1227

Ghose NC, Kent RW, Saunders AD (eds) (1996) Mesozoic Magmatism of the Eastern Margin of India. J Asian Earth Sci 13:75–158

Gilg HA, Morteani G, Kostitsyn Y, Preinfalk C, Gatter I, Strieder AJ (2003) Genesis of amethyst geodes in basaltic rocks of the Serra Geral Formation (Ametista do Sul, Rio Grande do Sul, Brazil): a fluid inclusion, REE, oxygen, carbon, and Sr isotope study on basalt, quartz, and calcite. Mineral Dep 38:1009–1025

Godchaux MM, Bonnichsen B (2002) Syneruptive magma-water and posteruptive lava-water interactions in the western Snake River Plain, Idaho, during the past 12 million years, *in* Bonnichsen B, White CM, McCurry M (eds) Tectonic and Magmatic Evolution of the Snake River Plain Volcanic Province. Idaho Geol Surv Bull 30:387–434

Godinot A (1988) Comment on "Pipe vesicles in Hawaiian basaltic lavas: their origin and potential as palaeoslope indicators". Geology 16:90

Goff F (1996) Vesicle cylinders in vapour-differentiated basalt flows. J Volcanol Geotherm Res 71:167–185

Götze J (2011) Agate – Fascination between legend and science, in Zenz J (ed) Agates III, 19–133. Bode Verlag, Lauenstein, Germany

Greeley R, Fagents SA (2001) Icelandic pseudocraters as analogs to some volcanic cones on Mars. J Geophys Res 106:20527–20546

Grossenbacher KA, McDuffie SM (1995) Conductive cooling of lava: columnar joint diameter and stria width as functions of cooling rate and thermal gradient. J Volcanol Geotherm Res 69:95–103

Gudmundsson A (2005) Effects of mechanical layering on the development of normal faults and dykes in Iceland. Geodin Acta 18:11–30

Guilbaud M-N, Self S, Thordarson T, Blake S (2005) Morphology, surface structures, and emplacement of lavas produced by Laki, A.D. 1783-84, *in* Manga M, Ventura G (eds) Kinematics and Dynamics of Lava Flows. Geol Soc Am Spec Pap 396, 81–102

Gumsley AP, Chamberlain KR, Bleeker W, Söderlund U, de Kock MO, Larsson ER, Bekker A (2017) Timing and tempo of the Great Oxidation Event. Proc Nat Acad Sci 114:1811–1816

Gunn BM (1966) Modal and element variation in Antarctic tholeiites. Geochim Cosmochim Acta 30: 881–920

Gunnell Y, Radhakrishna BP (eds) (2001) Sahyadri: The Great Escarpment of the Indian Subcontinent. Geol Soc Ind Mem 47(1-2), 1054 p

Halls HC (1982) The importance and potential of mafic dyke swarms in studies of geodynamic processes. Geosci Can 9:145–154

Halls HC, Hamilton MA, Denyszyn SW (2011) The Melville Bugt dyke swarm of Greenland: a connection to the 1.5-1.6 Ga Fennoscandian rapakivi granite province?, *in* Srivastava RK

(ed) Dyke Swarms: Keys for Geodynamic Interpretation. Springer 509–535

Hames WE, McHone JG, Renne PR, Ruppel C (eds) (2003) The Central Atlantic Magmatic Province: Insights from Fragments of Pangaea. Am Geophys Union Geophys Monogr 136, 267 p

Hamilton WB (1965) Diabase Sheets of the Taylor Glacier Region, Victoria Land, Antarctica. US Geol Surv Prof Pap 456-B, 71 p

Harris AJL, Rowland SK, Villeneuve N, Thordarson T (2017) Pāhoehoe, 'a'ā, and block lava: an illustrated history of the nomenclature. Bull Volcanol 79:7, doi: 10.1007/s00445-016-1075-7

Hazlett RW, Hyndman DW (1996) Roadside Geology of Hawaii. Mountain Press Publ Co (Missoula, Montana), 304 p

Head JW, Coffin MF (1997) Large igneous provinces: a planetary perspective, *in* Mahoney JJ, Coffin MF (eds) Large Igneous Provinces: Continental, Oceanic, and Planetary Flood Volcanism. Am Geophys Union Geophys Monogr 100:411–438

Higgins MD, Chandrasekharam D (2007) Nature of sub-volcanic magma chambers, Deccan province, India: evidence from quantitative textural analysis of plagioclase megacrysts in the giant plagioclase basalts. J Petrol 48:885–900

Hill PA (1965) Curviplanar (radial, bow-tie, festoon) and concentric jointing in Jurassic dolerite, Mersey Bluff, Tasmania. J Geol 73:255–270

Hoang N, Flower M (1998) Petrogenesis of Cenozoic basalts from Vietnam: implication for origins of a 'Diffuse Igneous Province'. J Petrol 39:369–395

Hooper PR (1997) The Columbia River flood basalt province: current status, *in* Mahoney JJ, Coffin MF (eds) Large Igneous Provinces: Continental, Oceanic, and Planetary Flood Volcanism. Am Geophys Union Geophys Monogr 100: 1–28

Hooper PR, Subbarao KV, Beane JE (1988) The giant plagioclase basalts (GPBs) of the Western Ghats, Deccan Traps, *in* Subbarao KV (ed) Deccan Flood Basalts. Geol Soc Ind Mem 10:135–144

Ivanov AV, He H, Yan L, Ryabov V, Shevko A, Palesskii SV, Nikolaeva IV (2013) Siberian Traps large igneous province: evidence for two flood basalt pulses around the Permo-Triassic boundary and in the Middle Triassic, and contemporaneous granitic magmatism. Earth-Sci Rev 122:58–76

Ivanov AV, Meffre S, Thompson J, Corfu F, Kamenetsky VS, Kamenetsky MB, Demonterova EI (2017) Timing and genesis of the Karoo-Ferrar large igneous province: new high precision U-Pb data for Tasmania confirm short duration of the major magmatic pulse. Chem Geol 455:32–43

Jarosch A, Gudmundsson T, Högnadóttir T, Axelsson G (2008) Progressive cooling of the hyaloclastite ridge at Gjálp, Iceland, 1996-2005. J Volcanol Geotherm Res 170:218–229

Jayananda M, Kano T, Peucat J-J, Channabasappa S (2008) 3.35 Ga komatiite volcanism in the Western Dharwar craton, southern India: constraints from Nd isotopes and whole rock geochemistry. Precamb Res 162:160–179

Jayananda M, Duraiswami RA, Aadhiseshan KR, Gireesh RV, Prabhakar BC, Kafo K-u, Tushipokla, Namratha R (2016) Physical volcanology and geochemistry of Palaeoarchaean komatiite lava flows from the Western Dharwar craton, southern India: implications for Archaean mantle evolution and crustal growth. Int Geol Rev 58:1569–1595

Jerram DA, Stollhofen H (2002) Lava-sediment interaction in desert settings; are all peperite-like textures the result of magma-water interaction? J Volcanol Geotherm Res 114:231–249

Jones JG (1969) Intraglacial volcanoes of the Laugarvatn region, south-west Iceland I. Quart J Geol Soc Lond 124:197–211

Kale VS (2010) The Western Ghat: The Great Escarpment of India, *in* Migon P (ed) Geomorphological Landscapes of the World, Springer, 257–264

Kapadia H (2003) Trek the Sahyadris. 5th Edn. Indus Publ Co, New Delhi, 176 p

Karmarkar BM, Kulkarni SR, Marathe SS, Sowani PV, Peshwa VV (1971) Giant phenocryst basalts in the Deccan Trap. Bull Volcanol 35:965–974

Kearey P (1996) The New Penguin Dictionary of Geology. Penguin, 366 p

Kerr AC, White RV, Saunders AD (2000) LIP reading: recognizing oceanic plateaux in the geological record. J Petrol 41:1041–1056

Keszthelyi LP, Jaeger WL (2015) A field investigation of the basaltic ring structures of

the Channeled Scabland and the relevance to Mars. Geomorphology 240:34–43

Keszthelyi L, Thordarson T (2000) Rubbly pāhoehoe: a previously undescribed but widespread lava type transitional between ‘a’ā and pāhoehoe. Geol Soc Am Abstr Progr 32, 7

Keszthelyi L, Self S, Thordarson T (1999) Application of recent studies on the emplacement of basaltic lava flows to the Deccan Traps, *in* Subbarao KV (ed) Deccan Volcanic Province. Geol Soc Ind Mem 43(1):485–520

Kilburn CRJ (2000) Lava flows and flow fields, *in* Sigurdsson H, Houghton BF, McNutt SR, Rymer H, Stix J (eds) Encyclopedia of Volcanoes. Academic Press, 291–306

Klausen MB (2004) Geometry and mode of emplacement of the Thverartindur cone sheet swarm, SE Iceland. J Volcanol Geotherm Res 138:18–204

Klausen MB (2006) Geometry and mode of emplacement of dyke swarms around the Birnudalstindur igneous centre, SE Iceland. J Volcanol Geotherm Res 151:340–356

Klausen MB, Larsen HC (2002) The East Greenland coast-parallel dyke swarm and its role in continental breakup, *in* Menzies MA, Klemperer SL, Ebinger CJ, Baker J (eds) Volcanic Rifted Margins. Geol Soc Am Spec Pap 362:133–158

Klausen MB, Nilsson M, Bartels A (2016a) Post-orogenic Proterozoic dyke swarms, *in* Kolb J, Stensgaard BM, Kokfelt TF (eds) Geology and Mineral Potential of South-East Greenland. GEUS Rep 2016/38, 75–83

Klausen MB, Nilsson M, Bothma R (2016b) Palaeoproterozoic dykes, *in* Kolb J, Stensgaard BM, Kokfelt TF (eds) Geology and Mineral Potential of South-East Greenland. GEUS Rep 2016/38, 41–53

Krauskopf KB (1948) Lava movement at Parícutin volcano, Mexico. Geol Soc Am Bull 59:1267–1283

Kristjánsdóttir H (2015) Sustainable Energy Resources and Economics in Iceland and Greenland. Springer (SpringerBriefs in Energy), 79 p

Kshirsagar PV, Sheth HC, Shaikh B (2011) Mafic alkalic magmatism in central Kachchh, India: a monogenetic volcanic field in the northwestern Deccan Traps. Bull Volcanol 73:595–612

Kshirsagar PV, Sheth HC, Seaman SJ, Shaikh B, Mohite P, Gurav T, Chandrasekharam D (2012) Spherulites and thundereggs from pitchstones of the Deccan Traps: geology, petrochemistry, and emplacement environments. Bull Volcanol 74:559–577

Larsen LM, Pedersen AK (2009) Petrology of the Paleocene picrites and flood basalts on Disko and Nuussuaq, West Greenland. J Petrol 50:1667–1711

Larsen LM, Watt WS, Watt M (1989) Geology and Petrology of the Lower Tertiary Plateau Basalts of the Scoresby Sund region, East Greenland. Bull Grønlands Geologiske Undersøgelse 157, 164 p

Lebedev VA, Bubnov SN, Dudauri OZ, Vashakidze GT (2008) Geochronology of Pliocene volcanism in the Dzhavakheti highland (the Lesser Caucasus) Part 1: Western part of the Dzhavakheti highland. Stratigr Geol Correl 16:204–224

Lenhardt N, Eriksson PG, Catuneanu O, Bumby AJ (2012) Nature of and controls on volcanism in the ca. 2.32-2.06 Ga Pretoria group, Transvaal Supergroup, Kaapvaal Craton, South Africa. Precamb Res 214-215:106–123

Lewis JV (1915) The pillow lavas of the Watchung Mountains. New Jersey Geol Surv Bull 16:51–56

Liégeois J-P, Benhallou A, Azzouni-Sekkal A, Yahiaoui R, Bonin B (2005) The Hoggar swell and volcanism: Reactivation of the Precambrian Tuareg shield during Alpine convergence and West African Cenozoic volcanism, *in* Foulger GR, Natland JH, Presnall DC, Anderson DL (eds) Plates, Plumes and Paradigms. Geol Soc Am Spec Pap 388:379–400

Lightfoot PC, Hawkesworth CJ (1997) Flood basalts and magmatic Ni, Cu, and PGE sulphide mineralization: comparative geochemistry of the Noril’sk (Siberian Traps) and West Greenland sequences, *in* Mahoney JJ Coffin MF (eds) Large Igneous Provinces: Continental, Oceanic, and Planetary Flood Volcanism. Am Geophys Union Geophys Monogr 100:357–380

Lipman (2000) Calderas, *in* Sigurdsson H, Houghton BF, McNutt SR, Rymer H, Stix J (eds) Encyclopedia of Volcanoes. Academic Press, 643–662

Lite Jr KE (2013) The influence of depositional environment and landscape evolution on groundwater flow in Columbia River basalt – examples from Mosier, Oregon, *in* Reidel SP, Camp

VE, Ross ME, Wolff JA, Martin BS, Tolan TL, Wells RE (eds) The Columbia River Flood Basalt Province. Geol Soc Am Spec Pap 497: 429–440

Lockwood JP, Hazlett RW (2010) Volcanoes: Global Perspectives. Wiley-Blackwell, 541 p

Lofgren G (1971) Spherulitic textures in glassy and crystalline rocks. J Geophys Res 76:5635–5648

Long PE, Wood BJ (1986) Structures, textures, and cooling histories of Columbia River basalt flows. Geol Soc Am Bull 97:1144–1155

Lyle P (2000) The eruption environment of multi-tiered columnar basalt lava flows. J Geol Soc Lond 157:715–722

Lyle P, Preston J (1993) Geochemistry and volcanology of the Tertiary basalts of the Giant's Causeway area, Northern Ireland. J Geol Soc Lond 150:109–120

Macdonald GA (1953) Pāhoehoe, 'a'ā, and block lava. Am J Sci 251:169–191

Macdougall JD (ed) (1988) Continental Flood Basalts. Kluwer Acad Publ, Dordrecht, 341 p

Mahoney JJ, Coffin MF (eds) (1997) Large Igneous Provinces: Continental, Oceanic, and Planetary Flood Volcanism. Am Geophys Union Geophys Monogr 100, 438 p

Maloof AC, Stewart ST, Weiss BP, Soule SA, Swanson-Hysell NL, Louzada KL, Garrick-Bethell I, Poussart PM (2010) Geology of Lonar Crater, India. Geol Soc Am Bull 122:109–126

Mangan MT, Marsh BD, Froelich AJ, Gottfried D (1993) Emplacement and differentiation of the York Haven diabase sheet, Pennsylvania. J Petrol 34 :1271–1302

Marsh BD (2004) A magmatic mush column rosetta stone: the McMurdo Dry Valleys of Antarctica. Eos, Trans Am Geophys Union 85:497–502

Marshall RR (1961) Devitrification of natural glass. Geol Soc Am Bull 72:1493–1520

Martins LT, Madeira J, Youbi N, Mata J, Munhá JM, Kerrich R (2008) Rift-related CAMP magmatism in Algarve (South Portugal). Lithos 101:102–124

Marzoli A, Bertrand H, Knight K, Cirilli S, Buratti N, Verati C, Nomade S, Renne PR, Youbi N, Martini R, Allenbach K, Neuwerth R, Rapaille C, Zaninetti L, Bellieni G (2004) Synchrony of the Central Atlantic magmatic province and the Triassic-Jurassic boundary climatic and biotic crisis. Geology 32:973–976

Mathur KK, Dubey VS, Sharma NL (1926) Magmatic differentiation in Mount Girnar. J Geol 34:289–307

Matthews WH (1947) "Tuyas", flat-topped volcanoes in northern British Columbia. Am J Sci 245:560–570

Mattsson H., Höskuldsson A (2003) Geology of the Heimaey volcanic centre, south Iceland: early evolution of a central volcano in a propagating rift? J Volcanol Geotherm Res 127:55–71

Maya JM, Bhutani R, Balakrishnan S, Sandhya SR (2017) Petrogenesis of 3.15 Ga old Banasandra komatiites from the Dharwar craton, India: implications for early mantle heterogeneity. Geosci Front 8:467–481

McHone JG (1992) Mafic dyke suites within Mesozoic igneous provinces of New England and Atlantic Canada, *in* Puffer JH, Ragland PC (eds), Eastern North American Mesozoic Magmatism. Geol Soc Am Spec Pap 268:1–11

Melluso L, Cucciniello C, Petrone CM, Lustrino M, Morra V, Tiepolo M, Vasconcelos L (2008) Petrology of Karoo volcanic rocks in the southern Lebombo monocline, Mozambique. J Afr Earth Sci 52:130–151

Melluso L, Sheth HC, Mahoney JJ, Morra V, Petrone CM, Storey M (2009) Geochemical correlations between silicic volcanic rocks of the St. Mary's Islands (southwestern India) and eastern Madagascar: a tool for India-Madagascar reconstructions for the Late Cretaceous. J Geol Soc Lond 166:283–294

Misra KS (1999) Deccan volcanics in Saurashtra and Kutch, Gujarat, India, *in* Subbarao KV (ed) Deccan Volcanic Province. Geol Soc Ind Mem 43(1):325–334

Misra KS (2002) Arterial system of lava tubes and channels in Deccan volcanics of western India. J Geol Soc Ind 59:115–124

Moraes LC, Seer HJ (2017) Pillow lavas and fluvio-lacustrine deposits in the northeast of Paraná continental magmatic province, Brazil. J Volcanol Geotherm Res, in press, doi: 10.1016/j.jvolgeores.2017.03.024

Mori L, Gomez-Tuena A, Schaaf P, Goldstein SL, Perez-Arvizu O, Solis-Pichardo G (2009) Lithospheric removal as a trigger for flood basalt magmatism in the Trans-Mexican Volcanic Belt. J Petrol 50:2157–2186

Moufti MR, Németh K (2016) Geoheritage of Volcanic Harrats in Saudi Arabia. Springer, 194 p

Muirhead DK, Bowden SA, Parnell J, Schofield N (2017) Source rock maturation owing to igneous intrusion in rifted margin petroleum systems. J Geol Soc Lond, in press, doi: https://doi.org/10.1144/jgs2017-011

Muirhead JD, Airoldi G, White JDL, Rowland JV (2014) Cracking the lid: sill-fed dykes are the likely feeders of flood basalt eruptions. Earth Planet Sci Lett 406:187–197

Murcia H, Németh K, Moufti MR, Lindsay JM, El-Masry N, Cronin SJ, Qaddah A, Smith IEM (2014) Late Holocene lava flow morphotypes of northern Harrat Rahat, Kingdom of Saudi Arabia: implications for the description of continental lava fields, *in* Sheth HC, Vanderkluysen L (eds) Flood Basalts of Asia. J Asian Earth Sci 84:131–145

Neal CR, Sager WW, Sano T, Erba E (eds) (2015) The Origin, Evolution, and Environmental Impact of Oceanic Large Igneous Provinces. Geol Soc Am Spec Pap 511, 339 p

Németh K (2004) The morphology and origin of wide craters at Al Haruj al Abyad, Libya: maars and phreatomagmatism in a large intracontinental flood lava field? Z Geomorph 48:417–439

Németh K, Martin U (2007) Practical Volcanology. Geol Inst Hungary, Budapest, 221 p

Németh K, Suwesi SK, Peregi Z, Gulacsi Z, Ujszaszi J (2003) Plio/Pleistocene flood basalt related scoria and spatter cones, rootless lava flows, and pit craters, Al Haruj al Abyad, Libya. GeoLines 15:98–103

Németh K, Martin U, Haller MJ, Alric VI (2007) Cenozoic diatreme field in Chubut (Argentina) as evidence of phreatomagmatic volcanism accompanied with extensive Patagonian plateau basalt volcanism? Episodes 30:217–223

Nichols RL (1936) Flow-units in basalt. J Geol 44:617–630

Nichols RL (1939) Squeeze-ups. J Geol 47:421–425

Nielsen TFD (1978) Dyke swarms of the Kangerdlugssuaq area, East Greenland and their bearing on the opening of the North Atlantic in Tertiary. Contrib Mineral Petrol 67:63–78

Nielsen TFD, Brooks CK (1981) The E Greenland rifted continental margin: an examination of the coastal flexure. J Geol Soc Lond 138:559–568

Nielsen TFD, Soper NJ, Brooks CK, Faller AM, Higgins AC, Matthews DW (1981) The pre-basaltic sediments and the Lower Basalts at Kangerdlugssuaq, East Greenland: their stratigraphy, lithology, palaeomagnetism and petrology. Meddelelser om Grønland, Geosci 6, 28 p

Nilsson MKM, Klausen MB, Soderlund U, Ernst RE (2013) Precise U-Pb ages and geochemistry of Palaeoproterozoic mafic dykes from southern West Greenland: linking the North Atlantic and the Dharwar cratons. Lithos 174:255–270

Noguchi R, Höskuldsson A, Kurita K (2016) Detailed topographical, distributional, and material analyses of rootless cones in Mývatn, Iceland. J Volcanol Geotherm Res 318:89–102

Ollier CD (1991) Laterite profiles, ferricrete and landscape evolution. Zeit Geomorph NF 35:165–173

Ollier CD, Pain CF (1996) Regolith, Soils and Landforms. John Wiley & Sons, 316 p

Ollier CD, Powar KB (1985) The Western Ghats and the morphotectonics of peninsular India. Zeit Geomorph Suppl NF 54:57–69

Ollier CD, Sheth HC (2008) The High Deccan duricrusts of India and their significance for the 'laterite' issue. J Earth Syst Sci 117:537–551

Ottens B (2003) Indian Zeolites and Related Species: Minerals of the Deccan Traps, India. The Min Record 34: 4–82

Ottens B (2011) Indien: Mineralien-Fundorte-Lagerstätten. TU Bergakademie Freiberg – Christian Weise Verlag, 384 p (in German)

Pacheco FERC, Caxito FA, Moraes LC, Marangoni YR, Santos RPZ (2017) Basaltic ring structures of the Serra Geral Formation at the southern Triângulo Mineiro, Água Vermelha region, Brazil. J Volcanol Geotherm Res, in press, doi: 10.1016/j.jvolgeores.2017.06.019

Pande K, Sheth HC, Bhutani R (2001) ^{40}Ar-^{39}Ar age of the St. Mary's Islands volcanics, southern India: record of India-Madagascar breakup on the Indian subcontinent. Earth Planet Sci Lett 193:39–46

Pande K, Cucciniello C, Sheth H, Vijayan A, Sharma KK, Purohit R, Jagadeesan KC, Shinde S (2017a) Polychronous (Early Cretaceous to Palaeogene) emplacement of the Mundwara alkaline complex, Rajasthan, India: ^{40}Ar/^{39}Ar geochronology, petrochemistry and geodynamics. Int J Earth Sci (Geol Rund) 106:1487–1504

Pande K, Yatheesh V, Sheth H (2017b) ^{40}Ar/^{39}Ar dating of the Mumbai tholeiites and Panvel

flexure: intense 62.5 Ma onshore-offshore Deccan magmatism during India-Laxmi Ridge-Seychelles breakup. Geophys J Int 210:1160–1170

Pawar NJ, Das S, Duraiswami RA (2012) Hydrogeology of Deccan Traps and Associated Formations in Peninsular India. Geol Soc Ind Mem 80, 202 p

Pebane M, Latypov R (2017) The significance of magmatic erosion for bifurcation of UG1 chromitite layers in the Bushveld Complex. Ore Geol Rev 90:65–93

Pedersen AK (1985) Reaction between picrite magma and continental crust: early Tertiary silicic basalts and magnesian andesites from Disko, West Greenland. Bull Grønlands Geologiske Undersøgelse 152, 126 p

Pedersen AK, Larsen LM, Dueholm KS (1993) Geological section along the south coast of Nuussuaq, central West Greenland. 1:20000 Coloured Geological Sheet. Geol Surv Greenland, Copenhagen

Peng P (2010) Reconstruction and interpretation of giant mafic dyke swarms : a case study of 1.78 Ga magmatism in the North China craton, *in* Kusky T, Zhai M-G, Xiao W (eds) The Evolving Continents: Understanding Processes of Continental Growth. Geol Soc Lond Spec Publ 338:163–178

Peng P, Bleeker W, Ernst RE, Soderlund U, McNicoll V (2011) U-Pb baddelyeite ages, distribution and geochemistry of 925 Ma mafic dykes and 900 Ma sills in the North China craton: evidence for a Neoproterozoic mantle plume. Lithos 127:210–221

Peterson GL, Hawkins Jr JW (1971) Inclined pipe vesicles as indicators of flow direction in basalts: a critical appraisal. Bull Volcanol 35:369–382

Philpotts AR, Lewis CL (1987) Pipe vesicles – an alternate model for their origin. Geology 15:971–974

Philpotts AR, Martello A (1986) Diabase feeder dykes for the Mesozoic basalts in southern New England. Am J Sci 286:105–126

Philpotts AR, Carroll M, Hill JM (1996) Crystal-mush compaction and the origin of pegmatitic segregation sheets in a thick flood-basalt flow in the Mesozoic Hartford Basin, Connecticut. J Petrol 37:811–836

Polteau S, Mazzini A, Galland O, Planke S, Malthe-Sørensen A (2008) Saucer-shaped intrusions: occurrences, emplacement and implications. Earth Planet Sci Lett 266:195–204

Prabhakar BC, Namratha R (2014) Morphology and textures of komatiite flows of J. C. Pura schist belt, Dharwar craton. J Geol Soc Ind 83:13–20

Price EH, Watkinson AJ (1989) Structural geometry and strain distribution within eastern Umtanum fold ridge, south-central Washington, *in* Reidel SP, Hooper PR (eds) Volcanism and Tectonism in the Columbia River Flood-Basalt Province. Geol Soc Am Spec Pap 239:265–282

Puffer JH, Student JJ (1992) Volcanic structures, eruptive style, and posteruptive deformation and chemical alteration of the Watchung flood basalts, New Jersey, *in* Puffer JH, Ragland PC (eds) Eastern North American Mesozoic Magmatism. Geol Soc Am Spec Pap 268:261–278

Puffer JH, Laskowich C (2012) Volcanic diapirs in the Orange Mountain flood basalt: New Jersey, USA. J Volcanol Geotherm Res 237-238:1–9

Puffer JH, Ragland PC (eds) (1992) Eastern North American Mesozoic Magmatism. Geol Soc Am Spec Pap 268, 398 p

Puffer JH, Block KA, Steiner JC (2009) Transmission of flood basalts through a shallow crustal sill and the correlation of sill layers with extrusive flows: the Palisades intrusive system and the basalts of the Newark Basin, New Jersey, USA. J Geol 117:139–155

Rainbird RH, Bédard JH, Williamson N (2013) Geology, Takiyuaqattak, Victoria Island, Northwest Territories. Geol Surv Canada, Canad Geosci Map (prelim. ed.), 1:50,000 scale, NTS 87/H4, 1 sheet, doi:10.4095/293344

Rampino MR, Stothers RB (1988) Flood basalt volcanism during the past 250 million years. Science 241:663–668

Rawlings DJ, Watkeys MK, Sweeney RJ (1999) Peperitic upper margin of an invasive flow, Karoo flood basalt province, northern Lebombo. S Afr J Geol 102:277–383

Ray R, Sheth HC, Mallik J (2007) Structure and emplacement of the Nandurbar-Dhule mafic dyke swarm, Deccan Traps, and the tectonomagmatic evolution of flood basalts. Bull Volcanol 69:537–551

Ray R, Shukla AD, Sheth HC, Ray JS, Duraiswami RA, Vanderkluysen L, Rautela CM, Mallik J (2008) Highly heterogeneous Precambrian

basement under the central Deccan Traps, India: direct evidence from xenoliths in dykes. Gondwana Res 13:275–285

Reidel SP (2006) Big Black Boring Rock: Essays on Northwest Geology. Battelle Press, Columbus (Ohio), 142 p

Reidel SP, Hooper PR (eds) (1989) Volcanism and Tectonism in the Columbia River Flood Basalt Province. Geol Soc Am Spec Pap 239, 379 p

Reidel SP, Tolan TL (1992) Eruption and emplacement of flood basalt: an example from the large-volume Teepee Butte Member, Columbia River Basalt Group. Geol Soc Am Bull 104:1650–1671

Reidel SP, Spane FA, Johnson VG (2002) Natural Gas Storage in Basalt Aquifers of the Columbia Basin, Pacific Northwest USA: A Guide to Site Characterization. Pacific Northwest National Laboratory Report PNNL-13962, Richland (Washington), 50 p

Reidel SP, Martin BS, Petcovic HL (2003) The Columbia River flood basalts and the Yakima fold belt, in Swanson DW (ed) Western Cordillera and Adjacent Areas. Geol Soc Am Field Guide 4:87–105

Reidel SP, Camp VE, Ross ME, Wolff JA, Martin BS, Tolan TL, Wells RE (eds) (2013a) The Columbia River Flood Basalt Province. Geol Soc Am Spec Pap 497, 440 p

Reidel SP, Camp VE, Tolan TL, Martin BS (2013b) The Columbia River flood basalt province: stratigraphy, areal extent, volume, and physical volcanology, *in* Reidel SP, Camp VE, Ross ME, Wolff JA, Martin BS, Tolan TL, Wells RE (eds) The Columbia River Flood Basalt Province. Geol Soc Am Spec Pap 497:1–43

Reidel SP, Camp VE, Tolan TL, Kauffman JD, Garwood DL (2013c) Tectonic evolution of the Columbia River flood basalt province, *in* Reidel SP, Camp VE, Ross ME, Wolff JA, Martin BS, Tolan TL, Wells RE (eds) The Columbia River Flood Basalt Province. Geol Soc Am Spec Pap 497:293–324

Reynolds P, Brown RJ, Thordarson T, Llewellin EW, Fielding K (2015) Rootless cone eruption processes informed by dissected tephra deposits and conduits. Bull Volcanol 77:72, doi: 10.1007/s00445-015-0958-3

Reynolds P, Brown RJ, Thordarson T, Llewellin EW (2016) The architecture and shallow conduits of Laki-type pyroclastic cones: insights into a basaltic fissure eruption. Bull Volcanol 78:36, doi: 10.1007/s00445-016-1029-0

Ross P-S, White JDL (2005) Mafic, large-volume, pyroclastic density current deposits from phreatomagmatic eruptions in the Ferrar large igneous province, Antarctica. J Geol 113:627–649

Ross P-S, White JDL (2006) Debris jets in continental phreatomagmatic volcanoes: a field study of their subterranean deposits in the Coombs Hills vent complex, Antarctica. J Volcanol Geotherm Res 149:62–84

Ross P-S, Ukstins-Peate I, McClintock MK, Xu Y-G, Skilling IP, White JDL, Houghton BF (2005) Mafic volcaniclastic deposits in flood basalt provinces: a review. J Volcanol Geotherm Res 145:281–314

Rossetti L, Lima EF, Waichel BL, Hole MJ, Simões MS, Scherer CMS (2017) Lithostratigraphy and volcanology of the Serra Geral Group, Parana-Etendeka igneous province in southern Brazil: towards a formal stratigraphical framework. J Volcanol Geotherm Res, in press, doi: 10.1016/j.jvolgeores.2017.05.008

Rossi MJ, Gudmundsson A (1996) The morphology and formation of flow-lobe tumuli on Icelandic shield volcanoes. J Volcanol Geotherm Res 72:291–308

Rougier S, Missenard Y, Gautheron C, Barbarand J, Zeyen H, Pinna R, Liégeois J-P, Bonin B, Ouabadi A, Derder MEM, Frizon de Lamotte D (2013) Eocene exhumation of the Tuareg Shield (Sahara, Africa). Geology 41:615–618

Rowland SK, Walker GPL (1987) Toothpaste lava: characteristics and origin of a lava structural type transitional between pāhoehoe and ‘a’ā. Bull Volcanol 49:631–641

Rowland SK, Walker GPL (1990) Pāhoehoe and ‘a’ā in Hawaii: volumetric flow rate controls the lava structure. Bull Volcanol 52:615–628

Ryan MP, Sammis CG (1978) Cyclic fracture mechanisms in cooling basalt. Geol Soc Am Bull 89:1295–1308

Saemundsson K (1970) Interglacial lava flows in the lowlands of southern Iceland and the problem of two-tiered columnar jointing. Jökull 20:62–77

Samant H, Pundalik A, D’Souza J, Sheth H, Carmo Lobo K, D’Souza K, Patel V (2017) Geology of the Elephanta Island fault zone, western Indian rifted margin, and its significance for

understanding the Panvel flexure. J Earth Syst Sci 126:9, doi: 10.1007/s12040-016-0793-8

Sangode SJ, Sharma R, Mahajan R, Basavaiah N, Srivastava P, Gudadhe SS, Meshram DC, Venkateswarlu M (2017) Anisotropy of magnetic susceptibility and rock magnetic applications in the Deccan volcanic province based on some case studies. J Geol Soc Ind 89:631–642

Sarkar PK, Mude SN (2010) Remnants of vertical and lateral migration of the entrapped volatiles and gases in the Deccan Trap basalts at Bhaja, Maval Taluka of Pune District, Maharashtra. J Geol Soc Ind 75:560–562

Sarkar PK, Upasani DV, Sikilkal NA, Moray GM (2015) Physical evidence of vesicular cylinders in pāhoehoe lava flow at Pataleshwar temple, Pune, India. J Geosci Res (Gondwana Geol Soc, Nagpur) 1:11–15

Scarth A, Tanguy J-C (2001) Volcanoes of Europe. Oxford Univ Press, New York, 243 p

Schaeffer B (1972) A Jurassic fish from Antarctica. Am Museum Nov 2495:1–17

Schmidt R, Schmincke H-U (2000) Seamounts and island building, *in* Sigurdsson H, Houghton BF, McNutt SR, Rymer H, Stix J (eds) Encyclopedia of Volcanoes. Academic Press, 383–402

Schmincke H-U (2004) Volcanism. Springer, 324 p

Schopka HH, Gudmundsson MT, Tuffen H (2006) The formation of Helgafell, southwest Iceland, a monogenetic subglacial hyaloclastite ridge: sedimentology, hydrology and volcano-ice interaction. J Volcanol Geotherm Res 152:359–377

Self S, Thordarson T, Keszthelyi L (1997) Emplacement of continental flood basalt lava flows, *in* Mahoney JJ Coffin MF (eds) Large Igneous Provinces: Continental, Oceanic, and Planetary Flood Volcanism. Am Geophys Union Geophys Monogr 100:381–410

Self S, Keszthelyi L, Thordarson T (1998) The importance of pāhoehoe. Ann Rev Earth Planet Sci 26:81–110

Self S, Schmidt A, Mather TA (2014) Emplacement characteristics, time scales, and volcanic gas release rates of continental flood basalt eruptions on Earth, *in* Keller G, Kerr AC (eds) Volcanism, Impacts, and Mass Extinctions: Causes and Effects. Geol Soc Am Spec Pap 505:319–337

Sen B (2017) Lava flow transition in pāhoehoe-dominated lower pile of Deccan Traps from Manmad-Chandwad area, western Maharashtra. J Geol Soc Ind 89:281–290

Sen B, Sabale AB (2011) Flow-types and lava emplacement history of Rajahmundry Traps, west of River Godavari, Andhra Pradesh. J Geol Soc Ind 78:457–467

Sen B, Sabale AB, Sukumaran PV (2012) Lava channel of Khedrai dam, northeast of Nasik in western Deccan volcanic province: detailed morphology and evidences of channel morphology and evidences of channel reactivation. J Geol Soc Ind 80:314–328

Senthil Kumar P (2005) Structural effects of meteorite impact on basalts: evidence from Lonar Crater, India. J Geophys Res 110:B12402, doi:10.1029/2005JB003662.

Senthil Kumar P, Lakshmi KJP, Krishna N, Menon R, Sruthi U, Keerthi V, Senthil Kumar A, Mysaiah D, Seshunarayana T, Sen MK (2014) Impact fragmentation of basalt at Lonar Crater, India: implications for impact cratering processes in basalt. J Geophys Res (Planets) 119:2029–2059

Sethna SF, Javeri P (1999) Geology and petrochemistry of Deccan spilitic basalts at and around Daman, India. J Geol Soc Ind 53:59–69

Shaub BM (1979) Genesis of thundereggs, geodes, and agates of igneous origin. Lapidary J 32:2340–2366

Shellnutt JG (2014) The Emeishan large igneous province: a synthesis. Geosci Front 5:369–394

Shellnutt JG, Bhat GM, Brookfield ME, Jahn B-M (2011) No link between the Panjal Traps (Kashmir) and the Late Permian mass extinctions. Geophys Res Lett 38, doi: 10.1029/2011GL049032

Shellnutt JG, Bhat GM, Wang K-L, Brookfield ME, Jahn B-M, Dostal J (2014) Petrogenesis of the flood basalts from the Early Permian Panjal Traps, Kashmir, India: geochemical evidence for shallow melting of the mantle. Lithos 204:159–171

Sheth HC (2006) The emplacement of pāhoehoe lavas on Kilauea and in the Deccan Traps. J Earth Syst Sci 115:615–629

Sheth HC (2007) 'Large Igneous Provinces (LIPs)': definition, recommended terminology,

and a hierarchical classification. Earth-Sci Rev 85:117–124

Sheth H (2016) Giant plagioclase basalts: Continental flood basalt-induced remobilization of anorthositic mushes in a deep crustal sill complex. Geol Soc Am Bull 128:916–925

Sheth HC, Cañón-Tapia E (2015) Are flood basalt eruptions monogenetic or polygenetic?, *in* Kämpf H, Németh K, Puziewicz J, Mrlina J, Geissler WH (eds) From Mantle Roots to Surface Eruptions: Cenozoic and Mesozoic Continental Basaltic Magmatism. Int J Earth Sci (Geol Rund) 104:2147–2162

Sheth HC, Pande K (2014) Geological and $^{40}Ar/^{39}Ar$ age constraints on late-stage Deccan rhyolitic volcanism, inter-volcanic sedimentation, and the Panvel flexure from the Dongri area, Mumbai, *in* Sheth HC, Vanderkluysen L (eds) Flood Basalts of Asia. J Asian Earth Sci 84:167–175

Sheth HC, Vanderkluysen L (eds) (2014) Flood Basalts of Asia. John J Mahoney Mem Vol, J Asian Earth Sci 84:1–200

Sheth HC, Ray JS, Ray R, Vanderkluysen L, Mahoney JJ, Kumar A, Shukla AD, Das P, Adhikari S, Jana B (2009) Geology and geochemistry of Pachmarhi dykes and sills, Satpura Gondwana Basin, central India: problems of dyke-sill-flow correlations in the Deccan Traps. Contrib Mineral Petrol 158:357–380

Sheth HC, Ray JS, Senthil Kumar P, Duraiswami RA, Chatterjee RN, Gurav T (2011a) Recyling of flow-top breccia crusts into molten interiors of flood basalt lava flows: field and geochemical evidence from the Deccan Traps, *in* Ray J, Sen G, Ghosh B (eds) Topics in Igneous Petrology, Springer, 161–180

Sheth HC, Ray JS, Kumar A, Bhutani R, Awasthi N (2011b) Toothpaste lava from the Barren Island volcano (Andaman Sea). J Volcanol Geotherm Res 202:73–82

Sheth HC, Zellmer GF, Kshirsagar PV, Cucciniello C (2013) Geochemistry of the Palitana flood basalt sequence and the Eastern Saurashtra dykes, Deccan Traps: clues to petrogenesis, dyke-flow relationships, and regional lava stratigraphy. Bull Volcanol 75:701, doi: 10.1007/s00445-013-0701-x

Sheth HC, Zellmer GF, Demonterova EI, Ivanov AV, Kumar R, Patel RK (2014) The Deccan tholeiite lavas and dykes of Ghatkopar-Powai area, Mumbai, Panvel flexure zone: geochemistry, stratigraphic status, and tectonic significance, *in* Sheth HC, Vanderkluysen L (eds) Flood basalts of Asia. J Asian Earth Sci 84:69–82

Sheth H, Meliksetian K, Gevorgyan H, Israyelyan A, Navasardyan G (2015) Intracanyon basalt lavas of the Debed River (northern Armenia), part of a Pliocene-Pleistocene continental flood basalt province in the South Caucasus. J Volcanol Geotherm Res 295:1–15

Sheth H, Samant H, Patel V, D'Souza J (2017a) The volcanic geoheritage of the Elephanta Caves, Deccan Traps, western India. Geoheritage 9:359–372

Sheth H, Pal I, Patel V, Samant H, D'Souza J (2017b) Breccia-cored columnar rosettes in a rubbly pāhoehoe lava flow, Elephanta Island, Deccan Traps, and a model for their origin. Geosci Front 8:1299–1307

Sheth H, Patel V, Samant H (2017c) Control of early-formed vesicle cylinders on upper crustal prismatic jointing in compound pāhoehoe lavas of Elephanta Island, western Deccan Traps, India. Bull Volcanol 79:63, doi: 10.1007/s00445-017-1147-3

Sheth H, Pande K, Vijayan A, Sharma KK, Cucciniello C (2017d) Recurrent Early Cretaceous, Indo-Madagascar (89-86 Ma) and Deccan (66 Ma) alkaline magmatism in the Sarnu-Dandali complex, Rajasthan: $^{40}Ar/^{39}Ar$ age evidence and geodynamic significance. Lithos 284-285:512–524

Shoemaker KA, Hart WK (2002) Temporal controls on basalt genesis and evolution on the Owyhee Plateau, Idaho and Oregon, *in* Bonnichsen B, White CM, McCurry M (eds) Tectonic and Magmatic Evolution of the Snake River Plain Volcanic Province. Idaho Geol Surv Bull 30:313–328

Shumlyanskyy L, Mitrokhin O, Billström K, Ernst RE, Vishnevska E, Tsymbal S, Cuney M, Soesoo A (2016) The ca. 1.8 Ga mantle plume related magmatism of the central part of the Ukrainian shield. GFF 138:86–101

Sigurdsson H (1999) Melting the Earth: The History of Ideas on Volcanic Eruptions. Oxford Univ Press, New York, 260 p

Singh SD (2000) Petrography and clay mineralogy of intertrappean beds of Mumbai, India. J Geol Soc Ind 55:275–288

Skilling IP, White JDL, McPhie J (2002) Peperite: a review of magma-sediment mingling. J Volcanol Geotherm Res 114:1–17

Smellie JL (2000) Subglacial volcanism, *in* Sigurdsson H, Houghton BF, McNutt SR, Rymer H, Stix J (eds) Encyclopedia of Volcanoes. Academic Press, 403–420

Smith RK, Tremallo RL, Lofgren GE (2001) Growth of megaspherulites in a rhyolitic vitrophyre. Am Mineral 86:589–600

Spry A (1962) The origin of columnar jointing, particularly in basalt flows. J Austr Geol Soc 8:191–216

Srivastava P, Sandoge SJ, Meshram DC, Gudadhe SS, Nagaraju E, Kumar A, Venkateshwarlu M (2012) Palaeoweathering and depositional conditions in the inter-flow sediment units (bole beds) of Deccan volcanic province, India: a mineral magnetic approach. Geoderma 177–178:90–109

Stigall AL, Babcock LE, Briggs DE, Leslie SA (2008) Taphonomy of lacustrine interbeds in the Kirkpatrick Basalt (Jurassic), Antarctica. Palaios 23:344–355

Subbarao KV (ed) (1988) Deccan Flood Basalts. Geol Soc Ind Mem 10, 393 p

Subbarao KV (ed) (1999) Deccan Volcanic Province. Geol Soc Ind Mem 43(1-2), 947 p

Subbarao KV, Sukheswala RN (eds) (1981) Deccan Volcanism and Related Basalt Provinces in Other Parts of the World. Geol Soc Ind Mem 3, 474 p

Sukheswala RN (1974) Gradation of tholeiitic Deccan basalt into spilite, Bombay, India, *in* Amstutz GC (ed) Spilites and Spilitic Rocks, Springer, 229–250

Sukheswala RN, Sethna SF (1967) Giant pseudoleucites of Ghori, Chhota Udaipur, India. Am Mineral 52:1904–1910

Sukheswala RN, Avasia RK, Gangopadhyay M (1974) Zeolites and associated secondary minerals in the Deccan Traps of western India. Min Mag 39:658–671

Swanson DA (1973) Pāhoehoe flows from the 1969-1971 Mauna Ulu eruption, Kilauea volcano, Hawaii. Geol Soc Am Bull 84:615–626

Swanson DA, Wright RL (1981) The regional approach to studying the Columbia River Basalt Group, *in* Subbarao KV, Sukheswala RN (eds) Deccan Volcanism and Related Basalt Provinces in Other Parts of the World. Geol Soc Ind Mem 3:58–80

Swanson DA, Wright RL, Helz RT (1975) Linear vent systems and estimated rates of magma production and eruption for the Yakima Basalt on the Columbia Plateau. Am J Sci 275:877–905

Tanner LH (2013) Surface morphology of basalt columns at Svartifoss, VatnajökulsÞjóðgarður, Southern Iceland. J Geol Res, art. 482067, doi: 10.1155/2013/482067

Tasch P, Gafford EL (1984) Central Transantarctic Mountains nonmarine deposits, *in* Turner MD, Splettstoesser JF (eds) Geology of the Central Transantarctic Mountains. Antarctic Res Ser, Am Geophys Union 36:75–96

Thorarinsson S (1953) The crater groups in Iceland. Bull Volcanol 14:3–44

Thordarson T, Larsen G (2007) Volcanism in Iceland in historical time: volcano types, eruption styles and eruptive history. J Geodyn 43:118–152

Thordarson T, Self S (1993) The Laki (Skaftár Fires) and Grímsvötn eruptions in 1783-85. Bull Volcanol 55:233–63

Thordarson T, Self S (1996) Sulfur, chlorine and fluorine degassing and atmospheric loading by the Roza eruption, Columbia River Basalt Group, Washington, USA. J Volcanol Geotherm Res 74:49–73

Thordarson T, Self S (1998) The Roza Member, Columbia River Basalt Group: a gigantic pāhoehoe lava flow field formed by endogenous processes? J Geophys Res 103:27411–27445

Tolan TL, Beeson MH (1984) Intracanyon flows of the Columbia River Basalt Group in the lower Columbia River gorge and their relationship to the Troutdale Formation. Geol Soc Am Bull 95:463–477

Tomkeieff SI (1940) The basalt lavas of the Giant's Causeway district of Northern Ireland. Bull Volcanol 6:89–146

Tyrrell GW (1932) The basalts of Patagonia. J Geol 40:374–383

U. S. Department of Energy (USDOE) (1988) Site Characterization Plan Reference Repository Location, Hanford Site, Washington.

U.S. Department of Energy, Washington D.C., DOE/RW-0164, two volumes

Vanderkluysen L, Mahoney JJ, Hooper PR, Sheth HC, Ray R (2011) The feeder system of the Deccan Traps (India): insights from dyke geochemistry. J Petrol 252:315–343

Verati C, Rapaille C, Féraud G, Marzoli A, Bertrand H, Youbi N (2007) $^{40}Ar/^{39}Ar$ ages and duration of the Central Atlantic Magmatic Province volcanism in Morocco and Portugal and its relation to the Triassic-Jurassic boundary. Palaeogeogr Palaeoclim Palaeoecol 244:308–325

Vergniolle S, Mangan M (2000) Hawaiian and Strombolian eruptions, *in* Sigurdsson H, Houghton BF, McNutt SR, Rymer H, Stix J (eds) Encyclopedia of Volcanoes. Academic Press, 447–461

Vespermann D, Schmincke H-U (2000) Scoria cones and tuff rings, *in* Sigurdsson H, Houghton BF, McNutt SR, Rymer H, Stix J (eds) Encyclopedia of Volcanoes. Academic Press, 447–461

Viladkar SG (2010) The origin of pseudoleucite in tinguaite, Ghori, India: a re-evaluation. Petrology 18:544–554

Wabo H, de Kock MO, Klausen MB, Söderlund U, Beukes NJ (2016) Paleomagnetism and chronology of B-1 marginal sills of the Bushveld Complex from the eastern Kaapvaal Craton, South Africa. GFF 138:133–151

Wadia DN (1975) Geology of India. 4th Ed. Tata McGraw-Hill, New Delhi, 508 p

Wager LR, Deer WA (1939) Geological Investigations in East Greenland, part III. The petrology of the Skaergaard Intrusion, Kangerdluqssuaq, East Greenland. Meddelelser on Grønland 105:1–352

Wager LR, Brown GM, Wadsworth WJ (1960) Types of igneous cumulates. J Petrol 1:73–85

Waichel BL, de Lima EF, Lubachevsky R, Sommer CA (2006) Pāhoehoe flows from the central Paraná continental flood basalts. Bull Volcanol 176:599–610

Walker GPL (1959) Geology of the Reydarfjördur area, eastern Iceland. Quat J Geol Soc 114:367–393

Walker GPL (1971) Compound and simple lava flows and flood basalts, *in* Aswathayarayana U (ed) Deccan Trap and other flood eruptions. Bull Volcanol 35:579–590

Walker GPL (1987) Pipe vesicles in Hawaiian basaltic lavas: their origin and potential as palaeoslope indicators. Geology 15:84–87

Walker GPL (1989) Spongy pāhoehoe in Hawaii: a study of vesicle-distribution patterns in basalt and their significance. Bull Volcanol 51:199–209

Walker GPL (1991) Structure, and origin by injection of lava under surface crust, of tumuli, "lava rises", "lava-rise pits", and "lava-inflation clefts" in Hawaii. Bull Volcanol 53:546–558

Walraven F (1997) Geochronology of the Rooiberg Group, Transvaal Supergroup, South Africa. Info Circ 316, Econ Geol Res Unit, Univ Witwatersrand, Johannesburg, South Africa.

Walraven F, Martini J (1995) Zircon Pb-evaporation age determinations for the Oak Tree Formation, Chuniespoort Group, Transvaal Sequence; implications for Transvaal-Griqualand West basin correlations. S Afr J Geol 98:58–67

Waters AC (1960) Determining directions of flow in basalts. Am J Sci 258A:350–366

Watkins J, Manga M, Huber C, Martin M (2009) Diffusion-controlled spherulite growth in obsidian inferred from H_2O concentration profiles. Contrib Mineral Petrol 157:163–172

Watters TR (1989) Periodically spaced anticlines of the Columbia plateau, *in* Reidel SP, Hooper PR (eds) Volcanism and Tectonism in the Columbia River Flood-Basalt Province. Geol Soc Am Spec Pap 239:283–292

Weatherley S, Keiding JK, Klausen MB, Kokfelt TF, Tegner C, Ulrich T (2016) Late Cretaceous to Palaeogene rocks, *in* Kolb J, Stensgaard BM, Kokfelt TF (eds) Geology and Mineral Potential of South-East Greenland. GEUS Report 2016/38:84-100

White JDL, Houghton BF (2000) Surtseyan and related phreatomagmatic eruptions, *in* Sigurdsson H, Houghton BF, McNutt SR, Rymer H, Stix J (eds) Encyclopedia of Volcanoes. Academic Press, 495–512

White JDL, McClintock MK (2001) Immense vent complex marks flood-basalt eruption in a wet, failed rift: Coombs Hills, Antarctica. Geology 29:935–938

White JDL, Bryan SE, Ross P-S, Self S, Thordarson T (2009) Physical volcanology of large igneous provinces: update and review, *in* Thordarson T, Larsen G, Self S, Rowland S, Höskuldsson A (eds) Studies in Volcanology: The legacy of George Walker. IAVCEI Spec Publ 2, Geol Soc Lond, 291–321

Widdowson M (1997) Tertiary palaeosurfaces of the SW Deccan, western India: implication for passive margin uplift, *in* Widdowson M (ed) Palaeosurfaces: Recognition, Reconstruction and Palaeoenvironmental Interpretation. Geol Soc Spec Publ 120:221–248

Widdowson M (2004) Ferricrete, *in* Goudie A (ed) Encylopedia of Geomorphology. Routledge, 365–367

Widdowson M, Gunnell Y (1999) Lateritization, geomorphology and geodynamics of a passive continental margin: the Konkan and Kanara coastal lowlands of western peninsular India. Spec Publ Int Assoc Sed 27:245–274

Wignall PB (2001) Large igneous provinces and mass extinctions. Earth-Sci Rev 53:1–33

Wignall PB (2005) The link between large igneous province eruptions and mass extinctions; Elements 1:293–297

Wilkins A, Subbarao KV, Ingram G, Walsh JN (1994) Weathering regimes within the Deccan basalts, *in* Subbarao KV (ed) Volcanism, 217–232. Wiley Eastern, New Delhi

Williamson IT, Bell BR (1994) The Palaeocene lava field of west-central Skye, Scotland: stratigraphy, palaeogeography and structure. Trans Roy Soc Edin: Earth Sci 85:39–75

Wilmoth RA, Walker GPL (1993) P-type and S-type pāhoehoe: a study of vesicle distribution patterns in Hawaiian lava flows. J Volcanol Geotherm Res 55:129–142

Wilson AH, Grant CE (2006) Physical volcanology and compositions of the basaltic lavas in the Archaean Nzuse Group, White Mfolozi inlier, South Africa, *in* Reimold WU, Gibson RL (eds) Processes on Early Earth. Geol Soc Am Spec Pap 405:255–289

Wilson CJN, Houghton BF (2000) Pyroclast transport and deposition, *in* Sigurdsson H, Houghton BF, McNutt SR, Rymer H, Stix J (eds) Encyclopedia of Volcanoes. Academic Press, 545–554

Winter JD (2001) Principles of Igneous and Metamorphic Petrology. 2nd ed. Prentice-Hall, 702 p

Wolff JA, Sumner JM (2000) Lava fountains and their products, *in* Sigurdsson H, Houghton BF, McNutt SR, Rymer H, Stix J (eds) Encyclopedia of Volcanoes. Academic Press, 321–330

Xu Y-G, Chung SL, Jahn BM, Wu GY (2001) Petrological and geochemical constraints on the petrogenesis of the Permo-Triassic Emeishan flood basalts in southwestern China. Lithos 58:145–168

Xu Y-G, He B, Chung SL, Menzies MA, Frey FA (2004) Geologic, geochemical, and geophysical consequences of plume involvement in the Emeishan flood-basalt province. Geology 32:917–920

Xu Y-G, Wang CY, Shen S (eds) (2014a) Permian Large Igneous Provinces: Characteristics, Mineralization and Palaeo-environmental Effects. Lithos 204, 268 p

Xu Y-G, Wei X, Luo ZY, Liu HQ, Cao J (2014b) The Early Permian Tarim large igneous province: main characteristics and a plume incubation model, *in* Xu Y-G, Wang CY, Shen S (eds) Permian Large Igneous Provinces: Characteristics, Mineralization and Palaeo-environmental Effects. Lithos 204:20–35

Youbi N, Martins LT, Munhá JM, Ibouh H, Madeira J, Aït Chayeb H, El Boukhari A (2003) The Late Triassic–Early Jurassic volcanism of Morocco and Portugal in the framework of the Central Atlantic Magmatic province: an overview, *in* Hames WE, McHone JG, Renne PR, Ruppel C (eds) The Central Atlantic Magmatic Province: Insights from Fragments of Pangaea. Am Geophys Union Geophys Monogr 136:179–207

Young DA (2003) Mind over Magma: The Story of Igneous Petrology. Princeton Univ Press, 686 p

Zellmer GF, Sheth HC, Iizuka Y, Lai Y-J (2012) Remobilization of granitoid rocks through mafic recharge: evidence from basalt-trachyte mingling and hybridization in the Manori-Gorai area, Mumbai, Deccan Traps. Bull Volcanol 74:47–66

Zhang CL, Xu YG, Li ZX, Wang HY (2010) Diverse Permian magmatism at the northern margin of the Tarim Block, NW China: genetically linked to the Permian Bachu mantle plume? Lithos 119:537–552

Suggested Reading[1]

Anderson AT, Swihart GH, Artioli G, Geiger CA (1984) Segregation vesicles, gas filter-pressing, and igneous differentiation. J Geol 92:55–72

Anderson SW, Stofan ER, Smrekar SE, Guest JE, Wood B (1999) Pulsed inflation of pāhoehoe lava flows: implications for flood basalt emplacement. Earth Planet Sci Lett 168:7–18

Annen C, Blundy JD, Sparks RSJ (2006) The genesis of intermediate and silicic magmas in deep crustal hot zones. J Petrol 47:505–539

Applegarth LJ, Pinkerton H, James MR, Calvari S (2010) Morphological complexities and hazards during the emplacement of channel-fed 'a'ā lava flow fields: a study of the 2001 lower flow field on Etna. Bull Volcanol 72:641–656

Arndt NT, Nisbet EG (eds) (1982) Komatiites. George Allen and Unwin, London

Ashwal LD, Bybee GM (2017) Crustal evolution and the temporality of anorthosites. Earth-Sci Rev 173:307–330

Auden JB (1949) Dykes in western India – a discussion of their relationships with the Deccan Traps. Trans Nat Inst Sci Ind 3:123–157

Aydin A, DeGraff JM (1988) Evolution of polygonal fracture patterns in lava flows. Science 239:471–476

Babiker M, Gudmundsson A (2004) Geometry, structure and emplacement of mafic dykes in the Red Sea Hills, Sudan. J Afr Earth Sci 38:279–292

Baer G, Heimann A (eds) (1995) Physics and Chemistry of Dykes. Balkema, Rotterdam, 339 p

Basaltic Volcanism Study Project (1981) Basaltic Volcanism on the Terrestrial Planets. Pergamon Press, New York, 1286 p

Batiza R, White JDL (2000) Submarine lavas and hyaloclastite, *in* Sigurdsson H, Houghton B, McNutt SR, Rymer H, Stix J (eds) Encyclopedia of Volcanoes, p 361–381. Academic Press, New York.

Bondre NR (2003) Discussion on: Analysis of vesicular basalts and lava emplacement processes for application as a palaeobarometer/palaeoaltimeter. J Geol 111:499–502

Boudreau A (2011) The evolution of texture and layering in layered intrusions. Int Geol Rev 53:330–353

Bryan SE, Ernst RE (2008) Revised definition of large igneous provinces (LIPs). Earth-Sci Rev 86:175–202

Bryan SE, Ferrari L (2013) Large igneous provinces and silicic large igneous provinces: progress in our understanding over the last 25 years. Geol Soc Am Bull 125:1053–1078

Bryan SE, Riley TR, Jerram DA, Leat PT, Stephens CJ (2002) Silicic volcanism: an undervalued component of large igneous provinces and volcanic rifted margins, in Menzies MA, Klemperer SL, Ebinger CJ, Baker J (eds) Volcanic Rifted Margins. Geol Soc Am Spec Pap 362, 99–120

Bryan SE, Ukstins-Peate I, Peate DW, Self S, Jerram DA, Mawby MR, Marsh JS, Miller JA

[1]What follows is a compilation of the definitions of technical terms used in this atlas, particularly for flood basalt nonspecialists, though specialists may also find the definitions and accompanying notes useful. The definitions are taken from several sources, and have been suitably edited in many cases. Additional sources which provide further information or clarification are also indicated. Note that some terms, such as "large igneous province", have definitions that are highly debated, and such controversies are best kept beyond the scope of this atlas, but ample reading material is indicated.

H. Sheth, *A Photographic Atlas of Flood Basalt Volcanism*, https://doi.org/10.1007/978-3-319-67705-7

(2010) The largest volcanic eruptions on Earth. Earth-Sci Rev 102:207–229

Budkewitsch P, Robin P-Y (1994) Modelling the evolution of columnar joints. J Volcanol Geotherm Res 59:219–239

Burchardt S, Galland O (2016) Studying volcanic plumbing systems – multidisciplinary approaches to a multifaceted problem, *in* Updates in Volcanology – From Volcano Modelling to Volcano Geology, Intech Publ, 23–53

Calvari S, Pinkerton H (1999) Lava tube morphology on Etna and evidence for lava flow emplacement mechanisms. J Volcanol Geotherm Res 90:263–280

Cañón-Tapia E (2009) Hydrostatic principles of volcanic systems, *in* Thordarson T, Self S, Larsen G, Rowland SK, Holkuldsson A (eds) Studies in Volcanology: The Legacy of George Walker. IAVCEI Spec Publ 2, Geol Soc Lond, 267–289

Cañón-Tapia E (2010) Origin of large igneous provinces: the importance of a definition, *in* Cañón-Tapia E, Szakács A (eds) What is a Volcano? Geol Soc Am Spec Pap 470:77–101

Cañón-Tapia E, Coe R (2002) Rock magnetic evidence of inflation of a flood basalt flow. Bull Volcanol 64:289–302

Cañón-Tapia E, Szakács A (eds) (2010) What is a Volcano? Geol Soc Am Spec Pap 470, 140 p

Cañón-Tapia E, Walker GPL (2004) Global aspects of volcanism: the perspectives of "plate tectonics" and "volcanic systems". Earth-Sci Rev 66:163–182

Cashman KV, Kauahikaua JP (1997) Reevaluation of vesicle distributions in basaltic lava flows. Geology 25:419–422

Cashman KV, Sparks RSJ (2013) How volcanoes work: a 25 year perspective. Geol Soc Am Bull 125:664–690

Cashman K, Pinkerton H, Stephenson J (eds) (1998) Introduction to special section: long lava flows. J Geophys Res 113:27281–27289

Cashman K V, Thornber C, Kauahikaua JP (1999) Cooling and crystallization of lava in open channels, and the transition of pāhoehoe lava to ʻa'ā. Bull Volcanol 61, 306–323

Cawthorn RG (ed) (1996) Layered Intrusions. Dev Petrol 15, Elsevier, Amsterdam, 530 p

Cawthorn RG (2015) The Bushveld Complex, South Africa, *in* Charlier B, Namur O, Latypov R, Teigner C (eds) Layered Intrusions, Springer, 517–587

Charlier B, Namur O, Latypov R, Teigner C (eds) (2015) Layered Intrusions. Springer, 748 p

Coffin MF, Eldholm O (1992) Volcanism and continental break-up: a global compilation of large igneous provinces, *in* Storey BC, Alabaster T, Pankhurst RJ (eds) Magmatism and the Causes of Continental Break-up. Geol Soc Lond Spec Publ 68:17–30

Coffin MF, Eldholm O (1993) Scratching the surface: estimating dimensions of large igneous provinces. Geology 21:515–518

Coffin MF, Eldholm O (1994) Large igneous provinces: crustal structure, dimensions, and external consequences. Rev Geophys 32:1–36.

Cox KG (1980) A model for flood basalt vulcanism. J Petrol 21:629–650

DeGraff JM, Aydin A (1987) Surface morphology of columnar joints and its significance to mechanics and direction of joint growth. Geol Soc Am Bull 99:605–617

DeGraff JM, Long PE, Aydin A (1989) Use of joint-growth directions and rock textures to infer thermal regimes during solidification of basaltic lava flows. J Volcanol Geotherm Res 38:309–324

Delaney PT, Pollard DD (1982) Solidification of basaltic magma during flow in a dyke. Am J Sci 282: 856–885

Deshmukh SS (1988) Petrographic variations in the compound flows in Deccan Traps and their significance, *in* Subbarao KV (ed) Deccan Flood Basalts. Geol Soc Ind Mem 10:305–319

Deshmukh SS, Sehgal MN (1988) Mafic dyke swarms in Deccan volcanic province of Madhya Pradesh and Maharashtra, *in* Subbarao KV (ed) Deccan Flood Basalts. Geol Soc Ind Mem 10:323–340

Duncan AM, Guest JE, Stofan ER, Anderson SW, Pinkerton H, Calvari S (2004) Development of tumuli in the medial portion of the 1983 ʻa'ā flow field, Mount Etna, Sicily. J Volcanol Geotherm Res 132:173–187

Duraiswami RA, Bondre NR, Managave S (2008) Morphology of rubbly pāhoehoe (simple) flows from the Deccan volcanic province : implications for style of emplacement. J Volcanol Geotherm Res 177:822–836

Ebinger CJ, Baker J, Menzies MA, Klemperer SL (eds) (2002) Volcanic Rifted Margins. Geol Soc Am Spec Pap 362, 236 p

Elliot DH, Fleming TH (2017) The Ferrar large igneous province: field and geochemical constraints on supra-crustal (high-level) emplacement of the magmatic system, *in* Sensarma S, Storey BC (eds) Large Igneous Provinces from Gondwana and Adjacent Regions. Geol Soc Lond Spec Publ 463, doi: 10.1144/SP463.1

Ernst RE (2014) Large Igneous Provinces. Cambridge Univ. Press, 653 p

Ernst RE, Youbi N (2017) How large igneous provinces affect global climate, sometimes cause mass extinctions, and represent natural markers in the geological record. Palaeogeogr, Palaeoclimatol, Palaeoecol 478:30–52

Ernst RE, Head JW, Parfitt E, Grosfils E, Wilson L (1995) Giant radiating dyke swarms on Earth and Venus. Earth-Sci Rev 39:1–58

Ernst RE, Grosfils EB, Mege D (2001) Giant dyke swarms on Earth, Venus, and Mars. Ann Rev Earth Planet Sci 29:489–534

Ernst RE, Buchan KL, Campbell IH (2005) Frontiers in large igneous province research. Lithos 79:271–279

Faust GT (1978) Joint systems in the Watchung basalt flows, New Jersey. US Geol Surv Prof Pap 864-B, 46 p

Fialko YA, Rubin AM (1999) Thermal and mechanical aspects of magma emplacement in giant dyke swarms. J Geophys Res 104:23033–23049

Finch RH (1933) Block lava. J Geol 41:769–770

Forbes AES, Blake S, Tuffen H (2014) Entablature: fracture types and mechanisms. Bull Volcanol 76:820, doi: DOI 10.1007/s00445-014-0820-z

Foulger GR, Jurdy DM (eds) (2007) Plates, Plumes, and Planetary Processes. Geol Soc Am Spec Pap 430, 974 p

Foulger GR, Natland JH, Presnall DC, Anderson DL (eds) (2005) Plates, Plumes, and Paradigms. Geol Soc Am Spec Pap 388, 861 p

Fowler AC, Rust AC, Vynnycky M (2015) The formation of vesicular cylinders in pāhoehoe lava flows. Geophys Astrophys Fluid Dyn 109:39–61

Gilman JJ (2009) Basalt columns: large scale constitutional supercooling? J Volcanol Geotherm res 184:347–350

Greeley R, Fagents SA, Harris RS, Kadel SD, Williams DA (1998) Erosion by flowing lava: field evidence. J Geophys Res 103:27325–27345

Goehring L, Morris SW (2008) Scaling of columnar joints in basalt. J Geophys Res 113: B10203, doi: 10.1029/2007JB005018

Gregg TKP (2017) Patterns and processes: subaerial lava flow morphologies: a review. J Volcanol Geotherm Res 342:3–12

Gregg TKP, Keszthelyi LP (2004) The emplacement of pāhoehoe toes: field observations and comparison to laboratory simulations. Bull Volcanol 66:381–391

Gregg TKP, Fink JH, Griffiths RW (1998) Formation of multiple fold generations on lava flow surfaces: influence of strain rate, cooling rate, and lava composition. J Volcanol Geotherm Res 80:281–292

Grossenbacher KA, McDuffie SM (1995) Conductive cooling of lava: columnar joint diameter and stria width as functions of cooling rate and thermal gradient. J Volcanol Geotherm Res 69:95–103

Gudmundsson A (1990) Dyke emplacement at divergent plate boundaries, *in* Parker AJ, Rickwood PC, Tucker DH (eds) Mafic Dykes and Emplacement Mechanisms, 47–62. Balkema, Rotterdam

Gudmundsson A (1995a) The geometry and growth of dykes, *in* Baer G, Heimann A (eds) Physics and Chemistry of Dykes, 23–24. Balkema, Rotterdam

Gudmundsson A (1995b) Infrastructure and mechanics of volcanic systems in Iceland. J Volcanol Geotherm Res 64:1–22

Gudmundsson A (2011) Rock Fractures in Geological Processes. Cambridge Univ Press, 578 p

Gudmundsson A, Brenner SL (2004) Local stresses, dyke arrest and surface deformation in volcanic edifices and rift zones. Annal Geophys 47:1433–1454

Gudmundsson A, Marinoni LB (2002) Geometry, emplacement, and arrest of dykes. Annal Tecto 13:71–92

Guest JE, Stofan ER (2005) The significance of slab-crusted lava flows for understanding controls on flow emplacement at Mount Etna, Sicily. J Volcanol Geotherm Res 142:193–205

Guilbaud M-N, Self S, Thordarson T, Blake S (2005) Morphology, surface structures, and emplacement of lavas produced by Laki, A.D. 1783-84, *in* Manga M, Ventura G (eds) Kinematics and Dynamics of Lava Flows. Geol Soc Am Spec Pap 396, 81–102

Halls HC, Fahrig WF (eds) (1987) Mafic Dyke Swarms. Geol Assoc Canada Pap 34, 503 p

Hames WE, McHone JG, Renne PR, Ruppel C (eds) (2003) The Central Atlantic Magmatic Province: Insights from Fragments of Pangaea. Am Geophys Union Geophys Monogr 136, 267 p

Harris AJL (2012) Lava flows, *in* Fagents SA, Gregg TKP, Lopes RMC (eds) Modelling Volcanic Processes: The Physics and Mathematics of Volcanism. Cambridge Univ Press, 85–106

Harris AJL, Rowland SK (2015) Lava flows and rheology, *in* Sigurdsson H, Houghton B, Rymer H, Stix J, McNutt S (eds) The Encyclopedia of Volcanoes, Elsevier, 321–342

Harris AJL, Rowland SK, Villeneuve N, Thordarson T (2017) Pāhoehoe, ‘a’ā, and block lava: an illustrated history of the nomenclature. Bull Volcanol 79:7, doi: 10.1007/s00445-016-1075-7

Hazlett RW, Hyndman DW (1996) Roadside Geology of Hawaii. Mountain Press Publ Co, Missoula, 304 p

Head JW, Coffin MF (1997) Large igneous provinces: a planetary perspective, *in* Mahoney JJ, Coffin MF (eds) Large Igneous Provinces: Continental, Oceanic, and Planetary Flood Volcanism. Am Geophys Union Geophys Monogr 100:411–438

Heimlich RA (1969) Cylindrical columnar joints in Precambrian mafic dykes, Bighorn Mountains, Wyoming. J Geol 77:371–374

Hetényi G, Taisne B, Garel F, Médard E, Bosshard S, Mattsson HB (2012) Scales of columnar jointing in igneous rocks: field measurements and controlling factors. Bull Volcanol 74:457–482

Hoblitt RP, Orr TR, Heliker C, Denlinger RP, Hon K, Cervelli PF (2012) Inflation rates, rifts, and bands in a pāhoehoe sheet flow. Geosphere 8:179–195

Holcomb RT (1981) Kilauea volcano, Hawaii: Chronology and morphology of the surficial lava flows. US Geol Surv Open File Rep 81-354, 335 p

Hon K, Kauahikaua J, Denlinger R, Mackay K (1994) Emplacement and inflation of pāhoehoe sheet flows – observations and measurements of active lava flows on Kilauea volcano, Hawaii. Geol Soc Am Bull 106:351–370

Hooper PR (2000) Flood basalt provinces, *in* Sigurdsson H, Houghton BF, McNutt SR, Rymer H, Stix J (eds) Encyclopedia of Volcanoes. Academic Press, 345–359

Huppert HE, Sparks RSJ (1985) Cooling and contamination of mafic and ultramafic magmas during ascent through continental crust. Earth Planet Sci Lett 74:371–386

James S, Walsh JN (1999) Zeolites from the Deccan basalts: chemistry and formation, *in* Subbarao KV (ed) Deccan Volcanic Province. Geol Soc Ind Mem 43(2):803–817

Jeffery KL, Henderson P, Subbarao KV, Walsh JN (1988) The zeolites of the Deccan basalt – a study of their distribution, *in* Subbarao KV (ed) Deccan Flood Basalts. Geol Soc Ind Mem 10:151–162

Jerram DA (2002) Volcanology and facies architecture of flood basalts, *in* Menzies MA, Klemperer SL, Ebinger CJ, Baker J (eds) Magmatic Rifted Margins. Geol Soc Am Spec Pap 362:119–132

Jerram DA, Widdowson M (2005) The anatomy of continental flood basalt provinces: geological constraints on the processes and products of flood volcanism. Lithos 79:385–405

Karlstrom L, Richards M (2011) On the evolution of large ultramafic magma chambers and timescales for flood basalt eruptions. J Geophys Res 116:B08216, doi: 10.1029/2010JB008159

Karlstrom L, Paterson SR, Jellinek M (2017) A reverse energy cascade for crustal magma transport. Nature Geosci 10:604–608

Kauahikaua J, Cashman CV, Mattox TN, Heliker C, Hon KA, Mangan MT, Thornber CR (1998) Observations on basaltic lava streams in tubes from Kilauea volcano, island of Hawaii. J Geophys Res 103:27303–27323

Kerr AC (2005) Oceanic LIPs: the kiss of death. Elements 1:289–292

Keszthelyi L (2002) Classification of mafic lava flows from ODP Leg 183. Proc Ocean Drill Progr Sci Res 183:1–28

Keszthelyi L, Denlinger R (1996) The initial cooling of pāhoehoe flow lobes. Bull Volcanol 58:5–18

Keszthelyi, LP, Self S (1998) Some physical requirements for the emplacement of long basaltic lava flows. J Geophys Res 103:27447-27464

Keszthelyi L, Thordarson T (2000) Rubbly pāhoehoe: a previously undescribed but widespread lava type transitional between ‘a’ā and pāhoehoe. Geol Soc Am Abstr Progr 32:7

Keszthelyi L, Thordarson T (2001) Rubbly pāhoehoe: implication for flood basalt eruptions and their atmospheric effects. Am Geophys Union Fall Mtg Abstr #V52A-1050

Keszthelyi L, Self S, Thordarson T (2006) Flood lavas on Earth, Io and Mars. J Geol Soc Lond 163:253–264

Kilburn CRJ (1981) Pāhoehoe and ‘a’ā lavas: a discussion and continuation of the model of Peterson and Tilling. J Volcanol Geotherm Res 11:373–382

Kilburn CRJ (1990) Surfaces of ‘a’ā flow fields on Mount Etna, Sicily – morphology, rheology, crystallization and scaling phenomena, *in* Fink JH (ed) Lava Flows and Domes, Springer, Berlin, 129–156

Kilburn CRJ (2000) Lava flows and flow fields, *in* Sigurdsson H, Houghton BF, McNutt SR, Rymer H, Stix J (eds) (2000) Encyclopedia of Volcanoes. Academic Press, 291–306

Kilburn CRJ (2004) Fracturing as a quantitative indicator of lava flow dynamics. J Volcanol Geotherm Res 139:209–224

Klausen MD (2009) The Lebombo monocline and associated feeder dyke swarm: diagnostic of a successful and highly volcanic rifted margin? Tectonophysics 468:42–62

Klausen MB, Larsen HC (2002) The East Greenland coast-parallel dyke swarm and its role in continental breakup, in Menzies MA, Klemperer SL, Ebinger CJ, Baker J (eds) Volcanic Rifted Margins. Geol Soc Am Spec Pap 362:133–158

Kontak DJ (2008) On the edge of CAMP: geology and volcanology of the Jurassic North Mountain Basalt, Nova Scotia. Lithos 101:74–101

Kontak DJ, Dostal J (2010) The late-stage crystallization history of the Jurassic North Mountain Basalt, Nova Scotia, Canada. II. Nature and origin of segregation pipes. Can Mineral 48:1141–1176

Latypov RM (2007) Noril’sk- and Lower Talnakh-type intrusions are not conduits for overlying flood basalts: insights from residual gabbroic sequence of intrusions. Appl Earth Sci (Trans Int Min Metall B) 116:215–225

Latypov RM (2009) Testing the validity of the petrological hypothesis ‘No phenocrysts, no post-emplacement differentiation’. J Petrol 50:1047–1059

Lister JR, Kerr RC (1991) Fluid-mechanical models of crack propagation and their application to magma transport in dykes. J Geophys Res 96:10049–10077

Long PE, Wood BJ (1986) Structures, textures, and cooling histories of Columbia River basalt flows. Geol Soc Am Bull 97:1144–1155

Lorenz V (1986) On the growth of maars and diatremes and its relevance to the formation of tuff rings. Bull Volcanol 48:265–274

Lyle P (2000) The eruption environment of multi-tiered columnar basalt lava flows. J Geol Soc Lond 157:715–722

Macdonald GA (1953) Pāhoehoe, ‘a’ā, and block lava. Am J Sci 251:169–191

Macdonald GA (1967) Forms and structures of extrusive basaltic rocks, *in* Hess HH, Poldervaart A (eds) The Poldervaart Treatise on Rocks of Basaltic Composition. Interscience, New York, 1–61

Macdonald GA, Abbott AT, Peterson FL (1983) Volcanoes in the Sea: The Geology of Hawaii. Univ Hawaii Press, Honolulu, 517 p

Macdougall JD (ed) (1988) Continental Flood Basalts. Kluwer Acad Publ, Dordrecht, 341 p

Mahoney JJ, Coffin MF (eds) (1997) Large Igneous Provinces: Continental, Oceanic, and Planetary Flood Volcanism. Am Geophys Union Geophys Monogr 100, 438 p

Manga M, Ventura G (eds) (2005) Kinematics and Dynamics of Lava Flows. Geol Soc Am Spec Pap 396, 218 p

Marinoni LB (2001) Crustal extension from exposed sheet intrusions: review and method proposal. J Volcanol Geotherm Res 107:27–46

Marshall PE, Widdowson M, Murphy DT (2016) The Giant Lavas of Kalkarindji: rubbly pāhoehoe lava in an ancient continental flood basalt province. Palaeogeogr, Palaeoclim, Palaeoecol 441:22–37

McHone JG, Ross ME, Greenough JD (1987) Mesozoic dyke swarms of eastern North America, *in* Halls HC, Fahrig WH (eds) Mafic Dyke Swarms. Geol Assoc Can Spec Pap 34:279–288

McHone JG, Anderson DL, Beutel EK, Fialko YA (2005) Giant dykes, rifts, flood basalts, and plate tectonics: a contention of mantle models, *in* Foulger GR, Natland JH, Presnall DC, Anderson DL (eds) Plates, Plumes, and Paradigms. Geol Soc Am Spec Pap 388:401–420

McLean DM (1985) Deccan Traps mantle degassing in the terminal Cretaceous marine extinctions. Cret Res 6:235–259

McMillan K, Long PE, Cross RW (1989) Vesiculation in Columbia River basalts, *in* Reidel SP, Hooper PR (eds) Volcanism and Tectonism in the Columbia River Flood-Basalt Province. Geol Soc Am Spec Pap 239:157–168

Mège D, Korme T (2004a) Fissure eruption of flood basalts from satistical analysis of dyke fracture length. J Volcanol Geotherm Res 131:77–92

Mège D, Korme T (2004b) Dyke swarm emplacement in the Ethiopian large igneous province: not only a matter of stress. J Volcanol Geotherm Res 132:283–310

Mohr P, Zanettin B (1988) The Ethiopian flood basalt province, *in* Macdougall JD (ed) Continental Flood Basalts. Kluwer Acad Publ, Doredrecht, 63–110

Muirhead JD, Airoldi G, Rowland JV, White JDL (2012) Interconnected sills and inclined sheet intrusions control shallow magma transport in the Ferrar large igneous province, Antarctica. Geol Soc Am Bull 124:162–180

Namur O, Abily B, Boudreau AE, Blanchette F, Bush JWM, Ceuleneer G, Charlier B, Donaldson CH, Duchesne JC, Higgins MD, Morata D, Nielsen TFD, O'Driscoll B, Pang KN, Peacock T, Spandler CJ, Toramaru A, Veksler IV (2015) Igneous layering in basaltic magma chambers, *in* Charlier B, Namur O, Latypov R, Teigner C (eds) Layered Intrusions, Springer, 75–152

Naslund HR, McBirney AR (1996) Mechanisms of formation of igneous layering, *in* Cawthorn RG (ed) Layered Intrusions. Dev Petrol 15:1–44, Elsevier

Németh K (2010) Monogenetic volcanic fields: origin, sedimentary record, and relationship with polygenetic volcanism, *in* Cañon-Tapia E, Szakács A (eds) What is a Volcano? Geol Soc Am Spec Pap 470:43–66

Németh K, Kereszturi G (2015) Monogenetic volcanism: personal views and discussion, *in* Kämpf H, Németh K, Puziewicz J, Mrlina J, Geissler WH (eds) From Mantle Roots to Surface Eruptions: Cenozoic and Mesozoic Continental Basaltic Magmatism. Int J Earth Sci (Geol Rund) 104:2131–2146

Németh K, Martin U (2007) Practical Volcanology. Geol Inst Hungary, Budapest, 221 p

Németh K, Suwesi SK, Peregi Z, Gulacsi Z, Ujszaszi J (2003) Plio/Pleistocene flood basalt related scoria and spatter cones, rootless lava flows, and pit craters, Al Haruj al Abyad, Libya. GeoLines 15:98–103

Németh K, Martin U, Haller MJ, Alric VI (2007) Cenozoic diatreme field in Chubut (Argentina) as evidence of phreatomagmatic volcanism accompanied with extensive Patagonian plateau basalt volcanism? Episodes 30:217–223

Nichols RL (1938) Grooved lava. J Geol 46:601–614

Noguchi R, Höskuldsson A, Kurita K (2016) Detailed topographical, distributional, and material analyses of rootless cones in Mývatn, Iceland. J Volcanol Geotherm Res 318:89–102

O'Hara MJ (2000) Flood basalts and lunar petrogenesis. J Petrol 41:1121–1125

O'Hara MJ (2000) Flood basalts, basalt floods or topless Bushvelds? Lunar petrogenesis revisited. J Petrol 41:1545–1651

Ollier CD (1991) Laterite profiles, ferricrete and landscape evolution. Zeit Geomorph NF 35:165–173

Ollier CD (1995) New concepts of laterite formation, *in* Wadia S, Korisettar R, Kale VS (eds) Quaternary Environments and Geoarchaeology in India: Essays in Honour of Professor S. N. Rajaguru. Geol Soc Ind Mem 32:309–323

Ollier CD (2004) The evolution of mountains on passive continental margins, *in* Owens PN, Slaymaker O (eds) Mountain Geomorphology, 59–88. Edward Arnold, London

Ollier CD, Galloway RW (1990) The laterite profile, ferricrete and unconformity. Catena 17:97–109

Ollier CD, Pain CF (1996) Regolith, Soils and Landforms. John Wiley & Sons, Chichester, 316 p

Ollier CD, Pain CF (1997) Equating the basal unconformity with the palaeoplain: a model for passive margins. Geomorphology 19:1–15

Pain CF, Ollier CD (1995) Inversion of relief – a component of landscape evolution. Geomorphology 12:151–165

Parker AJ, Rickwood PC, Tucker DH (eds) (1990) Mafic Dykes and Emplacement Mechanisms. Balkema, Rotterdam, 541 p

Parfitt EA, Wilson L (2008) Fundamentals of Physical Volcanology. Blackwell Publ, 230 p

Passey SR, Bell BR (2007) Morphologies and emplacement mechanisms of the lava flows of the Faroe Islands Basalt Group, Faroe Islands, NE Atlantic Ocean. Bull Volcanol 70:139–156

Perugini D, Poli G (2012) The mixing of magmas in plutonic and volcanic environments: analogies and differences. Lithos 153:261–277

Petcovic HL, Dufek JD (2005) Modelling magma flow and cooling in dykes: implications for emplacement of Columbia River flood basalts. J Geophys Res 110:1–15

Peterson DW, Tilling RI (1980) Transition of basaltic lava from pāhoehoe to ‘a’ā, Kilauea volcano, Hawaii: field observations and key factors. J Volcanol Geotherm Res 7:271–293

Philipp SL, Afşar F, Gudmundsson A (2013) Effects of mechanical layering on hydrofracture emplacement and fluid transport in reservoirs. Front Earth Sci 1, doi: 10.3389/feart.2013.00004

Philpotts AR (1992) A model for emplacement of magma in the Mesozoic Hartford Basin, *in* Puffer JH, Ragland PC (eds) Eastern North American Mesozoic Magmatism. Geol Soc Am Spec Pap 268:137–148

Philpotts AR, Ague JJ (2009) Principles of Igneous and Metamorphic Petrology. 2nd Edn. Cambridge Univ Press, 667 p

Philpotts AR, Dickson LD (2000) The formation of plagioclase chains during convective transfer in basaltic magma. Nature 406:59–61

Philpotts AR, Dickson LD (2002) Millimeter-scale modal layering and the nature of the upper solidification zone in thick flood-basalt flows and other sheets of magma. J Struc Geol 24:1171–1177

Philpotts AR, Lewis CL (1987) Pipe vesicles – an alternate model for their origin. Geology 15:971–974

Philpotts AR, Carroll M, Hill JM (1996) Crystal-mush compaction and the origin of pegmatitic segregation sheets in a thick flood-basalt flow in the Mesozoic Hartford Basin, Connecticut. J Petrol 37:811–836

Pinkerton H, Wilson L (1994) Factors controlling the lengths of channel-fed lava flows. Bull Volcanol 56:108–120

Polacci M, Cashman KV, Kauahikaua JP (1999) Textural characterization of the pāhoehoe-‘a’ā transition in Hawaiian basalt. Bull Volcanol 60:595–609

Pollard DD (1987) Elementary fracture mechanics applied to the structural interpretation of dykes, *in* Halls HC, Fahrig WF (eds) Mafic Dyke Swarms. Geol Assoc Canada Spec Pap 34:5–24

Puffer JH, Ragland PC (eds) (1992) Eastern North American Mesozoic Magmatism. Geol Soc Am Spec Pap 268, 398 p

Puffer JH, Horter DL (1993) Origin of pegmatitic segregation veins within flood basalts. Geol Soc Am Bull 105:738–748

Rader E, Vanderkluysen L, Clarke A (2017) The role of unsteady effusion rates on inflation in long-lived lava flow fields. Earth Planet Sci Lett 477:73–83

Ray R, Sheth HC, Mallik J (2007) Structure and emplacement of the Nandurbar-Dhule mafic dyke swarm, Deccan Traps, and the tectonomagmatic evolution of flood basalts. Bull Volcanol 69:537–531

Reidel SP (1998) Emplacement of Columbia River flood basalt. J Geophys Res 103:27393–27410

Reidel SP, Camp VE, Ross ME, Wolff JA, Martin BS, Tolan TL, Wells RE (eds) (2013a) The Columbia River Flood Basalt Province. Geol Soc Am Spec Pap 497, 440 p

Rohrman M (2013) Intrusive large igneous provinces below sedimentary basins: an example from the Exmouth Plateau (NW Australia). J Geophys Res 118:4477–4487

Rossi MJ, Gudmundsson A (1996) The morphology and formation of flow-lobe tumuli on Icelandic shield volcanoes. J Volcanol Geotherm Res 72:291–308

Rowland SK, Walker GPL (1988) Mafic-crystal distributions, viscosities, and lava structures of some Hawaiian lava flows. J Volcanol Geotherm Res 35:55–66

Rubin AM (1995) Propagation of magma-filled cracks. Ann Rev Earth Planet Sci 23:287–336

Ryan MP, Sammis CG (1978) Cyclic fracture mechanisms in cooling basalt. Geol Soc Am Bull 89:1295–1308

Ryan MP, Sammis CG (1981) The glass transition in basalt. J Geophys Res 86:9519–9535

Saemundsson K (1970) Interglacial lava flows in the lowlands of southern Iceland and the problem of two-tiered columnar jointing. Jökull 20:62–77

Sahagian DL, Proussevitch AA, Carlson WD (2002) Analysis of vesicular basalts and lava emplacement processes for application as a palaeobarometer/palaeoaltimeter. J Geol 110:671–685

Saunders AD (ed) (2005) Large Igneous Provinces: Origin and environmental consequences. Elements 1:259–297

Schultz RA, Mège D, Diot H (2008) Emplacement conditions of igneous dykes in Ethiopian Traps. J Volcanol Geotherm Res 178:683–692

Self S, Thordarson T, Keszthelyi L, Walker GPL, Hon K, Murphy MT, Long P, Finnemore S (1996) A new model for the emplacement of Columbia River basalts as large, inflated pāhoehoe lava flow fields. Geophys Res Lett 23:2689–2692

Self S, Thordarson T, Keszthelyi L (1997) Emplacement of continental flood basalt lava flows, *in* Mahoney JJ, Coffin MF (eds) Large Igneous Provinces: Continental, Oceanic, and Planetary Flood Volcanism. Am Geophys Union Geophys Monogr 100:381–410

Self S, Thordarson T, Widdowson M (2005) Gas fluxes from flood basalt eruptions. Elements 1:283–287

Self S, Schmidt A, Mather TA (2014) Emplacement characteristics, time scales, and volcanic gas release rates of continental flood basalt eruptions on Earth, *in* Keller G, Kerr AC (eds) Volcanism, Impacts, and Mass Extinctions: Causes and Effects. Geol Soc Am Spec Pap 505:319–337

Self S, Coffin MF, Rampino MR, Wolff JA (2015) Large igneous provinces and flood basalt volcanism, *in* Sigurdsson H, Houghton B, Rymer H, Stix J, McNutt S (eds) The Encyclopedia of Volcanoes, Elsevier, 441–455

Sensarma S, Storey BC (eds) (2017) Large Igneous Provinces from Gondwana and Adjacent Regions. Geol Soc Lond Spec Publ 463, in press

Sensarma S, Paul DK, Chalapathi Rao NVC (2013) Large igneous provinces – global perspectives and prospects in India. Current Sci 105:182–191

Shaw HR, Swanson DA (1970) Eruption and flow rates of flood basalts, *in* Gilmour EH, Stradling D (eds) Proc 2nd Columbia River Basalt Symp, 271-299. Eastern Washington State College Press, Cheney

Sheridan MF, Wohletz KH (1983) Hydrovolcanism: basic considerations and review. J Volcanol Geotherm Res 17:1–29

Sheth HC (2007) 'Large Igneous Provinces (LIPs)': definition, recommended terminology, and a hierarchical classification. Earth-Sci Rev 85:117–124

Sheth, HC, Cañón-Tapia E (2015) Are flood basalt eruptions monogenetic or polygenetic?, *in* Kämpf H, Németh K, Puziewicz J, Mrlina J, Geissler WH (eds) From Mantle Roots to Surface Eruptions: Cenozoic and Mesozoic Continental Basaltic Magmatism. Int J Earth Sci (Geol Rund) 104:2147–2162

Shellnutt JG (2017) The Panjal Traps, *in* Sensarma S, Storey BC (eds) Large Igneous Provinces from Gondwana and Adjacent Regions. Geol Soc Lond Spec Publ 463, doi: 10.1144/SP463.4

Sheridan MF, Wohletz KH (1983) Hydrovolcanism: basic considerations and review, *in* Sheridan MF, Barberi F (eds), Explosive Volcanism. J Volcanol Geotherm Res 17:1–29

Sigurdsson H, Houghton BF, McNutt SR, Rymer H, Stix J (eds) (2000) Encyclopedia of Volcanoes. Academic Press, 1417 p

Silver PG, Behn MD, Kelley K, Schmitz M, Savage B (2006) Understanding cratonic flood basalts. Earth Planet Sci Lett 245:190–201

Smith IEM, Németh K (2017) Source to surface model of monogenetic volcanism: a critical review, *in* Németh K, Carrasco-Núñez G, Aranda-Gómez JJ, Smith IEM (eds) Monogenetic volcanism. Geol Soc Lond Spec Publ 446:1–28

Snyder D (2000) Thermal effects of the intrusion of basaltic magma into a more silicic magma chamber and implications for eruption triggering. Earth Planet Sci Lett 175:257–273

Soule SA, Cashman KV (2005) Shear rate dependence of the pāhoehoe-to-'a'ā transition: analog experiments. Geology 31:361–364

Sparks RSJ, Marshall LA (1986) Thermal and mechanical constraints on mixing between mafic and silicic magmas. J Volcanol Geotherm Res 29:99–124

Spry A (1962) The origin of columnar jointing, particularly in basalt flows. J Austr Geol Soc 8:191–216

Srivastava RK (2011) Dyke Swarms: Keys for Geodynamic Interpretation. Springer, 601 p

Stolper E, Walker D (1980) Melt density and the average composition of basalt: Contrib Mineral Petrol 74:7–12

Storey BC, Alabaster T, Pankhurst RJ (eds) Magmatism and the Causes of Continental Breakup. Geol Soc Lond Spec Publ 68, 416 p

Swanson DA (1973) Pāhoehoe flows from the 1969-1971 Mauna Ulu eruption, Kilauea volcano, Hawaii. Geol Soc Am Bull 84:615–626

Szakács A (2010) From a definition of volcano to conceptual volcanology, *in* Cañón-Tapia E, Szakács A (eds) What is a Volcano? Geol Soc Am Spec Pap 470:67–76

Thordarson T, Self S (1993) The Laki (Skaftár Fires) and Grímsvötn eruptions in 1783-1785. Bull Volcanol 55:233–263

Thordarson T, Self S (1998) The Roza Member, Columbia River Basalt Group: a gigantic pāhoehoe lava flow field formed by endogenous processes? J Geophys Res 103:27411–27445

Thordarson T, Self S, Oskarsson N, Hulsebosch T (1996) Sulfur, chlorine, and fluorine degassing and atmospheric loading by the 1783-84 AD Laki (Skaftár Fires) eruption in Iceland. Bull Volcanol 58:205–225

Thordarson T, Self S, Larsen G, Rowland SK, Höskuldsson A (2009) Studies in Volcanology: The Legacy of George Walker. IAVCEI Spec Publ 2, Geol Soc Lond, 413 p

Tibaldi A (2015) Structure of volcano plumbing systems: a review of multi-parametric effects. J Volcanol Geotherm Res 298:85–135

Tomkeieff SI (1940) The basalt lavas of the Giant's Causeway district of Northern Ireland. Bull Volcanol 6:89–146

Tyrrell GW (1937) Flood basalts and fissure eruption. Bull Volcanol 2, 89–111

Valentine GA, Gregg TKP (2008) Continental basaltic volcanoes – processes and problems. J Volcanol Geotherm Res 177:857–873

Vergniolle S, Mangan M (2000) Lava flows and flow fields, *in* Sigurdsson H, Houghton BF, McNutt SR, Rymer H, Stix J (eds) (2000) Encyclopedia of Volcanoes. Academic Press, 447–462

Vye-Brown C, Self S, Barry TL (2013) Architecture and emplacement of flood basalt flow fields: case studies from the Columbia River Basalt Group, NW USA. Bull Volcanol 75:697, doi: 10.1007/s00445-013-0697-2

Walker GPL (1960) Zeolite zones and dyke distribution in relation to the structure of the basalts of eastern Iceland. J Geol 68:515–528

Walker GPL (1986) The dyke complex of Koolau volcano, Oahu: intensity and origin of a sheeted-dyke complex high in a Hawaiian volcanic edifice. Geology 14:310–313

Walker GPL (1987) Pipe vesicles in Hawaiian basaltic lavas: their origin and potential as palaeoslope indicators. Geology 15:84–87

Walker GPL (1992a) Coherent intrusion complexes in large basaltic volcanoes – a new structural model. J Volcanol Geotherm Res 50:41–54

Walker GPL (1992b) Morphometric study of pillow-size spectrum among pillow lavas. Bull Volcanol 54:459–474

Walker GPL (1993) Basaltic-volcano systems, *in* Prichard HM, Alabaster T, Harris NBW, Neary CR (eds) Magmatic Processes and Plate Tectonics. Geol Soc Spec Publ 76:3–38

Walker GPL (1995) Flood basalts versus central volcanoes and the British Tertiary Volcanic

Province, *in* Le Bas MJ (ed) Milestones in Geology. Geol Soc Lond Mem 16:195–202
Walker GPL (1999) Volcanic rift zones and their intrusion swarms. J Volcanol Geotherm Res 94:21–34
Walker GPL (2000) Basaltic volcanoes and volcanic systems, *in* Sigurdsson H, Houghton BF, McNutt SR, Rymer H, Stix J (eds) Encylopedia of Volcanoes, 283–289. Academic Press, New York
Walker GPL, Skelhorn RR (1966) Some associations of acid and basic igneous rocks. Earth Sci Rev 2:93–109
Walker GPL, Eyre R, Spengler SR, Knight MD, Kennedy K (1995) Congruent dyke-widths in large basaltic volcanoes, *in* Baer G, Heimann A (eds) Physics and Chemistry of Dykes, 35–40. Balkema, Rotterdam
Washington HS (1922) Deccan Traps and other plateau basalts. Geol Soc Am Bull 33:765–805
Waters AC (1960) Determining directions of flow in basalts. Am J Sci 258A:350–366
Waters AC, Myers CW, Brown DJ, Ledgerwood RK (1981) Columbia Plateau with special emphasis on the basalt stratigraphy of the Pasco basin, *in* Subbarao KV, Sukheswala RN (eds) Deccan Volcanism and Related Basalt Provinces in Other Parts of the World. Geol Soc Ind Mem 3:19–44
White JDL, Bryan SE, Ross P-S, Self S, Thordarson T (2009) Physical volcanology of large igneous provinces: update and review, *in* Thordarson T, Larsen G, Self S, Rowland S, Höskuldsson A (eds) Studies in Volcanology: The legacy of George Walker. IAVCEI Spec Publ 2, Geol Soc Lond, 291–321
Wignall PB (2001) Large igneous provinces and mass extinctions. Earth-Sci Rev 53:1–33
Wignall PB (2005) The link between large igneous province eruptions and mass extinctions; Elements 1:293–297
Wilson L (2009) Volcanism in the Solar System. Nat Geosci 2:389–397
Yoder HS Jr (1973) Contemporaneous basaltic and rhyolitic magmas. Am Mineral 58:153–171

Recommended Websites

www.largeigneousprovinces.org
www.mantleplumes.org
www.geology.sdsu.edu/how_volcanoes_work/
https://volcanoes.usgs.gov/observatories/hvo/
http://icelandicvolcanoes.is

Flood Basalt Index

H. Sheth, *A Photographic Atlas of Flood Basalt Volcanism*, https://doi.org/10.1007/978-3-319-67705-7

Author Index

H. Sheth, *A Photographic Atlas of Flood Basalt Volcanism*, https://doi.org/10.1007/978-3-319-67705-7